Master Thesis

Construction of a test rig of a mixed flow pump

Johann Hopfgartner

Institute for Hydraulic Fluid Machinery
Graz University of Technology
Head of the institute: O. Univ.-Prof. Dr. Ing. Helmut Jaberg

Appraiser: O. Univ.-Prof. Dr.-Ing. Helmut Jaberg
Supervisor: Ass. Prof. Dipl.-Ing. Dr. techn. Helmut Benigni

Graz, September 9, 2013

Abstract

Construction of a test rig of a mixed flow pump
The aim of this master thesis is to design and build up a test rig for a mixed flow pump, its hydraulic having been designed within the Institute for Hydraulic Fluid Machinery. Finally, a measurement analysis has to be carried out.
The construction of the pump, which was on a scale of 1:3.6, turned out to be an iterative and time-consuming process as the tight time schedule made it necessary to design the hydraulic and the test rig simultaneously.
The single parts were mainly manufactured in the workshop of the institute and only partly external because of capacity problems. The purpose of the final measurement analysis was, to generate a characteristic curve of the pump with the help of different positions of the impeller vanes, and thus to be able to provide evidence of the required warranty point.

Kurzfassung

Konstruktion eines Prüfstandes für eine Halbaxialpumpe
Inhalt dieser Masterarbeit ist es, einen Versuchsaufbau für eine Halbaxialpumpe, deren Hydraulik institutsintern entworfen wurde, zu konstruieren und aufzubauen sowie abschließend eine Messauswertung durchzuführen.
Die Konstruktion der im Maßstab 1:3,6 gefertigten Pumpe stellte sich als ein iterativer und zeitaufwendiger Prozess dar, da seitens der Auftraggeber ein straffer Zeitplan eingehalten werden musste und dadurch die Hydraulik zeitgleich mit dem Pumpenprüfstand entworfen wurde.
Die Einzelteile wurden hauptsächlich in der institutseigenen Werkstätte und lediglich wegen Kapazitätsproblemen teilweise auch extern gefertigt. Die abschließende Messung hatte zum Ziel, mithilfe verschiedener Laufradstellungen eine Pumpenkennlinie zu ermitteln, um den Nachweis für den geforderten Garantiepunkt erbringen zu können.

English version:

Statutory declaration

I declare, that I have authored this thesis independently, that I have not used other than the declared sources/resources, and that I have explicitly marked all material which has been quoted either literally or by content from the used sources.

Graz, ...
(Signature)

German version:
Beschluss der Curricula-Kommission für Bachelor-, Master- und Diplomstudien vom 10.11.2008
Genehmigung des Senates am 1.12.2008

Eidestattliche Erklärung

Ich erkläre an Eides statt, dass ich die vorliegende Arbeit selbstständig verfasst, andere als die angegebenen Quellen/Hilfsmittel nicht benutzt und die den benutzten Quellen wörtlich und inhaltlich entnommenen Stellen als solche kenntlich gemacht habe.

Graz, am ....
(Unterschrift)

Preface

Nowadays, as cost of energy is rapidly rising and the environmental damage which is caused by the production of electricity is getting worse, it is very important to use energy efficiently. There is a huge amount of pumps in various fields of application all over the world with an incredibly high consumption of energy. Therefore it is clear, that high efficiency of these pumps can save a lot of energy, but this is only possible if the pumps are not oversized and if they are operated at design points.

I would like to thank Mr. Helmut Jaberg for the opportunity to write this master thesis at the Institute for Hydraulic Fluid Machinery. Furthermore, I thank Mr. Helmut Benigni for the supervision and the support during the realization of this master thesis. Finally, I would like to thank all the others who supported me.

Contents

List of abbreviations

C	kN	Dynamic load rating
E	N/mm^2	Young's modulus of elasticity
e_r		Random error
e_s		Systematic error
g	m/s^2	Acceleration due to gravity
H	m	Differential head
I_y	Nmm^2	Area moment of inertia
K_A		Application factor
L_h	h	Nominal life expectancy
M	Nm	Engine torque
n	rpm	Rotational speed
NPSE	J/kg	Net positive suction specific energy
NPSH	m	Net positive suction head
n_q	rpm	Specific speed
NSS	rpm	Net suction specific speed
p		Load-life exponent
P	kW	Input power
P_H	kW	Hydraulic power
P_M	kW	Mechanical power
Q	m^3/s	Discharge
$R_{\mathrm{p}\ 0,2}$	N/mm^2	Yield strength
T_{eq}	Nm	Maximum occurring torque
$\bar{x}$		Expectation value
Y	J/kg	Specific hydraulic energy
μ		Friction coefficient
ω	s^{-1}	Angular velocity
φ		Flow coefficient
ψ		Head coefficient
ρ	kg/m^3	Density
$\tau_{\mathrm{tW\ N}}$	N/mm^2	Torsional stress under alternating loads

1 Introduction

The object of this master thesis is the construction and the measurement analysis of a mixed flow pump model in order to check, if the new hydraulic, which was designed within the Institute of Hydraulic Fluid Machinery, is able to fulfill the requirements of the customer. Although modern three-dimensional calculation methods are very helpful for the designing of a new hydraulic, they are not able to describe the real flow conditions satisfactorily enough so that a verification with a test rig is indispensable.
Due to the fact that the prototype of the pump should be designed for a very high discharge and power consumption, which is impossible to generate at our institute, a model on a scale of 1:3.6 is used instead. To ensure the best comparability, the scale was chosen as small as possible and results from the ratio between the inner sphere diameter of the prototype and the model.
On account of the tight time schedule, it was necessary to adapt an existing concept [5]. This concept was designed some years ago for a test rig of an axial pump.

1.1 Setting of tasks

- Construction of the test rig
- Calculation of several single parts
- Making single part drawings for the workshop
- Measurement and analysis of the measurements

1.2 Requirements

The customer of this new hydraulic, an Asian pump manufacturer, stated the following requirements for the prototype, which are listed in table 1.1.

Table 1.1: Requirements of the customer

Quantity	Value	Unit
Discharge	5	m^3/s
Differential head	27	m
Rotational speed	507	rpm
Specific speed	95.713	rpm
Net suction specific speed NSS_3	1,600	rpm

The pump efficiency should be as good as possible, but at least 88.5% at the test rig. Furthermore, at 130% of the discharge of the designed point, a net suction specific speed of NSS=1,500 has to be realized.

To fulfill the demands of the customer, the following requirements should be met:

- To ensure that the incident flow onto the impeller vanes is optimal at every operating point, the vanes must be adjustable.
- It must be possible to look inside the pump in order to watch the cavitation behavior of the whole area of the impeller vanes and especially of the inlet of the pump. Therefore, an impeller casing made of acrylic glass is needed.
- All requirements to carry out the measurements conforming to standards have to be fulfilled.

1.3 Arrangement of the test rig

To be able to minimize the costs, existing parts should be integrated as often as possible. Therefore, it is important to use the existing electric motor with the appropriate manifold. Due to this situation, the positions of the main axes of the test rig are already fixed.
The arrangement of the test rig is schematically displayed in figures 1.1 and 1.2 with dimensions in mm.

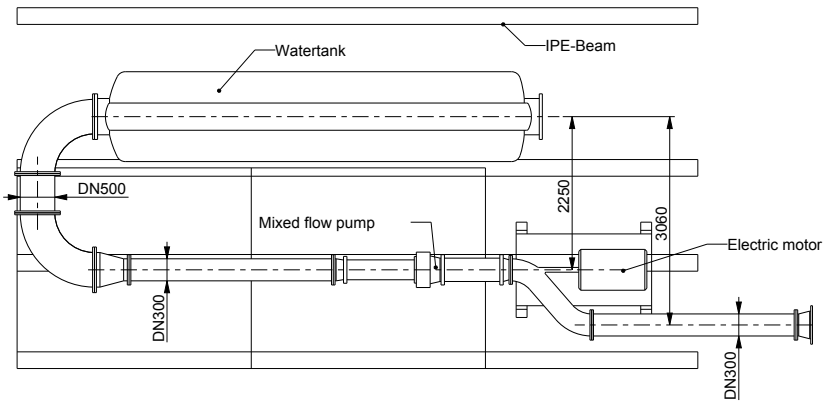

Figure 1.1: Arrangement of the test rig, plan view

1.4 Mode of action

Rotodynamic pumps are hydrodynamic fluid machines which increase the pressure level of a flow. The main parts of a pump are the impeller wheel, the casing and the bearing for the pump shaft. The energy from the electric motor is transferred to the flow from the shaft and the impeller wheel. The flow is accelerated in peripheral direction after which the static pressure is raised. To be able to use a large part of the remaining kinetic energy of the flow, in general, a diffuser is used to increase the pressure [3].

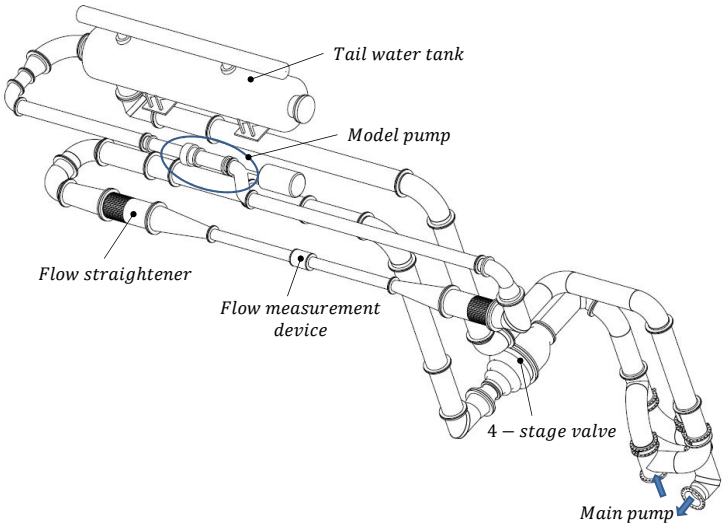

Figure 1.2: Arrangement of the test rig, 3D-view

The various fields of application of rotodynamic pumps range from small pumps for circulating pumps, used in heating systems, with some W drive power, up to pump turbines with more than 250 MW. This fact proves the high technical and economical meaning of pumps [3].
Pumps can be sub-divided according to different aspects depending on the delivery task and the field of application. One aspect is the direction of the flow at the impeller outlet. Thus, rotodynamic pumps can be divided into [3]:

- Radial flow pumps
- Mixed flow pumps
- Axial flow pumps

Other points of view to characterize pumps are listed in [3].

In order to be able to characterize the delivery task of a pump, the differential head, the discharge and the rotational speed are necessary. A relation between these parameters can be described by n_q, which is explained in chapter 2.2.1 in detail. By means of this value n_q, the shape of the meridional section and its impeller vanes can be approximated [3].
In general, a pump with a smaller n_q is used for a small discharge and a high differential head. The lower limit of n_q is approximately 8 (as of economical reasons $\Rightarrow$ the pump efficiency under n_q=20 decreases very fast). To enable a higher differential head, a second stage is used instead [3].
In contrast to a pump with a small n_q, a pump with a higher n_q is used for a higher discharge and a relatively low differential head. The upper limit of n_q is about 400. For a higher discharge, more pumps working in parallel are used [3].

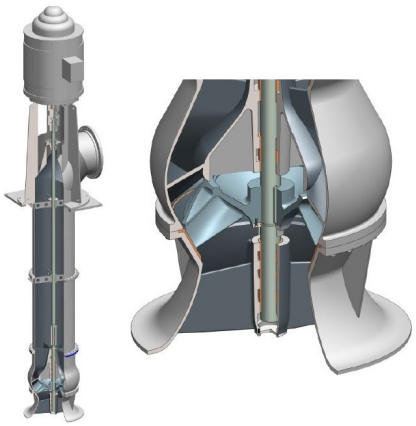

Figure 1.3: Sulzer mixed flow pump: SJM [20]

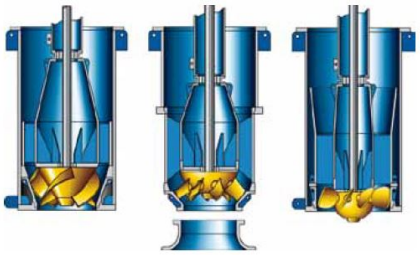

Figure 1.4: KSB mixed flow pumps: SEZ, PNZ, PHZ [6]

1.5 Area of application of mixed flow pumps

The outer diameter of the impeller wheel of a mixed flow pump compared to the spiral casing of a radial flow pump is considerably smaller. On this account, mixed flow pumps are often used as vertical pumps, where the diameter is limited because of economic reasons. The hydraulic optimal range can be given with a specific speed from n_q=50 up to n_q=170 [3].
These pumps are very often used in cooling water and circulating water pumping systems in power stations as well as in irrigation or drainage pumping systems. Some examples of mixed flow pumps can be seen in figures 1.3 and 1.4.

1.6 CFD calculation

For the design of the pump, the commercial program CFX and its authorized tools were used. For the impeller as well for the diffuser, different variants were generated. Based on their numerical results, a final version was chosen.
Figure 1.5 shows the results of the differential head and the pump efficiency, which are lined out for each of the impeller positions, calculated with the full model in stationary mode. The CFD calculations were carried out for the real prototype [2].

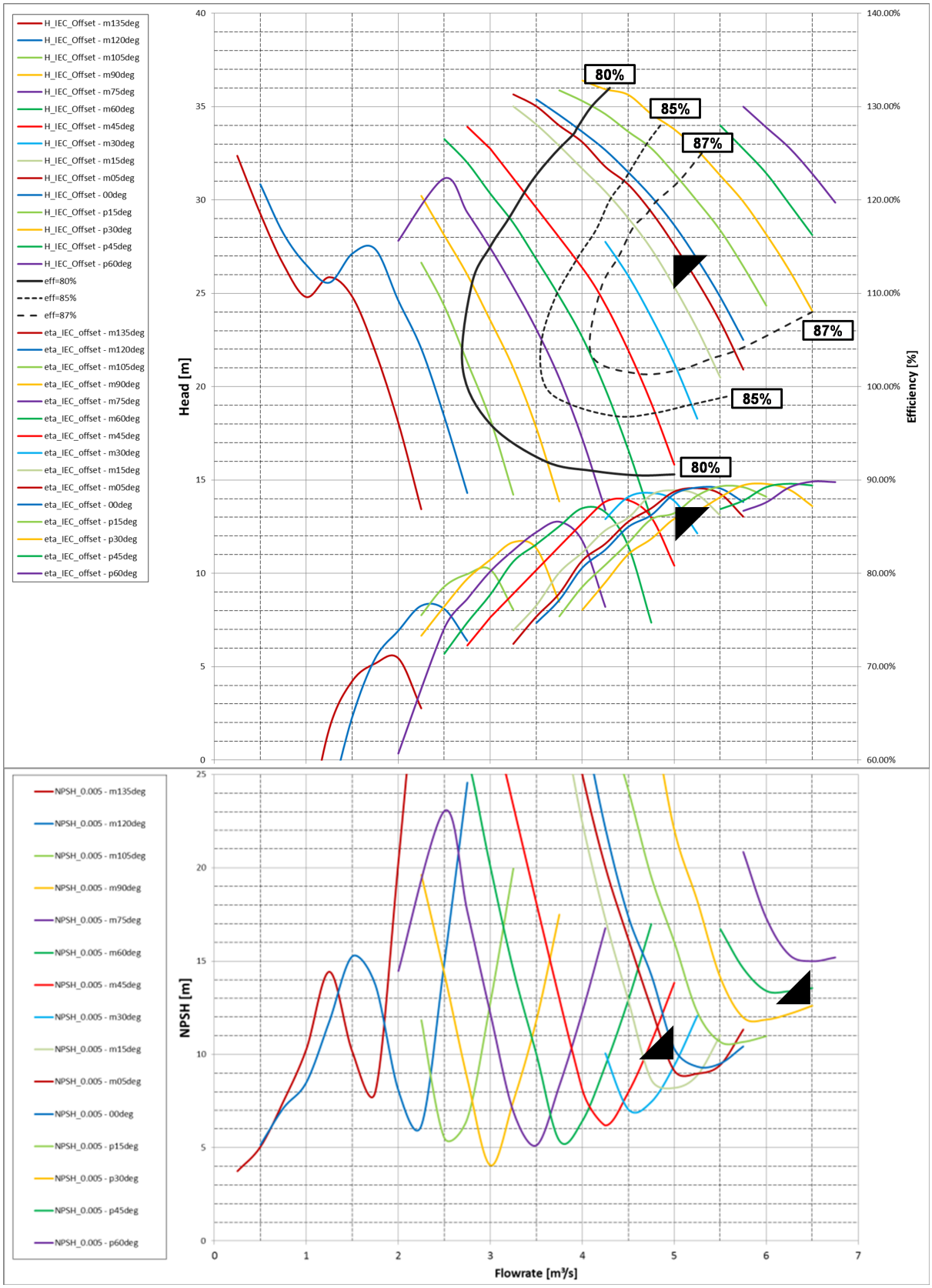

Figure 1.5: Results of the CFD calculation [2]

2 Theoretical foundations

2.1 Cavitation

Cavitation is the partial vaporization of a fluid in a system with a flowing medium and the following collapsing of the steam filled cavity. A cavity arises when the static pressure in a flow declines under the local saturated vapour of the fluid which is caused by the accelerated flow. This can be retraced by Bernoulli's equation (the geodetic height is not considered)[3]:

$$\left(\frac{u^2}{2}\right) + \left(\frac{p}{g}\right) = const. \tag{2.1}$$

The saturated vapour, which is shown for water in figure 2.1, depends strongly on the temperature of the fluid.

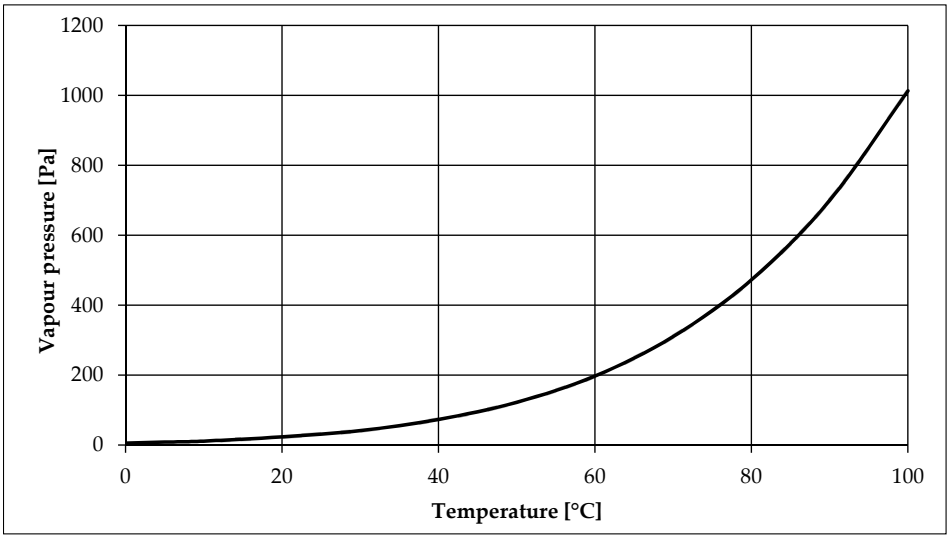

Figure 2.1: Vapour pressure curve [19]

The steam condensates abruptly like an implosion, when it is transported to a region with a higher static pressure than the saturated vapour. The higher static pressure is caused by the decelerated flow. The consequences of the cavitation are vibrations, noises and the decreasing of the efficiency and the differential head. Furthermore, the pump might even be destroyed by cavitation erosion [18].

2.1.1 Net positive suction head *NPSH*

For centrifugal pumps, the danger of cavitation depends on the local energy and the flow conditions inside the pump. The most susceptible area for cavitation is the inlet of the impeller. It is important to find a value which characterizes the operating behaviour at the inlet.
Such behaviour is specified by the „net positive suction head“ or *NPSH*. This value is corresponding to the energy (*NPSE*) which is needed to compensate the friction losses of the suction area and to accelerate the flow. The *NPSE* can be converted into the *NPSH* by dividing it by the acceleration of gravity g [18].
The *NPSH* is defined by the absolute energy head at the inlet minus the pressure head of the vaporisation as shown in equations 2.2 to 2.4 [3].

$$NPSH = H_s + \frac{p_{amb} - p_v}{\rho \cdot g} \tag{2.2}$$

With:

$$H_s = \frac{p_s}{\rho \cdot g} + z_s + \frac{c_s^2}{2 \cdot g} \tag{2.3}$$

the net positive suction head results in:

$$NPSH = \frac{p_s + p_{amb} - p_v}{\rho \cdot g} + z_s + \frac{c_s^2}{2 \cdot g} = \frac{p_{s,abs} - p_v}{\rho \cdot g} + z_s + \frac{c_s^2}{2 \cdot g} \tag{2.4}$$

H_s	m	Inlet total head
p_{amb}	Pa	Ambient pressure
p_s	Pa	Static pressure at the inlet
$p_{s,abs}$	Pa	Absolute pressure at the inlet
p_v	Pa	Vapour pressure
c_s	m/s	Velocity at the inlet
z_s	m	Level at the inlet referred to the reference level

If the reference level for the geodetic height and the horizontal axis of the pump shaft coincide. *NPSH* can be written as:

$$NPSH = \frac{p_{s,abs} - p_v}{\rho \cdot g} + \frac{c_s^2}{2 \cdot g} \tag{2.5}$$

According to the extent of the area of cavitation, the effect of cavitation can hardly be detected (first bubbles) up to the breakdown of the pump (total cavitation). This makes it necessary to introduce different criteria. When the minimal static pressure is equal to p_v, the first steam bubbles occur. The *NPSH* value corresponding to this situation is called $NPSH_{\mathrm{i}}$ and represents the minimal suction head needed to run the pump without cavitation [3].
If the pressure at the inlet is further reduced, the differential head will be influenced negatively. Consequently, there are different corresponding *NPSH*-values which dimension of cavitation is accepted [3]. Some of the most common criteria[1] are:

[1] All the criteria are tested at constant discharge and constant rotational speed.

- $NPSH_{\mathrm{i}}$: start of visual cavitation: first steam bubbles occur
- $NPSH_0$: start of decreasing differential head
- $NPSH_1$: differential head decreases by 1%
- $NPSH_3$: differential head decreases by 3%
- $NPSH_{\mathrm{x}}$: differential head decreases by x%

The determination of $NPSH_3$ is shown in figure 2.2. The required $NPSH$-value of the pump, $NPSHR$, indicates the suction head which is needed to meet the desired criteria of cavitation ($NPSH_{\mathrm{avail}} \geq NPSHR$).

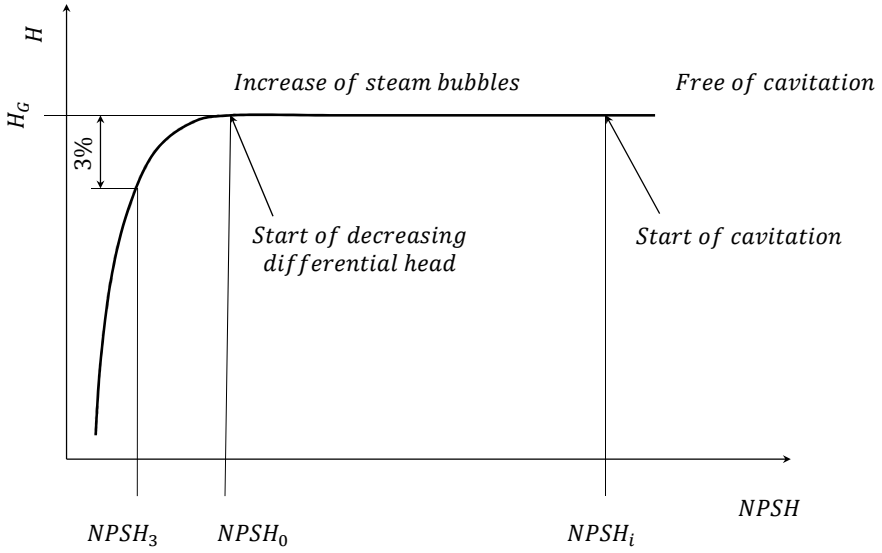

Figure 2.2: Decrease of the differential head [14]

2.1.2 Net suction specific speed NSS_3

The net suction specific speed is introduced in order to be able to compare the suction behavior of pumps which are not geometrically similar. NSS_3 is calculated for the pump performance at best efficiency point and is based on the $NPSH_3$. It can be written as [3]:[2]

$$NSS_3 = n \cdot \frac{\sqrt{Q}}{NPSH_3^{0.75}} \tag{2.6}$$

[2]In equation 2.6, the following units must be used: n in rpm, Q in $\mathrm{m}^3/\mathrm{min}$ and $NPSH_3$ in m.

2.2 Law of similitude and non-dimensional values

In practice, tests are very often carried out with the model and not with the prototype. In such cases, certain laws of similitude have to be considered in order to be able to convert the model results measured to the desired results of the prototype. Different non-dimensional values can be helpful to compare the model and the prototype.

2.2.1 Non-dimensional values

To be able to compare geometrically similar pumps to each other, non-dimensional values are needed. The most important ones are described in the following chapter. One of these values can be illustrated with the velocity triangle, where all velocities are based on the peripheral velocity (figure 2.3) [3].

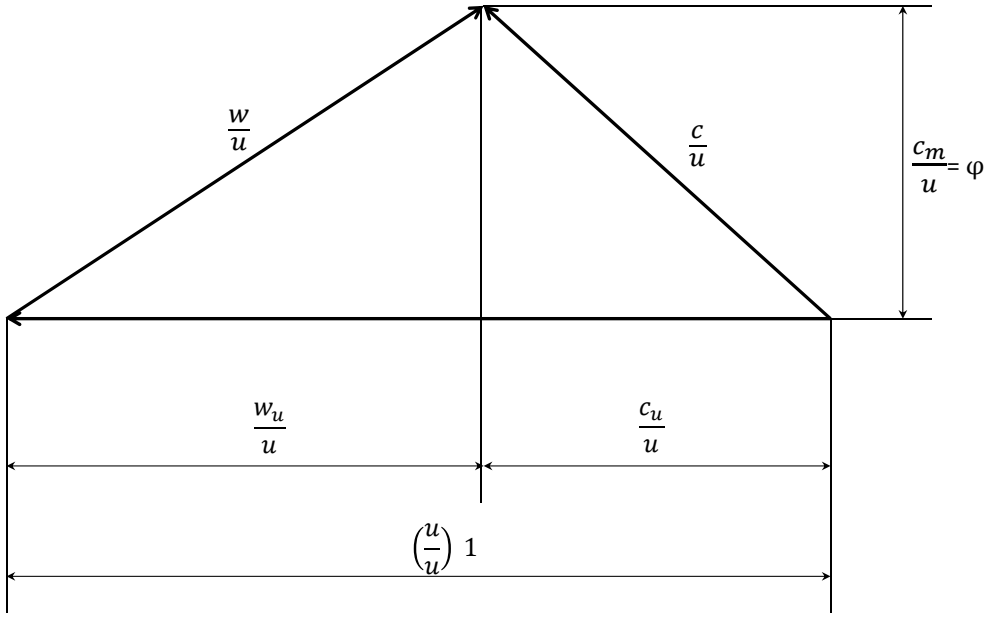

Figure 2.3: Velocity triangle [3]

u	m/s	Peripheral velocity
c	m/s	Absolute velocity
w	m/s	Relative velocity
c_m	m/s	The meridional component of the absolute velocity

This velocity triangle is non-dimensional. Due to the fact that the peripheral velocity depends on the diameter, a standard reference diameter D is needed (shown in figure 2.4) [3].

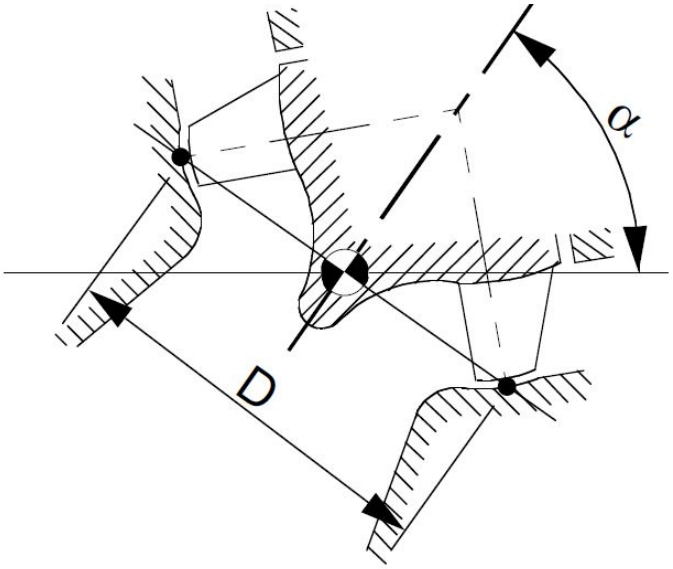

Figure 2.4: Reference diameter [17]

Flow coefficient φ

The flow coefficient is defined as the meridional component of the absolute velocity c_m divided by the peripheral velocity u. The velocity c_m is proportional to the discharge and inversely proportional to the sectional area.

$$\varphi = \frac{c_m}{u} = \frac{Q}{A \cdot u} = \frac{Q}{\frac{D^2\pi}{4} \cdot \frac{D\pi n}{60}} = \frac{Q}{D^3 n} \cdot \frac{240}{\pi^2} \tag{2.7}$$

Head coefficient ψ

The head coefficient is defined as the specific hydraulic energy of the machine divided by the velocity pressure.

$$\psi = \frac{Y}{\frac{u^2}{2}} = \frac{gH}{\frac{u^2}{2}} = \frac{2gH}{(\frac{D\pi n}{60})^2} = \frac{H}{D^2 n^2} \cdot \frac{7,200 \cdot g}{\pi^2} \tag{2.8}$$

Specific speed

To describe a hydraulic fluid machine, the specific speed is used beside the head- and flow-coefficient. The specific speed gives information about the shape of the pump.
If formulas 2.7 and 2.8 are transformed, the differential head and the discharge can be written as (whereas k_1 and k_2 are constants):

$$Q = \varphi \cdot D^3 \cdot n \cdot k_1 \tag{2.9}$$

$$H = \psi \cdot D^2 \cdot n^2 \cdot k_2. \tag{2.10}$$

If the differential head and the discharge of the dimensional condition are related to those of a „standard condition“ with Q_q=1 m^3/s and H_q=1 m, and the diameter is eliminated

by inserting H into Q, the formula for the specific speed can be found.[3]

$$n_q = n \cdot \frac{\sqrt{Q}}{H^{0.75}} \tag{2.11}$$

The definition of the specific speed in formula 2.11 has the dimension rpm and therefore it is dimensional. If the rotational speed is inserted in rad/s and the differential head is multiplied by the acceleration due to gravity g, the specific speed can be made non-dimensional and can be written as [3]:[4]

$$n_{\text{s dimless}} = n \cdot \frac{\sqrt{Q}}{(g \cdot H)^{0.75}} \tag{2.12}$$

Other common values for the specific speed can be received, if in formula 2.11 the discharge is inserted into m^3/min.

2.2.2 Hydraulic similitude

In order to ensure hydraulic similitude, two conditions should be theoretically met [17]:

- Geometrical similitude between the model and the prototype
- Identical ratios of the various forces acting between the fluid and the components of each machine

From the second condition it can be derived, that the velocity triangles of all comparable points of both machines have to be geometrically similar. Thus follows, that both machines have identical discharge, energy and cavitation coefficients at corresponding operation points [17].[5]

- Discharge coefficient: $(Q_{nD})_A = (Q_{nD})_B$
- Energy coefficient: $(E_{nD})_A = (E_{nD})_B$
- Cavitation coefficient: $(\sigma_{nD})_A = (\sigma_{nD})_B$

The discharge, the energy and the cavitation coefficient are expressed mathematically by the following equations [17]:

$$Q_{nD} = \frac{Q}{n \cdot D^3} \tag{2.13}$$

$$E_{nD} = \frac{Y}{n^2 \cdot D^2} \tag{2.14}$$

$$\sigma_{nD} = \frac{NPSE}{n^2 \cdot D^2} \tag{2.15}$$

[3] In equation 2.11, the following units must be used: n in rpm, Q in m^3/s and H in m.
[4] In equation 2.12, the following units must be used: n in rad/s, Q in m^3/s, H in m and g in m/s^2.
[5] A stands for the model and B for the prototype.

2.3 Principles of measurement analysis

Every measuring system has an uncertainty arising from random and systematic measurement errors.
The systematic measurement errors e_s partially result from the imperfect measuring system and the measuring method, influences like self-heating or wear of the measurement device and some others. Under the same conditions, a systematic error has the same sign and the same magnitude. The systematic error consists of a known systematic error and an unknown systematic error. The first one can be determined by a measuring system which is more exact but not by repeating the measurement more often. The second one cannot be determined and has to be handled like a random error. Very often a tolerance of a measuring device is denoted, which describes the systematic error [17].

The random errors e_r are deviations from the mean value with a normal distribution, which are caused by numerous small and independent influences. That means, that the measuring system delivers different readings although the input value of the quantity is the same. The repetition of the measurements at the same operating conditions makes it possible to specify the measurement uncertainty with statistical methods [17].

The measured value x consists of the two measurement errors e_r and e_s and the true value x_w.

$$x = x_w + e_r + e_s \tag{2.16}$$

2.3.1 Systematic measurement error

The systematic error e_s for a measured value is the deviation of the expectation value $\bar{x}$ from the true value x_w and can be written as:

$$e_s = \bar{x} - x_w \tag{2.17}$$

The known systematic error $e_{s,b}$ is balanced with the negative value of the correction K. The second part of the systematic error, the unknown systematic error $e_{s,u}$, is described with an uncertainty. In general, an upper limit b and a lower limit a are given to describe the systematic error. These limits are very often determined by experience [12].
The values for $e_{s,b}$ and $e_{s,u}$ are supposed to be rectangularly distributed and can be described with formulas 2.18 and 2.19 [12].

$$e_{s,b} = -K = \frac{a+b}{2} \tag{2.18}$$

$$e_{s,u} = \frac{b-a}{\sqrt{12}} \tag{2.19}$$

2.3.2 Random measurement error

If the influencing values are independent, evenly distributed and the number of single measurements is high enough (theoretical infinite), the measured values x_i will be normally distributed (Gaussian distribution) [7].

In the theoretical case of an infinite amount of single measurements and without a systematic error, the arithmetic mean value μ would be equal to the true value [11].

$$\mu = \lim_{N\to\infty} \frac{1}{N} \sum_{i=1}^{N} x_i \tag{2.20}$$

In reality, $\bar{x}$ is used to estimate the arithmetic mean value of all values measured [11].

$$\bar{x} = \frac{1}{N} \sum_{i=1}^{N} x_i \tag{2.21}$$

The standard deviation σ is a parameter to indicate the deviation of the single measurement values from the mean value μ [7].

$$\sigma = \sqrt{\lim_{N\to\infty} \frac{1}{N} \sum_{i=1}^{N} (x_i - \mu)^2} \tag{2.22}$$

If the amount of single measurements is endless, the experimental standard deviation s is used to estimate σ [11].

$$s = \sqrt{\frac{1}{N-1} \sum_{i=1}^{N} (x_i - \bar{x})^2} \tag{2.23}$$

The probability density $p(x)$ describes, how often deviations occur [7].

$$p(x) = \frac{1}{\sigma \cdot \sqrt{2\pi}} \cdot e^{-\frac{1}{2}\cdot(\frac{x-\mu}{\sigma})^2} \tag{2.24}$$

$$P = \int_{x_1}^{x_2} p(x)dx \tag{2.25}$$

In figure 2.5, the Gaussian distribution of the probability density is plotted. The area under the curve is equal to the probability P which is maximum one. The deviation of the limits x_1 and x_2 from the mean value are very often expressed by multiples of the standard deviation. These multiples, which depend on the probability and the number of single measurements, are called student factors t and are listed in tables [7].

The random error e_r of a single measurement value is, with a probability of P, within the interval $\pm\sigma \cdot t$.[6]

$$e_r = \pm\sigma \cdot t \tag{2.26}$$

e.g.: With a probability of 95.5%, the random error e_r is within the interval $\pm\sigma \cdot 2$ for a student factor of t=2.

To describe the random error in a practical case when only a finite amount of single measurements is determined, the uncertainty of the random error can be written as [7]:

$$e_r = \pm\frac{t \cdot s}{\sqrt{N}} \tag{2.27}$$

[6]For an indefinite amount of single measurements.

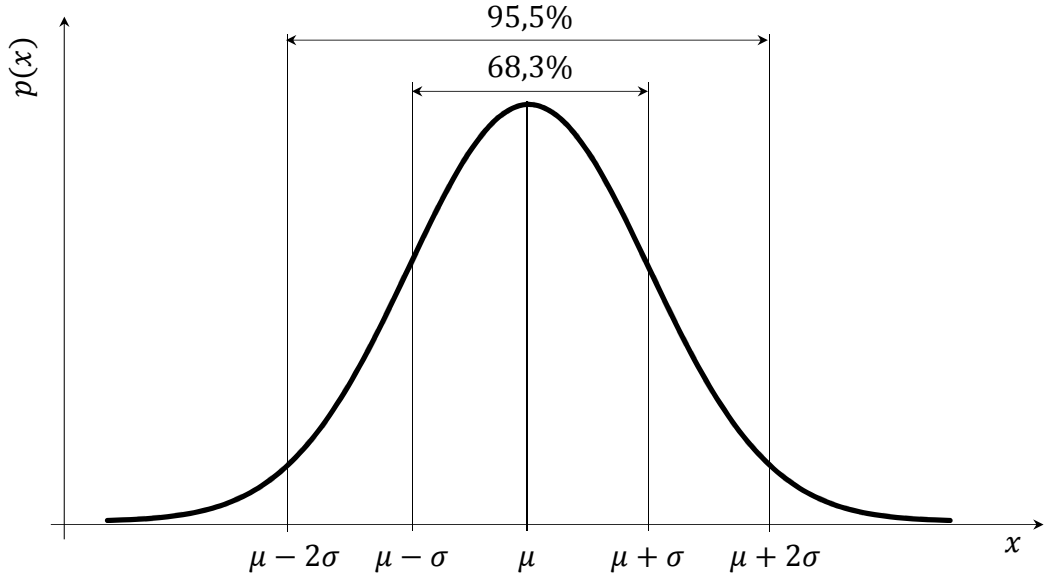

Figure 2.5: Gaussian distribution function [7]

2.3.3 Evaluation of the measurements

First of all, the function of a model that describes the value of the result of the measurement has to be formulated. This function can have the form of equation 2.28 where X_i represents the input quantities [12].

$$Y = f(X_1, ..., X_m) \tag{2.28}$$

The complete result can be calculated with the estimated value y for the true value of the measurand Y and the overall uncertainty e_y (see equation 2.34). In formula 2.29 the estimated values x_i are inserted in the function of the model. Equations 2.31 and 2.32 describe the transmission of the uncertainties [12].

$$y = f(x_i, ..., x_m) \tag{2.29}$$

$$x_i = \bar{x_i} - e_{x_i,s,b} \tag{2.30}$$

If the single systematic error $e_{x_i,s}$ is small in relation to the single measurement value ($|e_{x_i,s}| << |x_i|$), the systematic error $e_{y,s}$ can be calculated with formula 2.32 which is based on a first-order Taylor series approximation. The random error $e_{y,r}$ can be calculated with the Gaussian error propagation law [7].

$$e_{y,r} = \sqrt{\sum_{i=1}^{N} (\frac{\partial y}{\partial x_i} e_{x,r})^2} \tag{2.31}$$

$$e_{y,s} = \sum_{i=1}^{N} \left| \frac{\partial y}{\partial x_i} e_{x,s} \right| \tag{2.32}$$

The overall uncertainty of the measurand e_y can be calculated with the quadratic error propagation law. The complete result of the measurement is shown in formula 2.34 [12].

$$e_y = \sqrt{e_{y,r}^2 + e_{y,s}^2} \tag{2.33}$$

$$Y = y \pm e_y \tag{2.34}$$

2.4 Hydraulic acceptance test for centrifugal pumps

2.4.1 Application area

The test carried out within this project is based on the standard EN IS0 9906. This is a standard for every centrifugal pump which operates with pure cold water. The characteristics of pure cold water are shown in table 2.1 [14].

Table 2.1: Characteristics of pure cold water [15]

Characteristics	Unit	Max. value
Temperature	°C	40
Kinematic viscosity	m^2/s	$1.75 \cdot 10^{-6}$
Density	kg/m^3	1,050
Rate of undissolved free solids	kg/m^3	2.5
Rate of solute solids	kg/m^3	50

The following test conditions should be complied with as well as possible [14]:

- Axially directed symmetrical velocity distribution
- Constant distribution of the static pressure
- No turbulences caused by the arrangement of the test rig

2.4.2 Guarantees

A guaranteed point is defined by a guaranteed discharge (Q_G) and a guaranteed differential head (H_G). Under the agreed conditions and at the agreed rotational speed, the measured $H(Q)$-line including the uncertainty of measurement has to intersect a tolerance area which encloses the guaranteed point [13].
To get the operating behavior of the prototype, the results of the measurements have to be converted into the agreed rotational speed. Then, they are plotted in dependency of the discharge. The curve which fits best with the measured points shows the operating behaviour of the pump [14].

The conversion to the agreed rotational speed is made according to [14].

$$Q_T = Q \cdot \frac{n_{sp}}{n} \tag{2.35}$$

$$H_T = H \cdot \left(\frac{n_{sp}}{n}\right)^2 \tag{2.36}$$

$$P_T = P \cdot \left(\frac{n_{sp}}{n}\right)^3 \cdot \frac{\rho_{sp}}{\rho} \tag{2.37}$$

$$\eta_T = \eta \tag{2.38}$$

$$NPSHR_T = NPSHR \cdot \left(\frac{n_{sp}}{n}\right)^x \tag{2.39}$$

X_T		Converted value
n_{sp}	rpm	Agreed rotational speed
x		Coefficient depends on different effects ⇒ see [14]

The International Standard EN ISO 9906 specifies three levels of acceptance:

- Grades 1B, 1E and 1U with tighter tolerance
- Grades 2B and 2U with broader tolerance
- Grade 3B with even broader tolerance

Table 2.2: Pump test acceptance grades and corresponding tolerance - EN ISO 9906 [14]

Grade	**1**			**2**		**3**
$\Delta\tau_Q$	10 %			16 %		18 %
$\Delta\tau_H$	6 %			10 %		14 %
Acceptance grade	**1U**	**1E**	**1B**	**2B**	**2U**	**3B**
τ_Q	+10 %	±5%		±8 %	+16 %	±9 %
τ_H	+6 %	±3 %		±5 %	+10 %	±7 %
τ_P	+10 %	±4 %		±8 %	+16 %	±9 %
τ_η	≥ 0 %		-3 %	-5 %		-7 %

Table 2.3 shows a comparison of EN ISO 9906 and EN ISO 13709 (API standard). These values are valid at the nominal rotational speed and the nominal discharge. The test rotational speed should be within 3% of the nominal speed and the rated discharge within 5% of the rated flow [16].

Table 2.3: Performance tolerances - EN ISO 13709 [16]

Value	Rated point [%]
Rated differential head	$-2 + 5$
Rated power	+4
Rated NPSH	0

With the tolerance factors, which are shown in table 2.2, a cross is formed. The center of this cross is located at the guaranteed point (see figure 2.6). If the measured $H(Q)$-curve intersects or tangents the cross, the guarantee for the differential head is complied [14]. A vertical line is drafted where a line between the origin and the guaranteed point intersects the $H(Q)$-curve. The guarantee of the pump efficiency is complied when the value

of the point where the vertical line crosses the pump-efficiency-curve is higher or at least equal to $\eta_U = \eta_G \cdot (1 - |\tau_\eta|)$ [14].
The guarantee of the *NPSH* is complied, when the measured $NPSH_3$ is lower than $NPSH_{3,G}$ [14].

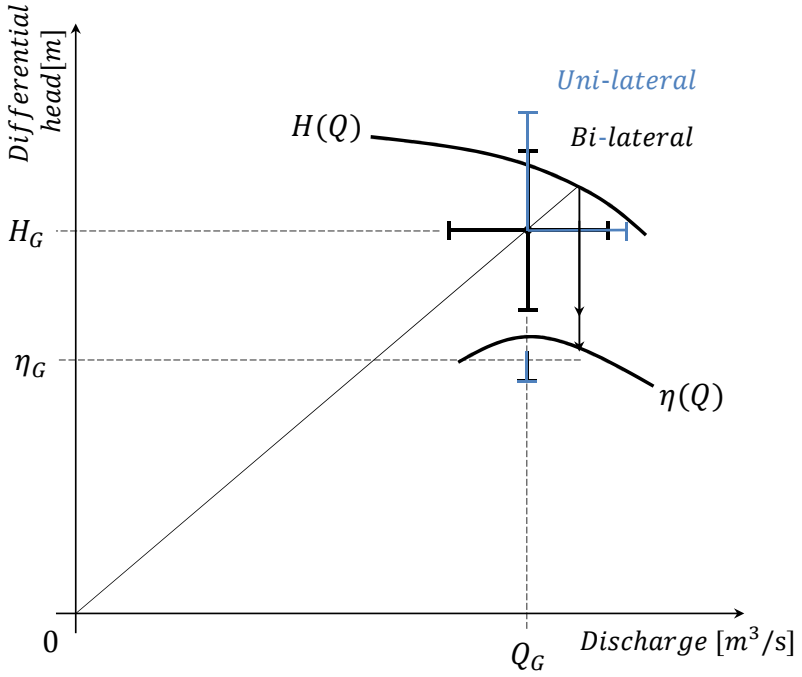

Figure 2.6: Implementation of the guaranteed differential head and pump efficiency [14]

2.4.3 Determination of the guaranteed values

Discharge

The discharge is the volume of water per unit time which is passing through any section in the arrangement of the pump. The volume flow rate is measured by an inductive flow meter (see chapter 5.1.1).

Differential head

The differential head is expressed by the discharged liquid column and corresponds to the energy which is transferred by the pump related to the discharged mass force. In the case, that the density of the water does not change, the differential head can be written as [14]:

$$H = H_2 - H_1 \tag{2.40}$$

H_1 Total head at the inlet
H_2 Total head at the outlet

The differential head can be calculated from the height of the reference levels, the pressure head and the kinetic head as shown in equation 2.41 [14].

$$H = z_2 - z_1 + \frac{p_2 - p_1}{\rho \cdot g} + \frac{U_2^2 - U_1^2}{2 \cdot g} \tag{2.41}$$

The guaranteed values refer to the inlet and outlet flanges. Due to the fact, that the pressure measurement cannot be located at the flanges directly, as the flow would be too turbulent, friction losses within the pipe should be considered [14][13].

$$H = z_2' - z_1' + \frac{p_2' - p_1'}{\rho \cdot g} + \frac{U_2'^2 - U_1'^2}{2 \cdot g} + H_{J2} + H_{J1} \tag{2.42}$$

X_1	Value at the inlet
X_1'	Value at the inlet measuring section
X_2	Value at the outlet
X_2'	Value at the outlet measuring section

In figure 2.7, the reference levels are shown.

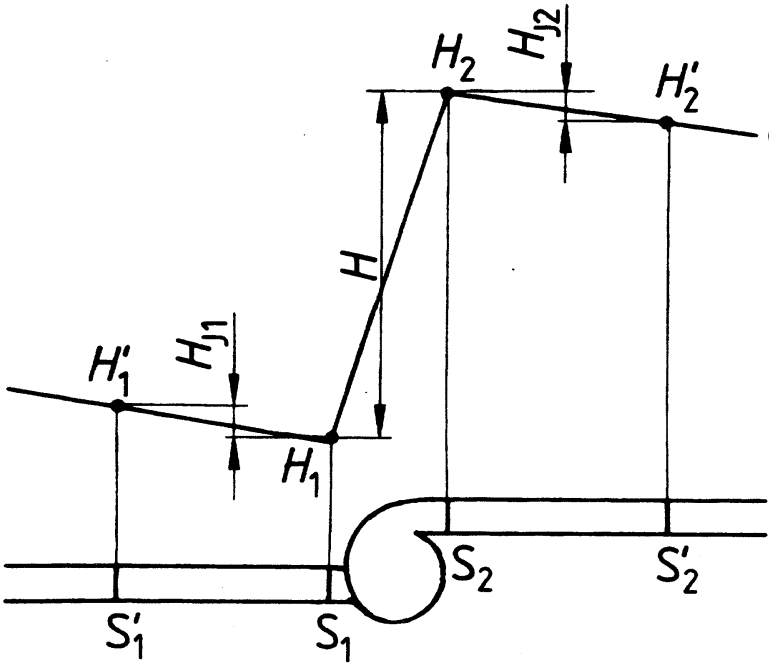

Figure 2.7: Determination of the differential head [13]

If the pipe between the measurement point and the pump is straight, with a constant diameter and without any barriers, the friction losses can be written as [13]:

$$H_J = \lambda \cdot \frac{L}{D} \cdot \frac{U^2}{2 \cdot g} \tag{2.43}$$

Whether the friction losses of the straight pipe have to be considered, can be looked up in the EN ISO 9906 norm. In case of a turbulent flow, λ can be calculated using one of

the following equations [13]:

for $Re < 23\frac{D}{k}$ (smooth pipe)

$$\frac{1}{\sqrt{\lambda}} = -2 \cdot log_{10} \frac{2.51}{Re \cdot \sqrt{\lambda}} \tag{2.44}$$

for $23\frac{D}{k} < Re < 560\frac{D}{k}$ (transient zone)

$$\frac{1}{\sqrt{\lambda}} = -2 \cdot log_{10} (\frac{2.51}{Re \cdot \sqrt{\lambda}} + \frac{k}{3.7 \cdot D}) \tag{2.45}$$

for $Re > 560\frac{D}{k}$ (rough pipe)

$$\frac{1}{\sqrt{\lambda}} = -2 \cdot log_{10} \frac{k}{3.7 \cdot D} \tag{2.46}$$

The velocity U is expressed mathematically by the following equation:

$$U = \frac{Q}{A} \tag{2.47}$$

H_J	m	Frictional loss
L	mm	Length of the pipe
D	mm	Diameter of the pipe
Re		Reynolds number
k	mm	Pipe equivalent uniform roughness (see EN ISO 9906)
λ		Coefficient of friction in a pipe

Measuring the pressure
The distance between the positions of the pressure measurement and the pump should be as small as possible but at least two times the diameter of the pipe. The measuring section has to be located within a straight pipe which is coaxial to the pump. Four drilling holes are evenly spaced around the circumference in order to be able to get an average pressure. The vertical height between the gauge and the middle of the measuring section should also be considered [14].
The pressure is measured by a pressure transmitter, which is described in chapter 5.1.2 in detail.

Measuring the density
After the temperature has been measured, the density can be looked up in a table [19].

Pump efficiency

The pump efficiency is equal to the hydraulic power divided by the mechanical power.

$$\eta = \frac{P_H}{P_M} = \eta_h \cdot \eta_{mech} \tag{2.48}$$

η_h	Hydraulic efficiency
η_{mech}	Mechanical efficiency ⇒ friction losses of sealing and bearing

The hydraulic power P_H can be written as:

$$P_H = \rho \cdot Q \cdot g \cdot H \tag{2.49}$$

The mechanical power P_M can be written as:

$$P_M = \frac{2 \cdot \pi \cdot n \cdot M}{60} \tag{2.50}$$

Measuring the rotational speed n
The rotational speed is measured by a torque measuring flange (see chapter 5.1.3).

Measuring the torque M
The torque of the electric motor is measured by a torque measuring flange (see chapter 5.1.3).

Cavitation

The standard EN ISO 9906 only deals with the hydraulic operation behavior like differences in the pump efficiency or the differential head and not with others like noises, vibrations or material damages.
In this test, the *NPSH* is reduced till the declining of the differential head at constant discharge and rotational speed is 3%. This *NPSH*-value is equal to the $NPSH_3$.

2.4.4 Measurement of the variables

To achieve meaningful values, the measurements have to be determined during constant operation conditions. If there are great amplitudes of fluctuation, they should be reduced by a damping device. The tolerated amplitude of fluctuation is shown in table 2.4 [14].

Table 2.4: Permissible amplitude of fluctuation as a percentage of the mean value for the quantity being measured [14]

Measured quantity	Grade 1 [%]	Grade 2 [%]	Grade 3 [%]
Discharge	±2	±3	±6
Differential head	±3	±4	±10
Outlet head	±2	±3	±6
Inlet head	±2	±3	±6
Inlet power	±2	±3	±6
Rotational speed	±0,5	±1	±2
Torque	±2	±3	±6
Temperature	0.3 °C	0.3 °C	0.3 °C

The mean value of a physical variable $x(t)$ over a time period T is expressed by equation 2.51 (analogue to equation 2.20) [13].

$$\mu_x = \frac{1}{T} \cdot \int_t^{t+T} x(t)dt \tag{2.51}$$

The length of the time period for determining the variables has to be considerably longer than the response time of the measuring instrument.

Uncertainty

In standard EN ISO 9906 the random measurement error is supposed to be two times the standard deviation s (see chapter 2.3.2). That means that the level of confidence is about 95%.

$$e_r = 2 \cdot s \tag{2.52}$$

The permitted values of the systematic measurement error are shown in table 2.5. The way, how the systematic error is determined, is shown in chapter 2.3.1 on page 12.

Table 2.5: Permissible values of the systematic measurement error [14]

Quantity	Grade 1	Grade 2,3
Discharge	±1.5%	±2.5%
Rotational speed	±0.35%	±1.4%
Torque	±0.9%	±2.0%
Differential head	±1.0%	±2.5%
Outlet head	±1.0%	±2.5%
Inlet head	±1.0%	±2.5%
Suction head for NPSH testing	±0.5%	±1%
Drive power input	±1.0%	±2.0%

The overall uncertainty e_y can be calculated with 2.33, and the permitted values of the overall uncertainty are listed in table 2.6. Regardless of the procedure to determine the uncertainty, which is described in chapter 2.3, the uncertainty of the differential head and the pump efficiency have to be calculated with formulas 2.53 and 2.54 according to EN ISO 9906.

$$e_H = \sum_{i=1}^{K} e_{x_i} \tag{2.53}$$

$$e_\eta = \sqrt{e_Q^2 + e_H^2 + e_T^2 + e_n^2} \tag{2.54}$$

Table 2.6: Permissible values of overall uncertainties [14]

Quantity	Symbol	Grade 1	Grade 2,3
Discharge	e_Q	±2.0%	±3.5%
Rotational speed	e_n	±0.5%	±2.0%
Torque	e_T	±1.4%	±3.0%
Differential head	e_H	±1.5%	±3.5%
Pump power input	e_P	±1.5%	±3.5%
Pump efficiency	e_η	±2.9%	±6.1%

3 Calculation

The present chapter describes the dimensioning of the single parts. It should be mentioned, that the forces which are calculated in chapter 3.1 are the maximum forces. Although these maximum forces cannot occur at the same time, they are used for the calculations in order to be on the safe side.

3.1 Calculation of forces appearing

In the following chapter, the main forces and torques which are needed to design the single parts of the pump model are calculated.

3.1.1 Axial thrust assessment

The assessment of the axial thrust is calculated according to [3]. At this point it should be mentioned that the shut-off head is inserted in equation 3.1 to get the maximum axial thrust.

$$F_{axial} = \rho \cdot g \cdot H \cdot f_{ha} \cdot \frac{\pi}{4} \left(d_1^2 - d_D^2 \right). \tag{3.1}$$

H	m	Differential head
ρ	kg/m^3	Density
d_1	m	Inlet diameter
d_D	m	Sealing diameter
n_q		Specific speed

With

$$\begin{aligned} f_{ha} &= \left(\frac{200}{n_q} \right)^{0.28} \\ &= \left(\frac{200}{95.713} \right)^{0.28} = 1.23 \end{aligned} \tag{3.2}$$

equation 3.1 leads to

$$\begin{aligned} F_{axial} &= 1,000\,\mathrm{kg/m^3} \cdot 9.81\,\mathrm{m/s^2} \cdot 33\,\mathrm{m} \cdot 1.23 \cdot \frac{\pi}{4} \left((0.285\,\mathrm{m})^2 - (0.07\,\mathrm{m})^2 \right) \\ &= 23,854\,\mathrm{N}. \end{aligned} \tag{3.3}$$

3.1.2 Torque

The torque can be calculated according to [8]. The maximum occurring torque T_{eq} can be calculated with formula 3.4. The application factor from [9] is for moderate impacts

of the driven machine and for regular impacts of the engine.

$$T_{eq} = K_A \cdot \frac{P}{2\pi n} = 1.25 \cdot \frac{90,000\,\mathrm{W}}{2 \cdot \pi \cdot \frac{1{,}600\,\mathrm{rpm}}{60}} \\ = 671.4\,\mathrm{Nm} \tag{3.4}$$

P	W	Input power
n	rpm	Rotational speed
K_A		Application factor

3.1.3 Radial forces

The radial forces caused by the flow are expected to offset each other, and the imbalance of the pump shaft is held to a minimum by balancing. To be on the safe side, a remaining radial force from the imbalance of F_R=2,000N is supposed. Another reason for radial forces is the weight of the single parts, which should be disregarded for convenience reasons.

3.2 Bearing

3.2.1 Reaction forces

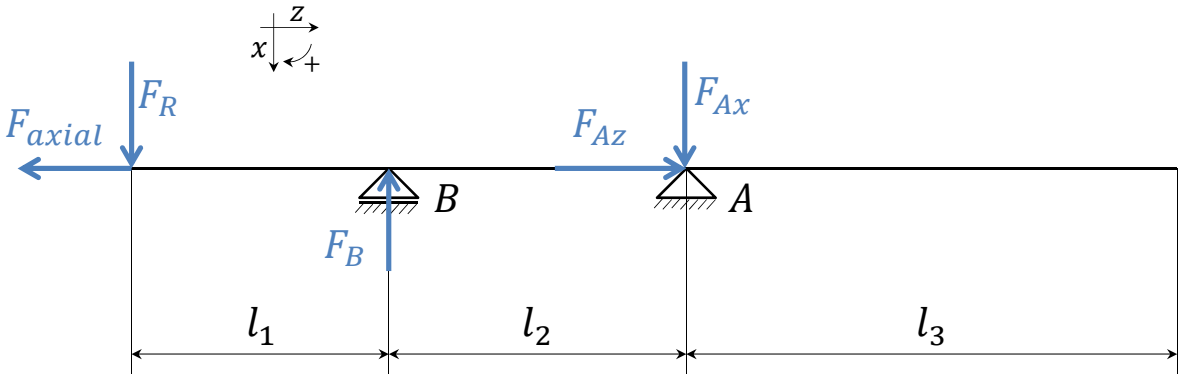

Figure 3.1: Reaction forces

In figure 3.1 the reaction forces are shown. From the 3-D model, the distances between the bearings and the force application point can be determined:

$$l_1 = 120\,\mathrm{mm} \qquad l_2 = 130\,\mathrm{mm} \qquad l_3 = 784\,\mathrm{mm}.$$

$$\sum M_A = 0: \qquad 0 = -F_R \cdot (l_1 + l_2) + F_B \cdot l_2 \tag{3.5}$$

$$\Rightarrow F_B = F_R \cdot \frac{(l_1 + l_2)}{l_2} = 2,000\,\mathrm{N} \cdot \frac{120\,\mathrm{mm} + 130\,\mathrm{mm}}{130\,\mathrm{mm}} \\ = 3,846\,\mathrm{N} \tag{3.6}$$

$$\sum F_x = 0: \qquad 0 = F_R - F_B + F_{Ax} \tag{3.7}$$

$$\Rightarrow F_{Ax} = F_B - F_R = 3,846\,\mathrm{N} - 2,000\,\mathrm{N} = 1,846\,\mathrm{N} \tag{3.8}$$

$$\sum F_z = 0: \qquad 0 = -F_{axial} + F_{Az} \tag{3.9}$$

$$\Rightarrow F_{Az} = F_{axial} = 23,854\,\mathrm{N} \tag{3.10}$$

3.2.2 Load carrying capacity

The static load carrying capacity is not calculated, because the forces which act on the pump at static conditions are insignificant.
The dynamic load carrying capacity of the bearings can be calculated according to [10]. Due to the fact, that the periods and rotational speeds of the different testing points are not ascertainable before, the maximum forces are used. The values of the parameters which are used to calculate the load carrying capacity are shown in table 3.1.

Table 3.1: Parameters for the calculation of the load carrying capacity [10]

Angular ball bearing	2x7213 BECBJ - DB
Boundary dimension	65 mm x 120 mm x 23 mm (dxDxB)
Dynamic load rating C_{r_A}	67 kN
Static load rating C_{0r_A}	50 kN
Deep groove ball bearing	6012-2RSR
Boundary dimension	60 mm x 95 mm x 18 mm (dxDxB)
Dynamic load rating C_{r_B}	29,4 kN
Static load rating C_{0r_B}	23,2 kN

Bearing A is designed as a fixed bearing. Therefore, two single row angular ball bearings in universal design, which are arranged back to back, are used. For bearing pairs mounted side by side, the dynamic load rating can be calculated with formula 3.12. If the ratio of the axial force to the radial force is higher than 1.14, the equivalent dynamic bearing load P_A can be calculated with:

$$P_A = 0.57 \cdot F_r + 0.93 \cdot F_a = 0.57 \cdot F_{Ax} + 0.93 \cdot F_{Az} = 0.57 \cdot 1,846\,\mathrm{N} + 0.93 \cdot 23,854\,\mathrm{N} = 23,236\,\mathrm{N} \tag{3.11}$$

$$C_{rpair_A} = C_{r_A} \cdot 1.62 = 67\,\mathrm{kN} \cdot 1.62 = 108.5\,\mathrm{kN} \tag{3.12}$$

F_r	N	Radial force
F_a	N	Axial force
P_A	N	Equivalent dynamic bearing load
p		Load-life exponent

With formula 3.13, the nominal life expectancy of bearing A for a default probability of 10 % can be calculated.

$$\begin{aligned} L_{h_A} &= \frac{16,666}{n} \cdot \left(\frac{C_{rpair_A}}{P_A}\right)^p = \frac{16,666}{1,600\,\text{rpm}} \cdot \left(\frac{108,500\,\text{N}}{23,236\,\text{N}}\right)^3 \\ &= 1,060\,\text{h} \end{aligned} \tag{3.13}$$

For the bearing B, a deep groove ball bearing is used. This bearing is designed as a floating bearing and is not able to absorb axial forces. This leads to an equivalent dynamic bearing load of:

$$\begin{aligned} P_B &= F_r = F_B \\ &= 3,846\,\text{N} \end{aligned} \tag{3.14}$$

With formula 3.15, the nominal life expectancy for a default probability of 10 % of bearing B can be calculated.

$$\begin{aligned} L_{h_B} &= \frac{16,666}{n} \cdot \left(\frac{C_{r_B}}{P_B}\right)^p = \frac{16,666}{1,600\,\text{rpm}} \cdot \left(\frac{29,400\,\text{N}}{3,846\,\text{N}}\right)^3 \\ &= 4,653\,\text{h} \end{aligned} \tag{3.15}$$

3.3 Pump shaft

To be able to estimate the minimal diameter of the solid pump shaft, formula 3.16 is used according to [8]. A pure torsional strain is expected, because the forces caused by weight are disregarded. The permitted torsional stress of the pump shaft, which is made out of steel (42CrMo4), is calculated with a minimum safety factor of 5.

$$\begin{aligned} d &\geq \sqrt[3]{\frac{16 \cdot T_{eq}}{\pi \cdot \frac{\tau_{\text{tW N}}}{5}}} \\ &\geq \sqrt[3]{\frac{16 \cdot 671.4 \cdot 10^3\,\text{Nmm}}{\pi \cdot \frac{330\,\text{N/mm}^2}{5}}} \\ &\geq 37.3\,\text{mm} \end{aligned} \tag{3.16}$$

3.3.1 Deflection of the shaft

To calculate the deflection of the pump shaft, a simplified model of the shaft is needed (see figure 3.2). Therefore, the shaft is divided into three parts with piecewise constant diameters. The area moment of inertia I_y for a circle is shown in formula 3.17.

$$I_y = \frac{d^4 \cdot \pi}{64} \tag{3.17}$$

$$I_{y_I} = \frac{d_I^4 \cdot \pi}{64} = \frac{(52\,\text{mm})^4 \cdot \pi}{64} = 3.59 \cdot 10^5\,\text{mm}^4 \tag{3.18}$$

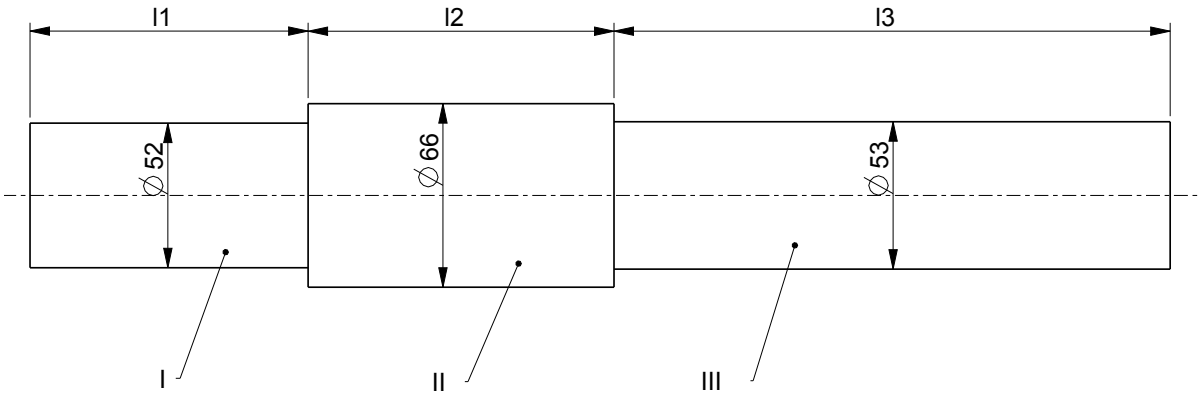

Figure 3.2: Simplified model for the deflection

$$I_{y_{II}} = \frac{d_{II}^4 \cdot \pi}{64} = \frac{(66\,\mathrm{mm})^4 \cdot \pi}{64} = 9.31 \cdot 10^5\,\mathrm{mm}^4 \tag{3.19}$$

$$I_{y_{III}} = \frac{d_{III}^4 \cdot \pi}{64} = \frac{(53\,\mathrm{mm})^4 \cdot \pi}{64} = 3.87 \cdot 10^5\,\mathrm{mm}^4 \tag{3.20}$$

To be able to calculate the whole deflection, the principle of superposition is used. Therefore, four different loading cases are distinguished:

- Dead load of the pump shaft
- Dead load of the impeller wheel
- Dead load of the coupling
- Radial force

Derivation of the bending stress equation for point loads

The dead load of the coupling and the impeller wheel are approached by point loads (F_R), which act at the end of the shaft. For domain I: $0 < z_I < l_1$, which is shown in figure 3.3, the second order differential equation for the deflection of the neutral axis for small deflections can be written as:

$$w_I'' \cdot E \cdot I_{y_I} = -M_{z_I} = F_R \cdot z_I \tag{3.21}$$

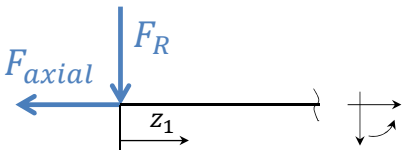

Figure 3.3: Domain I for point loads

By integration of formula 3.21, the slope of the deflected neutral axis w' can be found as a function of z_I. Another integration leads to the displacement of the neutral axis which is actually in demand.

$$w'_I E I_{y_I} = F_R \cdot \frac{z_I^2}{2} + C_1 \tag{3.22}$$

$$w_I E I_{y_I} = F_R \cdot \frac{z_I^3}{6} + C_1 \cdot z_I + C_2 \tag{3.23}$$

For domain II: $0 \leq z_{II} \leq l_2$ (see figure 3.4), the procedure is analog to domain I.

$$w''_{II} E I_{y_{II}} = -M_{z_{II}} = F_R \cdot (l_1 + z_{II}) - F_B \cdot z_{II} = F_R \cdot l_1 + (F_R - F_B) \cdot z_{II} \tag{3.24}$$

$$w'_{II} E I_{y_{II}} = F_R \cdot l_1 \cdot z_{II} + (F_R - F_B) \cdot \frac{z_{II}^2}{2} + C_3 \tag{3.25}$$

$$w_{II} E I_{y_{II}} = F_R \cdot l_1 \cdot \frac{z_{II}^2}{2} + (F_R - F_B) \cdot \frac{z_{II}^3}{6} + C_3 \cdot z_{II} + C_4 \tag{3.26}$$

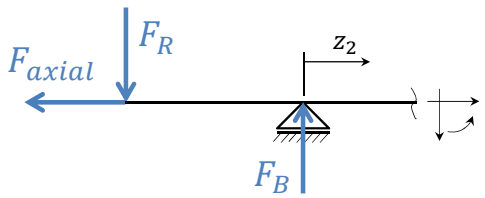

Figure 3.4: Domain II for point loads

Now the constants of integration C_i have to be evaluated by using boundary conditions. The following conditions are used:

- Because of bearing B: $w_{II}\,(z_{II} = 0) = 0$
- Because of bearing B: $w_I\,(z_I = l_1) = 0$
- Because of bearing A: $w_{II}\,(z_{II} = l_2) = 0$
- Because of the transition condition: $w'_I\,(z_I = l_1) = w'_{II}\,(z_{II} = 0)$

$w_{II}\,(z_{II} = 0) = 0$ leads to:

$$0 = C_4 \tag{3.27}$$

$w_{II}\,(z_{II} = l_2) = 0$ leads to:

$$0 = F_R \cdot l_1 \cdot \frac{l_2^2}{2} + (F_R - F_B) \cdot \frac{l_2^3}{6} + C_3 \cdot l_2 \tag{3.28}$$

$$\Rightarrow C_3 = -F_R \cdot l_1 \cdot \frac{l_2}{2} - (F_R - F_B) \cdot \frac{l_2^2}{6} \tag{3.29}$$

If the constants C_3 and C_4 are put into equation 3.26, the displacement can be written as:

$$w_{II} = \frac{1}{EI_{y_{II}}} \cdot \left\{ F_R \cdot \frac{l_1}{2} \cdot \left(z_{II}^2 - z_{II} \cdot l_2 \right) + (F_R - F_B) \cdot \frac{1}{6} \cdot \left(z_{II}^3 - z_{II} \cdot l_2^2 \right) \right\} \tag{3.30}$$

With formula 3.6 the difference between F_R and F_B can be expressed by:

$$F_R - F_B = -F_R \cdot \frac{l_1}{l_2} \tag{3.31}$$

Finally the displacement of the second domain can be written as:

$$w_{II} = \frac{F_R \cdot l_1}{6EI_{y_{II}}} \cdot \left\{ -\frac{z_{II}^3}{l_2} + 3z_{II}^2 - 2z_{II} \cdot l_2 \right\} \tag{3.32}$$

$w_I'(z_I = l_1) = w_{II}'(z_{II} = 0)$ leads to:

$$\frac{1}{EI_{y_I}} \cdot \left(F_R \cdot \frac{l_1^2}{2} + C_1 \right) = \frac{1}{EI_{y_{II}}} \cdot C_3 \tag{3.33}$$

$$\Rightarrow C_1 = -F_R \cdot \frac{I_{y_I}}{I_{y_{II}}} \cdot \frac{l_1 \cdot l_2}{3} - F_R \cdot \frac{l_1^2}{2} \tag{3.34}$$

$w_I(z_I = l_1) = 0$ leads to:

$$0 = F_R \cdot \frac{l_1^3}{6} + C_1 \cdot l_1 + C_2 \tag{3.35}$$

$$\begin{aligned} \Rightarrow C_2 = & -F_R \cdot \frac{l_1^3}{6} - C_1 \cdot l_1 \\ = & F_R \cdot \frac{I_{y_I}}{I_{y_{II}}} \cdot \frac{l_1^2 \cdot l_2}{3} + F_R \cdot \frac{l_1^3}{3} \end{aligned} \tag{3.36}$$

If the constants C_1 and C_2 are put into equation 3.23, the displacement can be written as:

$$w_I = \frac{F_R}{EI_{y_I}} \cdot \left\{ \frac{z_I^3}{6} - \frac{I_{y_I}}{3I_{y_{II}}} \cdot \left(l_1 \cdot l_2 \cdot z_I - l_1^2 \cdot l_2 \right) - \frac{l_1^2 \cdot z_I}{2} + \frac{l_1^3}{3} \right\} \tag{3.37}$$

Derivation of the bending stress equation for line loads

The dead load of the pump shaft is approximated by a line load (see figure 3.5). To express the line load, the specific weight quotients a_i are necessary.

$$\begin{aligned} m &= m_1 + m_2 + m_3 \\ &= a_1 \cdot m + a_2 \cdot m + a_3 \cdot m \end{aligned} \tag{3.38}$$

$$m_1 = \rho \cdot \frac{\pi}{4} \cdot d_1^2 \cdot l_1 \tag{3.39}$$

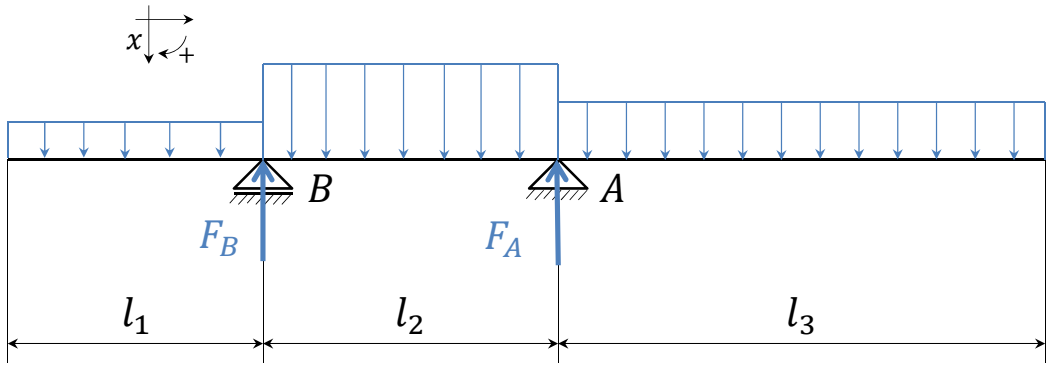

Figure 3.5: Line load of the shaft

$$\Rightarrow a_1 = \frac{m_1}{m} = \frac{d_1^2 \cdot l_1}{d_1^2 \cdot l_1 + d_2^2 \cdot l_2 + d_3^2 \cdot l_3}$$
$$= \frac{(52\,\text{mm})^2 \cdot 120\,\text{mm}}{(52\,\text{mm})^2 \cdot 120\,\text{mm} + (66\,\text{mm})^2 \cdot 130\,\text{mm} + (53\,\text{mm})^2 \cdot 784\,\text{mm}} \tag{3.40}$$
$$= 0.105$$

$$m_2 = \rho \cdot \frac{\pi}{4} \cdot d_2^2 \cdot l_2 \tag{3.41}$$

$$\Rightarrow a_2 = \frac{m_2}{m} = \frac{d_2^2 \cdot l_2}{d_1^2 \cdot l_1 + d_2^2 \cdot l_2 + d_3^2 \cdot l_3}$$
$$= \frac{(66\,\text{mm})^2 \cdot 130\,\text{mm}}{(52\,\text{mm})^2 \cdot 120\,\text{mm} + (66\,\text{mm})^2 \cdot 130\,\text{mm} + (53\,\text{mm})^2 \cdot 784\,\text{mm}} \tag{3.42}$$
$$= 0.183$$

$$m_3 = \rho \cdot \frac{\pi}{4} \cdot d_3^2 \cdot l_3 \tag{3.43}$$

$$\Rightarrow a_3 = \frac{m_3}{m} = \frac{d_3^2 \cdot l_3}{d_1^2 \cdot l_1 + d_2^2 \cdot l_2 + d_3^2 \cdot l_3}$$
$$= \frac{(53\,\text{mm})^2 \cdot 784\,\text{mm}}{(52\,\text{mm})^2 \cdot 120\,\text{mm} + (66\,\text{mm})^2 \cdot 130\,\text{mm} + (53\,\text{mm})^2 \cdot 784\,\text{mm}} \tag{3.44}$$
$$= 0.712$$

For domain I: $0 < z_I < l_1$ (see figure 3.6), the second order differential equation for the deflection of the neutral axis for small deflections can be written as:

$$w_I'' E I_{y_I} = -M_{z_I} = \int_0^{z_I} (z_I - \tilde{z_I}) \cdot q_{z_I} \cdot d\tilde{z_I}$$
$$= q_{z_I} \cdot \frac{z_I^2}{2} = \frac{m \cdot g \cdot a_1}{l_1} \cdot \frac{z_I^2}{2} \tag{3.45}$$

The slope of the deflected neutral axis w' can be found as a function of z_I by integration

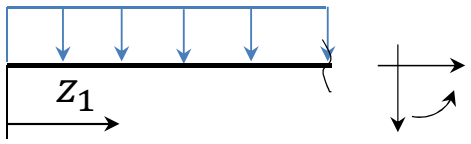

Figure 3.6: Domain I for line loads

of formula 3.45. Another integration leads to the displacement of the neutral axis.

$$w'_I EI_{y_I} = \frac{m \cdot g \cdot a_1}{l_1} \cdot \left(\frac{z_I^3}{6} + D_1 \right) \tag{3.46}$$

$$w_I EI_{y_I} = \frac{m \cdot g \cdot a_1}{l_1} \cdot \left(\frac{z_I^4}{24} + D_1 \cdot z_I + D_2 \right) \tag{3.47}$$

For domain II: $0 \leq z_{II} \leq l_2$, the reaction forces caused by the dead load of the pump shaft are needed:

$$\sum M_A = 0: \qquad 0 = F_B \cdot l_2 + \frac{l_3^2}{2} \cdot q_{z_{III}} - \frac{l_2^2}{2} \cdot q_{z_{II}} - \left(\frac{l_1}{2} + l_2 \right) \cdot l_1 \cdot q_{z_I} \tag{3.48}$$

$$\Rightarrow F_B = g \cdot m \cdot \left\{ \frac{a_2}{2} + a_1 \cdot \left(\frac{l_1}{2 \cdot l_2} + 1 \right) - a_3 \cdot \frac{l_3}{2 \cdot l_2} \right\} \tag{3.49}$$

$$\sum F_x = 0: \qquad 0 = m \cdot g - F_B - F_A \tag{3.50}$$

$$\Rightarrow F_A = g \cdot m \cdot \left\{ 1 + a_3 \cdot \frac{l_3}{2 \cdot l_2} - \frac{a_2}{2} - a_1 \cdot \left(\frac{l_1}{2 \cdot l_2} + 1 \right) \right\} \tag{3.51}$$

According to figure 3.7, the second order differential equation for the deflection of the neutral axis for small deflections can be written as:

$$\begin{aligned} w''_{II} EI_{y_{II}} = & -M_{z_{II}} = q_{z_I} \cdot l_1 \cdot \left(\frac{l_1}{2} + z_{II} \right) + \int_0^{z_{II}} (z_{II} - \tilde{z_{II}}) \cdot q_{z_{II}} \cdot d\tilde{z_{II}} - F_B \cdot z_{II} \\ & = m \cdot g \cdot \left\{ a_1 \cdot \frac{l_1}{2} \cdot \left(1 - \frac{z_{II}}{l_2} \right) + \frac{a_2}{2} \cdot \left(\frac{z_{II}^2}{l_2} - z_{II} \right) + \frac{a_3}{2} \cdot z_{II} \cdot \frac{l_3}{l_2} \right\} \end{aligned} \tag{3.52}$$

The slope and the displacement of the neutral axis are:

$$\begin{aligned} w'_{II} EI_{y_{II}} = & \frac{m \cdot g}{2} \cdot \left\{ a_1 \cdot l_1 \cdot \left(z_{II} - \frac{z_{II}^2}{2 \cdot l_2} \right) + a_2 \cdot \left(\frac{z_{II}^3}{3 \cdot l_2} - \frac{z_{II}^2}{2} \right) + \right. \\ & \left. + a_3 \cdot \frac{z_{II}^2}{2} \cdot \frac{l_3}{l_2} + D_3 \right\} \end{aligned} \tag{3.53}$$

$$\begin{aligned} w_{II} EI_{y_{II}} = & \frac{m \cdot g}{2} \cdot \left\{ a_1 \cdot l_1 \cdot \left(\frac{z_{II}^2}{2} - \frac{z_{II}^3}{6 \cdot l_2} \right) + a_2 \cdot \left(\frac{z_{II}^4}{12 \cdot l_2} - \frac{z_{II}^3}{6} \right) + \right. \\ & \left. + a_3 \cdot \frac{z_{II}^3}{6} \cdot \frac{l_3}{l_2} + D_3 \cdot z_{II} + D_4 \right\} \end{aligned} \tag{3.54}$$

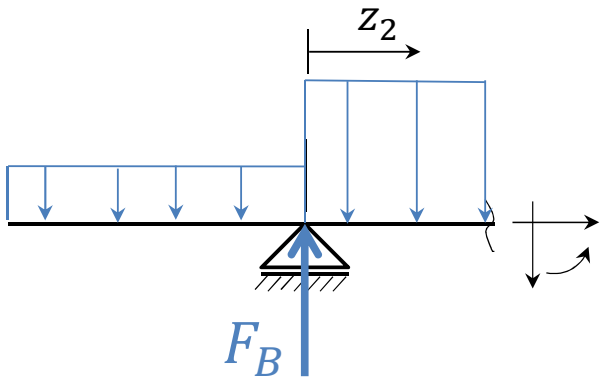

Figure 3.7: Domain II for line loads

For the third domain, which is shown in figure 3.8, the other end of the section is used to make it simpler.

$$\begin{aligned} w''_{III} EI_{y_{III}} = & -M_{z_{III}} = \int_0^{z_{III}} (z_{III} - \tilde{z_{III}}) \cdot q_{z_{III}} \cdot d\tilde{z_{III}} \\ & = q_{z_{III}} \cdot \frac{z_{III}^2}{2} = \frac{m \cdot g \cdot a_3}{l_3} \cdot \frac{z_{III}^2}{2} \end{aligned} \tag{3.55}$$

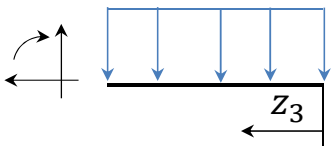

Figure 3.8: Domain III for line loads

$$w'_{III} EI_{y_{III}} = \frac{m \cdot g \cdot a_3}{6 \cdot l_3} \cdot \left(z_{III}^3 + D_5 \right) \tag{3.56}$$

$$w_{III} EI_{y_{III}} = \frac{m \cdot g \cdot a_3}{6 \cdot l_3} \cdot \left(\frac{z_{III}^4}{4} + D_5 \cdot z_{III} + D_6 \right) \tag{3.57}$$

Now the six constants of integration D_i have to be evaluated by using six boundary conditions. The following conditions are used:

- Because of bearing B: $w_{II}\left(z_{II} = 0\right) = 0$
- Because of bearing B: $w_I\left(z_I = l_1\right) = 0$
- Because of bearing A: $w_{II}\left(z_{II} = l_2\right) = 0$
- Because of bearing A: $w_{III}\left(z_{III} = l_3\right) = 0$
- Because of the transition condition: $w'_I\left(z_I = l_1\right) = w'_{II}\left(z_{II} = 0\right)$
- Because of the transition condition: $w'_{II}\left(z_{II} = l_2\right) = w'_{III}\left(z_{III} = l_3\right)$

$w_{II}\left(z_{II}=0\right)=0$ leads to:

$$0 = D_4 \tag{3.58}$$

$w_{II}\left(z_{II}=l_2\right)=0$ leads to:

$$0 = \frac{a_1 \cdot l_1}{3} \cdot l_2^2 - a_2 \cdot \frac{l_2^3}{12} + a_3 \cdot l_3 \cdot \frac{l_2^2}{6} + D_3 \cdot l_2 \tag{3.59}$$

$$\Rightarrow D_3 = -a_1 \cdot \frac{l_1 \cdot l_2}{3} + a_2 \cdot \frac{l_2^2}{12} - a_3 \cdot \frac{l_2 \cdot l_3}{6} \tag{3.60}$$

If the constants D_3 and D_4 are put into equation 3.54, the displacement can be written as:

$$\begin{aligned} w_{II} = \frac{m \cdot g}{2EI_{y_{II}}} \Bigg\{ & \frac{a_1 \cdot l_1}{6} \left(3z_{II}^2 - \frac{z_{II}^3}{l_2} - 2l_2 \cdot z_{II} \right) + \frac{a_2}{12} \left(\frac{z_{II}^4}{l_2} - 2z_{II}^3 + z_{II} \cdot l_2^2 \right) + \\ & + \frac{a_3 \cdot l_3}{6} \left(\frac{z_{II}^3}{l_2} - l_2 \cdot z_{II} \right) \Bigg\} \end{aligned} \tag{3.61}$$

$w_I'\left(z_I=l_1\right)=w_{II}'\left(z_{II}=0\right)$ leads to:

$$\frac{m \cdot g \cdot a_1}{l_1 \cdot E \cdot I_{y_I}} \left(\frac{l_1^3}{6} + D_1 \right) = \frac{m \cdot g}{2 \cdot E \cdot I_{y_{II}}} \cdot D_3 \tag{3.62}$$

$$\Rightarrow D_1 = \frac{l_1 \cdot I_{y_I}}{2 \cdot I_{y_{II}} \cdot a_1} \left\{ -a_1 \cdot \frac{l_1 \cdot l_2}{3} + a_2 \cdot \frac{l_2^2}{12} - a_3 \cdot \frac{l_2 \cdot l_3}{6} \right\} - \frac{l_1^3}{6} \tag{3.63}$$

$w_I\left(z_I=l_1\right)=0$ leads to:

$$\frac{l_1^4}{24} + D_1 \cdot l_1 + D_2 = 0 \tag{3.64}$$

$$\Rightarrow D_2 = \frac{3l_1^4}{24} + \frac{l_1^2 \cdot I_{y_I}}{2 \cdot I_{y_{II}} \cdot a_1} \left\{ a_1 \cdot \frac{l_1 \cdot l_2}{3} - a_2 \cdot \frac{l_2^2}{12} + a_3 \cdot \frac{l_2 \cdot l_3}{6} \right\} \tag{3.65}$$

If the constants D_1 and D_2 are put into equation 3.47, the displacement can be written as:

$$\begin{aligned} w_I = \frac{m \cdot g \cdot a_1}{l_1 \cdot E \cdot I_{y_I}} \Bigg\{ & \frac{z_I^4 + 3l_1^4 - 4l_1^3 \cdot z_I}{24} + \\ & + \frac{l_1 \cdot I_{y_I} \cdot (l_1 - z_I)}{2 \cdot I_{y_{II}} \cdot a_1} \left(a_1 \cdot \frac{l_1 \cdot l_2}{3} - a_2 \cdot \frac{l_2^2}{12} + a_3 \cdot \frac{l_2 \cdot l_3}{6} \right) \Bigg\} \end{aligned} \tag{3.66}$$

$w_{II}'\left(z_{II}=l_2\right)=w_{III}'\left(z_{III}=l_3\right)$ leads to:

$$\frac{m \cdot g}{2 \cdot E \cdot I_{y_{II}}} \left(\frac{a_1 \cdot l_1 \cdot l_2}{6} - \frac{a_2 \cdot l_2^2}{12} + \frac{a_3 \cdot l_2 \cdot l_3}{3} \right) = \frac{m \cdot g \cdot a_3}{6 \cdot E \cdot I_{y_{III}} \cdot l_3} \left(z_{III}^3 + D_5 \right) \tag{3.67}$$

$$\Rightarrow D_5 = \frac{l_3 \cdot I_{y_{III}}}{a_3 \cdot I_{y_{II}}} \left(\frac{a_1 \cdot l_1 \cdot l_2}{2} - \frac{a_2 \cdot l_2^2}{4} + a_3 \cdot l_2 \cdot l_3 \right) - l_{III}^3 \tag{3.68}$$

$w_{III}\left(z_{III}=l_3\right)=0$ leads to:

$$\frac{l_3^4}{4}+D_5\cdot l_3+D_6=0 \tag{3.69}$$

$$\Rightarrow D_6=\frac{3}{4}l_3^4-\frac{l_3^2\cdot I_{y_{III}}}{a_3\cdot I_{y_{II}}}\left\{a_1\cdot\frac{l_1\cdot l_2}{2}-a_2\cdot\frac{l_2^2}{4}+a_3\cdot l_2\cdot l_3\right\} \tag{3.70}$$

If the constants D_5 and D_6 are put into equation 3.57, the displacement can be written as:

$$\begin{aligned} w_{III}=\frac{m\cdot g\cdot a_3}{6\cdot l_3\cdot E\cdot I_{y_{III}}}\Bigg\{&\frac{z_{III}^4+3l_3^4-4l_3^3\cdot z_{III}}{4}+\\ &+\frac{l_3\cdot I_{y_{III}}\cdot\left(z_{III}-l_3\right)}{a_3\cdot I_{y_{II}}}\left(a_1\cdot\frac{l_1\cdot l_2}{2}-a_2\cdot\frac{l_2^2}{4}+a_3\cdot l_2\cdot l_3\right)\Bigg\}\end{aligned} \tag{3.71}$$

Deflection at the shaft endings

Concerning the gab between the impeller and the casing, it is important to know the deflection of the pump shaft ending at the suction side. A further interesting value is the deflection at the other end of the pump shaft, because at this side a coupling has to be mounted.
The overall deflection at the shaft endings are determined by the principle of superposition.

The deflections caused by the radial force from the imbalance can be written as:

$$\begin{aligned} w_I\left(z_I=0\right)&=\frac{F_R\cdot l_1^2}{3EI_{y_I}}\cdot\left\{l_1+l_2\cdot\frac{I_{y_I}}{I_{y_{II}}}\right\}\\ &=\frac{2{,}000\,\mathrm{N}\cdot\left(120\,\mathrm{mm}\right)^2}{3\cdot 210{,}000\,\mathrm{N/mm^2}\cdot 3.59\cdot 10^5\,\mathrm{mm^4}}\cdot\\ &\quad\cdot\left\{120\,\mathrm{mm}+130\,\mathrm{mm}\cdot\frac{3.59\cdot 10^5\,\mathrm{mm^4}}{9.31\cdot 10^5\,\mathrm{mm^4}}\right\}\\ &=0.0217\,\mathrm{mm}\end{aligned} \tag{3.72}$$

The deflection of the shaft ending at the outlet can be calculated with the angular offset at $z_{II}=l_2$.

$$\begin{aligned} w'_{II}\left(z_{II}=l_2\right)&=\tan\alpha\\ &=\frac{F_R}{EI_{y_{II}}}\cdot\frac{l_1\cdot l_2}{6}\end{aligned} \tag{3.73}$$

$$\begin{aligned} w_{III}\left(z_{III}=l_3\right)&=\tan\alpha\cdot l_3\\ &=\frac{2{,}000\,\mathrm{N}}{210{,}000\,\mathrm{N/mm^2}\cdot 9.31\cdot 10^5\,\mathrm{mm^4}}\cdot\frac{120\,\mathrm{mm}\cdot 130\,\mathrm{mm}}{6}\cdot 784\,\mathrm{mm}\\ &=0.0208\,\mathrm{mm}\end{aligned} \tag{3.74}$$

The deflections caused by the dead load of the impeller wheel can be written as:

$$\begin{aligned} w_I\left(z_I = 0\right) &= \frac{F_R \cdot l_1^2}{3EI_{y_I}} \cdot \left\{ l_1 + l_2 \cdot \frac{I_{y_I}}{I_{y_{II}}} \right\} \\ &= \frac{17.8\,\mathrm{kg} \cdot 9.81\,\mathrm{m/s^2} \cdot (120\,\mathrm{mm})^2}{3 \cdot 210,000\,\mathrm{N/mm^2} \cdot 3.59 \cdot 10^5\,\mathrm{mm^4}} \cdot \\ &\quad \cdot \left\{ 120\,\mathrm{mm} + 130\,\mathrm{mm} \cdot \frac{3.59 \cdot 10^5\,\mathrm{mm^4}}{9.31 \cdot 10^5\,\mathrm{mm^4}} \right\} \\ &= 0.0019\,\mathrm{mm} \end{aligned} \tag{3.75}$$

The deflection of the shaft ending at the outlet can be calculated with the angular offset at $z_{II} = l_2$.

$$\begin{aligned} w'_{II}\left(z_{II} = l_2\right) &= \tan\alpha \\ &= \frac{F_R}{EI_{y_{II}}} \cdot \frac{l_1 \cdot l_2}{6} \end{aligned} \tag{3.76}$$

$$\begin{aligned} w_{III}\left(z_{III} = l_3\right) &= \tan\alpha \cdot l_3 \\ &= \frac{17.8\,\mathrm{kg} \cdot 9.81\,\mathrm{m/s^2}}{210,000\,\mathrm{N/mm^2} \cdot 9.31 \cdot 10^5\,\mathrm{mm^4}} \cdot \frac{120\,\mathrm{mm} \cdot 130\,\mathrm{mm}}{6} \cdot 784\,\mathrm{mm} \\ &= 0.0018\,\mathrm{mm} \end{aligned} \tag{3.77}$$

To calculate the deflections caused by the dead load of the coupling, the model has to be reflected.

$$\begin{aligned} w_{III}\left(z_{III} = l_3\right) &= \frac{F_R \cdot l_3^2}{3EI_{y_{III}}} \cdot \left\{ l_3 + l_2 \cdot \frac{I_{y_{III}}}{I_{y_{II}}} \right\} \\ &= \frac{6\,\mathrm{kg} \cdot 9.81\,\mathrm{m/s^2} \cdot (784\,\mathrm{mm})^2}{3 \cdot 210,000\,\mathrm{N/mm^2} \cdot 3.87 \cdot 10^5\,\mathrm{mm^4}} \cdot \\ &\quad \cdot \left\{ 784\,\mathrm{mm} + 130\,\mathrm{mm} \cdot \frac{3.87 \cdot 10^5\,\mathrm{mm^4}}{9.31 \cdot 10^5\,\mathrm{mm^4}} \right\} \\ &= 0.1244\,\mathrm{mm} \end{aligned} \tag{3.78}$$

The deflection of the shaft ending at the outlet can be calculated with the angular offset at $z_{II} = l_2$.

$$\begin{aligned} w'_{II}\left(z_{II} = l_2\right) &= \tan\alpha \\ &= \frac{F_R}{EI_{y_{II}}} \cdot \frac{l_3 \cdot l_2}{6} \end{aligned} \tag{3.79}$$

$$\begin{aligned} w_I\left(z_I = l_1\right) &= \tan\alpha \cdot l_1 \\ &= \frac{6\,\mathrm{kg} \cdot 9.81\,\mathrm{m/s^2}}{210,000\,\mathrm{N/mm^2} \cdot 9.31 \cdot 10^5\,\mathrm{mm^4}} \cdot \frac{784\,\mathrm{mm} \cdot 130\,\mathrm{mm}}{6} \cdot 120\,\mathrm{mm} \\ &= 0.0006\,\mathrm{mm} \end{aligned} \tag{3.80}$$

The deflections caused by the dead load of the pump shaft can be written as:

$$\begin{aligned} w_I\left(z_I=0\right) &= \frac{m\cdot g\cdot a_1}{l_1\cdot E\cdot I_{y_I}}\left\{\frac{3l_1^4}{24}+\right. \\ &\quad \left.+\ \frac{l_1^2\cdot I_{y_I}}{2\cdot a_1\cdot I_{y_{II}}}\left(a_1\cdot\frac{l_1\cdot l_2}{3}-a_2\cdot\frac{l_2^2}{12}+a_3\cdot\frac{l_2\cdot l_3}{6}\right)\right\} \\ &= \frac{19.2\,\mathrm{kg}\cdot 9.81\,\mathrm{m/s^2}\cdot 0.105}{120\,\mathrm{mm}\cdot 210,000\,\mathrm{N/mm^2}\cdot 3.59\cdot 10^5\,\mathrm{mm^4}}\cdot\left\{\frac{3}{24}\left(120\,\mathrm{mm}\right)^4+\right. \\ &\quad +\frac{\left(120\,\mathrm{mm}\right)^2\cdot 3.59\cdot 10^5\,\mathrm{mm^4}}{2\cdot 0.105\ \cdot 9.31\cdot 10^5\,\mathrm{mm^4}}\cdot\left(0.105\ \cdot\frac{120\,\mathrm{mm}\cdot 130\,\mathrm{mm}}{3}\ -\right. \\ &\quad \left.\left.-\ 0.183\ \cdot\frac{\left(130\,\mathrm{mm}\right)^2}{12}+0.712\ \cdot\frac{130\,\mathrm{mm}\cdot 784\,\mathrm{mm}}{6}\right)\right\} \\ &= 0.0008\,\mathrm{mm} \end{aligned} \tag{3.81}$$

$$\begin{aligned} w_{III}\left(z_{III}=0\right) &= \frac{m\cdot g\cdot a_3}{6\cdot l_3\cdot E\cdot I_{y_{III}}}\left\{\frac{3}{4}l_3^4-\right. \\ &\quad \left.-\ \frac{l_3^2\cdot I_{y_{III}}}{a_3\cdot I_{y_{II}}}\left(a_1\cdot\frac{l_1\cdot l_2}{2}-a_2\cdot\frac{l_2^2}{4}+a_3\cdot l_2\cdot l_3\right)\right\} \\ &= \frac{19.2\,\mathrm{kg}\cdot 9.81\,\mathrm{m/s^2}\cdot 0.712}{6\cdot 784\,\mathrm{mm}\cdot 210,000\,\mathrm{N/mm^2}\cdot 3.87\cdot 10^5\,\mathrm{mm^4}}\cdot\left\{\frac{3}{4}\left(784\,\mathrm{mm}\right)^4-\right. \\ &\quad -\frac{\left(784\,\mathrm{mm}\right)^2\cdot 3.87\cdot 10^5\,\mathrm{mm^4}}{0.712\ \cdot 9.31\cdot 10^5\,\mathrm{mm^4}}\cdot\left(0.105\ \cdot\frac{120\,\mathrm{mm}\cdot 130\,\mathrm{mm}}{2}\ -\right. \\ &\quad \left.\left.-\ 0.183\ \cdot\frac{\left(130\,\mathrm{mm}\right)^2}{4}+0.712\ \cdot 130\,\mathrm{mm}\cdot 784\,\mathrm{mm}\right)\right\} \\ &= -\,0.009\,\mathrm{mm} \end{aligned} \tag{3.82}$$

The overall deflections can be calculated with:

$$\begin{aligned} w_{I_{sum}} &= \sum_{i=1}^{n} w_{I_i} = 0.0217\,\mathrm{mm}+0.0019\,\mathrm{mm}+0.0006\,\mathrm{mm}+0.0008\,\mathrm{mm} \\ &= 0.025\,\mathrm{mm} \end{aligned} \tag{3.83}$$

$$\begin{aligned} w_{III_{sum}} &= \sum_{i=1}^{n} w_{III_i} = 0.0208\,\mathrm{mm}+0.0018\,\mathrm{mm}+0.1244\,\mathrm{mm}-(-0.009\,\mathrm{mm}) \\ &= 0.156\,\mathrm{mm} \end{aligned} \tag{3.84}$$

3.3.2 Critical bending speed ω_k

The lowest critical bending speed of a shaft with more than one single mass can be determined with the Dunkerley method 3.85 [8]. Therefore, the natural frequencies of the pump shaft alone ω_{k0} and of the single masses ω_{ki}[1] are needed. These frequencies can

[1]Here: the shaft is expected to be massless.

be calculated with formula 3.88, where the biggest deflection is inserted, because only the lowest frequency is interesting.

$$\frac{1}{\omega_k^2} = \frac{1}{\omega_{k0}^2} + \frac{1}{\omega_{k1}^2} + \frac{1}{\omega_{k2}^2} \tag{3.85}$$

The natural frequency can be written as:

$$\omega_k = \sqrt{\frac{c}{m}} \tag{3.86}$$

$$F = g \cdot m = c \cdot w \tag{3.87}$$

c	N/m	Spring rigidity
m	kg	Mass

With the spring load F the natural frequency is:

$$\omega_k = \sqrt{\frac{g}{w}} \tag{3.88}$$

The natural frequencies of the single parts are:

- Pump shaft:

$$\omega_{k0} = \sqrt{\frac{g}{w_0}} = \sqrt{\frac{9.81\,\mathrm{m/s^2}}{0.009 \cdot 10^{-3}\,\mathrm{m}}} = 1,044\,\mathrm{Hz} \tag{3.89}$$

- Coupling:

$$\omega_{k1} = \sqrt{\frac{g}{w_1}} = \sqrt{\frac{9.81\,\mathrm{m/s^2}}{0.1244 \cdot 10^{-3}\,\mathrm{m}}} = 281\,\mathrm{Hz} \tag{3.90}$$

- Impeller wheel:

$$\omega_{k2} = \sqrt{\frac{g}{w_2}} = \sqrt{\frac{9.81\,\mathrm{m/s^2}}{0.0019 \cdot 10^{-3}\,\mathrm{m}}} = 2,272\,\mathrm{Hz} \tag{3.91}$$

If the natural frequencies are put into formula 3.85, the lowest critical bending speed can be written as:

$$\begin{aligned} n_k = \omega_k \cdot \frac{30}{\pi} &= \sqrt{\frac{1}{\frac{1}{\omega_{k0}^2} + \frac{1}{\omega_{k1}^2} + \frac{1}{\omega_{k2}^2}}} = \sqrt{\frac{1}{\frac{1}{(1{,}044\,\mathrm{Hz})^2} + \frac{1}{(281\,\mathrm{Hz})^2} + \frac{1}{(2{,}272\,\mathrm{Hz})^2}}} \cdot \frac{30}{\pi} = \\ &= 2,573\,\mathrm{rpm} \end{aligned} \tag{3.92}$$

According to [8], the approximation of the critical bending speed is expected to be 5% to 10% lower than in reality. Another aspect is, that the bearing rigidity was supposed to be endless. If the real bearing rigidity would be considered, the calculated critical bending speed would be too high. It is suspected, that these two sources of errors will counterbalance each other.

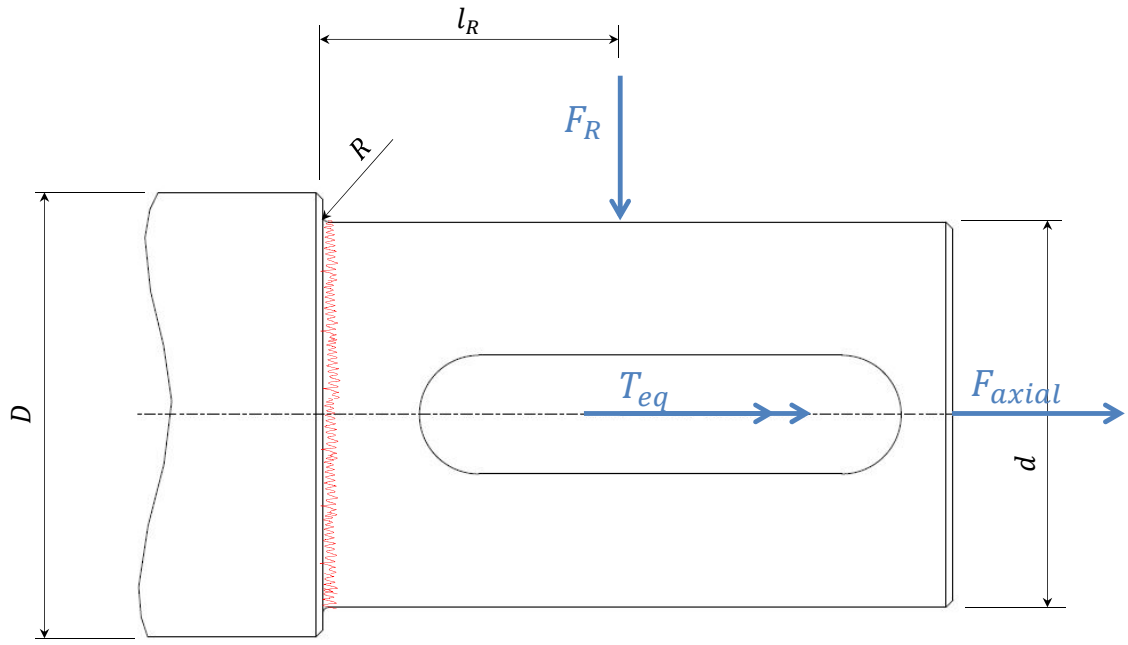

Figure 3.9: Critical section of the pump shaft

3.3.3 Strength verification

To provide evidence that the pump shaft can resist the strains which act on it, the most endangered section of the shaft is chosen, which is shown in figure 3.9. The procedure to calculate the coefficient of safety against breakage is according to [4].
Calculation of the nominal stresses:

- Tensile stress:

$$\sigma_{\mathrm{z\,a}} = \sigma_{te,max} = \frac{F_{axial}}{A} = \frac{F_{axial}}{\frac{d^2 \cdot \pi}{4}} = \frac{23,854\,\mathrm{N}}{\frac{(52\,\mathrm{mm})^2 \cdot \pi}{4}} = 11.23\,\mathrm{N/mm^2} \tag{3.93}$$

- Bending stress:

$$\sigma_{\mathrm{b\,a}} = \sigma_{b,max} = \frac{M_b}{W} = \frac{F_R \cdot l_R}{\frac{d^3 \cdot \pi}{32}} = \frac{2,000\,\mathrm{N} \cdot 42.5\,\mathrm{mm}}{\frac{(52\,\mathrm{mm})^3 \cdot \pi}{32}} = 6.16\,\mathrm{N/mm^2} \tag{3.94}$$

- Torsional stress:

$$\tau_{\mathrm{t\,a}} = \tau_{t,max} = \frac{T_{eq}}{W_p} = \frac{T_{eq}}{\frac{d^3 \cdot \pi}{16}} = \frac{671.4 \cdot 10^3\,\mathrm{Nmm}}{\frac{(52\,\mathrm{mm})^3 \cdot \pi}{16}} = 24.32\,\mathrm{N/mm^2} \tag{3.95}$$

Due to the fact that the nominal stresses are static without amplitudes, the safety against fatigue fracture has not to be considered. The safety against exceeding the yield strength S_F can be calculated with:

$$\frac{1}{S_F} = \sqrt{\left(\frac{\sigma_{te,max}}{\sigma_{te,YS}} + \frac{\sigma_{b,max}}{\sigma_{b,YS}}\right)^2 + \left(\frac{\tau_{t,max}}{\tau_{t,YS}}\right)^2} \tag{3.96}$$

The yield strength of the component can be calculated with:

$$\begin{aligned}\sigma_{te,YS} &= K_1 \cdot K_{2,te} \cdot \gamma_{Y,te} \cdot R_{\mathrm{p\ 0,2\ N}} \\ &= 0.93 \cdot 1 \cdot 1.1 \cdot 900\,\mathrm{N/mm^2} \\ &= 921\,\mathrm{N/mm^2}\end{aligned} \tag{3.97}$$

$$\begin{aligned}\sigma_{b,YS} &= K_1 \cdot K_{2,b} \cdot \gamma_{Y,b} \cdot R_{\mathrm{p\ 0,2\ N}} \\ &= 0.93 \cdot 0.871 \cdot 1.1 \cdot 900\,\mathrm{N/mm^2} \\ &= 802\,\mathrm{N/mm^2}\end{aligned} \tag{3.98}$$

$$\begin{aligned}\tau_{t,YS} &= K_1 \cdot K_{2,t} \cdot \gamma_{Y,t} \cdot \frac{R_{\mathrm{p\ 0,2\ N}}}{\sqrt{3}} \\ &= 0.93 \cdot 0.871 \cdot 1.05 \cdot \frac{900\,\mathrm{N/mm^2}}{\sqrt{3}} \\ &= 442\,\mathrm{N/mm^2}\end{aligned} \tag{3.99}$$

K_1	Size factor
$K_{2,i}$	Factor of the static support effect
$\gamma_{Y,i}$	Increase factor of the yield strength

With the yield strength of the component, equation 3.96 leads to:

$$\frac{1}{S_F} = \sqrt{\left(\frac{11.23\,\mathrm{N/mm^2}}{921\,\mathrm{N/mm^2}} + \frac{6.16\,\mathrm{N/mm^2}}{802\,\mathrm{N/mm^2}}\right)^2 + \left(\frac{24.32\,\mathrm{N/mm^2}}{442\,\mathrm{N/mm^2}}\right)^2} \tag{3.100}$$

$$\Rightarrow S_F = 17.1 \tag{3.101}$$

The safety against exceeding the yield strength is much bigger than the required safety of 2.

3.3.4 Fitting key

The fitting keys are designed according to [8].

Hub

$$p_m \approx \frac{2 \cdot T_{eq} \cdot K_\lambda}{d \cdot h' \cdot l' \cdot z \cdot \kappa} = \frac{2 \cdot 671.4 \cdot 10^3\,\mathrm{Nmm} \cdot 1.13}{52\,\mathrm{mm} \cdot 3.8\,\mathrm{mm} \cdot 53\,\mathrm{mm} \cdot 1 \cdot 1} = 144.9\,\mathrm{N/mm^2} \leq p_{zul}$$
$$144.9\,\mathrm{N/mm^2} \leq 433\,\mathrm{N/mm^2}\ \checkmark \tag{3.102}$$

Coupling

$$p_m \approx \frac{2 \cdot T_{eq} \cdot K_\lambda}{d \cdot h' \cdot l' \cdot z \cdot \kappa} = \frac{2 \cdot 671.4 \cdot 10^3\,\mathrm{Nmm} \cdot 1.26}{52\,\mathrm{mm} \cdot 3.8\,\mathrm{mm} \cdot 53\,\mathrm{mm} \cdot 2 \cdot 0.75} = 107.7\,\mathrm{N/mm^2} \leq p_{zul}$$
$$107.7\,\mathrm{N/mm^2} \leq 187.5\,\mathrm{N/mm^2}\ \checkmark \tag{3.103}$$

K_λ		Load distribution factor
h'	mm	Bearing height of the fitting key
l'	mm	Bearing lenght of the fitting key
z		Number of fitting keys
κ		Carrying factor
p_m	$\mathrm{N/mm^2}$	Contact pressure
p_{zul}	$\mathrm{N/mm^2}$	Permitted contact pressure

3.4 Impeller vane pivot

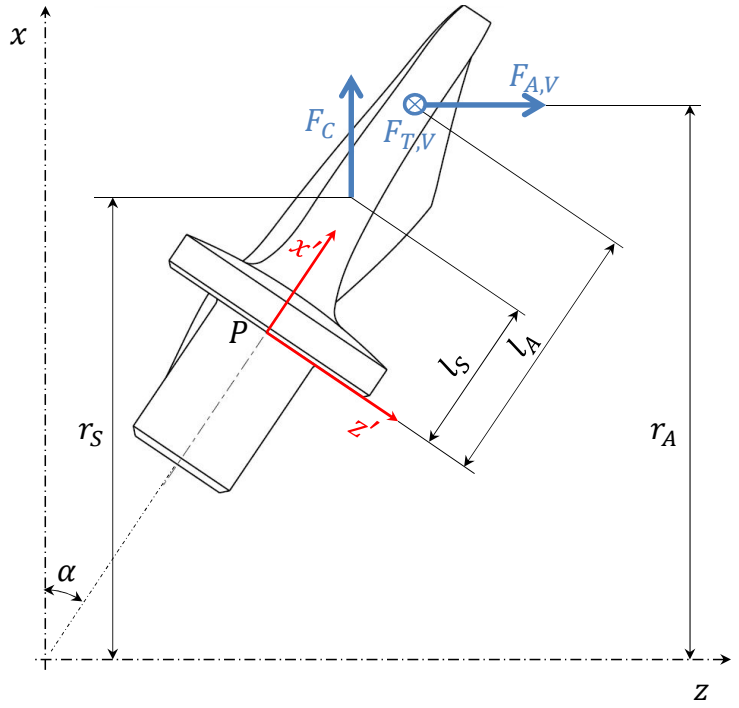

Figure 3.10: Forces which act on the impeller vane pivot

The forces, which are shown in figure 3.10, act on the impeller vane and lead to torques which have to be absorbed by the pivot. The pivot has to be mounted that way, that a lifting of the impeller vane from the hub cannot occur. To be on the safe side, it is supposed that the maximum forces occur at the same time, although this would be improbable. Furthermore, the centrifugal force F_C is expected to act in the center of gravity which is supposed to be in the z-x plane. The point of application of the tangential force $F_{T,V}$ and the axial force $F_{A,V}$ is supposed to act at a height of 2/3 of the impeller vane.

3.4.1 Reaction forces and torques

$$\begin{aligned} F_C &= m \cdot \omega^2 \cdot r_S = m \cdot \left(\frac{\pi \cdot n}{30}\right)^2 \cdot r_S \\ &= 1.04\,\mathrm{kg} \cdot \left(\frac{\pi \cdot 1,600\,\mathrm{rpm}}{30}\right)^2 \cdot 116.5 \cdot 10^{-3}\,\mathrm{m} \\ &= 3,401\,\mathrm{N} \end{aligned} \tag{3.104}$$

$$F_{T,V} = \frac{T_{eq}}{6 \cdot r_A} = \frac{674.1\,\mathrm{Nm}}{6 \cdot 140 \cdot 10^{-3}\,\mathrm{m}} = 803\,\mathrm{N} \tag{3.105}$$

Reaction forces and torques at point P

$$\sum M_{P,y'} = 0: \qquad 0 = M_{y'} + F_C \cdot \sin\alpha \cdot l_S - F_{A,V} \cdot \cos\alpha \cdot l_A \tag{3.106}$$

$$\Rightarrow M_{y'} = -F_C \cdot \sin\alpha \cdot l_S + \frac{F_{axial}}{6} \cdot \cos\alpha \cdot l_A \tag{3.107}$$

$$\begin{aligned} &= -3,401\,\mathrm{N} \cdot \sin 34^\circ \cdot 0.0257\,\mathrm{m} + \frac{23,854\,\mathrm{N}}{6} \cdot \cos 34^\circ \cdot 0.0536\,\mathrm{m} \\ &= 128\,\mathrm{Nm} \end{aligned}$$

$$\sum M_{P,z'} = 0: \qquad 0 = M_{z'} - F_{T,V} \cdot l_A \tag{3.108}$$

$$\Rightarrow M_{z'} = F_{T,V} \cdot l_A = 803\,\mathrm{N} \cdot 0.0536\,\mathrm{m} \tag{3.109}$$

$$= 43\,\mathrm{Nm}$$

$$\sum F_{x'} = 0: \qquad 0 = F_C \cdot \cos\alpha + F_{A,V} \cdot \sin\alpha + F_{x'} \tag{3.110}$$

$$\Rightarrow F_{x'} = -\frac{F_A}{6} \cdot \sin\alpha - F_C \cdot \cos\alpha \tag{3.111}$$

$$= -\frac{23,854\,\mathrm{N}}{6} \cdot \sin 34^\circ - 3,401\,\mathrm{N} \cdot \cos 34^\circ = -5,043\,\mathrm{N}$$

$F_{x'}$ is equal to the operating force F_B, which is considered in the calculation of the thread.

Twisting moment of the pivot

The twisting moment of the pivot consists of a term which is caused by the flow ($T_{P,F}$) and a term which is caused by the moment of inertia ($T_{P,I}$). The first term is given from the CFD-calculation with 65 Nm. The second term can be derived as follows:

$$dF = \omega_z^2 \cdot r \cdot dm \tag{3.112}$$

$$dM_y = z \cdot dF_x = z \cdot dF \cdot \cos\beta = z \cdot \omega_z^2 \cdot \underbrace{r \cdot \cos\beta}_{x} \cdot dm \tag{3.113}$$

$$\Rightarrow M_y = \omega_z^2 \cdot \underbrace{\int z \cdot x \cdot dm}_{I_{zx}} = \omega_z^2 \cdot I_{zx} \tag{3.114}$$

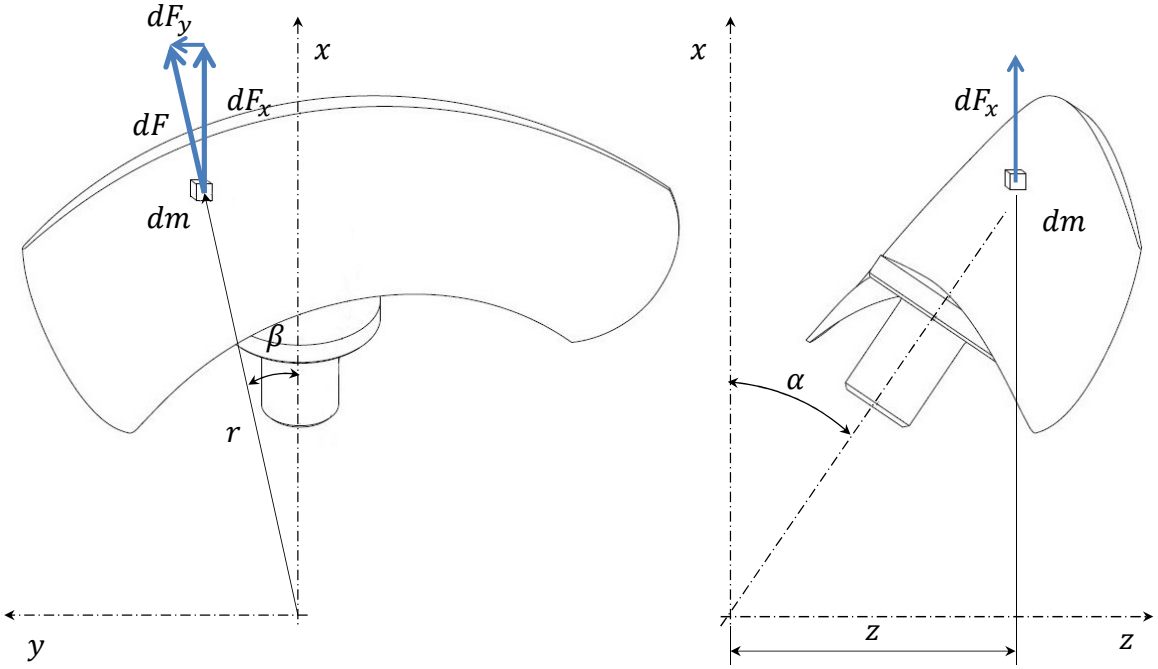

Figure 3.11: Derivation of the moments of inertia

$$dM_x = -z \cdot dF_y = -z \cdot dF \cdot \sin\beta = -z \cdot \omega_z^2 \cdot \underbrace{r \cdot \sin\beta}_{y} \cdot dm \tag{3.115}$$

$$\Rightarrow M_x = -\omega_z^2 \cdot \underbrace{\int z \cdot y \cdot dm}_{I_{zy}} = -\omega_z^2 \cdot I_{zy} \tag{3.116}$$

The term which acts in the direction of the pivot-axis can be written as:

$$T_{P,I} = \cos\alpha \cdot M_x = -\cos\alpha \cdot \omega_z^2 \cdot I_{zy} \tag{3.117}$$

This term depends on the moment of inertia I_{zy}, which varies depending on the position of the impeller vane (see table 3.2). The moments of inertia are determined by means of the 3D-drawing program. Therefore, the maximum twisting moment is:

$$\begin{aligned} T_P &= T_{P,F} + T_{P,I_{max}} = 65\,\text{Nm} + 5\,\text{Nm} \\ &= 70\,\text{Nm} \end{aligned} \tag{3.118}$$

3.4.2 Required clamping force

Required clamping force due to the bending moments

The required clamping force has to ensure that a lifting of the impeller vane from the hub cannot occur. Therefore, the contact pressure between the plate of the vane and the hub always has to be bigger than zero. The contact pressure is supposed to be linear along the radius (see figure 3.12). As a result, the contact pressure can be written as:

$$p(z') = k \cdot z' + d \tag{3.119}$$

Table 3.2: Twisting moment of the pivot

Stagger angle [°]	I_{zx} [kgmm^2]	I_{zy} [kgmm^2]	M_y [Nm]	M_x [Nm]	$T_{P,I}$ [Nm]
6.0	-10,335	-215	-291.7	6.1	5.0
4.5	-10,361	-190	-292.4	5.4	4.4
3.0	-10,386	-164	-293.1	4.6	3.8
1.5	-10,410	-136	-293.8	3.8	3.2
0.0	-10,433	-107	-294.5	3.0	2.5
-1.5	-10,456	-77	-295.1	2.2	1.8
-3.0	-10,477	-46	-295.7	1.3	1.1
-4.5	-10,497	-14	-296.3	0.4	0.3
-6.0	-10,516	18	-296.8	-0.5	-0.4
-7.5	-10,534	52	-297.3	-1.5	-1.2
-9.0	-10,550	86	-297.8	-2.4	-2.0
-10.5	-10,565	121	-298.2	-3.4	-2.8
-12.0	-10,579	157	-298.6	-4.4	-3.7
-13.5	-10,592	192	-298.9	-5.4	-4.5
-15.0	-10,603	228	-299.3	-6.4	-5.3
-16.5	-10,613	265	-299.6	-7.5	-6.2

To evaluate the two unknown parameters, two boundary conditions are needed:

- The balance of forces:

$$0 = \int p(z') \cdot dA \tag{3.120}$$

- The balance of moments:

$$0 = \int p(z') \cdot z' \cdot dA - M \tag{3.121}$$

The first boundary condition leads to:

$$0 = \int (k \cdot z' + d) \cdot dA \tag{3.122}$$

or with polar coordinates:

$$\begin{aligned} 0 &= \int_{r_i}^{r_o} \int_0^{2\pi} (k \cdot \cos\delta \cdot r + d) \cdot r \cdot dr \cdot d\delta \\ &= k \cdot \sin\delta \cdot \frac{r^3}{3} + d \cdot \frac{r^2}{2} \cdot \delta \Bigg|_{r_i}^{r_o} \Bigg|_0^{2\pi} = \pi \left(r_o^2 - r_i^2\right) \cdot d \\ \Rightarrow d &= 0 \end{aligned} \tag{3.123}$$

With $d = 0$ the second boundary condition can be written as:

$$M = \int z' \cdot (k \cdot z') \cdot dA \tag{3.124}$$

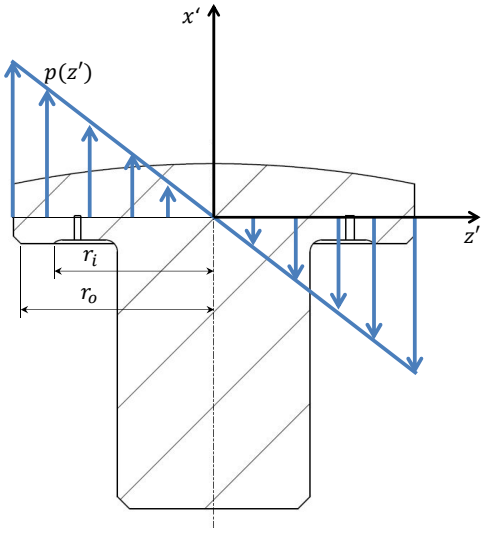

Figure 3.12: Contact pressure along the radius of the pivot

or with polar coordinates:

$$\begin{aligned} M &= \int\int r \cdot \cos\delta \cdot (k \cdot r \cdot \cos\delta) \cdot r \cdot dr \cdot d\delta \\ &= \int\int k \cdot \cos^2\delta \cdot r^3 \cdot dr \cdot d\delta \\ &= k \cdot \frac{r^4}{4} \cdot \frac{1}{2} \left(\delta + \sin\delta \cdot \cos\delta\right) \Big|_{r_i}^{r_o} \Big|_{0}^{2\pi} = k \cdot \frac{(r_o^4 - r_i^4)}{4} \cdot \pi \\ \Rightarrow k &= \frac{M \cdot 4}{\pi \left(r_o^4 - r_i^4\right)} \end{aligned} \tag{3.125}$$

Now, the contact pressure can be written as:

$$p(r,\delta) = \frac{M \cdot 4}{\pi \left(r_o^4 - r_i^4\right)} \cdot r \cdot \cos\delta \tag{3.126}$$

The contact pressure caused by $M_{P,y'}$ and by $M_{P,z'}$ leads to:

$$p_{z'}(r,\delta) = \frac{M_{P,y'} \cdot 4}{\pi \left(r_o^4 - r_i^4\right)} \cdot r \cdot \cos\delta \tag{3.127}$$

$$p_{y'}(r,\delta) = -\frac{M_{P,z'} \cdot 4}{\pi \left(r_o^4 - r_i^4\right)} \cdot r \cdot \sin\delta \tag{3.128}$$

The resulting contact pressure can be found by accumulating $p_{y'}(r,\delta)$ and $p_{z'}(r,\delta)$.

$$p_{res}(r,\delta) = \frac{r \cdot 4}{\pi \left(r_o^4 - r_i^4\right)} \cdot \left(M_{P,y'} \cdot \cos\delta - M_{P,z'} \cdot \sin\delta\right) \tag{3.129}$$

To find the minimum of the resulting contact pressure, its first derivation has to be zero.

$$\begin{aligned} 0 = \frac{dp_{res}(r,\delta)}{d\delta} &= \frac{r \cdot 4}{\pi \left(r_o^4 - r_i^4\right)} \cdot \left(-M_{P,y'} \cdot \sin\delta - M_{P,z'} \cdot \cos\delta\right) \\ &= M_{P,y'} \cdot \sin\delta + M_{P,z'} \cdot \cos\delta \end{aligned} \tag{3.130}$$

$$\Rightarrow \tan\delta = -\frac{M_{P,z'}}{M_{P,y'}} \tag{3.131}$$

$$\Rightarrow \delta = \tan^{-1}\left(-\frac{M_{P,z'}}{M_{P,y'}}\right) = \tan^{-1}\left(-\frac{43\,\mathrm{Nm}}{128\,\mathrm{Nm}}\right) = -18.57\,^\circ \tag{3.132}$$

As of the tangent function, a second solution for the extrema exists at $\delta + 180° = 161.43°$. The minimum of the resulting contact pressure will occur at the outer diameter. This leads to:

$$p_{\text{res ex}}(\delta) = \frac{r_o \cdot 4}{\pi\left(r_o^4 - r_i^4\right)} \cdot \left(M_{P,y'} \cdot \cos\delta - M_{P,z'} \cdot \sin\delta\right) \tag{3.133}$$

$$\begin{aligned} p_{\text{res max}}(-18.57\,^\circ) = &\frac{24.65\,\mathrm{mm} \cdot 4}{\pi\left((24.65\,\mathrm{mm})^4 - (19.9\,\mathrm{mm})^4\right)} \cdot \\ &\cdot \left(128 \cdot 10^3\,\mathrm{Nmm} \cdot \cos\left(-18.57\,^\circ\right) - 43 \cdot 10^3\,\mathrm{Nmm} \cdot \sin\left(-18.57\,^\circ\right)\right) \\ = &\,20\,\mathrm{N/mm^2} \end{aligned} \tag{3.134}$$

$$\begin{aligned} p_{\text{res min}}(161.43\,^\circ) = &\frac{24.65\,\mathrm{mm} \cdot 4}{\pi\left((24.65\,\mathrm{mm})^4 - (19.9\,\mathrm{mm})^4\right)} \cdot \\ &\cdot \left(128 \cdot 10^3\,\mathrm{Nmm} \cdot \cos\left(161.43\,^\circ\right) - 43 \cdot 10^3\,\mathrm{Nmm} \cdot \sin\left(161.43\,^\circ\right)\right) \\ = &\,-20\,\mathrm{N/mm^2} \end{aligned} \tag{3.135}$$

To ensure that the resulting contact pressure is always positive, the required clamping force due to the moments $M_{P,y'}$ and $M_{P,z'}$ leads to:

$$\begin{aligned} F_{\text{req b}} = &-p_{\text{res min}} \cdot A = -p_{\text{res min}} \cdot \left(r_o^2 - r_i^2\right) \cdot \pi \\ = &-20\,\mathrm{N/mm^2} \cdot \left((24.65\,\mathrm{mm})^2 - (19.9\,\mathrm{mm})^2\right) \cdot \pi = 13,296\,\mathrm{N} \end{aligned} \tag{3.136}$$

Required clamping force due to the twisting moment

A further purpose of the clamping force is, to transfer the twisting moment of the impeller vane. The friction is supposed to act at the averaged radius r_m.

$$r_m = \frac{r_o + r_i}{2} = \frac{24.65\,\mathrm{mm} + 19.9\,\mathrm{mm}}{2} = 22.28\,\mathrm{mm} \tag{3.137}$$

$$\begin{aligned} F_{\text{req t}} &\geq \frac{T_P}{\mu \cdot r_m} \\ &\geq \frac{70 \cdot 10^3\,\mathrm{Nmm}}{0.12 \cdot 22.28\,\mathrm{mm}} \\ &\geq 26,182\,\mathrm{N} \end{aligned} \tag{3.138}$$

For the further calculation of the thread, $F_{\text{req t}}$ is used because this required clamping force can also ensure that the vane cannot lift from the hub.

3.4.3 Calculation of the thread of the pivot

The calculation is according to [8], and the values for the parameters can be found in [9]. The situation of the fastening of the impeller vane is shown in figure 3.13.

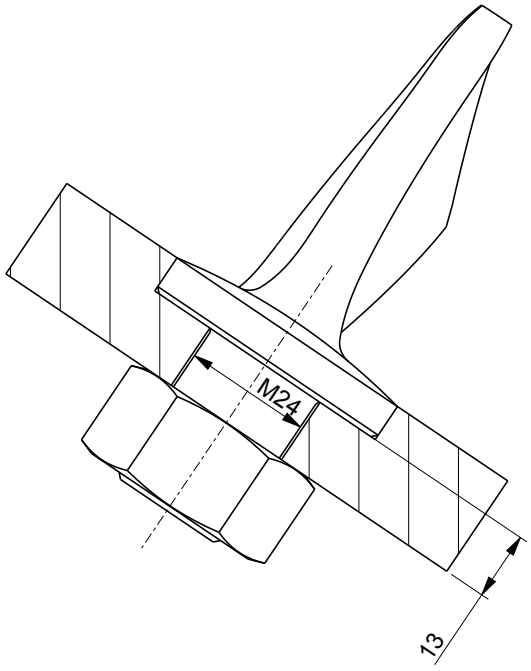

Figure 3.13: Fastening of the impeller vane

Loss of the preload force caused by creep processes F_Z

The elastic resilience of the pivot δ_s

$$A_N = \frac{d^2 \cdot \pi}{4} = \frac{(24\,\mathrm{mm})^2 \cdot \pi}{4} = 452.4\,\mathrm{mm}^2 \tag{3.139}$$

$$A_3 = \frac{d_3^2 \cdot \pi}{4} = \frac{(22.16\,\mathrm{mm})^2 \cdot \pi}{4} = 385.7\,\mathrm{mm}^2 \tag{3.140}$$

$$\begin{aligned}
\delta_s &= \delta_H + \delta_C + \delta_T + \delta_N \\
&= \frac{1}{E}\left\{\frac{0.4 \cdot d}{A_N} + \frac{l_{thr}}{A_3} + \frac{0.5 \cdot d}{A_3} + \frac{0,4 \cdot d}{A_N}\right\} \\
&= \frac{1}{210,000\,\mathrm{N/mm}^2}\left\{\frac{0.4 \cdot 24\,\mathrm{mm}}{452.4\,\mathrm{mm}^2} + \frac{13\,\mathrm{mm}}{385.7\,\mathrm{mm}^2} + \frac{0.5 \cdot 24\,\mathrm{mm}}{385.7\,\mathrm{mm}^2} + \frac{0.4 \cdot 24\,\mathrm{mm}}{452.4\,\mathrm{mm}^2}\right\} \\
&= 5.11 \cdot 10^{-7}\,\mathrm{mm/N}
\end{aligned} \tag{3.141}$$

A_N	mm^2	Area of the major section
A_3	mm^2	Area of the core section of the thread
d	mm	Outer diameter of the thread / major diameter

The elastic resilience of the deformed parts δ_t

$$D_A = l_k + d_w = 13\,\text{mm} + 36\,\text{mm} = 49\,\text{mm} \tag{3.142}$$

$$x = \sqrt[3]{\frac{l_k \cdot d_w}{D_A^2}} = \sqrt[3]{\frac{13\,\text{mm} \cdot 36\,\text{mm}}{(49\,\text{mm})^2}} = 0.58 \tag{3.143}$$

$$\begin{aligned} A_{rep} &= \frac{\pi}{4} \cdot \left(d_w^2 - d_h^2\right) + \frac{\pi}{8} \cdot d_w \cdot (D_A - d_w) \left[(x+1)^2 - 1\right] \\ &= \frac{\pi}{4} \cdot \left((36\,\text{mm})^2 - (25\,\text{mm})^2\right) + \frac{\pi}{8} \cdot 36\,\text{mm} \cdot (49\,\text{mm} - 36\,\text{mm}) \left[(0.58\ + 1)^2 - 1\right] \\ &= 802\,\text{mm}^2 \end{aligned} \tag{3.144}$$

A_{rep}	mm^2	Replacement area
d_w	mm	Outer diameter of the head contact
d_h	mm	Diameter of the drilling hole
D_A	mm	Outer diameter of the deformed parts
l_k	mm	Clamping length

$$\delta_t = \frac{l_k}{A_{rep} \cdot E} = \frac{13\,\text{mm}}{802\,\text{mm}^2 \cdot 210,000\,\text{N/mm}^2} = 0.77 \cdot 10^{-7}\,\text{mm/N} \tag{3.145}$$

$$F_Z = \frac{f_z}{\delta_s + \delta_t} = \frac{0.012\,\text{mm}}{5.11 \cdot 10^{-7}\,\text{mm/N} + 0.77 \cdot 10^{-7}\,\text{mm/N}} = 20,408\,\text{N} \tag{3.146}$$

Forces at the thread

$$\begin{aligned} F_{VM} &= k_A \left\{ F_{\text{req}} + F_B \left(1 - \frac{\delta_t}{\delta_t + \delta_s}\right) + F_Z \right\} \\ &= 1.6 \left\{ 26,182\,\text{N} + 5,043\,\text{N} \left(1 - \frac{0.77 \cdot 10^{-7}\,\text{mm/N}}{0.77 \cdot 10^{-7}\,\text{mm/N} + 5.11 \cdot 10^{-7}\,\text{mm/N}}\right) + 20,408\,\text{N} \right\} \\ &= 81,556\,\text{N} \end{aligned} \tag{3.147}$$

$$\begin{aligned} F_{Smax} &= F_{VM} + k_A \cdot \frac{\delta_t}{\delta_t + \delta_s} \cdot F_B \\ &= 81,556\,\text{N} + 1.6 \cdot \frac{0.77 \cdot 10^{-7}\,\text{mm/N}}{0.77 \cdot 10^{-7}\,\text{mm/N} + 5.11 \cdot 10^{-7}\,\text{mm/N}} \cdot 5,043\,\text{N} \\ &= 82,613\,\text{N} \end{aligned} \tag{3.148}$$

k_A		Tightening factor
F_{req}	N	Required clamping force
F_B	N	Operating force
F_Z	N	Loss of the preload force
F_{Smax}	N	Maximum screw force
F_{VM}	N	Assembling preload force

Torques at the thread

$$\varphi = \tan^{-1}\left(\frac{P_h}{d_2 \cdot \pi}\right) = \tan^{-1}\left(\frac{1.5\,\text{mm}}{23.026\,\text{mm} \cdot \pi}\right) = 1.19\,^\circ \tag{3.149}$$

$$\rho' = \tan^{-1}\left(\frac{\mu}{\cos\frac{\beta}{2}}\right) = \tan^{-1}\left(\frac{0.14}{\cos\frac{60\,^\circ}{2}}\right) = 9.18\,^\circ \tag{3.150}$$

$$\begin{aligned} M_G &= F_{VM} \cdot \frac{d_2}{2} \cdot \tan\left(\varphi + \rho'\right) \\ &= 81,556\,\text{N} \cdot \frac{23.026 \cdot 10^{-3}\,\text{m}}{2} \cdot \tan\left(1.19\,^\circ + 9.18\,^\circ\right) \\ &= 172\,\text{Nm} \end{aligned} \tag{3.151}$$

$$\begin{aligned} M_A &= F_{VM}\frac{d_2}{2}\left\{\mu_{ges}\left(\frac{1}{\cos\frac{\beta}{2}} + \frac{d_w + d_h}{2 \cdot d_2}\right) + \tan\varphi\right\} \\ &= 81,556\,\text{N}\ \frac{23.026\,\text{mm}}{2}\left\{0.13\ \left(\frac{1}{\cos\frac{60\,^\circ}{2}} + \frac{36\,\text{mm} + 25\,\text{mm}}{2 \cdot 23.026\,\text{mm}}\right) + \tan 1.19\,^\circ\right\} \\ &= 322,137\,\text{Nmm} \approx 322\,\text{Nm} \end{aligned} \tag{3.152}$$

M_G	Nm	Torque within the thread
M_A	Nm	Assembly tightening torque
P_h	mm	Thread pitch
β	°	Thread angle
φ	°	Helix angle of the thread
ρ'	°	Angle of friction
d_2	mm	Pitch diameter of the thread

Verification of compliance of the admissible limiting values

$$\sigma_M = \frac{F_{Smax}}{A_s} = \frac{82,613\,\text{N}}{401\,\text{mm}^2} = 206\,\text{N/mm}^2 \tag{3.153}$$

A_s	mm^2	Stress cross-section of the screw

$$\tau_t = \frac{M_G}{W_p} = \frac{M_G}{\frac{\pi \cdot d_3^3}{16}} = \frac{172,000\,\text{Nmm}}{\frac{\pi \cdot (22.16\,\text{mm})^3}{16}} = 80.5\,\text{N/mm}^2 \tag{3.154}$$

$$\sigma_{red} = \sqrt{\sigma_M^2 + 3 \cdot \tau_t^2} = \sqrt{(206\,\text{N/mm}^2)^2 + 3 \cdot (80.5\,\text{N/mm}^2)^2} = 249\,\text{N/mm}^2 \tag{3.155}$$

$$\begin{aligned} \sigma_{red} &\leq 0.9 \cdot R_{\text{p }0,2} \\ 249\,\text{N/mm}^2 &\leq 450\,\text{N/mm}^2\ \checkmark \end{aligned} \tag{3.156}$$

σ_M	N/mm^2	Tensile stress
τ_t	N/mm^2	Shear stress
σ_{red}	N/mm^2	Equivalent stress

$$p = \frac{F_{Smax}}{A_p} = \frac{F_{Smax}}{\frac{\pi \cdot \left(d_w^2 - d_h^2\right)}{4}} = \frac{82,613\,\text{N}}{\frac{\pi \cdot \left[(36\,\text{mm})^2 - (25\,\text{mm})^2\right]}{4}} = 157\,\text{N/mm}^2 \tag{3.157}$$

$$\begin{aligned} p &\leq p_G \\ 157\,\text{N/mm}^2 &\leq 220\,\text{N/mm}^2\ \checkmark \end{aligned} \tag{3.158}$$

p	N/mm^2	Contact pressure
p_G	N/mm^2	Permissible contact pressure

3.5 Fastening of the hub

The calculation is according to [8], and the values for the parameters can be found in [9]. For the explanations of the parameters see chapter 3.4.3. The situation of the fastening of the hub is shown in figure 3.14.

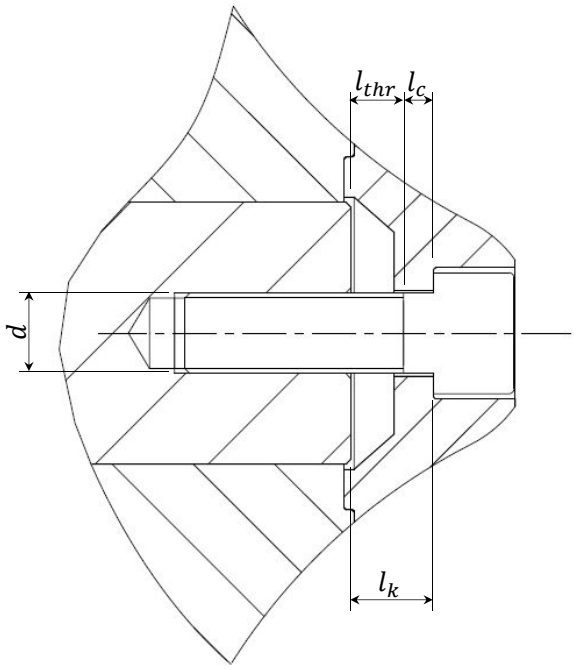

Figure 3.14: Fastening of the hub

3.5.1 Loss of the preload force caused by creep processes F_Z

The elastic resilience of the screw

$$A_N = \frac{d^2 \cdot \pi}{4} = \frac{(16\,\mathrm{mm})^2 \cdot \pi}{4} = 201.1\,\mathrm{mm}^2 \tag{3.159}$$

$$A_3 = \frac{d_3^2 \cdot \pi}{4} = \frac{(13.546\,\mathrm{mm})^2 \cdot \pi}{4} = 144.1\,\mathrm{mm}^2 \tag{3.160}$$

$$\begin{aligned}
\delta_s &= \delta_H + \delta_{C_1} + \delta_{C_2} + \delta_T + \delta_N \\
&= \frac{1}{E}\left\{\frac{0.4 \cdot d}{A_N} + \frac{l_c}{A_N} + \frac{l_{thr}}{A_3} + \frac{0.5 \cdot d}{A_3} + \frac{0.4 \cdot d}{A_N}\right\} \\
&= \frac{1}{210,000\,\mathrm{N/mm}^2}\left\{\frac{0.4 \cdot 16\,\mathrm{mm}}{201.1\,\mathrm{mm}^2} + \frac{6\,\mathrm{mm}}{201.1\,\mathrm{mm}^2} + \right. \\
&\quad \left. + \frac{9.7\,\mathrm{mm}}{144.1\,\mathrm{mm}^2} + \frac{0.5 \cdot 16\,\mathrm{mm}}{144.1\,\mathrm{mm}^2} + \frac{0.4 \cdot 16\,\mathrm{mm}}{201.1\,\mathrm{mm}^2}\right\} \\
&= 10.3 \cdot 10^{-7}\,\mathrm{mm/N}
\end{aligned} \tag{3.161}$$

The elastic resilience of the deformed parts

$$D_A = l_k + d_w = 15.7\,\text{mm} + 24\,\text{mm} = 39.7\,\text{mm} \tag{3.162}$$

$$x = \sqrt[3]{\frac{l_k \cdot d_w}{D_A^2}} = \sqrt[3]{\frac{15.7\,\text{mm} \cdot 24\,\text{mm}}{(39.7\,\text{mm})^2}} = 0.62 \tag{3.163}$$

$$\begin{aligned} A_{rep} &= \frac{\pi}{4} \cdot \left(d_w^2 - d_h^2\right) + \frac{\pi}{8} \cdot d_w \cdot (D_A - d_w) \left[(x+1)^2 - 1\right] \\ &= \frac{\pi}{4} \cdot \left((24\,\text{mm})^2 - (17\,\text{mm})^2\right) + \frac{\pi}{8} \cdot 24\,\text{mm} \cdot (39.7\,\text{mm} - 24\,\text{mm}) \left[(0.62\ +1)^2 - 1\right] \\ &= 466\,\text{mm}^2 \end{aligned} \tag{3.164}$$

$$\delta_t = \frac{l_k}{A_{rep} \cdot E} = \frac{15.7\,\text{mm}}{466\,\text{mm}^2 \cdot 210,000\,\text{N/mm}^2} = 1.6 \cdot 10^{-7}\,\text{mm/N} \tag{3.165}$$

$$F_Z = \frac{f_z}{\delta_s + \delta_t} = \frac{0.008\,\text{mm}}{10.3 \cdot 10^{-7}\,\text{mm/N} + 1.6 \cdot 10^{-7}\,\text{mm/N}} = 6,723\,\text{N} \tag{3.166}$$

3.5.2 Forces at the thread

$$\begin{aligned} F_{VM} &= k_A \left\{ F_{\text{clamp}} + F_B \left(1 - \frac{\delta_t}{\delta_t + \delta_s}\right) + F_Z \right\} \\ &= 1.6 \left\{ 0\,\text{N} + 23,854\,\text{N} \left(1 - \frac{1.6 \cdot 10^{-7}\,\text{mm/N}}{1.6 \cdot 10^{-7}\,\text{mm/N} + 10.3 \cdot 10^{-7}\,\text{mm/N}}\right) + 6,723\,\text{N} \right\} \\ &= 43,792\,\text{N} \end{aligned} \tag{3.167}$$

$$\begin{aligned} F_{Smax} &= F_{VM} + k_A \cdot \frac{\delta_t}{\delta_t + \delta_s} \cdot F_B \\ &= 45,392\,\text{N} + 1.6\ \cdot \frac{1.6 \cdot 10^{-7}\,\text{mm/N}}{1.6 \cdot 10^{-7}\,\text{mm/N} + 10.3 \cdot 10^{-7}\,\text{mm/N}} \cdot 23,854\,\text{N} \\ &= 48,923\,\text{N} \end{aligned} \tag{3.168}$$

3.5.3 Torques at the thread

$$\varphi = \tan^{-1}\left(\frac{P_h}{d_2 \cdot \pi}\right) = \tan^{-1}\left(\frac{2\,\text{mm}}{14.701\,\text{mm} \cdot \pi}\right) = 2.48\,^\circ \tag{3.169}$$

$$\rho' = \tan^{-1}\left(\frac{\mu}{\cos\frac{\beta}{2}}\right) = \tan^{-1}\left(\frac{0.14}{\cos\frac{60\,^\circ}{2}}\right) = 9.18\,^\circ \tag{3.170}$$

$$\begin{aligned} M_G &= F_{VM} \cdot \frac{d_2}{2} \cdot \tan\left(\varphi + \rho'\right) \\ &= 43,792\,\text{N} \cdot \frac{14.701 \cdot 10^{-3}\,\text{m}}{2} \cdot \tan\left(2.48\,^\circ + 9.18\,^\circ\right) \\ &= 66.4\,\text{Nm} \end{aligned} \tag{3.171}$$

$$\begin{aligned} M_A &= F_{VM}\frac{d_2}{2}\left\{\mu_{ges}\left(\frac{1}{\cos\frac{\beta}{2}}+\frac{d_w+d_h}{2\cdot d_2}\right)+\tan\varphi\right\} \\ &= 43,792\,\mathrm{N}\ \frac{14.701\,\mathrm{mm}}{2}\left\{0.13\ \left(\frac{1}{\cos\frac{60\,^\circ}{2}}+\frac{24\,\mathrm{mm}+17\,\mathrm{mm}}{2\cdot 14.701\,\mathrm{mm}}\right)+\tan 2.48\,^\circ\right\} \\ &= 120,614\,\mathrm{Nmm}\approx 121\,\mathrm{Nm} \end{aligned} \tag{3.172}$$

3.5.4 Verification of compliance of the admissible limiting values

$$\sigma_M = \frac{F_{Smax}}{A_s} = \frac{48,923\,\mathrm{N}}{157\,\mathrm{mm}^2} = 312\,\mathrm{N/mm}^2 \tag{3.173}$$

$$\tau_t = \frac{M_G}{W_p} = \frac{M_G}{\frac{\pi\cdot d_3^3}{16}} = \frac{66,400\,\mathrm{Nmm}}{\frac{\pi\cdot(13.546\,\mathrm{mm})^3}{16}} = 136.1\,\mathrm{N/mm}^2 \tag{3.174}$$

$$\sigma_{red} = \sqrt{\sigma_M^2+3\cdot\tau_t^2} = \sqrt{(312\,\mathrm{N/mm^2})^2+3\cdot(136.1\,\mathrm{N/mm^2})^2} = 391.1\,\mathrm{N/mm}^2 \tag{3.175}$$

$$\begin{aligned} \sigma_{red} &\le 0.9\cdot R_{\mathrm{p}\,0,2} \\ 391.1\,\mathrm{N/mm}^2 &\le 900\,\mathrm{N/mm}^2\ \checkmark \end{aligned} \tag{3.176}$$

$$p = \frac{F_{Smax}}{A_p} = \frac{F_{Smax}}{\frac{\pi\cdot\left(d_w^2-d_h^2\right)}{4}} = \frac{48,923\,\mathrm{N}}{\frac{\pi\cdot\left[(24\,\mathrm{mm})^2-(17\,\mathrm{mm})^2\right]}{4}} = 217\,\mathrm{N/mm}^2 \tag{3.177}$$

$$\begin{aligned} p &\le p_G \\ 217\,\mathrm{N/mm}^2 &\le 220\,\mathrm{N/mm}^2\ \checkmark \end{aligned} \tag{3.178}$$

4 Details of the construction

4.1 Fastening of the impeller vanes

The fastening of the impeller vane has to absorb forces and torques caused by the flow and the rotation. The production of the impeller vanes can be seen in figure 4.1. In addition to the main function of a fastening, the impeller vanes have to be rotatable to ensure various positions of the vanes from $-15°$ to $+6°$. This is necessary to make different attempts at different stagger angles. Due to these requirements the position has to be fixed exactly and in a reliable way.

Figure 4.1: Production of the impeller vanes

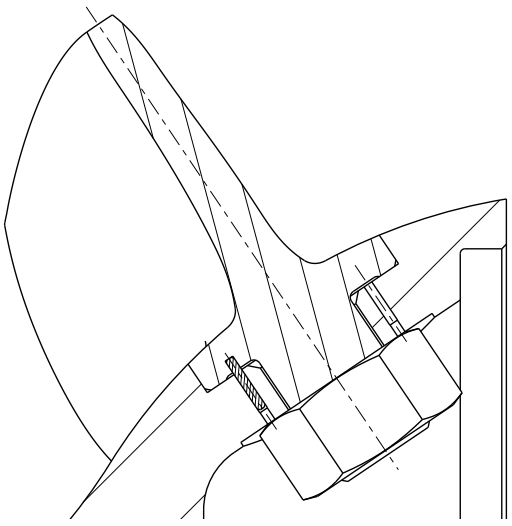

Figure 4.2: Fastening of the impeller vanes

Hereafter, the disadvantages of the various possibilities for the fastening are discussed:

Cylindrical pens

- They have to be very thick to absorb the whole torque.
- They need a lot of space ⇒ the required angle between the different positions would be too big.

Cone-press-connection

- The axial position of the vanes is indeterminate.

Frictional fastening

- It is difficult to ensure the right rotational position.

Due to these drawbacks, the final technical execution, which is shown in figure 4.2, uses a combination of two of these possibilities. A long and thin cylindrical pen makes it possible to guarantee the right position, and the frictional fastening absorbs the forces and torques. The diameter of the plate of the fastening is made as big as possible to reduce the preload force of the screw by enabling a big friction radius. Additionally, the stiffness of the plate is reduced a little bit to keep the rest of the clamping force larger. The cylindrical pens are long enough in order to make visible in which drilling hole they are put during the assembly.

4.2 Bearing

The bearing of the mixed flow pump, which is shown in figure 4.3, has to be very stiff to ensure a small gap between the vanes and the casing and thus very little leakage loss. Furthermore, it has to be as simple as possible to mount and it should have a lifetime of more than 200 hours. Angular contact ball bearings are used for the fixed bearing, since thrust bearings are harder to mount than other bearings and most of the radial bearings cannot withstand the high axial force. They are arranged back-to-back to make the bearing stiffer. A simple radial roller bearing is used as floating bearing, because this bearing does not need to absorb high forces.

4.3 Fastening of the impeller hub

The fastening of the impeller hub has to transfer the torque and the axial force. Furthermore, it has to enable an adjustment of the axial position of the hub. Another requirement is, that the dismounting should be as simple as possible, because it is necessary to remove the hub to adjust the impeller vanes.
Due to these constraints, a press-fit connection and also the cone-frictional-connection would be impractical. A shaft clamping element would have the advantage that the axial force and the torque may be transmitted, but it requires too much space. In the final solution (see figure 4.4), a fitting key transfers the torque and the axial force is transmitted by a central screw.

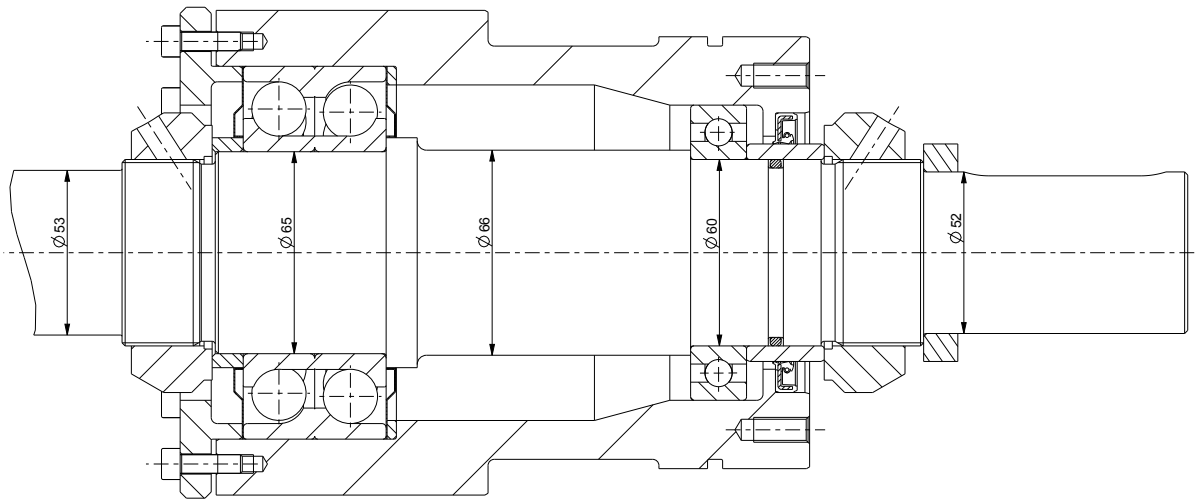

Figure 4.3: Bearing of the pump shaft

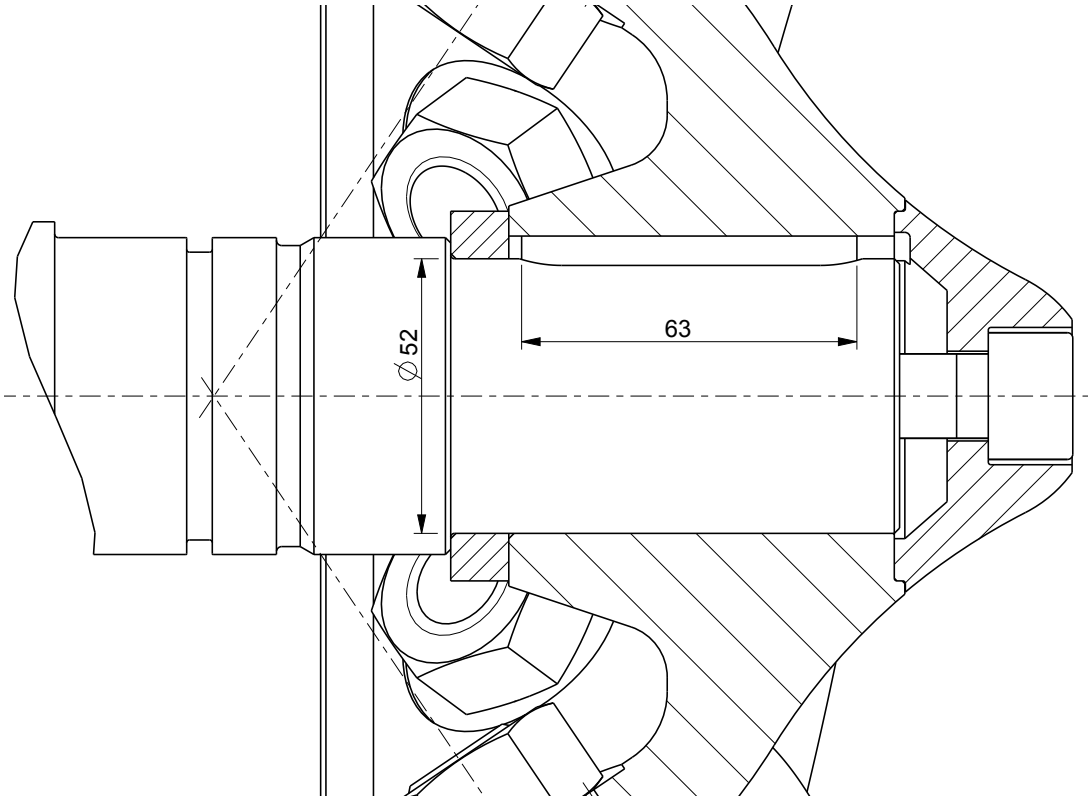

Figure 4.4: Fastening of the impeller hub

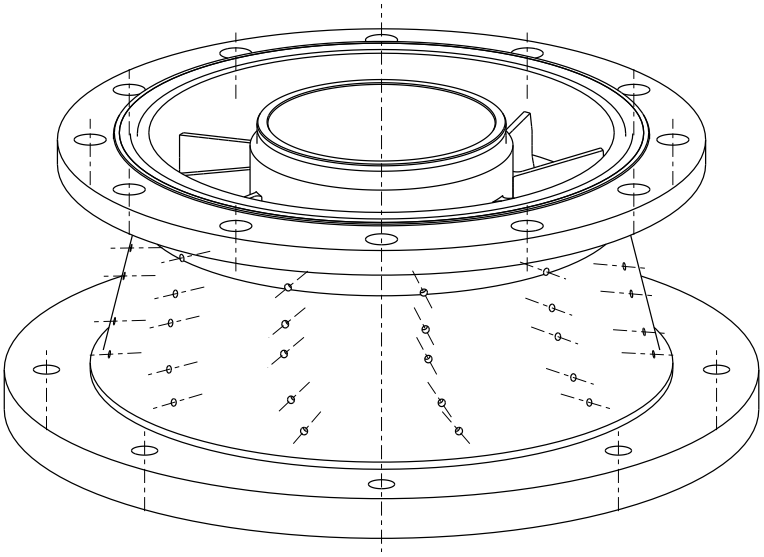

Figure 4.5: Diffuser casing

4.4 Diffuser casing

The diffuser and the casing are mounted together by welding. Therefore, six holes for every vane, which are shown in figure 4.5, are drilled into the casing. After the diffuser is put in the right position, welding points are made to fix them together. The diffuser of the mixed flow pump is milled from one piece, as it would be very difficult to generate the required shape otherwise. To prevent corrosion, the diffuser and the casing are made of stainless steel (1.4301).

4.5 Impeller casing

The impeller casing, which is shown in figures 4.6 and 4.7, has to be lucent to provide an insight into the suction area and the impeller vanes. It is required for the monitoring of cavitation. Therefore, the casing is made of two thick acrylic glass plates which are bonded together. The casing is fixed between O-rings to ensure that it will not be damaged by the mounting forces. To chuck the casing, eight M16 screws with bushings are used. With these screws, the two flanges are braced.

4.6 Coupling

The shaft to drive the pump has to be very long, as the pipe positioned directly behind the impeller and the diffuser has to have a certain length in order to allow measuring the pressure according to standards. Due to the long distance between the electric motor and the impeller, the shaft has to be divided into two parts. To connect these two shafts together, the coupling shown in figure 4.8 is needed. In order to enable the mounting, a pluggable coupling has to be installed. Therefore, a jaw coupling is used which also allows to adjust an offset or a squint.

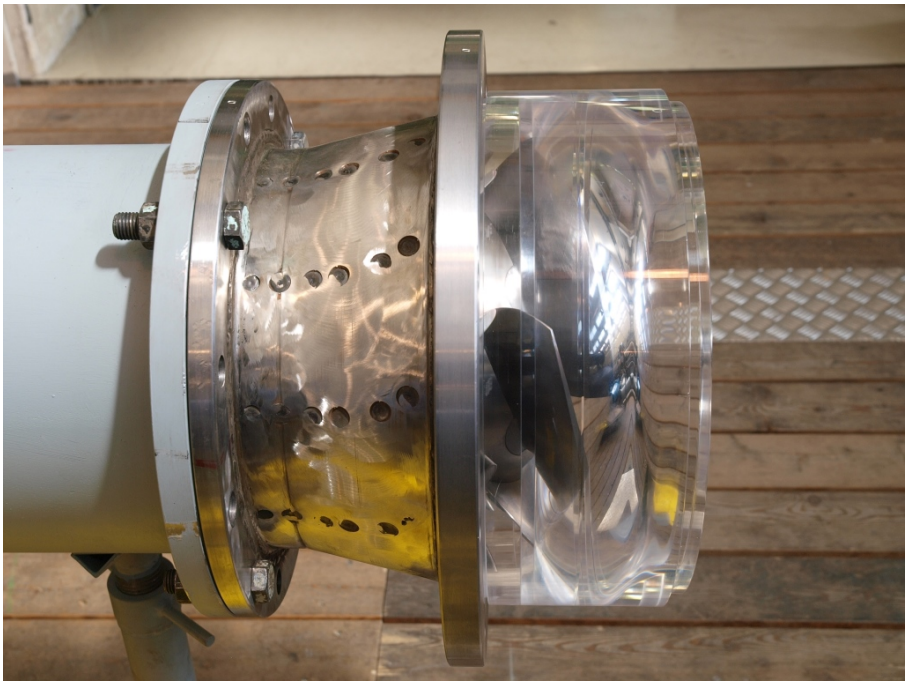

Figure 4.6: Impeller and diffuser casing

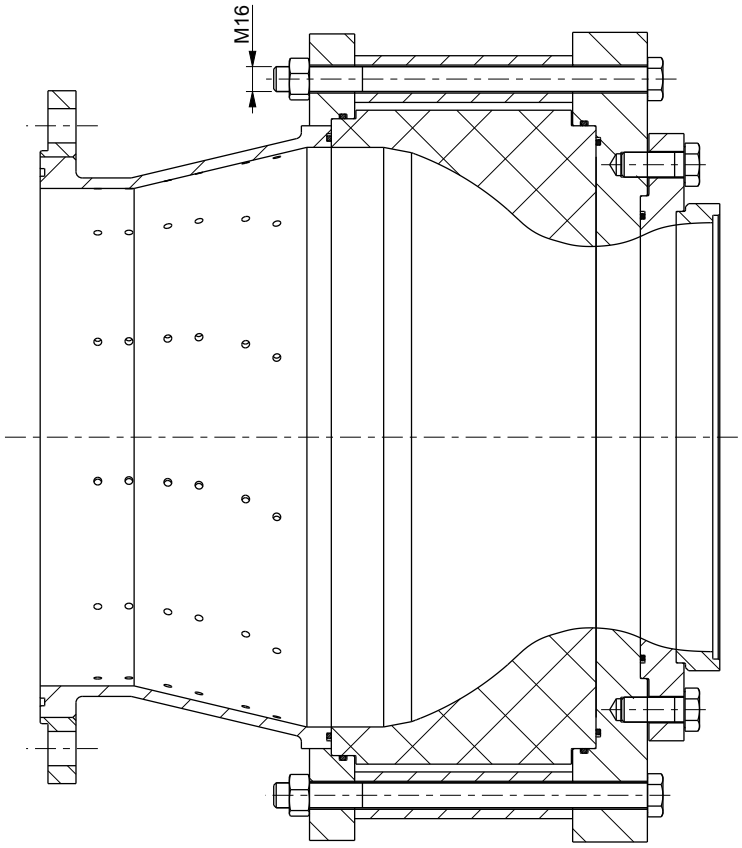

Figure 4.7: Impeller casing

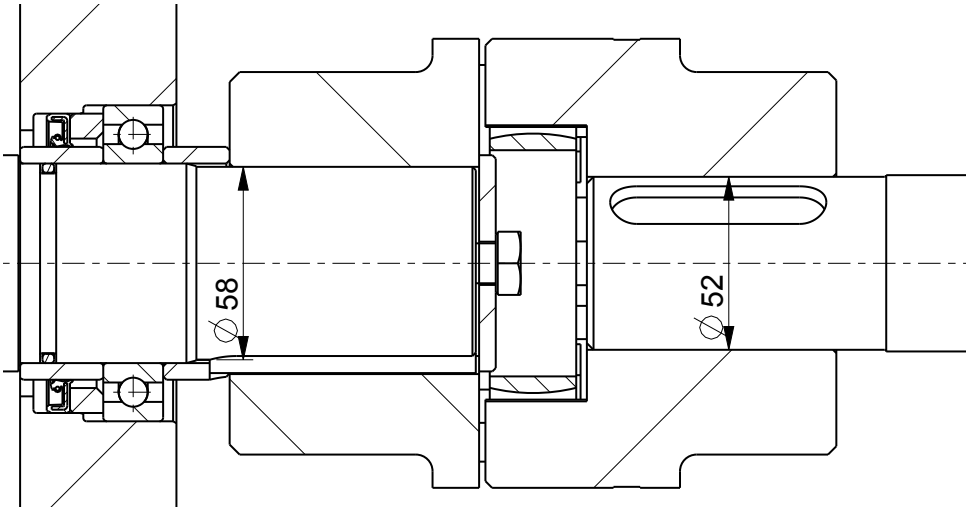

Figure 4.8: Coupling

4.7 Sealing

O-rings are used to seal two stagnated parts like two flanges or the inner pipe and the diffuser. To seal the rotating shaft against the stagnated bearing bushing, a radial shaft sealing is used (see figure 4.3). On the data sheet of the manufacturer (see appendix A.1) the scope of application is shown. It is obvious, that the sealing is able to withstand a pressure of more than 2.5 bars at 1,600 rpm (the flowing medium is oil). The manufacturer declared, that the sealing is able to withstand high pressure over a short period of time (50h) operated with water even if it would be possible that the wear of the touching parts is remarkable. Therefore, an exchangeable hardened inner ring is used.

4.8 Stagger angle of the impeller vane

The stagger angles can be reached with different combinations of the positions of the hub and the vane, which are shown in table 4.1. Figure 4.9 shows these positions.
To be able to control the positions of the vanes, a control value, which is shown in figure 4.12, is given. This value z is the distance between the front edge of the hub and the outlet edge of the vane on the suction side at the outer diameter.

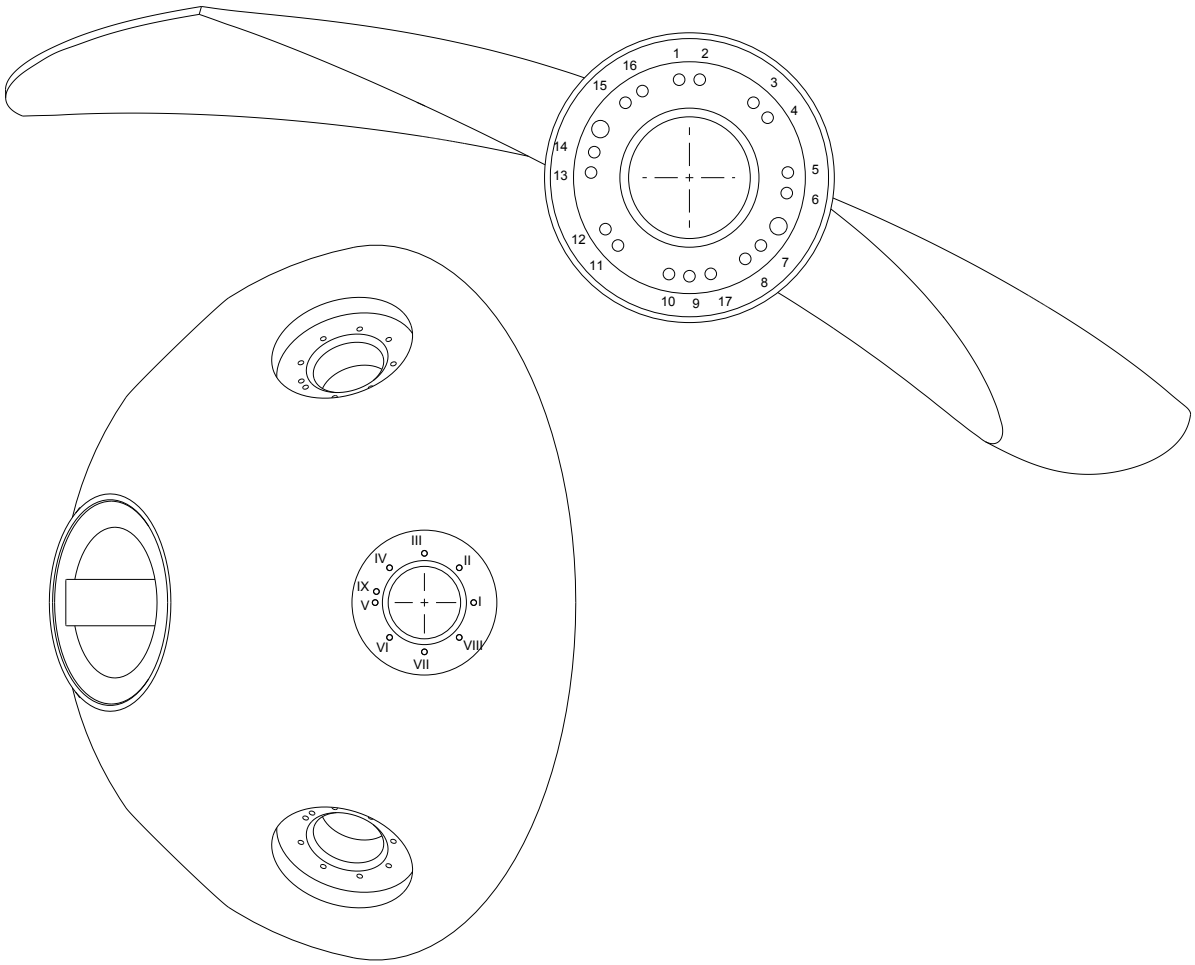

Figure 4.9: Positions of the impeller vane and the hub

Figure 4.10: Impeller

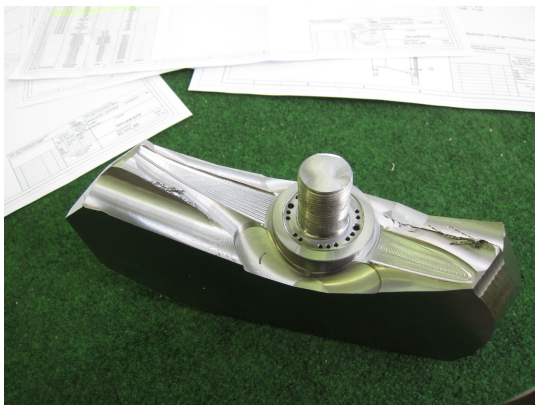

Figure 4.11: Impeller vane

Table 4.1: Stagger angle of the impeller vane

Stagger angle [°]	Position hub	Position vane	Control value z [mm]
6.0	I	1	62.1
4.5	II	3	59.6
3.0	III	5	57.2
1.5	IV	7	54.7
0.0	V	9	52.2
-0.5	IX	17	51.4
-1.5	VI	11	49.7
-3.0	VII	13	47.2
-4.5	VIII	15	44.7
-6.0	I	2	42.2
-7.5	II	4	39.7
-9.0	III	6	37.2
-10.5	IV	8	34.7
-12.0	V	10	32.2
-13.5	VI	12	29.7
-15.0	VII	14	27.2
-16.5	VIII	16	24.7

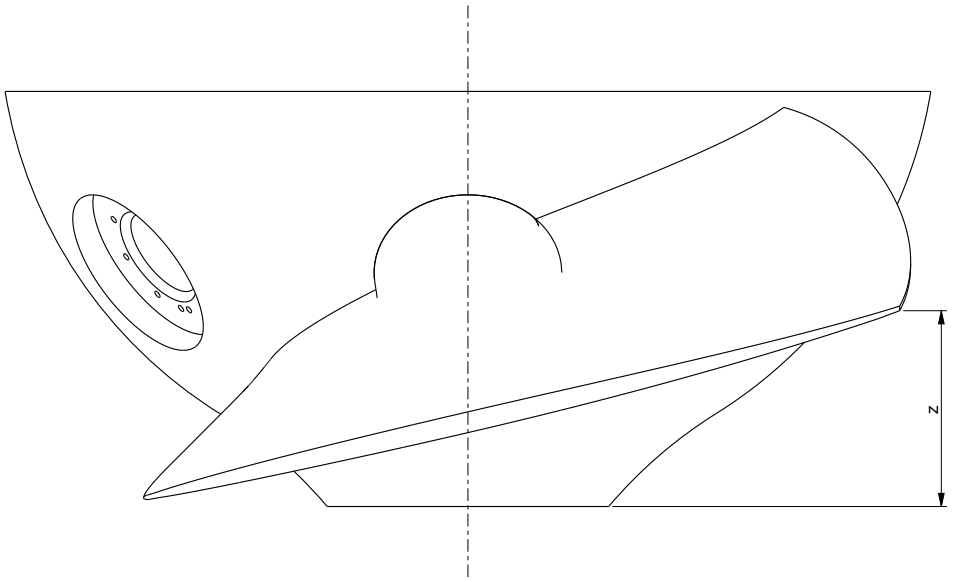

Figure 4.12: Control value z

5 Measurement

The following chapter deals with the measurement procedure in general. Especially the results of the measurements and details about the measurement devices are the main components of this chapter.

5.1 Measurement devices

5.1.1 Flow meter

To be able to measure the discharge, an inductive flow measuring device, with general specifications as shown in table 5.1, is integrated into the test rig.

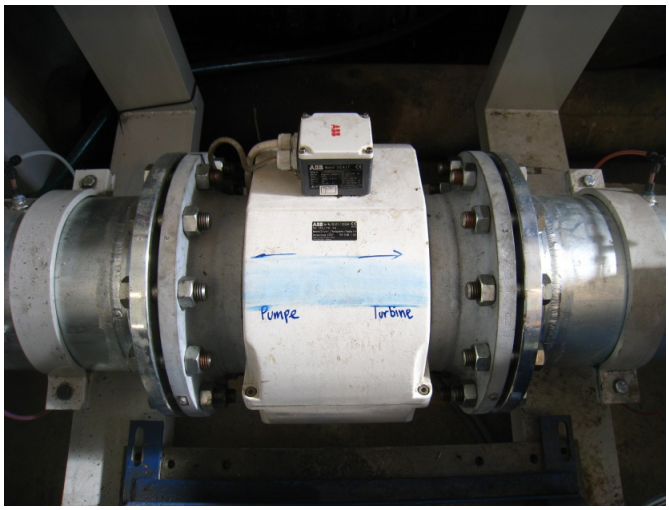

Figure 5.1: Inductive flow measuring device [1]

Table 5.1: General specifications of the flow meter [1]

Manufacturer	ABB
Model	SM4000
Serial no.	SE41F/010461
Nominal diameter	DN250
Max. flow rate	$1,800\,\mathrm{m^3/h}$
Output signal	$4-20\,\mathrm{mA}$

The inductive flow measuring device, which is shown in figure 5.1, is located in a horizontal pipe section between the first and the second floor of the test rig (see figure 1.2).

5.1.2 Pressure gauge

The pressure measuring taps were manufactured according to ISO 9906 [14] (see figure 5.2) and are located two times the diameter away from the flange. At each pressure tapping position, there are four pressure measuring taps, which are displaced by 90° to each other (see figure 5.3). Each single measuring tap is connected to a manifold and separately valved so that it can be read individually. All connecting pipes were carried out with an inner diameter of 6mm.

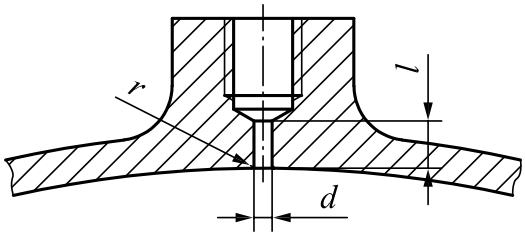

Figure 5.2: Pressure tappings [14]

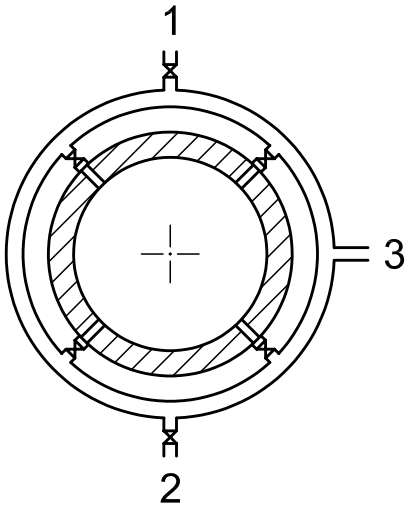

Figure 5.3: Pressure tappings connected by a ring manifold [14]

Differential pressure

A differential pressure transmitter, which is shown in figure 5.4, is integrated into the test rig in order to measure the static differential pressure between the inlet and the outlet of the pump model. The general specifications of the pressure measuring device can be seen in table 5.2.

Absolute pressure

The absolute pressure transmitter, which is shown in figure 5.5, is connected to the pressure measuring tap at the suction pipe. The general specification of this measuring device can be seen in table 5.3.

Table 5.2: General specifications of the differential pressure transmitter [1]

Manufacturer	Rosemount
Model	3051 CD4
Serial no.	7886438 04/04
Measuring range	$Dp = \pm 20\,\text{bar}$
Output signal	$4 - 20\,\text{mA}$

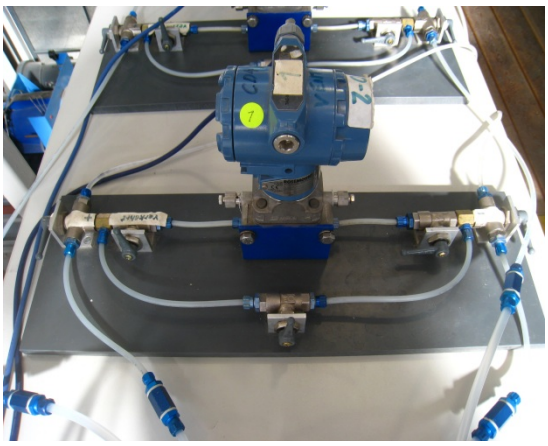

Figure 5.4: Differential pressure transmitter [1]

Table 5.3: General specifications of the absolute pressure transmitter [1]

Manufacturer	Rosemount
Model	3051 CA2
Serial no.	7079927 / 1197
Measuring range	p_{abs} = 0-10 bar
Output signal	$4 - 20\,\text{mA}$

Figure 5.5: Absolute pressure transmitter [1]

5.1.3 Torque meter

The HBM (Hottinger Baldwin) torque and speed measurement flange, which is shown in figure 5.6, is located between the driving shaft of the electric motor and the driving shaft of the pump model. The two shafts and the measurement flange are connected by a curved tooth coupling (Tacke SBG50 Spezial Bogenzahn-Kupplung®), which is part of the measurement device. The general specifications of the torque meter are shown in table 5.4.

Table 5.4: General specifications of the torque meter

Manufacturer	HBM
Model	T30FNA
Serial no.	G 65993
Measuring range	M = ± 1000 Nm
Output signal (speed)	inductive, 30 impulses p. rev.
Output signal (torque)	5-15kHz

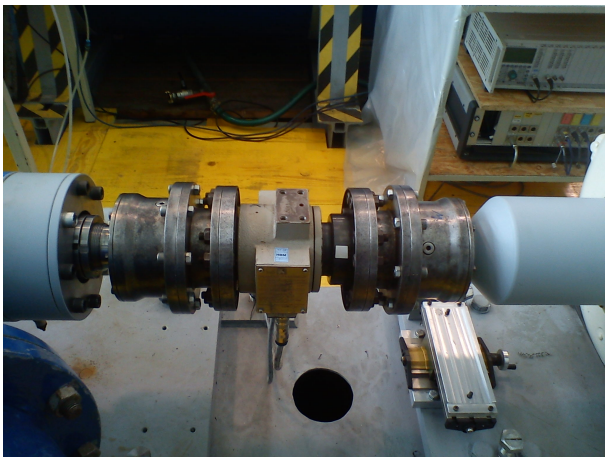

Figure 5.6: Torque meter

5.1.4 Temperature transmitter

For the measurement of the water temperature, a PT100 temperature sensor with the following general specifications is used.

Table 5.5: General specifications of the temperature transmitter [1]

Manufacturer	Conatex
Accuracy class	DIN EN 60751 Class B
Output signal	4-20 mA

5.1.5 Calibration of the flow measurement device

To calibrate the flow measurement device, the volumetric method using a calibrated volumetric tank according to the IEC standard 60193 [17] was used. This method delivers an averaged value of the discharge during the measuring time, which can be calculated with formula 5.1. The measurement is carried out during a steady-state and stable operating point as long as a certain quantity of water in the volumetric tank is collected [1].

$$Q_{Ave} = \frac{\int_0^{t_{meas}} Q(t)dt}{t_{meas}} \cong \frac{V_{water}}{t_{meas}} \tag{5.1}$$

Q_{Ave}	l/s	Averaged value of the discharge
$Q(t)$	l/s	Discharge at the moment t
t_{meas}	s	Measuring time
V_{water}	l	Increase of the water volume in the tank

To be able to switch from the main water cycle of the test rig to the calibration cycle, a swinging chute is used. When the swinging chute is switched to the calibration mode, the measuring time starts and water is collected with the calibrated water tank. The increase of the water volume in the tank is measured by the measurement of the water level inside the tank. The relation between the water volume and the water level in the tank is shown in figure 5.7, which is based on a separate calibration of the volumetric tank. The maximum relative measurement error using the linear approximation shown in figure 5.7 is 0.04% [1].

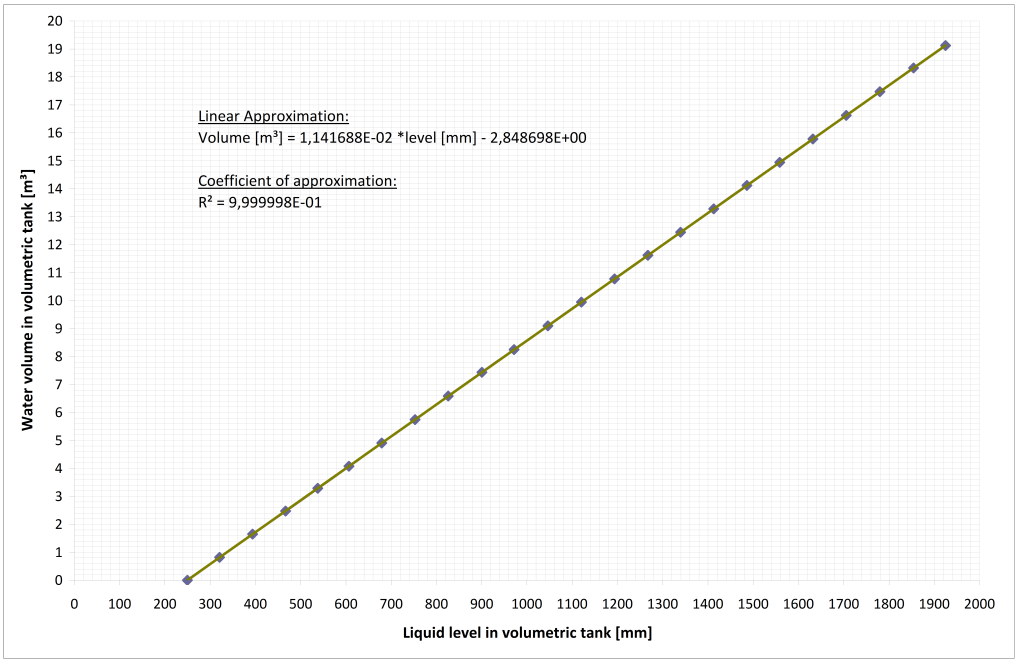

Figure 5.7: Calibration of the volumetric water tank-relation between the water level and the water volume [1]

During the measurements, the increase of the water volume in the volumetric tank was kept constant at $V_{water} = 7\,\mathrm{m}^3$ for different values of the discharge. Due to the different

flow rates the measuring time t_{meas} varied between 15 seconds for high flow rates and 600 seconds for low flow rates. Therefore, the maximum relative error in time appearing during the calibration can be written as [1]:

$$f_{tS} = \frac{t_{switch}}{t_{meas}} = \frac{0.02\,\mathrm{s}}{15\,\mathrm{s}} = \pm 0.133\% \tag{5.2}$$

The calibration of the inductive flow measurement device was carried out for a flow rate between $Q = 10\,\mathrm{l/s}$ and $Q = 375\,\mathrm{l/s}$. The calibration line shows the relation between the indicated measurement value, which can be determined by means of the measured reference value of the discharge and the current output of the flow measurement device. Due to the nonlinearity of the calibration line for flow rates below $Q = 50\,\mathrm{l/s}$, a polynomial relation with a strongly developed linear part was needed. The calibration line for the flow direction in pump-mode is shown in figure 5.8 [1].

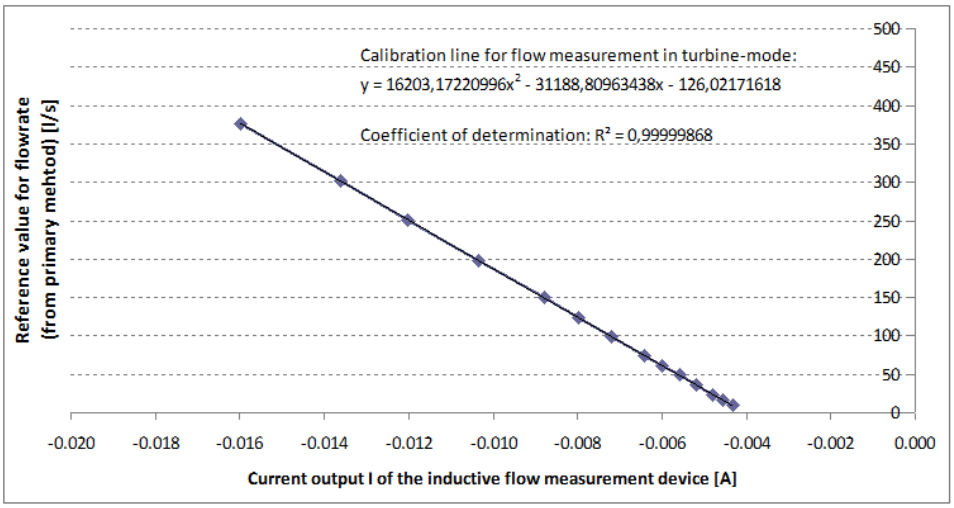

Figure 5.8: Calibration line for the flow rate in pump-mode [1]

The absolute measurement error F_{abs}, which is shown in figure 5.9, was determined by means of a repeated measurement series in the range of $Q = 10 - 375\,\mathrm{l/s}$ using the calibration line shown in figure 5.8. The red dotted line refers to a relative measurement error of 0.3%. The calculation of the relative measurement error is shown in formula 5.3 [1].

$$F_{rel} = \frac{Q_{\text{reference}} - Q_{\text{indicated}}}{Q_{\text{reference}}} \cdot 100 \tag{5.3}$$

F_{rel}	%	Relative measurement error
$Q_{\text{reference}}$	l/s	Flow rate gained from primary method
$Q_{\text{indicated}}$	l/s	Flow rate actually indicated by the flow measurement device

ABB, the manufacturer of the inductive flow measurement device, guarantees a maximum relative measurement error of $F_{rel} < 0.5\%$ within a measurement range of $Q = 30{-}500\,\mathrm{l/s}$. The calibration results indicate that they are considerably better than the guarantees of ABB in a wide range of flow rates. On the other hand, figure 5.9 shows a quadratic increase of the relative measurement error for flow rates below $Q = 50\,\mathrm{l/s}$ [1].

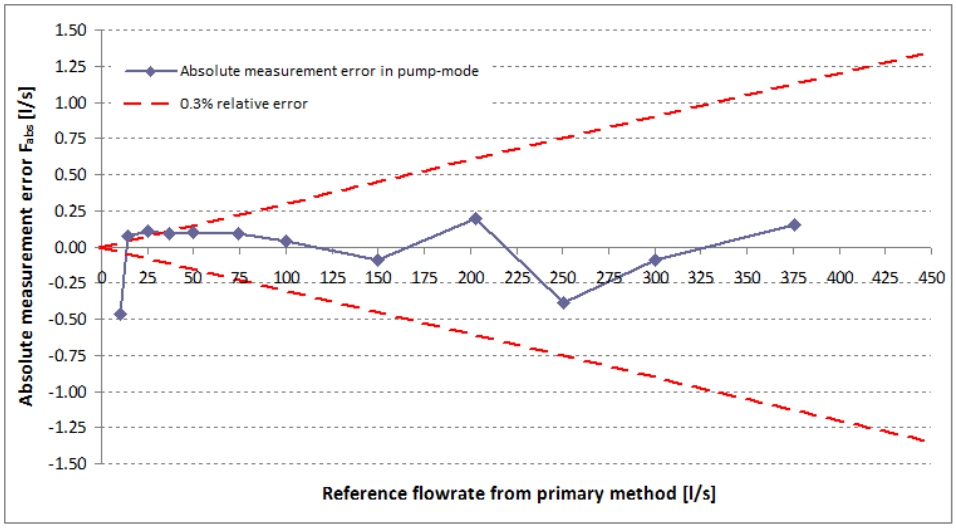

Figure 5.9: Absolute measurement error for each measured value of flow rate in pump-mode [1]

5.1.6 Measuring uncertainties

The measuring uncertainties are determined with the help of the individual uncertainties of the main parameters, which characterize the hydraulic performance. The values $e_{*,s}$ describe the systematic uncertainties based on previous measurements or manufacturer informations.
According to measurement results, the random uncertainty $e_{*,r}$ (based on the determined repeatability) accounts for maximum $\pm 0.15\,\%$ [1].

Discharge

a)	Calibration of volumetric tank	$\pm 0.04\,\%$ [1]
b)	Error in density of water	$\pm 0.02\,\%$ [1]
c)	Error in time	$\pm 0.133\,\%$ [1]
d)	Calibration of volumetric tank	$\pm 0.30\,\%$ [1]

The systematic uncertainty of the discharge can be calculated with formula 5.4.

$$\begin{aligned} e_{Q,s} &= \sqrt{e_{a,s}^2 + e_{b,s}^2 + e_{c,s}^2 + e_{d,s}^2} \\ &= \sqrt{(0.04\,\%)^2 + (0.02\,\%)^2 + (0.133\,\%)^2 + (0.30\,\%)^2} = \pm 0.331\,\% \end{aligned} \tag{5.4}$$

The overall uncertainty of the discharge can be written as:

$$e_Q = \sqrt{e_{Q,s}^2 + e_{Q,r}^2} = \sqrt{(0.331\,\%)^2 + (0.15\,\%)^2} = \pm 0.363\,\% \tag{5.5}$$

Differential head

$$e_{H,s} = \pm 0.15\,\%[1]$$

The overall uncertainty of the differential head can be written as:

$$e_H = \sqrt{e_{H,s}^2 + e_{H,r}^2} = \sqrt{(0.15\,\%)^2 + (0.15\,\%)^2} = \pm 0.212\,\% \tag{5.6}$$

Torque

$$e_{T,s} = \pm 0.15\,\%[1]$$

The overall uncertainty of the torque can be written as:

$$e_T = \sqrt{e_{T,s}^2 + e_{T,r}^2} = \sqrt{(0.15\,\%)^2 + (0.15\,\%)^2} = \pm 0.212\,\% \tag{5.7}$$

Rotational speed

$$e_{n,s} = \pm 0.1\,\%[1]$$

The overall uncertainty of the rotational speed can be written as:

$$e_n = \sqrt{e_{n,s}^2 + e_{n,r}^2} = \sqrt{(0.1\,\%)^2 + (0.15\,\%)^2} = \pm 0.18\,\% \tag{5.8}$$

Pump efficiency

The uncertainty of the pump efficiency can be calculated according to chapter 2.4.4.

$$\begin{aligned} e_{\eta,s} &= \sqrt{e_{Q,s}^2 + e_{H,s}^2 + e_{T,s}^2 + e_{n,s}^2} \\ &= \sqrt{(0.331\,\%)^2 + (0.15\,\%)^2 + (0.15\,\%)^2 + (0.1\,\%)^2} = \pm 0.406\,\% \end{aligned}$$

The overall uncertainty of the pump efficiency can be written as:

$$e_\eta = \sqrt{e_{\eta,s}^2 + e_{\eta,r}^2} = \sqrt{(0.406\,\%)^2 + 4 \cdot (0.15\,\%)^2} = \pm 0.505\,\% \tag{5.9}$$

The overall uncertainties in this measurement compared with the permissible values (see chapter 2.4.4) show, that this measurement is considerably more precise than it has to be.

5.2 Measurement results

For each point of measurement, the averaged values for all relevant quantities are determined and digitally stored in a table. The averaged value of a quantity is equivalent to the arithmetic average of 20 single measuring points (one measurement per second). The measuring values of the relevant quantities are determined with the measurement devices described in chapter 5.1.

To enable the comparability between the prototype and the model, the determined pump efficiency has to be corrected. One reason for the correction is the friction torque caused by the sealing and bearings. The other reason is, that the model and the prototype are operated at flowing conditions with different Reynolds numbers. The Reynolds number

describes the influences of the pump dimension, the rotational speed and the viscosity.

The friction torque was measured in a way, that the influence of the flowing water was kept to a minimum. So, this measurement was carried out without the impeller wheel at different pressures and rotational speeds. The correction of the mechanic power was realized with the help of a fourth order polynomial interpolation of the measured friction torque curve (p-abs=4.5bar). The measured curves and the interpolation (black line) can be seen in figure 5.10.

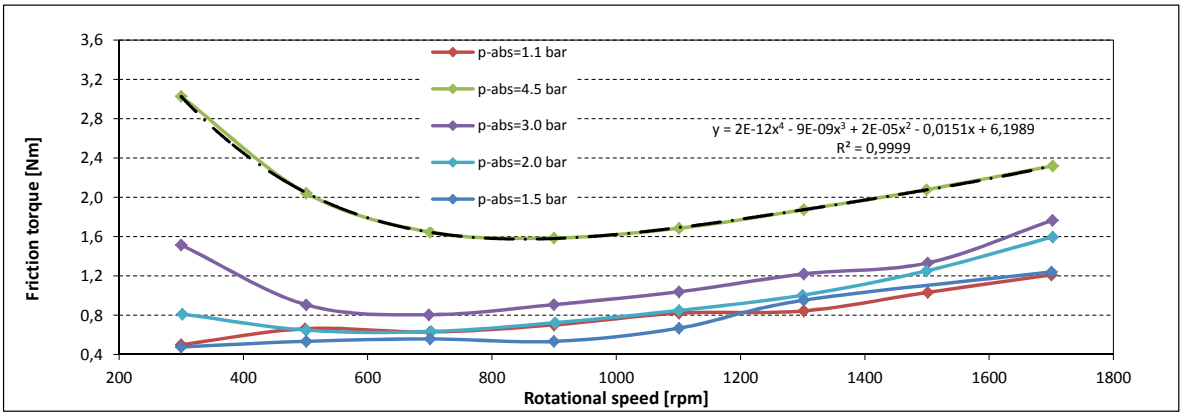

Figure 5.10: Measured friction torque and polynomial approximation

The corrected mechanical power $P_{M,cor}$ can be calculated with:

$$P_{M,cor} = P_M - \left(a \cdot n^4 - b \cdot n^3 + c \cdot n^2 - d \cdot n + e\right) \cdot \frac{2 \cdot \pi \cdot n}{60} \tag{5.10}$$

a		$1.572042 \cdot 10^{-12}$	$\mathrm{Nm} \cdot \mathrm{min}^4$
b		$8.501480 \cdot 10^{-9}$	$\mathrm{Nm} \cdot \mathrm{min}^3$
c		$1.744264 \cdot 10^{-5}$	$\mathrm{Nm} \cdot \mathrm{min}^2$
d		$1.509014 \cdot 10^{-2}$	$\mathrm{Nm} \cdot \mathrm{min}$
e		6.198855	Nm
n	Rotational speed		rpm

With $P_{M,cor}$, the corrected pump efficiency of the model $\eta_{cor,M}$ can be written as:

$$\eta_{cor,M} = \frac{P_H}{P_{M,cor}} \tag{5.11}$$

The procedure of the scale-up of the pump efficiency is according to the IEC standard [17]. There, the losses are divided into parts which can be scaled-up (dependent on the Reynolds number) and parts which cannot be scaled-up. The part of the hydraulic losses which is caused by friction is an example for losses which can be scaled-up.

The corrected pump efficiency η_{cor} can be calculated with equation 5.12.

$$\eta_{cor} = \eta_{cor,M} + (\Delta\eta)_{M \to P} \tag{5.12}$$

With equations 5.13, 5.14 and 5.15, the difference of the pump efficiency caused by the scale-up $(\Delta\eta)_{M\to P}$ can be calculated [17].

$$(\Delta\eta)_{M\to P} = \delta_{ref} \cdot \left[\left(\frac{Re_{ref}}{Re_M} \right)^{0.16} - \left(\frac{Re_{ref}}{Re_P} \right)^{0.16} \right] \tag{5.13}$$

$$\delta_{ref} = \frac{1 - \eta_{opt,M}}{\left(\frac{Re_{ref}}{Re_{opt,M}} \right)^{0.16} + \frac{1 - V_{ref}}{V_{ref}}} \tag{5.14}$$

$$Re_P = \frac{\omega \cdot D_{ref,P}^2}{\nu} = \frac{\frac{\pi \cdot n}{60} \cdot D_{ref,P}^2}{\nu} = \frac{\frac{\pi \cdot 507\,\mathrm{rpm}}{60} \cdot (1.16064\,\mathrm{m})^2}{1 \cdot 10^{-6}\,\mathrm{m^2/s}} = 35,760,341 \tag{5.15}$$

ν	$\mathrm{m^2/s}$	Kinematic viscosity
ω	$\mathrm{s^{-1}}$	Angular velocity
$D_{ref,P}$	m	Reference diameter of the prototype
Re_M		Reynolds number of the model
$Re_{opt,M}$		Reynolds number of the model at $\eta_{opt,M}$
Re_P		Reynolds number of the prototype
Re_{ref}	$7 \cdot 10^6$	Reference Reynolds number (see [17])
V_{ref}	0.6	Loss distribution coefficient (see [17])
$\eta_{opt,M}$		Maximum of the pump efficiency of the model

For the sake of simplicity, figures 5.11 to 5.14 are plotted without any details about the uncertainties. To be able to compare the results of the measurements of the pump model with the guarantees of the prototype, non-dimensional characteristics are used. In figure 5.11, the measured head curves of the pump model at different stagger angles can be seen. The head coefficient and the flow coefficient were standardized and refer to the coefficients of the guaranteed operating point.

Furthermore, the tolerance of the guaranteed point is plotted to show, at which position of the impeller vanes the implementation of the guarantees can be achieved best. It can be seen, that the head curve of the $-0.5°$position hits the guaranteed point best. Furthermore, in figure 5.11 an instability at about 60 percent of the discharge at the best point, caused by complex flow conditions, can be recognized.

In figure 5.12 the corrected pump efficiencies depending on the flow coefficient are shown. The efficiency and the flow coefficient were standardized and refer to the values of the guaranteed operation point.

The implementation of the guaranteed operating point is shown in figure 5.13. A detailed description of the procedure to provide evidence of the implementation of the guarantees is given in chapter 2.4.2.

As seen in figure 5.11, the position of the impeller vanes with a stagger angle of $-0.5°$provides the best result to implement the guarantees. In figure 5.13, the tolerances refer to the pump test acceptance grade 2B.

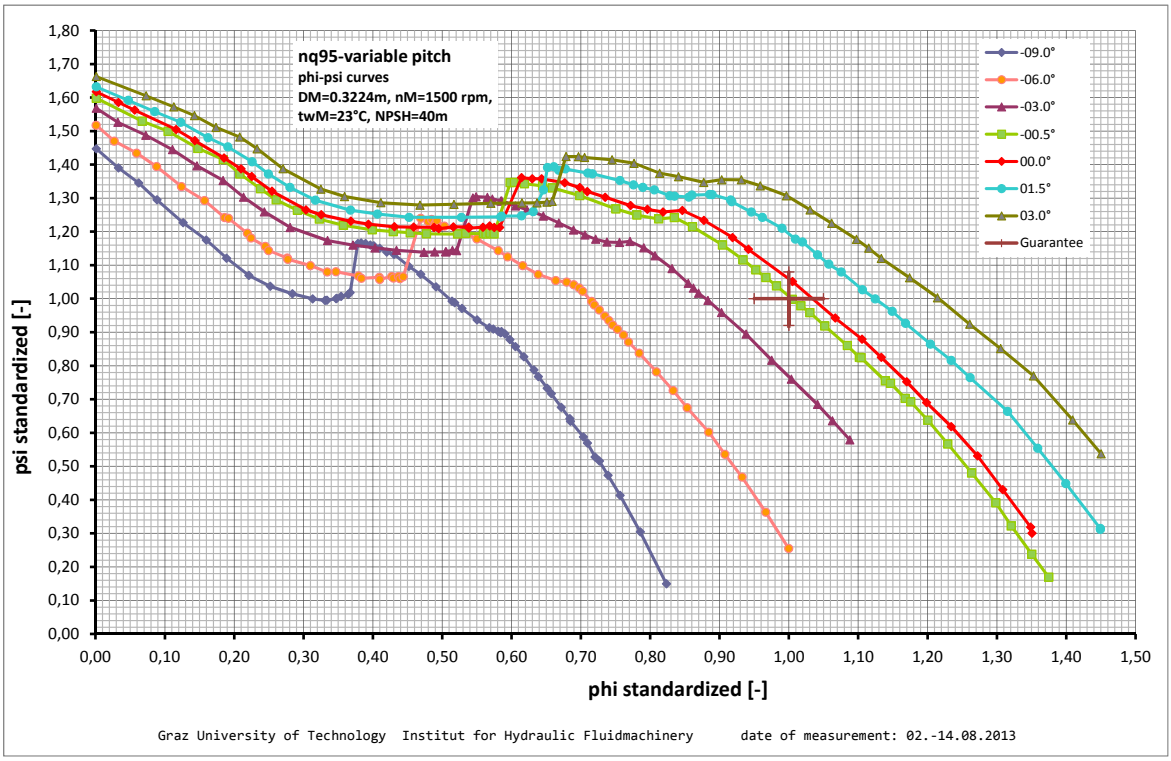

Figure 5.11: Phi-psi curves for different impeller vane positions

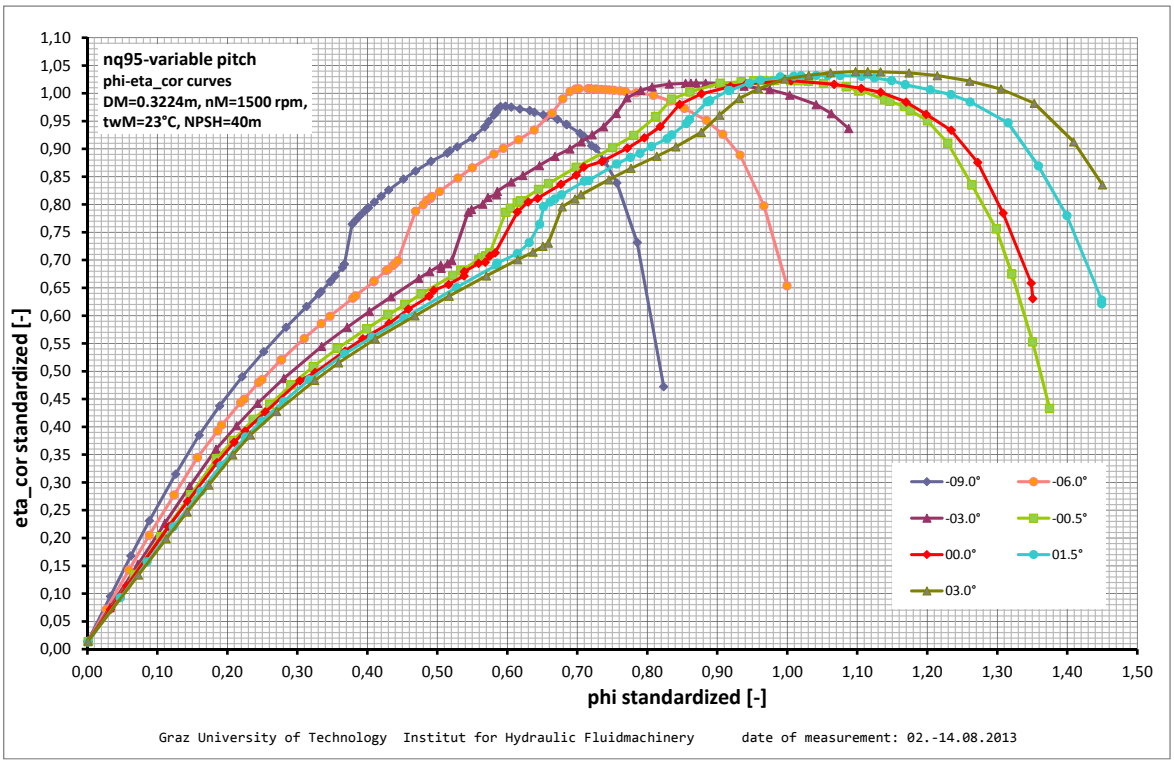

Figure 5.12: Eta-psi curves for different impeller vane positions

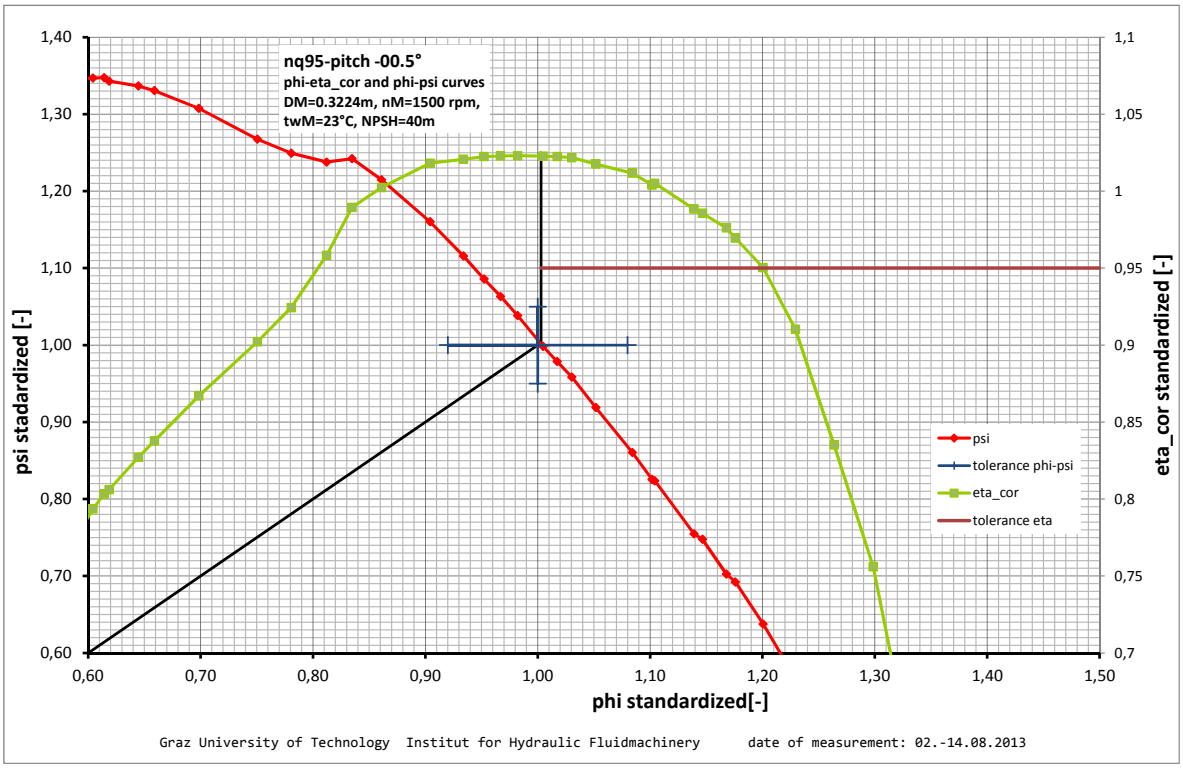

Figure 5.13: Implementation of the guarantees

Figure 5.14 shows the measured NSS_3 values at different stagger angles. The NSS_3 values and the flow coefficient were standardized and refer to the values of the guaranteed operation point.

In figures 5.13 and 5.14 it can be seen, that the requirements were met. For the definitions of single characteristics see chapter 2. For reasons of discretion all characteristics used had to be standardized, but their qualitative meaning is still the same.

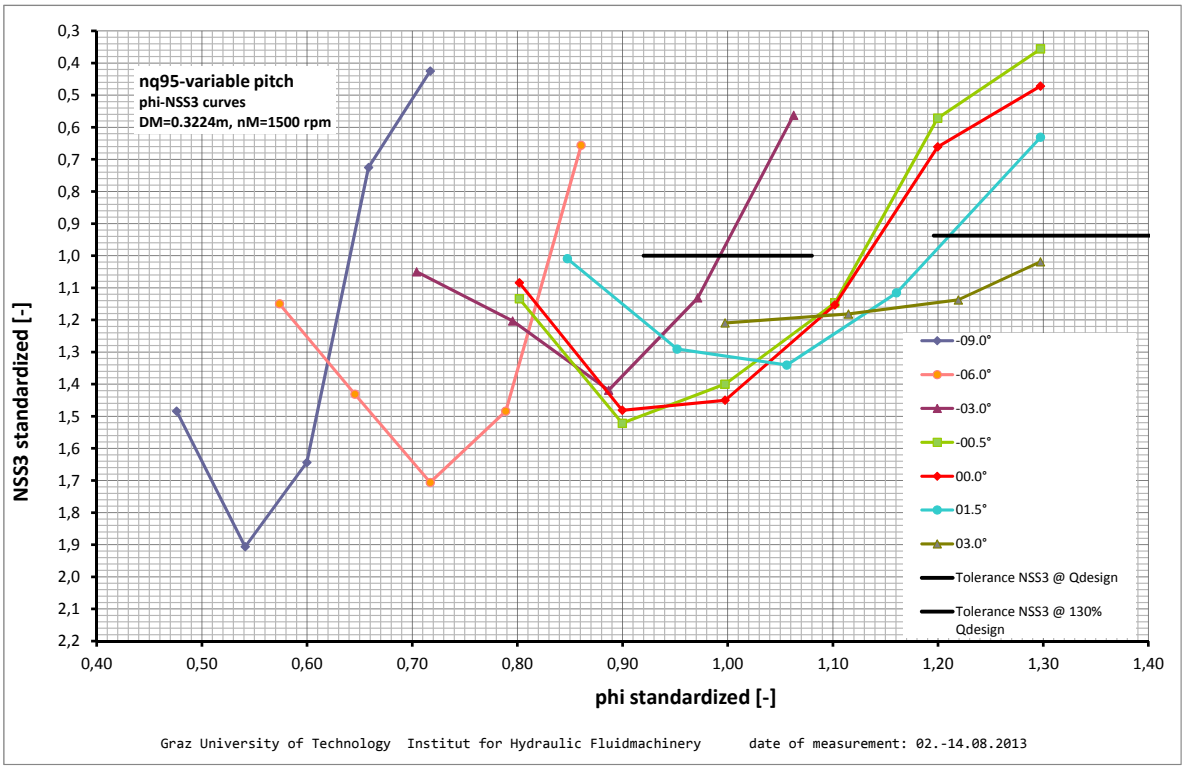

Figure 5.14: NSS_3-phi curves for different impeller vane positions

6 Summary and outlook

The measurements of the model pump prove that the requirements of the customer were met. The results of the measurements also show that the expectations of the CFD calculation were fulfilled for the most part. The results of the CFD calculation were a little bit too conservative. The CFD-result was corrected with a small offset to lower values to be on the safe side. The correlation between the results of the *NPSH*-value of the CFD and experimental set up is remarkable. It follows, that the position of the impeller vanes, to reach the guaranteed point, was not 0.0°. This fact was considered in advance with an additional position of the impeller vane at an angel of −0.5°.

After the first diffuser was designed and manufactured, the customer decided to try out another diffuser, which should be weldable (see figures 6.1 and 6.2). Another set of measurements with the new type of diffuser is going to be the next step in this project. It is suspected, that the second diffuser will lead to worse results, however it should be able to meet the guarantees too. As of time requirements, the results of the second diffuser are not part of this master thesis.

Finally, this master thesis has been a valuable project in order to see how a pump is manufactured and tested and which challenges have to be met.

Figure 6.1: Diffuser with eleven vanes (tested type)

Figure 6.2: Diffuser with seven vanes (new type)

List of Figures

List of Tables

References

[1] Benigni H., Höller S., Jaberg H.: *Mixed Flow Pump: Answers to Appendix C*, Version: $28^{th}$of June 2013, Rev. 1.0.

[2] Benigni H., Höller S., Jaberg H.: *Mixed Flow Pump: Hydraulic profile, meridional section*, Version: $5^{th}$of May 2013, Rev. 1.0.

[3] Gülich Johann F.: *Kreiselpumpen*, 3. Auflage, Springer, Berlin-Heidelberg 2010.

[4] Haberhauer H., Bodenstein F.: *Maschinenelemente: Gestaltung, Berechnung, Anwendung*, 16. Auflage, Springer, Heidelberg/Berlin 2011.

[5] Handl J.: *Aufbau eines Axialpumpenprüfstandes, Diplomarbeit*, Institut für hydraulische Strömungsmaschinen TU Graz, Graz 2009.

[6] KSB Aktiengesellschaft, Frankenthal: *Nass aufgestellte Pumpen*, www.ksb.com, Abfrage 12.08.2013.

[7] Lerch R.: *Elektrische Messtechnik*, 6. Auflage, Springer, Berlin-Heidelberg 2012.

[8] Matek W., Muhs D., Wittel H., Becker M., Jannasch D.: *Roloff/Matek Maschinenelemente*, 15. Auflage, Vieweg, Braunschweig/Wiesbaden 2001.

[9] Matek W., Muhs D., Wittel H., Becker M., Jannasch D.: *Roloff/Matek Maschinenelemente Tabellen*, 15. Auflage, Vieweg, Braunschweig/Wiesbaden 2001.

[10] NKE: *General Catalogue*, 2012/04.

[11] Norm DIN 1319: *Grundlagen der Meßtechnik, Teil 1: Grundbegriffe*, 1995-01.

[12] Norm DIN 1319: *Grundlagen der Meßtechnik, Teil 3: Auswertung von Messungen einer einzelnen Meßgröße, Meßunsicherheit*, 1996-05.

[13] Norm EN ISO 5198: *Kreiselpumpen (Radial-, Halbaxial- und Axialkreiselpumpen) Regeln für die Messung des hydraulischen Betriebsverhaltens, Präzisionsklasse*, Ausgabe 1999-08-01.

[14] Norm EN ISO 9906: *Rotodynamic pumps − Hydraulic performance acceptance tests − Grades 1,2 and 3*, English version: 2013/03.

[15] Norm EN ISO 9906: *Kreiselpumpen − Hydraulische Abnahmeprüfung Klassen 1 und 2*, Ausgabe: 2002-07-01.

[16] Norm EN ISO 13709: *Centrifugal pumps for petroleum, petrochemical and natural gas industries*, 2003.

[17] Norm IEC 60193: *Hydraulic turbines, storage pumps and pump-turbines – Model acceptance tests*, 2. Auflage, 1999.

[18] Pfleiderer C., Pettermann H.: *Strömungsmaschinen*, 7. Auflage, Springer, Berlin-Heidelberg 2005.

[19] Sigloch H.: *Technische Fluidmechanik*, 8. Auflage, Springer, Berlin-Heidelberg 2012.

[20] Sulzer Pumps: *Vertikalpumpen für die Nassaufstellung*, www.sulzer.com, Abfrage 12.08.2013.

Appendix

A Datasheets

A.1 Datasheet of the radial shaft sealing

Simmerring BABSL (NBR)

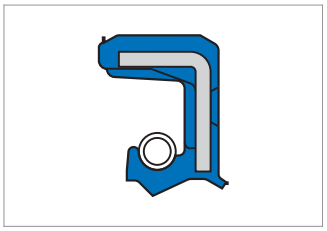

Produktbeschreibung

Druckbelastbare, ohne Stützring verwendbare Bauform für den Einsatz in druckbeaufschlagten Aggregaten wie Hydropumpen, -motoren und hydrodynamischen Kupplungen. Mit zusätzlicher Staublippe gegen Schmutzanfall von außen.

Produktvorteile

- Einsatz vorzugsweise in druckbeaufschlagten Aggregaten
- Sichere Abdichtung zur Gehäusebohrung, auch bei erhöhter Rauheit der Bohrung, Wärmedehnung und geteilten Gehäusen
- Vorteile bei Abdichtung von dünnflüssigen und gasförmigen Medien
- Zusätzliche Schutzlippe gegen mäßigen und mittleren Staub- und Schmutzanfall von außen
- Geringer axialer Bauraum (Hinweis: kann zu Temperaturerhöhung durch Reibungswärme führen)

Produkteigenschaften

- Außenmantel: Elastomer
- Kurze, flexible, federbelastete Dichtlippe
- Zusätzliche Schutzlippe

Anwendungsbereich

- 2-Takt Motoren
- Hydrostatische Antriebe (Pumpen, Motoren aller Art)

Werkstoff

Werkstoff	Acrylnitril-Butadien-Kautschuk
Bezeichnung	72 NBR 902
Farbe	blau
Härte	75 Shore A

Komponenten

Versteifungsblech	unlegierter Stahl DIN EN 10027-1
Feder	Federstahl DIN EN 10270-1

Einsatzbereich

Medien	Mineralöle, synthetische Öle*
T	−40 ... +100 °C
P	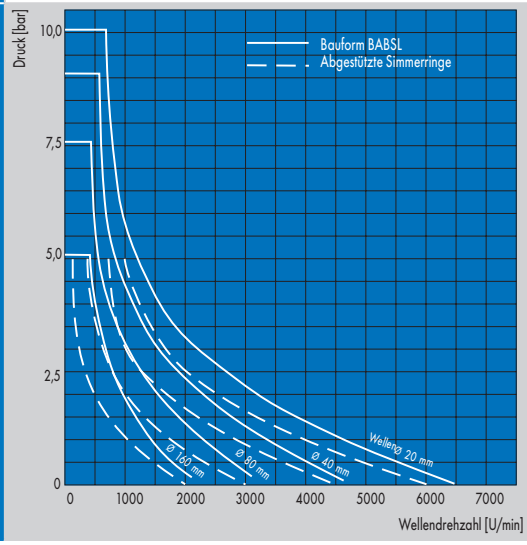

Zulässiger Druck im Aggregat für Simmerringe (Bauform BABSL), sowie für abgestützte Simmerringe.
* Bei synthetischen Ölen (Polyalkylenglykolen/Polyalphaolefinen, → Technisches Handbuch ist zu beachten, dass die maximale Einsatztemperatur 80 °C nicht übersteigen darf.

Zulässige Maximalwerte in Abhängigkeit der übrigen Betriebsbedingungen.

Einbau und Montage

Welle

Toleranz	ISO h 11
Rundheit	IT 8
Rauheit	R_a = 0,2 ... 0,4 µm
	R_z = 1,0 ... 3,0 µm
	R_{max} ≤ 6,3 µm
Härte	45 ... 60 HRC
Beschaffenheit	drallfrei, vorzugsweise im Einstich geschliffen

Gehäusebohrung

Toleranz	ISO H8
Rauheit, metallischer Haftsitz	R_z = 10 ... 25 µm

Voraussetzung für einwandfreie Funktion der Dichtung ist die sorgfältige Montage nach DIN 3760 → Technisches Handbuch.

Abmessungsbereich für Wellen-Ø d1

Simmerring BABSL (NBR)	8 ... 340 mm

B Drawings of the construction

B.1 Mixed flow pump

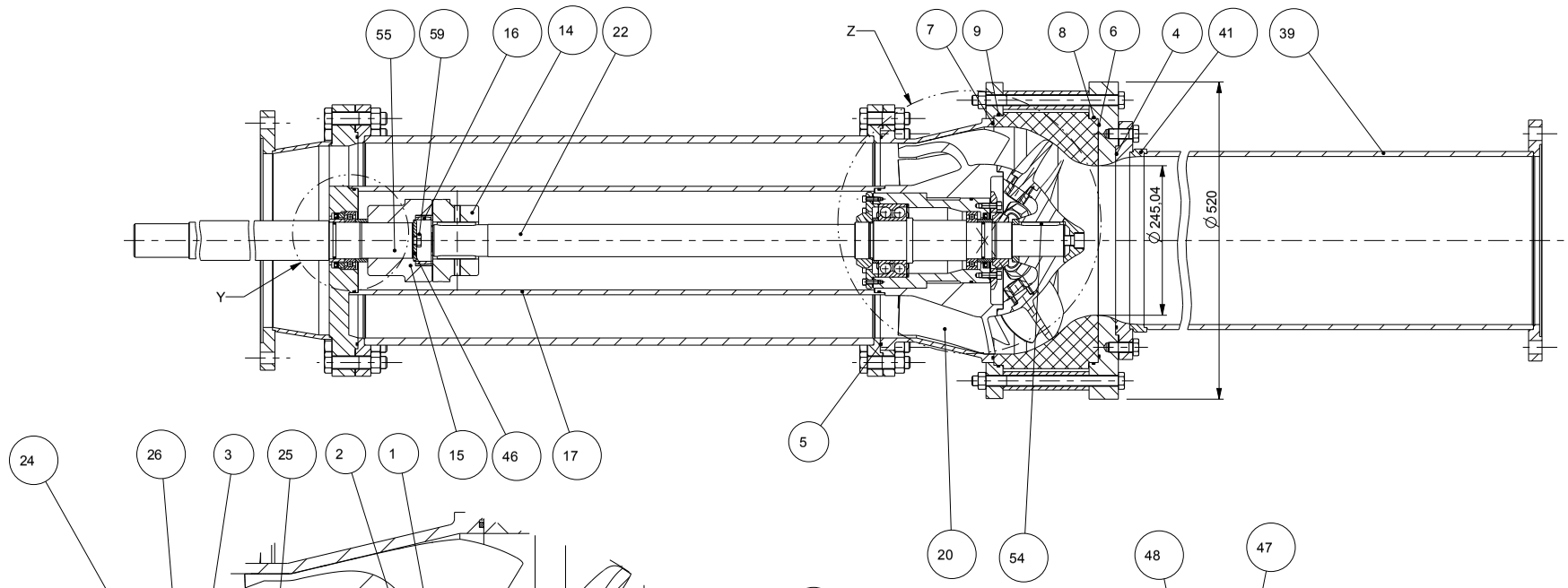

Detail Z
Scale 0.500

Detail Y
Scale 0.500

Dateiname des Zeichnungsobjektes /Name of the drawing object: 1010_000_HALBAXIALPUMPE		Dateityp. File-type: ASSEM	Dateiname der Zeichnung / Name of the drawing: 1010_000_HALBAXIALPUMPE
	Tolerierung/Tolerance ISO 8015 Allg. Toleranz/Gen. tolerance DIN ISO 2768 m-K	Oberfläche Surface quality DIN ISO 1302 Werkst.-Kanten Pyrhedges DIN ISO 13715	Maßstab/Scale 0,200 Gew./Weight 453.2 kg
			Werkstoff Material: Halbzug Raw material:
	Datum/Date	Name	Benennung Denotation:
Bearb./Draft.	31-04-28	Hofgärtner	Mixed flow pump
Gepr./Cert.			
Norm/Standard			
Graz, University of Technology Institute for Hydraulic Fluidmachinery			Zeichnungsnummer/Drawing number: BG 1010_000
			Blatt/Pages 1 2 Bl./P.

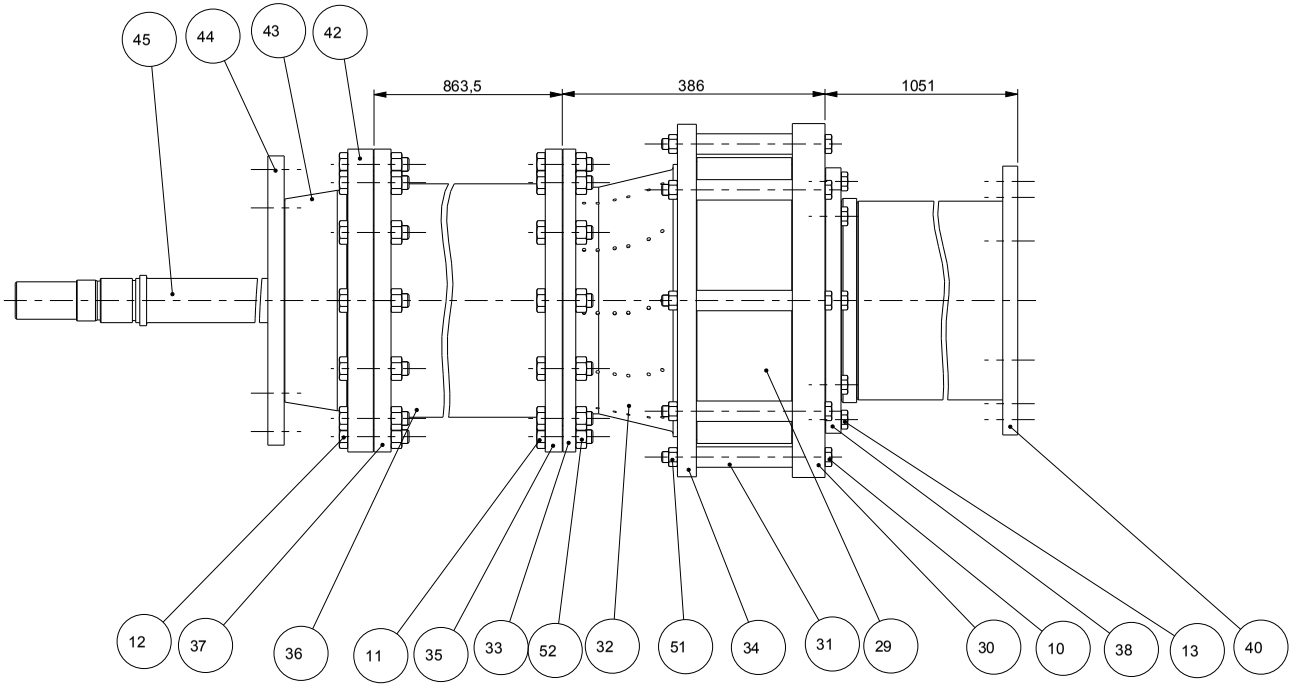

No.	Qnty	DRAWING No.	DENOTATION	STANDARD	MATERIAL	RAW MATERIAL
63	2		Radial shaft sealing	Simrit BABSL1 70x90x7x0	72 NBR 902	
62	2		NILOS-Ring	Nilos 7213 JVH		
61	2		Lock nut	KMT 12		
60	2		Inner ring	IR 60x70x25		
59	1		Hexagonal screw	DIN 933 M12x30	A2-70	
58	8		Cylindrical screw	DIN 912 M8x25	A2-70	
57	8		Cylindrical screw	DIN 912 M6x20	A2-70	
56	1		Cylindrical Screw	DIN 912 M16x50	Steel 10.9	
55	1		Fitting key	DIN 6885 A 16x10x80		
54	3		Fitting key	DIN 6885 A 16x10x63		
53	6		Hexagonal nut	DIN 555 M24	A2-80	
52	24		Hexagonal nut	DIN 555 M20	Steel 8.8	
51	8		Hexagonal nut	DIN 555 M16	Steel 8.8	
50	2		Grooved ball bearing	6012-2RSR		
49	1		Angular ball bearing	2x7213 BECBJ DB		
48	1	BT 1090_004	Space ring		1.4301	
47	1	BT 1090_003	Space ring		1.4301	
46	1	BT 1090_002	Disk		1.4301	
45	1	BT 1090_001	Shaft		42CrMo4	
44	1	BT 1080_003	Flange		S355J2	
43	1	BT 1080_002	Casing		S355J2	
42	1	BT 1080_001	Flange		S355J2	
41	1	BT 1070_006	Adapter flange		S355J2	
40	1	BT 1070_003	Flange		S355J2	
39	1	BT 1070_002	Pipe		S355J2	292x10
38	1	BT 1070_001	Flange		S355J2	
37	1	BT 1060_004	Flange		S355J2	
36	1	BT 1060_002	Casing		S355J2	343x17,5
35	1	BT 1060_001	Flange		S355J2	
34	1	BT 1050_003	Flange		S355J2	
33	1	BT 1050_002	Flange		S355J2	
32	1	BT 1050_001	Casing		1.4301	
31	8	BT 1040_004	Bushing		S355J2	
30	1	BT 1040_003	Flange		S355J2	
29	1	BT 1040_001	Casing		Acrylic glass	
28	6	BT 1030_006	Impeller vane		1.4571	
27	1	BT 1030_001	Hub		1.4122	
26	1	BT 1020_007	Space ring		1.4301	
25	1	BT 1020_006	Space ring		1.4301	
24	1	BT 1020_005	Cover plate		1.4301	
23	1	BT 1020_004	Space ring		1.4301	
22	1	BT 1020_003	Shaft		42CrMo4	
21	1	BT 1020_002	Bearing bushing		1.4301	
20	1	BT 1010_006	Diffusor		1.4301	
19	1	BT 1010_004	Cap		1.4301	
18	1	BT 1010_003	Lid		1.4301	
17	1	BT 1010_002	Inner pipe		S355J2	
16	1		Cuppling - toothed ring	GE-T 65 E	94 Shore	
15	1		Cuppling d=58	GE-T 65		
14	1		Cuppling d=52	GE-T 65		
13	8		Hexagonal screw	DIN 933 M16x40	Steel 8.8	
12	12		Hexagonal screw	DIN 931 M20x90	Steel 8.8	
11	12		Hexagonal screw	DIN 931 M20x70	Steel 8.8	
10	8		Hexagonal screw	DIN 931 M16x280	Steel 8.8	
9	1		O-ring d=409		NBR70Sh	Cord 3.6
8	1		O-ring d=400		NBR70Sh	Cord 3.6
7	1		O-ring d=380		NBR70Sh	Cord 3.6
6	1		O-ring d=375		NBR70Sh	Cord 3.6
5	2		O-ring d=335		NBR70Sh	Cord 3.6
4	1		O-ring d=280		NBR70Sh	Cord 3.6
3	2		O-ring d=165		NBR70Sh	Cord 3.6
2	1		O-ring d=132		NBR70Sh	Cord 3.6
1	2		O-ring d=54		NBR70Sh	Cord 3.6

Datei name des Zeichnungsobjektes /Name of the drawing object:
1010_000_HALBAXIALPUMPE

Dateityp
File type:
ASSEM

Datei name der Zeichnung / Name of the drawing:
1010_000_HALBAXIALPUMPE

Toleranzung / Tolerance
ISO 8015
Allg. Toleranz / Gen. tolerance
DIN ISO 2768 m-K

Oberfläche
Surface quality
DIN ISO 1302
Werkst.-Kanten
Part edges
DIN ISO 13715

Maßstab/Scale 0,200

Gew./Weight 453.2 kg

Werkstoff/Material:

Halbzeug/Raw material:

	Datum/Date	Name
Bearb./Draft.	21.04.15	Hofgärtner
Gepr./Check.		
Norm/Standard		

Benennung/Denotation:

Mixed flow pump

Graz, University of Technology
Institute for Hydraulic Fluidmachinery

Zeichnungsnummer/Drawing number:
BG 1010_000

Bl. / Pg. 2
2 Bl.P.

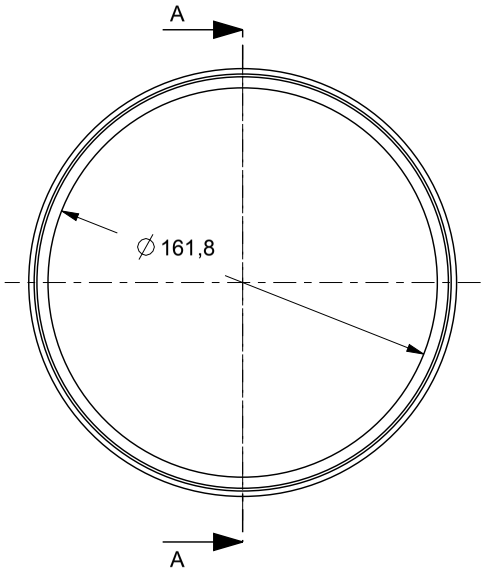

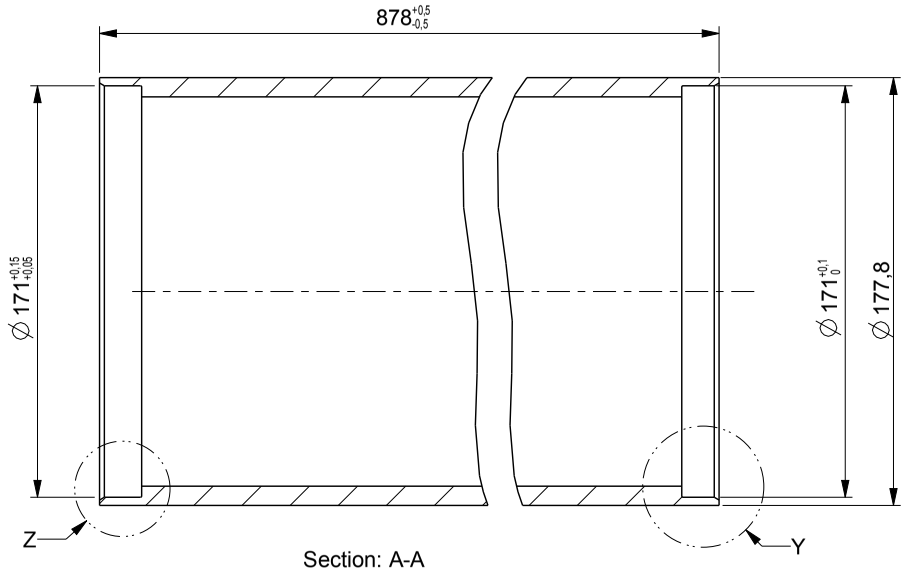

Section: A-A

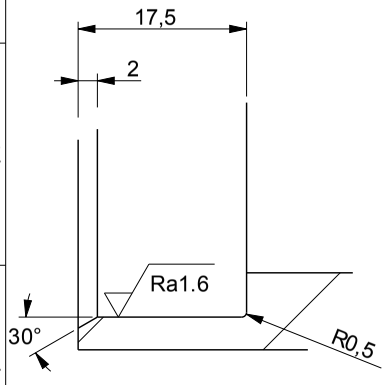

Detail Z
Scale 2.000

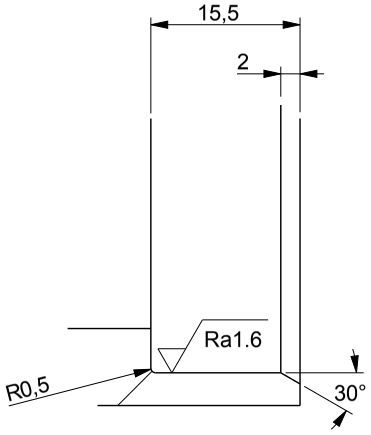

Detail Y
Scale 2.000

0.3 +0.3

Ra12.5 (Ra1.6)

Dateiname des Zeichnungsobjektes / Name of the drawingobject: 1010_002_INNENROHR		Dateityp File-type: PART	Dateiname der Zeichnung / Name of the drawing: 1010_002_INNENROHR
	Tolerierung/Tolerance ISO 8015 Allg. Toleranz/Gen. tolerance DIN ISO 2768 m-K	Oberflaeche Surface quality DIN ISO 1302 Werkst.-Kanten Part-edges DIN ISO 13715	Maßstab/Scale 0,500 Gew./Weight: 28.6 kg
			Werkstoff / Material: S355J2
			Halbzeug / Raw material: Pipe 177.8x8
	Datum/Date	Name	Benennung/Denotation: Inner Pipe Mixed flow pump
	Bearb. Edit. 2013-04-22	Hopfgartner	
	Gepr. Cert.		
	Norm Standard		
	Graz, University of Technology Institute for Hydraulic Fluidmachinery		Zeichnungsnummer/Drawing number: BT 1010_002
			Blatt/Page 1
			1 Bl./P.

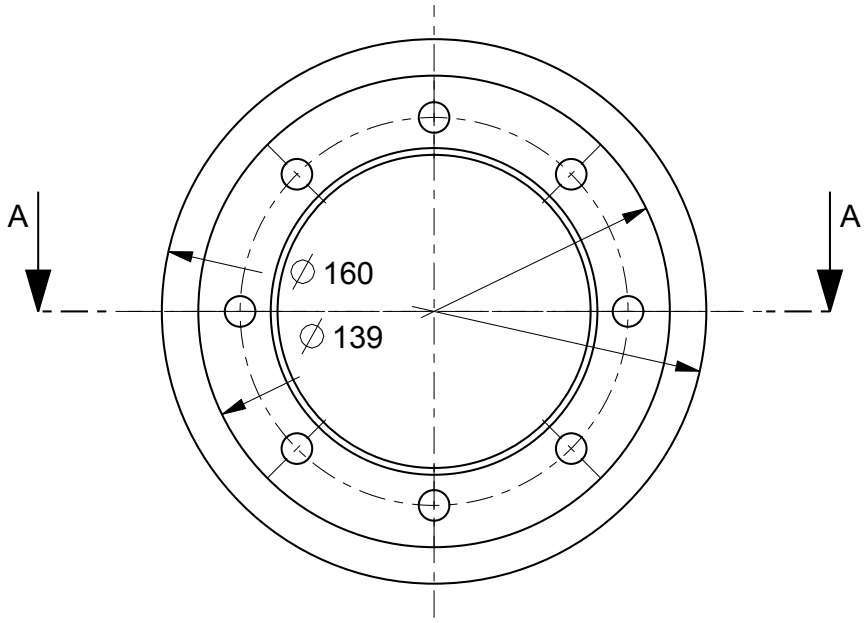

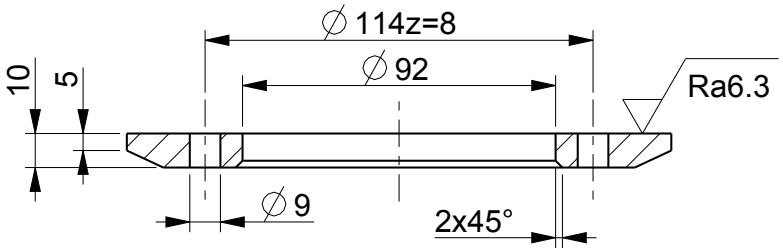

Section A-A

Dateiname des Zeichnungsobjektes / Name of the drawingobject: 1010_003_DECKEL		Dateityp File-type: PART	Dateiname der Zeichnung / Name of the drawing: 1010_003_DECKEL
	Tolerierung/Tolerance ISO 8015 Allg. Toleranz/Gen. tolerance DIN ISO 2768 m-K	Oberflaeche Surface quality DIN ISO 1302 Werkst.-Kanten Part-edges DIN ISO 13715	Maßstab/Scale 0,500 Gew./Weight: 0.9 kg Werkstoff/Material: 1.4301 Halbzeug/Raw material: Round steel bar d=170mm
	Datum/Date / Name Bear. / Edit. 2013-04-22 Hopfgartner Gepr. / Cert. Norm / Standard		Benennung/Denotation: Cover plate Mixed flow pump
	Graz, University of Technology Institute for Hydraulic Fluidmachinery		Zeichnungsnummer / Drawing number: BT 1010_003 Blatt/Page 1 1 Bl./P.

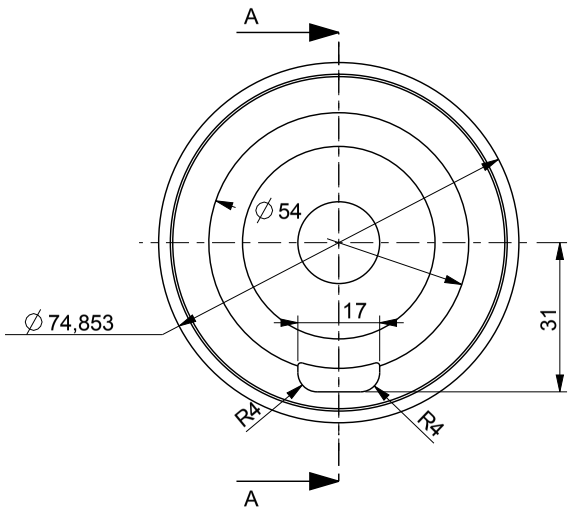

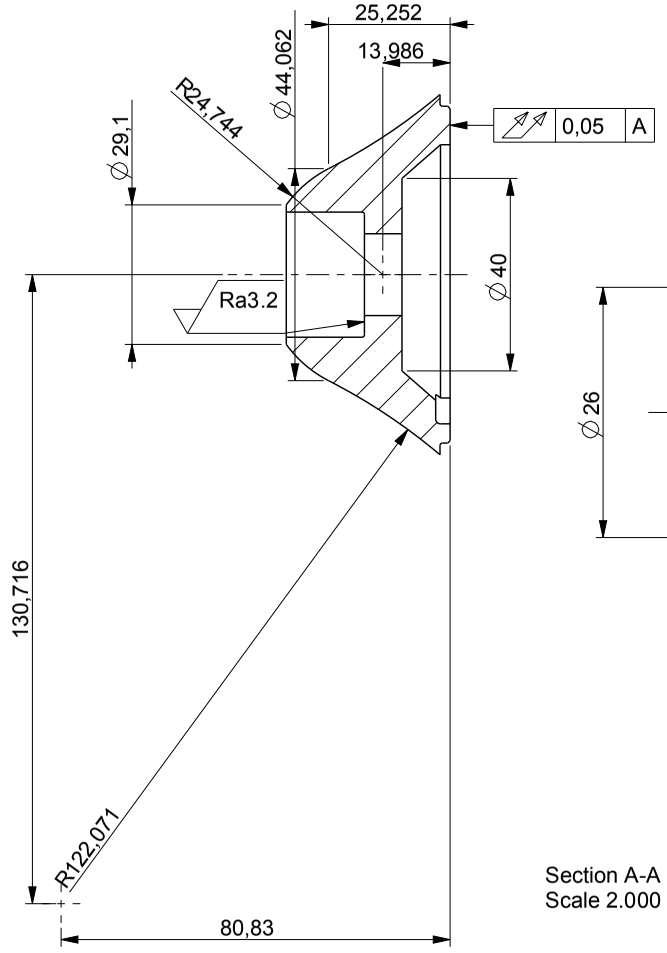

Section A-A

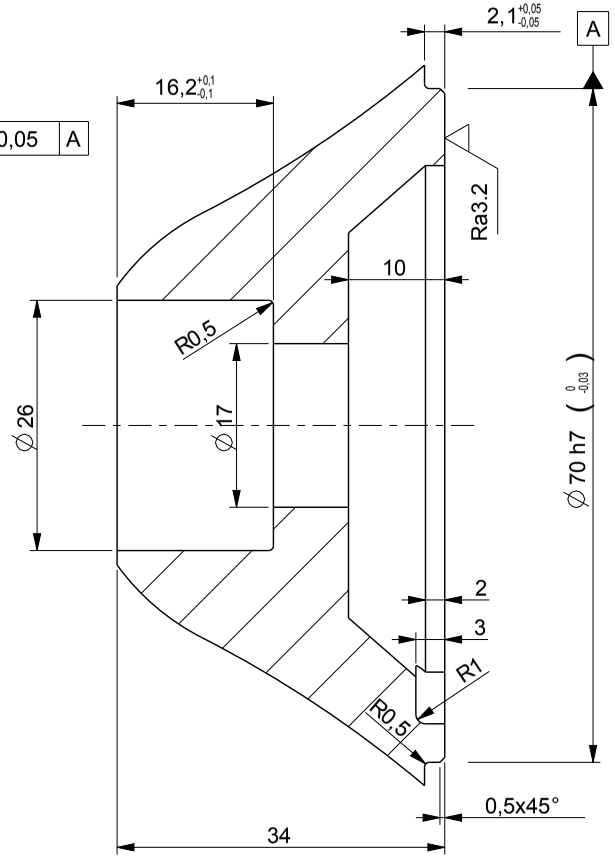

Section A-A
Scale 2.000

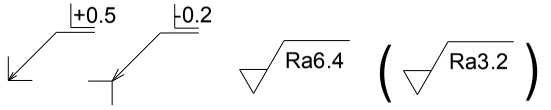

Dateiname des Zeichnungsobjektes / Name of the drawingobject: 1010_004_KAPPE		Dateityp File-type: PART	Dateiname der Zeichnung / Name of the drawing: 1010_004_KAPPE
	Tolerierung/Tolerance ISO 8015; Allg. Toleranz/Gen. tolerance DIN ISO 2768 m-K	Oberflaeche Surface quality DIN ISO 1302; Werkst.-Kanten Part-edges DIN ISO 13715	Maßstab/Scale 1,000; Gew./Weight: 0.6 kg; Werkstoff / Material: 1.4301; Halbzeug / Raw material: Round steel bar d=90mm
	Datum/Date	Name	Benennung/Denotation: Cap, Mixed flow pump
Bearb. Edit.	2013-04-22	Hopfgartner	
Gepr. Cert.			
Norm Standard			
Graz, University of Technology, Institute for Hydraulic Fluidmachinery			Zeichnungsnummer/Drawing number: BT 1010_004; Blatt/Page 1; 1 Bl./P.

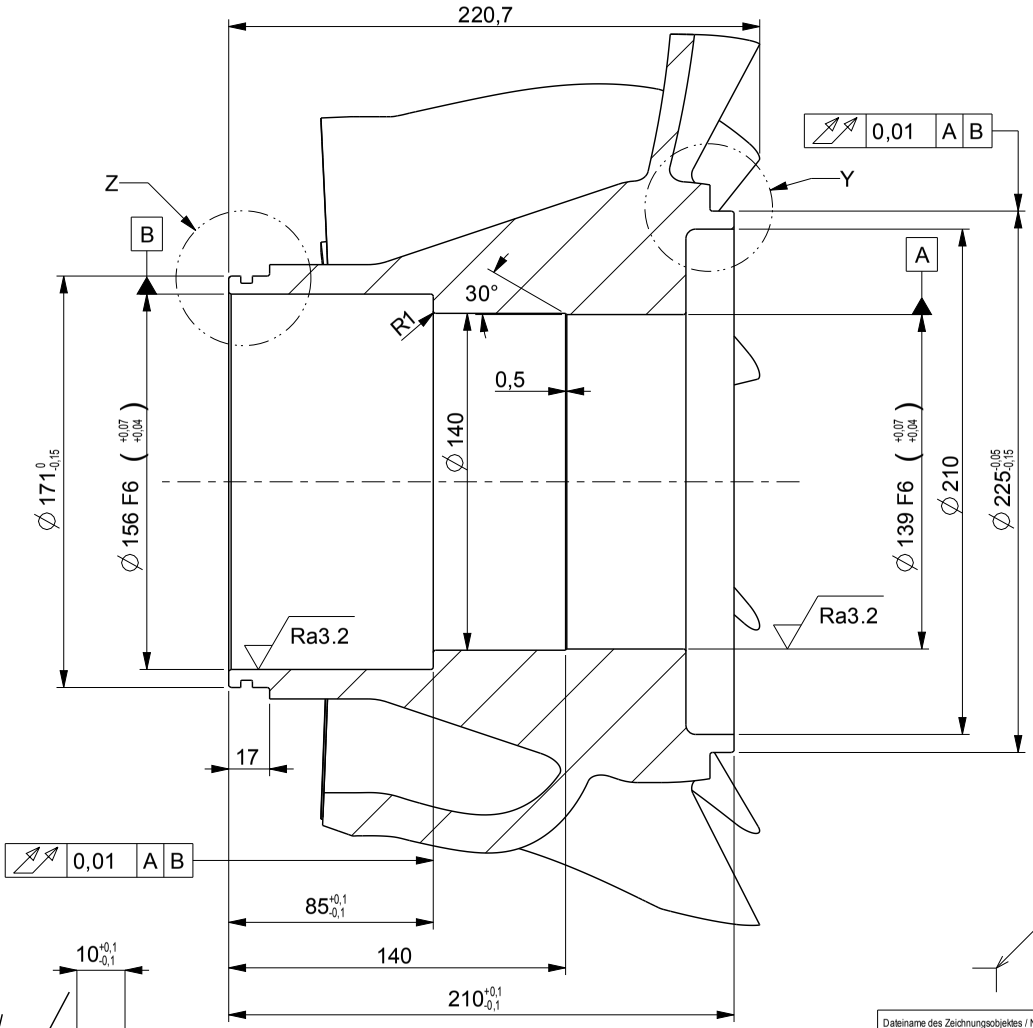

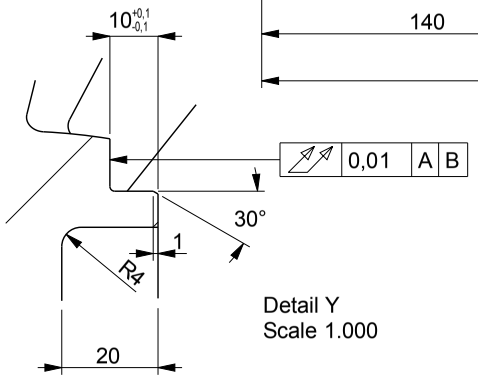

Detail Y
Scale 1.000

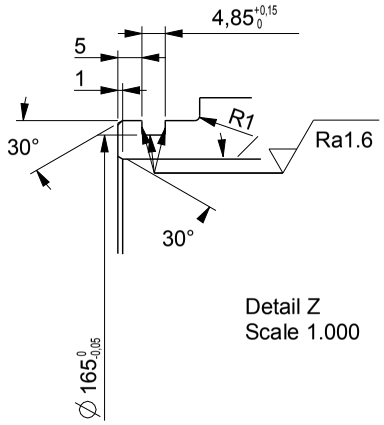

Detail Z
Scale 1.000

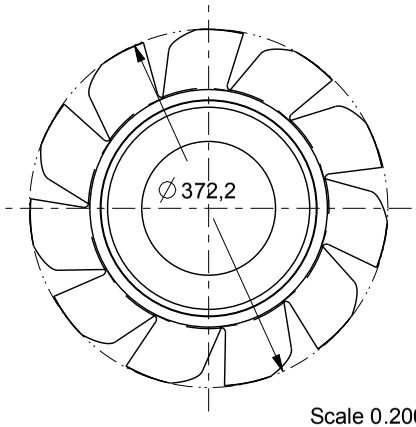

Scale 0.200

-0.2 +0.5

Ra6.3 (Ra1.6 Ra3.2)

Missing dimensions are shown in the 3D-CAD-file!

Dateiname des Zeichnungsobjektes / Name of the drawingobject: 1010_006_LEITAPPARAT		Dateityp File-type: PART	Dateiname der Zeichnung / Name of the drawing: 1010_006_LEITAPPARAT
	Tolerierung/Tolerance ISO 8015 Allg. Toleranz/Gen. tolerance DIN ISO 2768 m-K	Oberflaeche Surface quality DIN ISO 1302 Werkst.-Kanten Part-edges DIN ISO 13715	Maßstab/Scale 0,500 Gew./Weight: 35.3 kg Werkstoff / Material: 1.4301 Halbzeug / Raw material:
	Datum/Date	Name	Benennung/Denotation: Diffuser Mixed flow pump
Bearb. Edit.	2013-04-22	Hopfgartner	
Gepr. Cert.			
Norm Standard			
Graz, University of Technology Institute for Hydraulic Fluidmachinery			Zeichnungsnummer/Drawing number: BT 1010_006 Blatt/Page 1 1 Bl./P.

B.2 Pump shaft

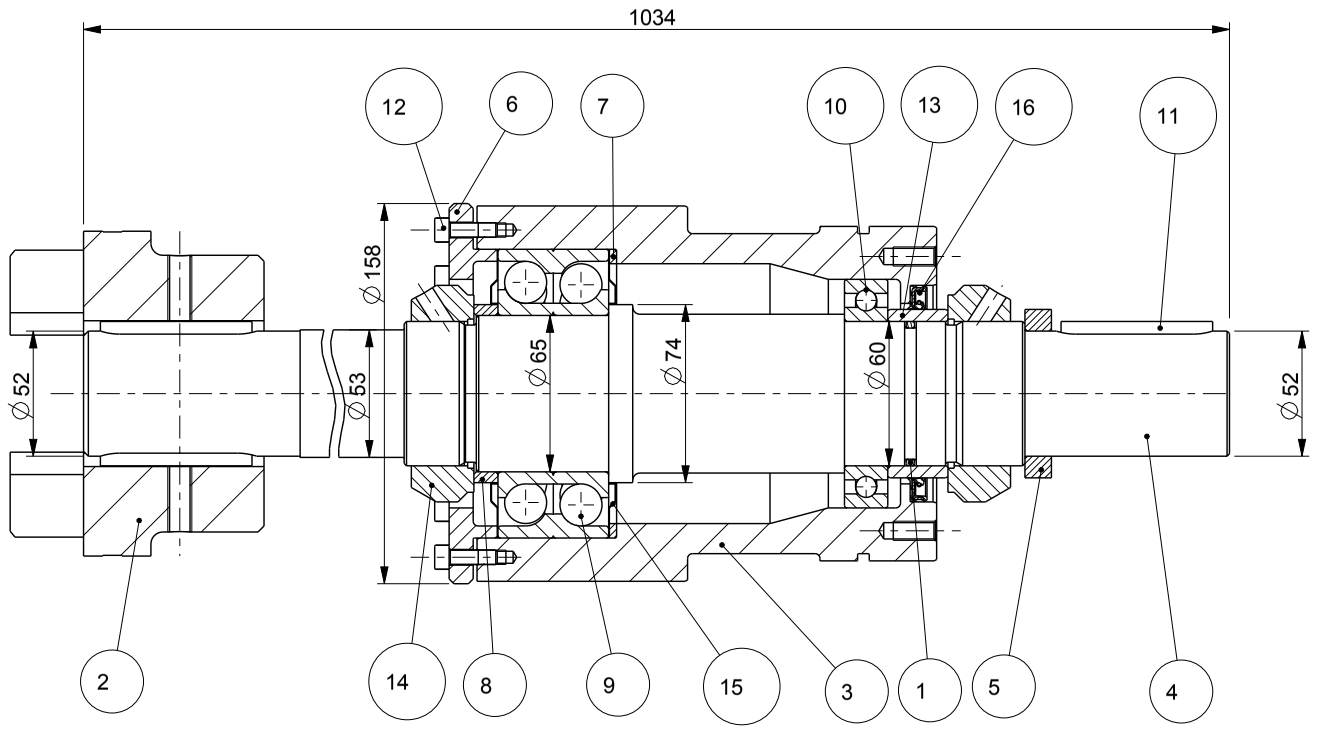

No.	Qnty	DRAWING No.	DENOTATION	STANDARD	MATERIAL	RAW MATERIAL
16	1		Radial shaft sealing	Simrit BABSL1 70x90x7x0	72 NBR 902	
15	2		NILOS-Ring	Nilos 7213 JVH		
14	2		Lock nut	KMT 12		
13	1		Inner ring	IR 60x70x25		
12	8		Cylindrical screw	DIN 912 M6x20	A2-70	
11	3		Fitting key	DIN 6885 A 16x10x63		
10	1		Grooved ball bearing	6012-2RSR		
9	1		Angular ball bearing	2x7213 BECBJ DB		
8	1	BT 1020_007	Space ring		1.4301	
7	1	BT 1020_006	Space ring		1.4301	
6	1	BT 1020_005	Cover plate		1.4301	
5	1	BT 1020_004	Space ring		1.4301	
4	1	BT 1020_003	Shaft		42CrMo4	
3	1	BT 1020_002	Bearing bushing		1.4301	
2	1		Cuppling d=52	GE-T 65		
1	1		O-ring d=54		NBR70Sh	Cord 3.6

Dateiname des Zeichnungsobjektes / Name of the drawingobject:
1020_000_PUMPENWELLE

Dateityp / File-type: ASSEM

Dateiname der Zeichnung / Name of the drawing:
1020_000_PUMPENWELLE

Tolerierung/Tolerance: ISO 8015
Allg. Toleranz/Gen. tolerance: DIN ISO 2768 m-K

Oberflaeche / Surface quality: DIN ISO 1302
Werkst.-Kanten / Part-edges: DIN ISO 13715

Maßstab/Scale: 0,500

Gew./Weight: 41.9kg

Werkstoff / Material:

Halbzeug / Raw material:

	Datum/Date	Name
Bearb. / Edit.	2013-04-23	Hopfgartner
Gepr. / Cert.		
Norm / Standard		

Benennung/Denotation:

Pump shaft

Graz, University of Technology
Institute for Hydraulic Fluidmachinery

Zeichnungsnummer/Drawing number:
BG 1020_000

Blatt/Page 1
1 Bl./P.

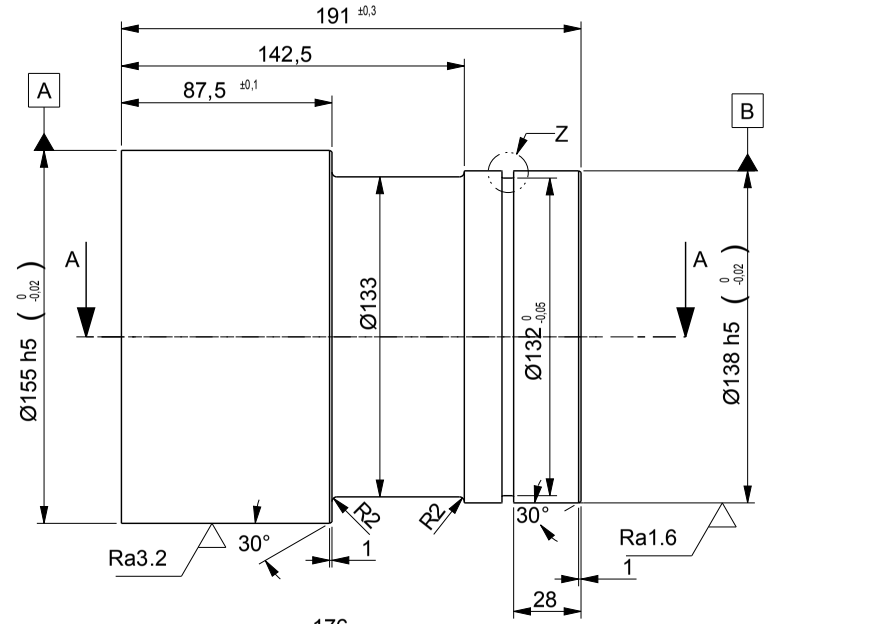

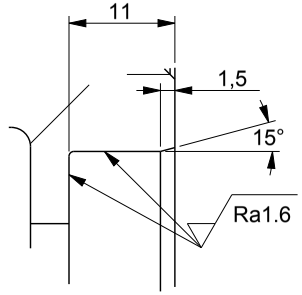

Detail Y
Scale 2.000

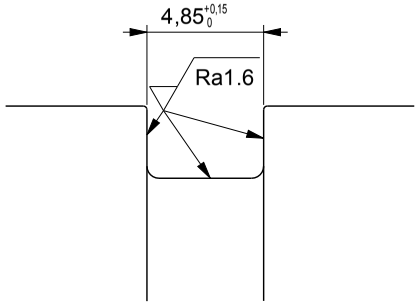

Detail Z
Scale 5.000

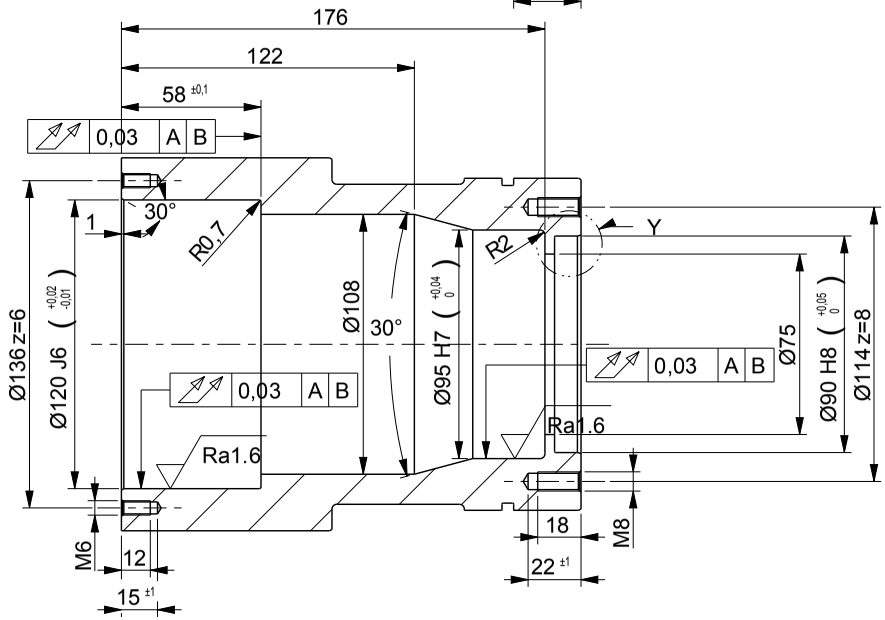

Section A-A

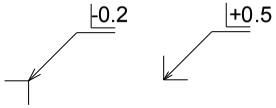

Dateiname des Zeichnungsobjektes / Name of the drawingobject: 1020_002_LAGERBUECHSE		Dateityp File-type: PART	Dateiname der Zeichnung / Name of the drawing: 1020_002_LAGERBUECHSE
	Tolerierung/Tolerance ISO 8015 Allg. Toleranz/Gen. tolerance DIN ISO 2768 m-K	Oberflaeche Surface quality DIN ISO 1302 Werkst.-Kanten Part-edges DIN ISO 13715	Maßstab/Scale 1,000 Gew./Weight: 11.1 kg
			Werkstoff / Material: 1.4301 Halbzeug / Raw material: Round steel bar d=170mm
	Datum/Date	Name	Benennung/Denotation: Bearing bushing Pump shaft
Bearr.	2013-04-22	Hopfgartner	
Edit.			
Gepr.			
Cert.			
Norm Standard			
Graz, University of Technology Institute for Hydraulic Fluidmachinery			Zeichnungsnummer/Drawing number: BT 1020_002
			Blatt/Page 1 1 Bl./P.

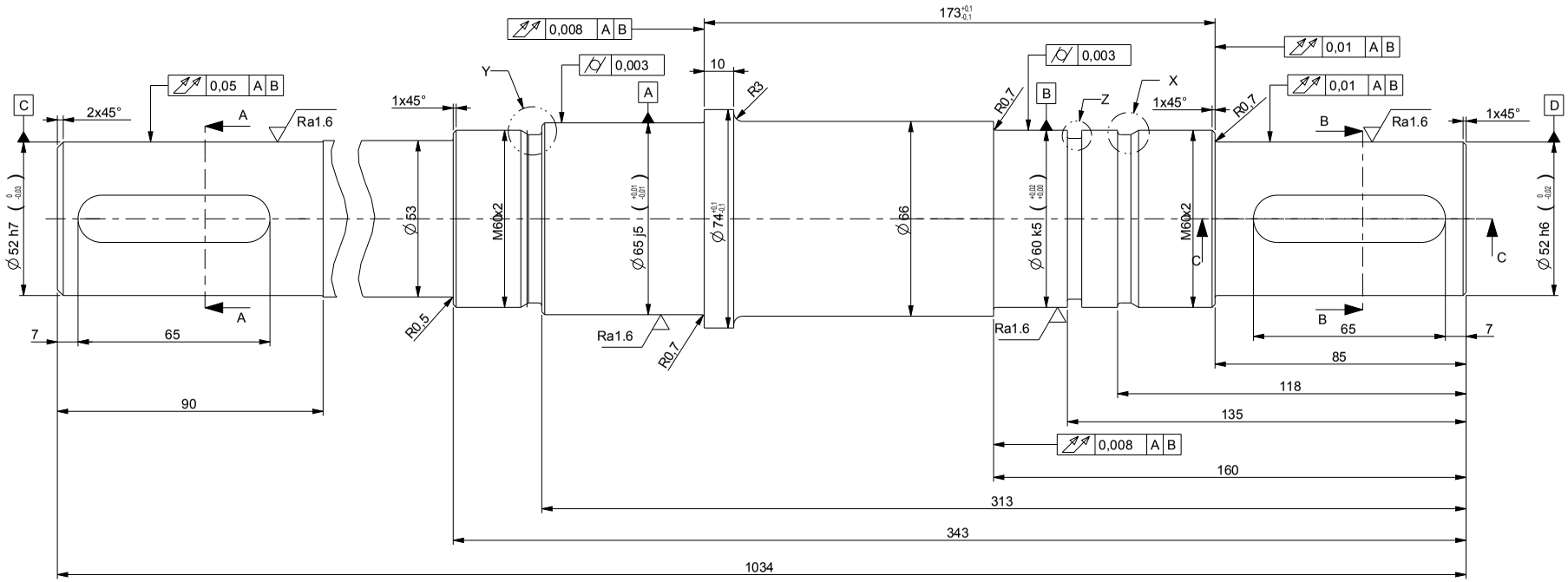

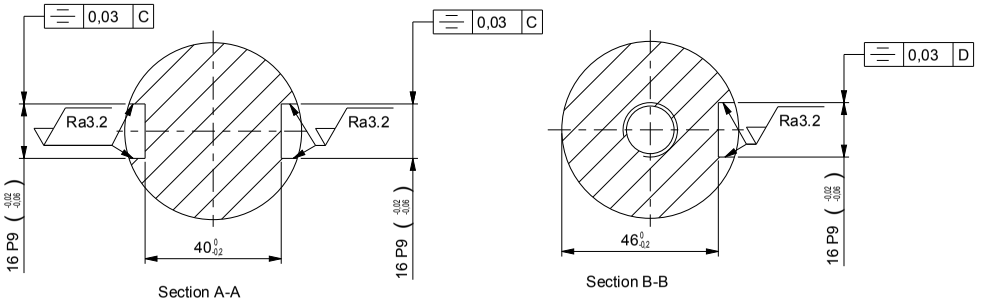

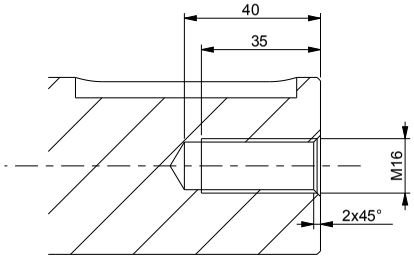

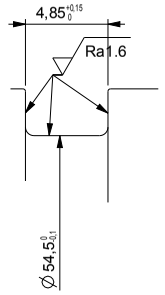

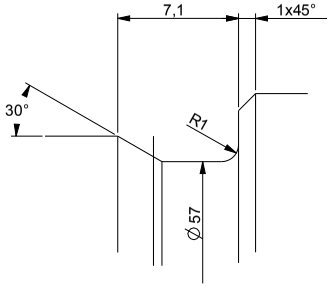

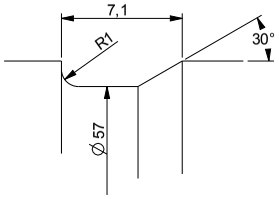

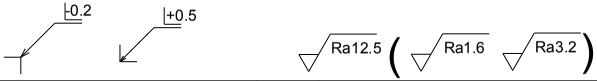

Dateiname des Zeichnungsobjektes /Name of the drawing object: 1020_003_WELLE	Dateityp File type: PART	Dateiname der Zeichnung / Name of the drawing: 1020_003_WELLE	
Tolerierung/Tolerance ISO 8015 Allg. Toleranz/Gen. tolerance DIN ISO 2768 m-K	Oberfläche Surface quality DIN ISO 1302 Werkst.-Kanten Part edges DIN ISO 13715	Maßstab/Scale 1,000	Gew./Weight 19.2 kg
		Werkstoff Material 42CrMo4	
Datum/Date: 2015-04-22	Name: Hofgärtner	Benennung Description: Shaft Pump shaft	
Graz, University of Technology Institute for Hydraulic Fluidmachinery		Zeichnungsnummer Drawing number: BT 1020_003	Blatt/Pag. 1 1 BLP

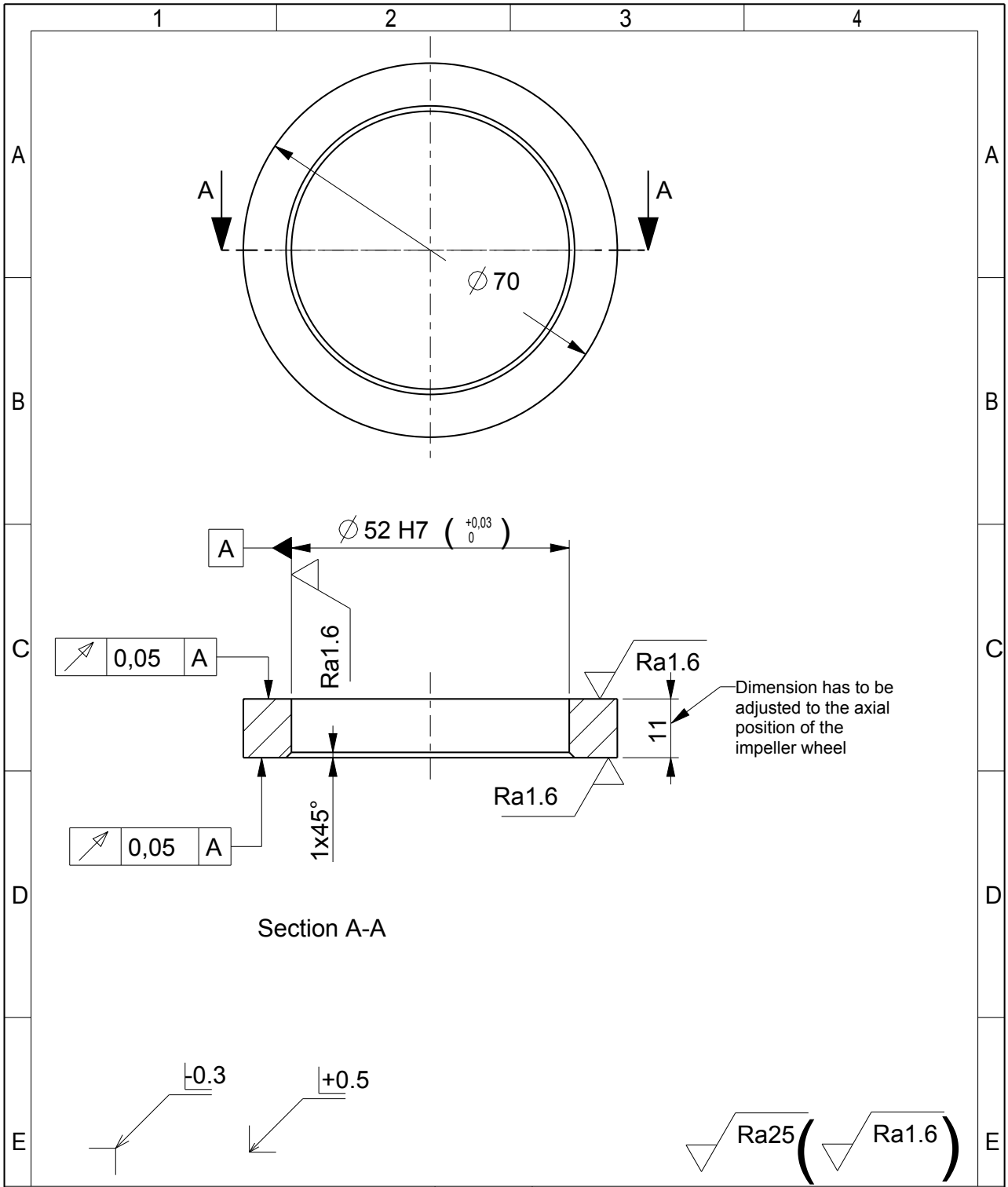

Dateiname des Zeichnungsobjektes / Name of the drawingobject: 1020_004_DISTANZRING		Dateityp File-type: PART	Dateiname der Zeichnung / Name of the drawing: 1020_004_DISTANZRING
	Tolerierung/Tolerance ISO 8015 Allg. Toleranz/Gen. tolerance DIN ISO 2768 m-K	Oberflaeche Surface quality DIN ISO 1302 Werkst.-Kanten Part-edges DIN ISO 13715	Maßstab/Scale 1,000 Gew./Weight: 0.1 kg Werkstoff/Material: 1.4122 Halbzeug/Raw material:
	Datum/Date	Name	Benennung/Denotation: Space ring Pump shaft
	Bear. Edit. 2013-04-22	Hopfgartner	
	Gepr. Cert.		
	Norm Standard		
Graz, University of Technology Institute for Hydraulic Fluidmachinery			Zeichnungsnummer / Drawing number: BT 1020_004 Blatt/Page 1 1 Bl./P.

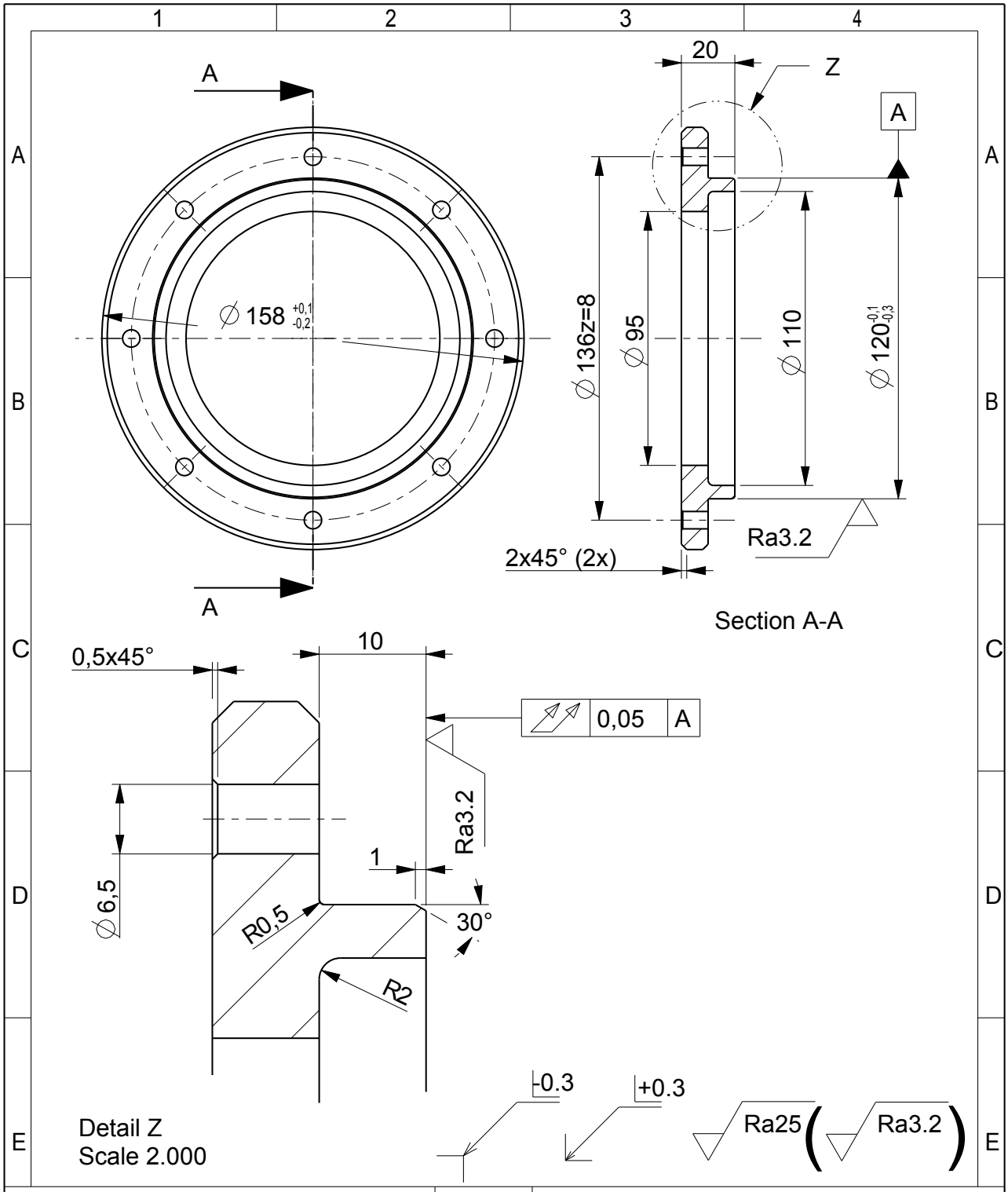

Dateiname des Zeichnungsobjektes / Name of the drawingobject: 1020_005_DECKEL	Dateityp File-type: PART	Dateiname der Zeichnung / Name of the drawing: 1020_005_DECKEL	
	Tolerierung/Tolerance ISO 8015 Allg. Toleranz/Gen. tolerance DIN ISO 2768 m-K	Oberflaeche Surface quality DIN ISO 1302 Werkst.-Kanten Part-edges DIN ISO 13715	Maßstab/Scale 1,000 Gew./Weight: 1.2 kg
			Werkstoff/Material: 1.4301
			Halbzeug/Raw material:

	Datum/Date	Name
Bear. Edit.	2013-04-22	Hopfgartner
Gepr. Cert.		
Norm Standard		

Benennung/Denotation:

Cover plate
Pump shaft

Graz, University of Technology
Institute for Hydraulic Fluidmachinery

Zeichnungsnummer / Drawing number: BT 1020_005

Blatt/Page 1

1 Bl./P.

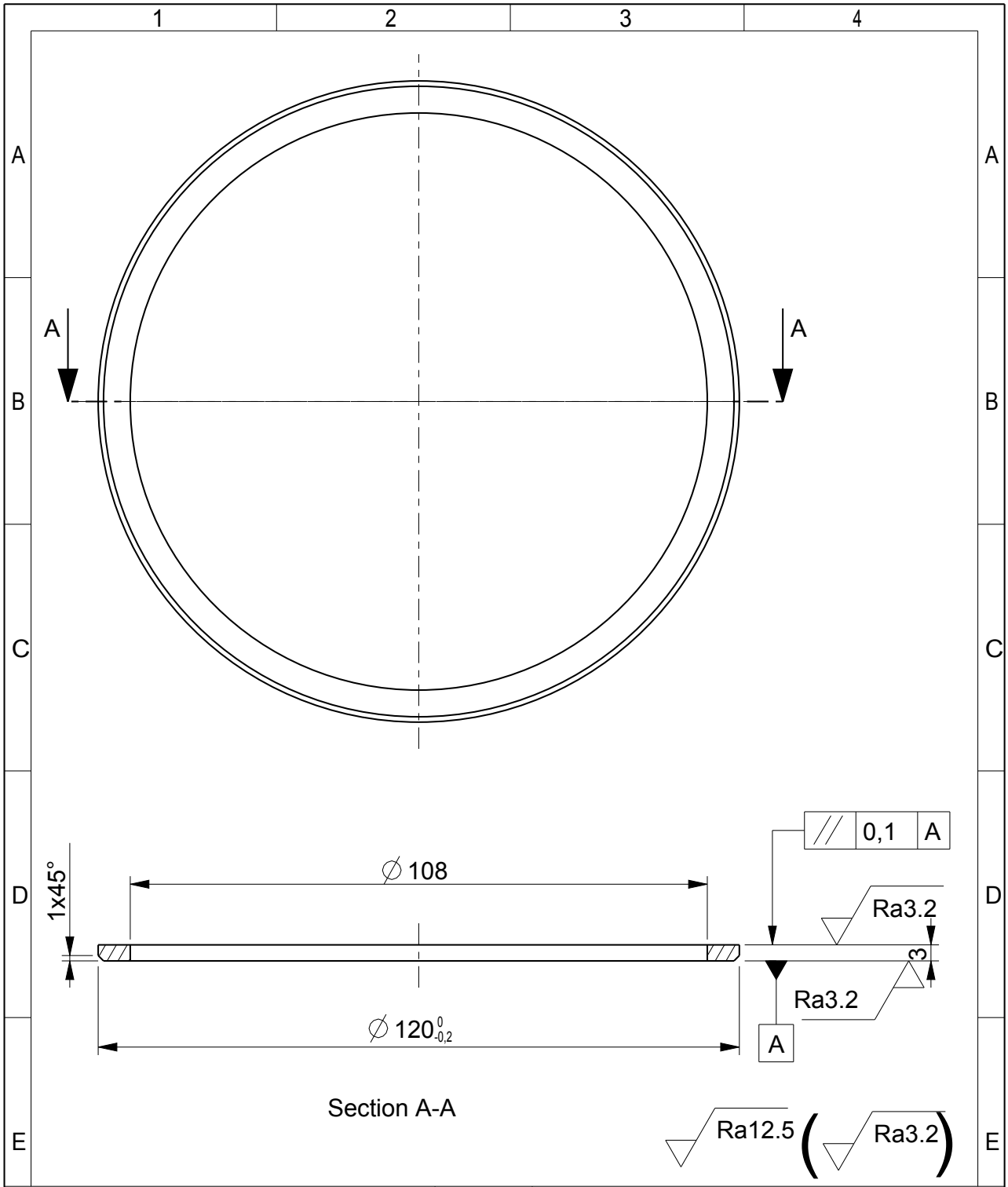

Dateiname des Zeichnungsobjektes / Name of the drawingobject: 1020_006_DISTANZRING		Dateityp File-type: PART	Dateiname der Zeichnung / Name of the drawing: 1020_006_DISTANZRING
	Tolerierung/Tolerance ISO 8015 Allg. Toleranz/Gen. tolerance DIN ISO 2768 m-K	Oberflaeche Surface quality DIN ISO 1302 Werkst.-Kanten Part-edges DIN ISO 13715	Maßstab/Scale 1,000 Gew./Weight: 0.05 kg Werkstoff/Material: 1.4122 Halbzeug/Raw material:
	Datum/Date / Name Bear. / Edit.: 2013-04-22 Hopfgartner Gepr. / Cert.: Norm / Standard:		Benennung/Denotation: Space ring Pump shaft
	Graz, University of Technology Institute for Hydraulic Fluidmachinery		Zeichnungsnummer / Drawing number: BT 1020_006 Blatt/Page 1 1 Bl./P.

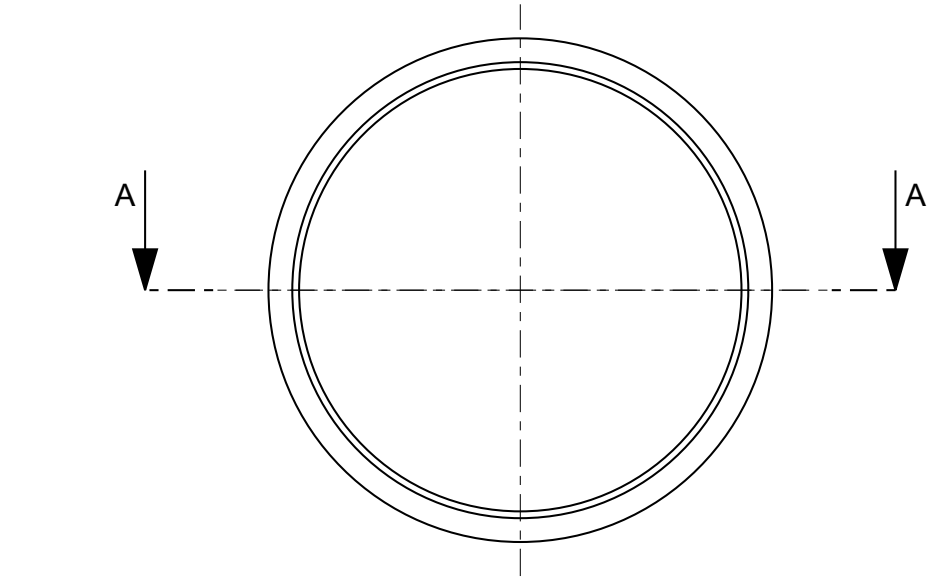

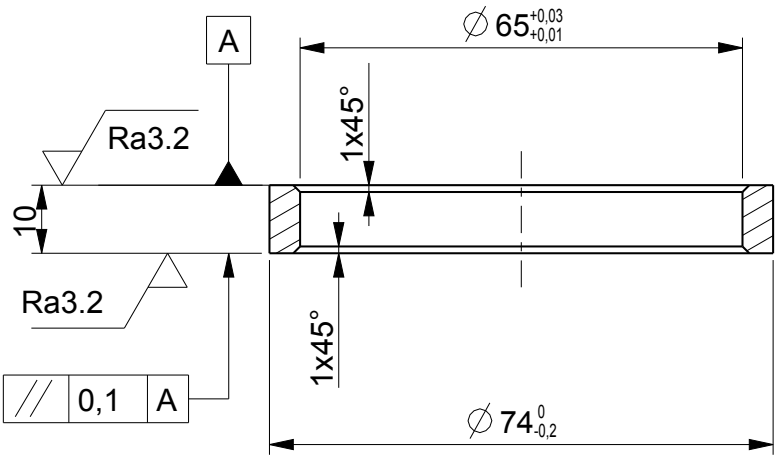

Section A-A

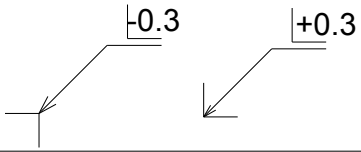

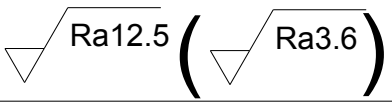

Dateiname des Zeichnungsobjektes / Name of the drawingobject: 1020_007_DISTANZRING		Dateityp File-type: PART	Dateiname der Zeichnung / Name of the drawing: 1020_007_DISTANZRING
	Tolerierung/Tolerance ISO 8015 Allg. Toleranz/Gen. tolerance DIN ISO 2768 m-K	Oberflaeche Surface quality DIN ISO 1302 Werkst.-Kanten Part-edges DIN ISO 13715	Maßstab/Scale 1,000 Gew./Weight: 0.07 kg Werkstoff/Material: 1.4301 Halbzeug/Raw material:
	Datum/Date / Name Bear. / Edit. 2013-04-22 Hopfgartner Gepr. / Cert. Norm / Standard		Benennung/Denotation: Space ring Pump shaft
	Graz, University of Technology Institute for Hydraulic Fluidmachinery		Zeichnungsnummer / Drawing number: BT 1020_007
			Blatt/Page 1 1 Bl./P.

B.3 Impeller

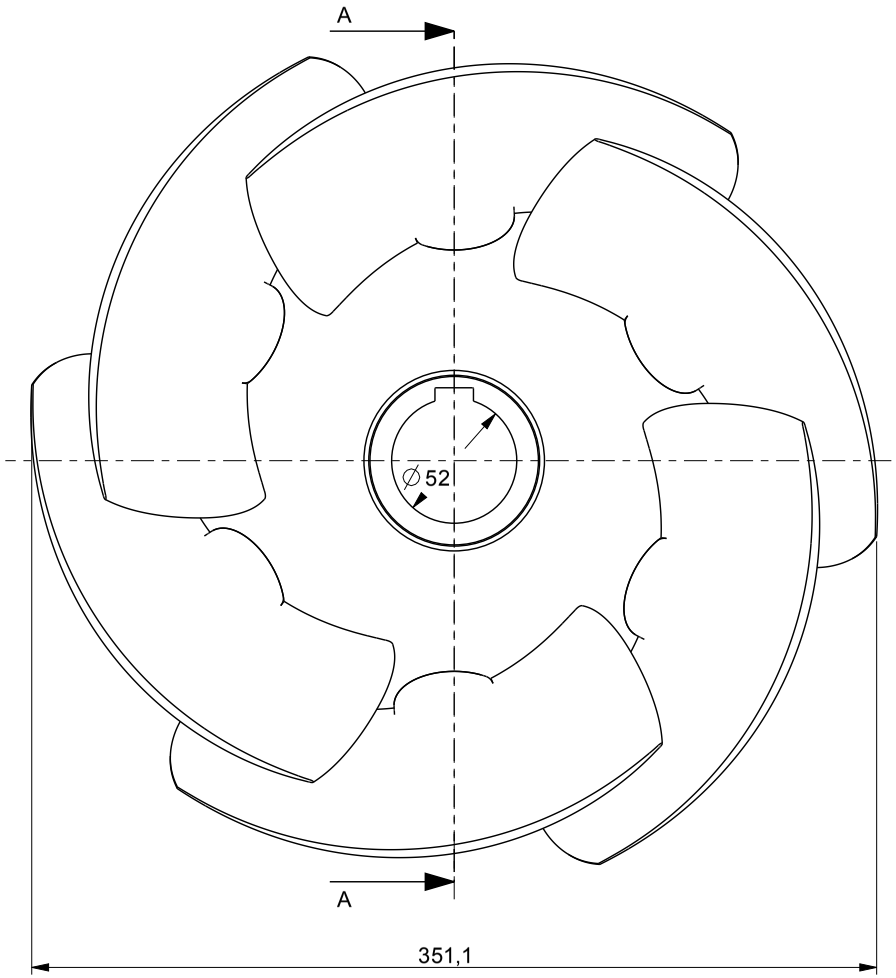

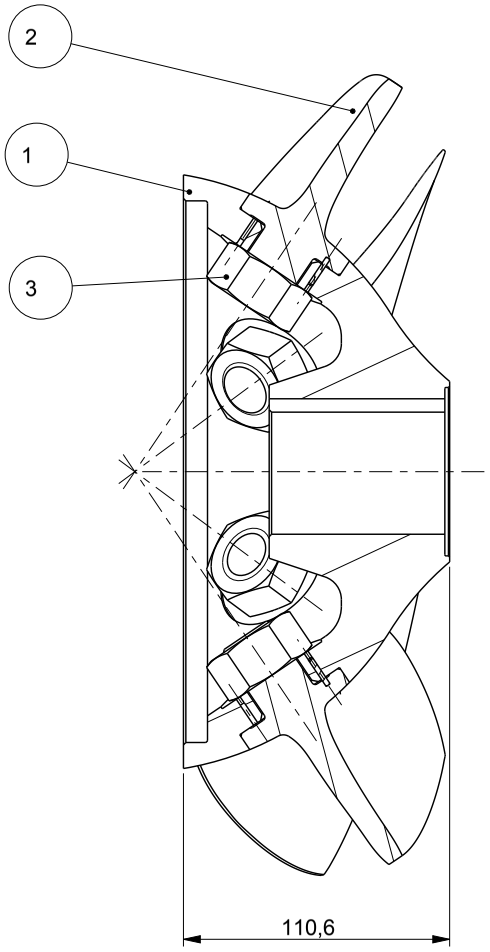

Section A-A

No.	Qnty	DRAWING No.	DENOTATION	STANDARD	MATERIAL	RAW MATERIAL
3	6		Hexagonal nut	DIN 555 M24	A2-80	
2	6	BT 1030_006	Impeller vane		1.4571	
1	1	BT 1030_001	Hub		1.4122	

Dateiname des Zeichnungsobjektes / Name of the drawingobject: FAST_IMP_GES		Dateityp / File-type: ASSEM	Dateiname der Zeichnung / Name of the drawing: FAST_IMP_1030_000		
	Tolerierung/Tolerance ISO 8015; Allg. Toleranz/Gen. tolerance DIN ISO 2768 m-K	Oberflaeche / Surface quality DIN ISO 1302; Werkst.-Kanten / Part-edges DIN ISO 13715	Maßstab/Scale 0,500	Gew./Weight: 17.8 kg	Werkstoff / Material: Halbzeug / Raw material:
		Datum/Date	Name	Benennung/Denotation:	
	Bearb. / Edit.	2013-07-09	Hopfgartner		
	Gepr. / Cert.			Impeller	
	Norm / Standard				
	Graz, University of Technology, Institute for Hydraulic Fluidmachinery			Zeichnungsnummer/Drawing number: BG 1030_000	Blatt/Page 1; 1 Bl./P.

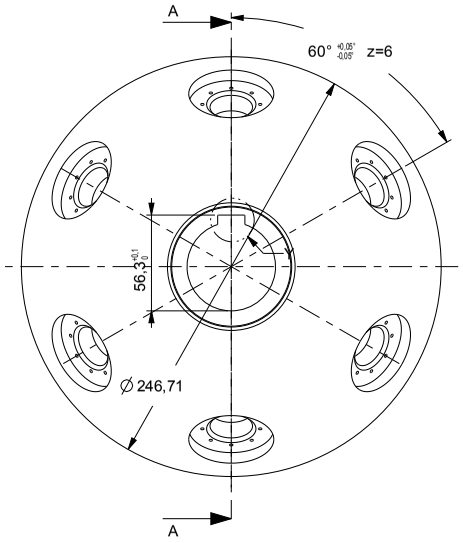

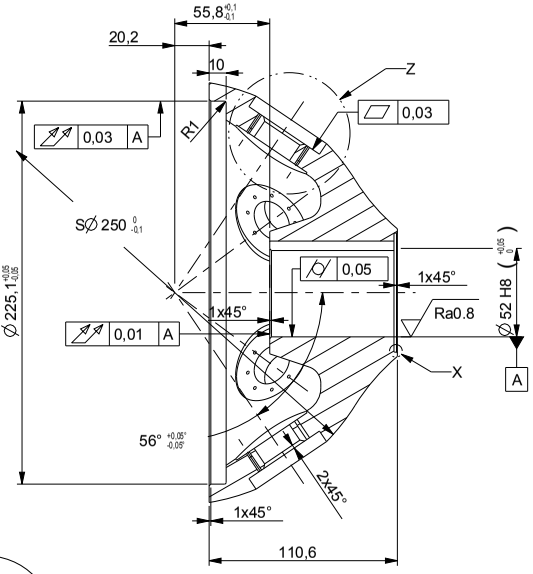

Scale A-A

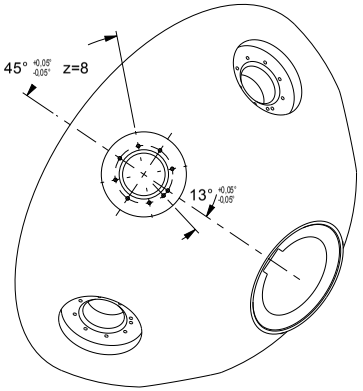

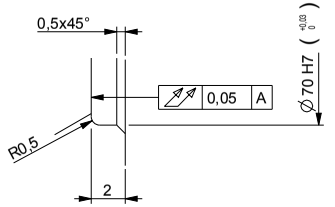

Detail X
Scale 5.000

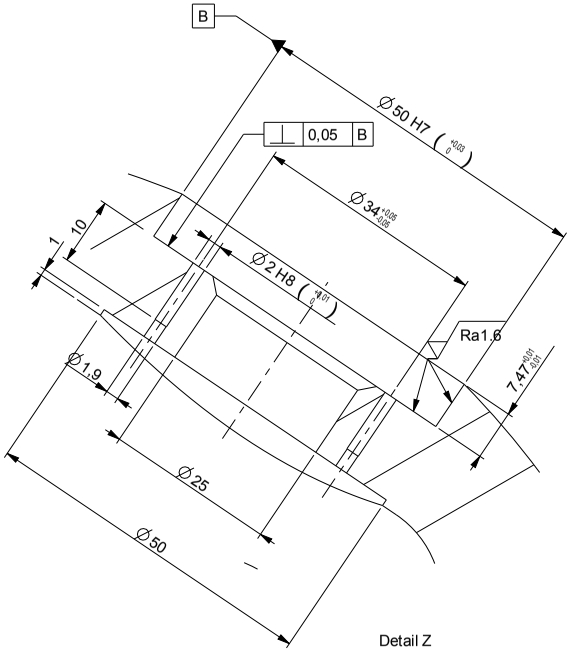

Detail Z
Scale 2.000

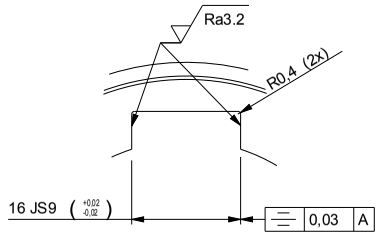

Detail Y
Scale 2.000

Missing dimensions are shown in the 3D-CAD-file!

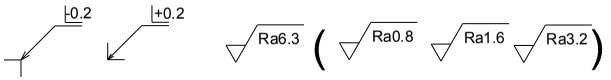

Datei name des Zeichnungsobjektes / Name of the drawing object: 1030_001_NABE		Dateityp / File type: PART	Datei name der Zeichnung / Name of the drawing: 1030_001_NABE
	Tolerierung / Tolerance: ISO 8015, Allg. Toleranz / Gen. tolerance: DIN ISO 2768 m-K	Oberfläche / Surface quality: DIN ISO 1302, Werkst.-Kanten / Part edges: DIN ISO 13715	Maßstab / Scale: 0,500 — Gew. / Weight: 11.2 kg; Werkstoff / Material: 1.4571; Härtung / Raw material:
	Datum / Date	Name	Benennung / Denomination: Hub Impeller
Bearb. / Edit.:	21-04-22	Hofgärtner	
Gepr. / Cert.:			
Norm / Standard:			
Graz, University of Technology, Institute for Hydraulic Fluidmachinery			Zeichnungsnummer / Drawing number: BT 1030_001 — Blatt / Pg.: 1 — 1 Bl. / P.

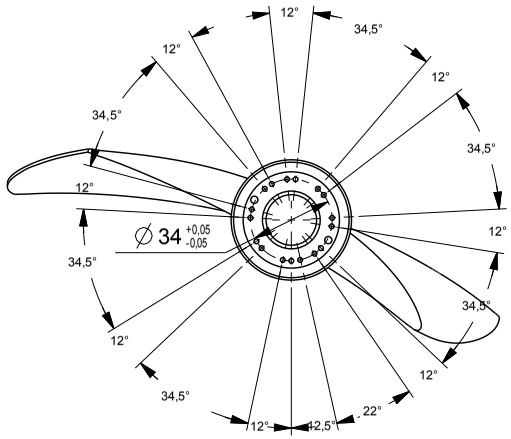

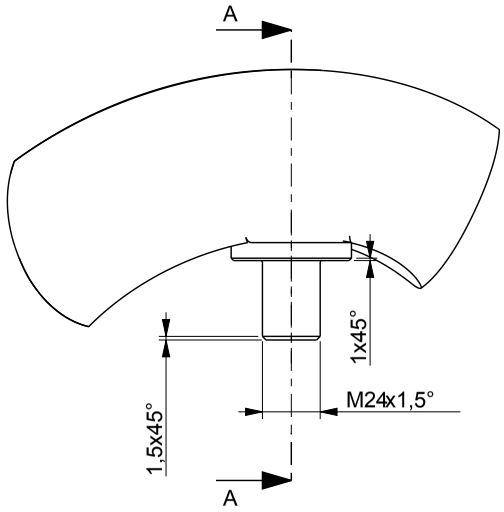

Section A-A

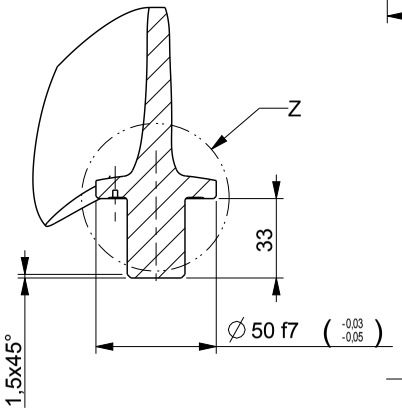

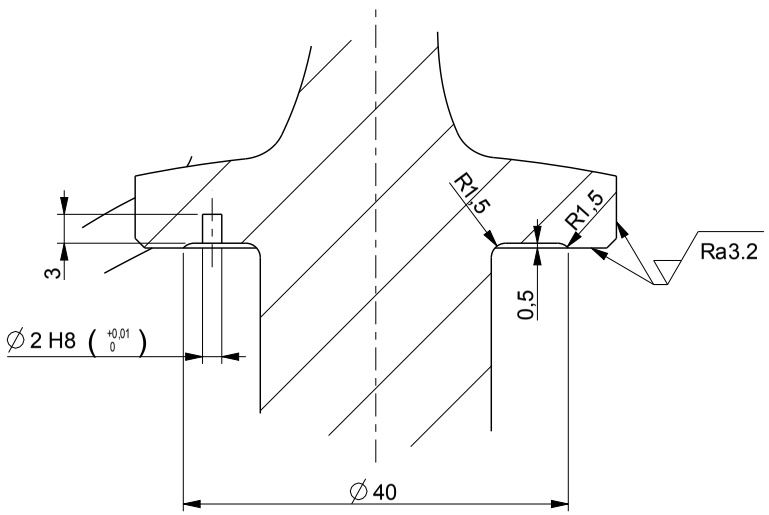

Detail Z
Scale 2.000

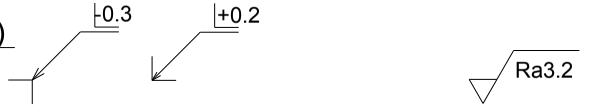

Missing dimensions are shown in the 3D-CAD-file!

Dateiname des Zeichnungsobjektes / Name of the drawingobject: 1030_006_SCHAUFEL		Dateityp File-type: PART	Dateiname der Zeichnung / Name of the drawing: 1030_006_SCHAUFEL
	Tolerierung/Tolerance ISO 8015; Allg. Toleranz/Gen. tolerance DIN ISO 2768 m-K	Oberflaeche Surface quality DIN ISO 1302; Werkst.-Kanten Part-edges DIN ISO 13715	Maßstab/Scale 0,500; Gew./Weight: 1.1 kg; Werkstoff / Material: 1.4122; Halbzeug / Raw material:
	Datum/Date	Name	Benennung/Denotation: Impeller vane Impeller
Bearb. Edit.	2013-04-23	Hopfgartner	
Gepr. Cert.			
Norm Standard			
Graz, University of Technology Institute for Hydraulic Fluidmachinery			Zeichnungsnummer/Drawing number: BT 1030_006; Blatt/Page 1; 1 Bl./P.

B.4 Impeller casing (Shroud)

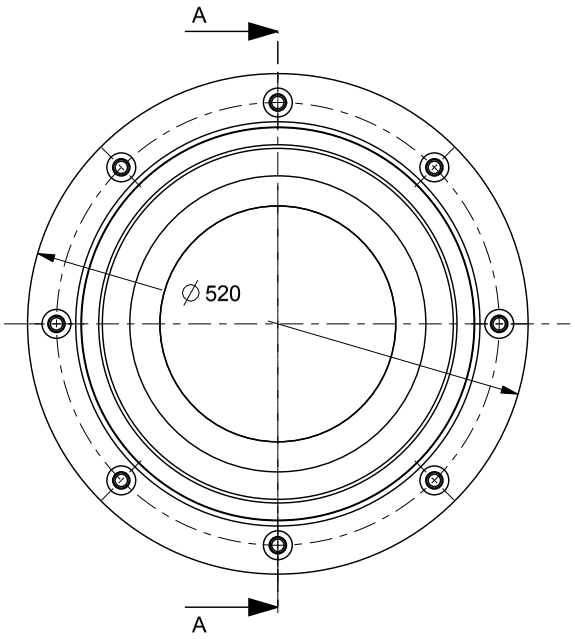

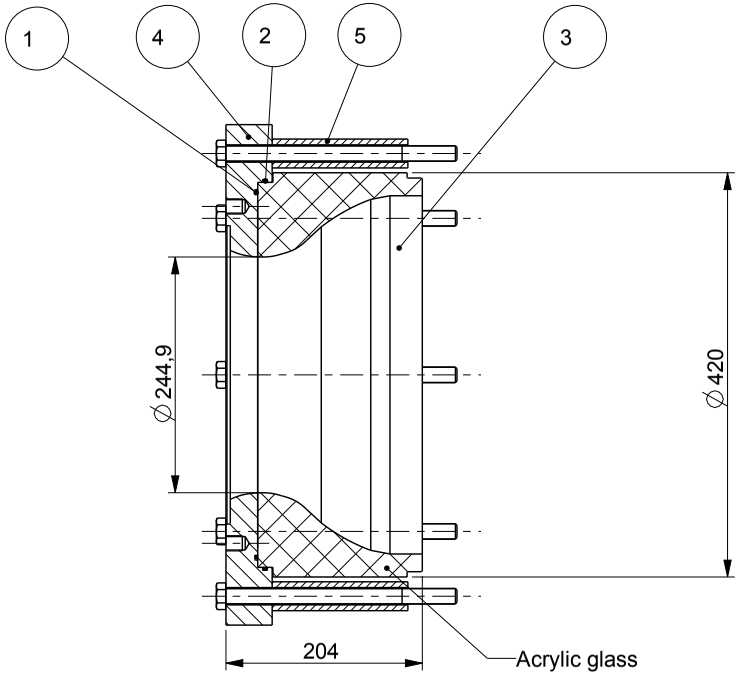

Section A-A

No.	Qnty	DRAWING No.	DENOTATION	STANDARD	MATERIAL	RAW MATERIAL
5	8	BT 1040_004	Bushing		S355J2	
4	1	BT 1040_003	Flange		S355J2	
3	1	BT 1040_001	Casing		Acrylic glass	
2	1		O-ring d=400		NBR70Sh	Cord 3.6
1	1		O-ring d=375		NBR70Sh	Cord 3.6

Dateiname des Zeichnungsobjektes / Name of the drawingobject: 1040_000_LAUFRADMANTEL

Dateityp / File-type: ASSEM

Dateiname der Zeichnung / Name of the drawing: 1040_000_LAUFRADMANTEL

Tolerierung/Tolerance: ISO 8015
Allg. Toleranz/Gen. tolerance: DIN ISO 2768 m-K

Oberflaeche / Surface quality: DIN ISO 1302
Werkst.-Kanten / Part-edges: DIN ISO 13715

Maßstab/Scale: 0,200

Gew./Weight: 68.5 kg

Werkstoff / Material:

Halbzeug / Raw material:

	Datum/Date	Name
Bearb. / Edit.	2013-04-23	Hopfgartner
Gepr. / Cert.		
Norm / Standard		

Benennung/Denotation:

Impeller casing (Shroud)

Graz, University of Technology
Institute for Hydraulic Fluidmachinery

Zeichnungsnummer/Drawing number: BG 1040_000

Blatt/Page 1

1 Bl./P.

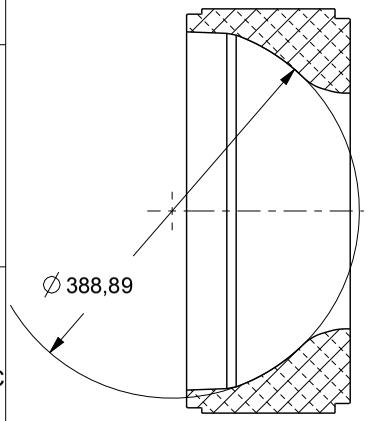

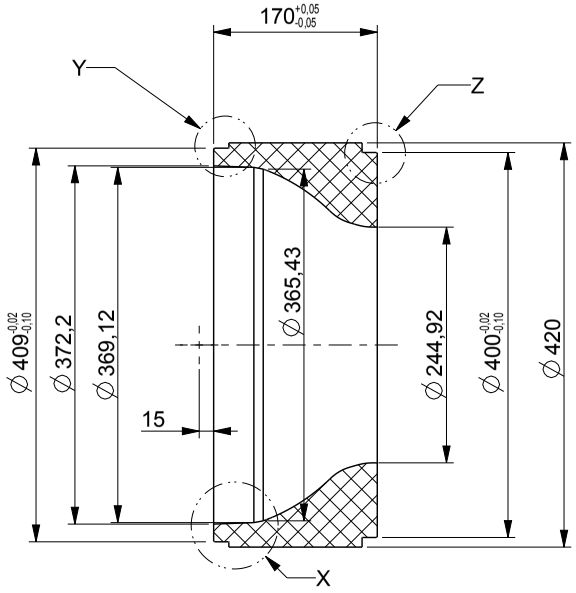

Section A-A

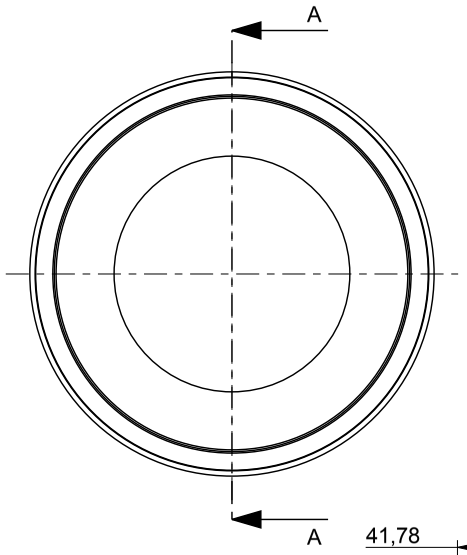

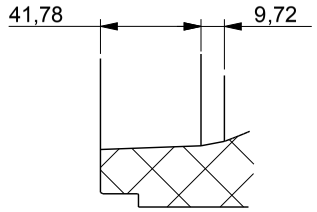

Detail X
Scale 0.500

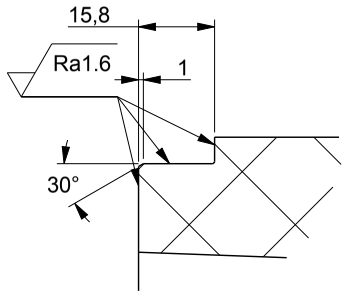

Detail Y
Scale 1.000

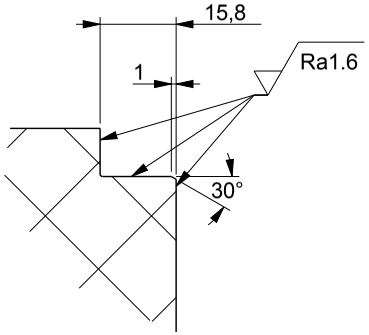

Detail Z
Scale 1.000

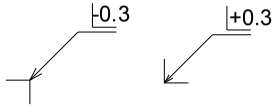

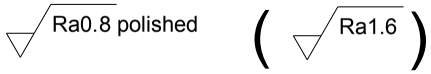

Dateiname des Zeichnungsobjektes / Name of the drawingobject: 1040_001_MANTEL_ZW		Dateityp File-type: PART	Dateiname der Zeichnung / Name of the drawing: 1040_001_MANTEL_ZW
	Tolerierung/Tolerance ISO 8015 Allg. Toleranz/Gen. tolerance DIN ISO 2768 m-K	Oberflaeche Surface quality DIN ISO 1302 Werkst.-Kanten Part-edges DIN ISO 13715	Maßstab/Scale 0,200 Gew./Weight: 11.1 kg Werkstoff / Material: Acrylic glass transparent colourless Halbzeug / Raw material:
	Datum/Date	Name	Benennung/Denotation: Casing Impeller casing
Bearb. Edit.	2013-05-29	Hopfgartner	
Gepr. Cert.			
Norm Standard			
Graz, University of Technology Institute for Hydraulic Fluidmachinery			Zeichnungsnummer/Drawing number: BT 1040_001 Blatt/Page 1 1 Bl./P.

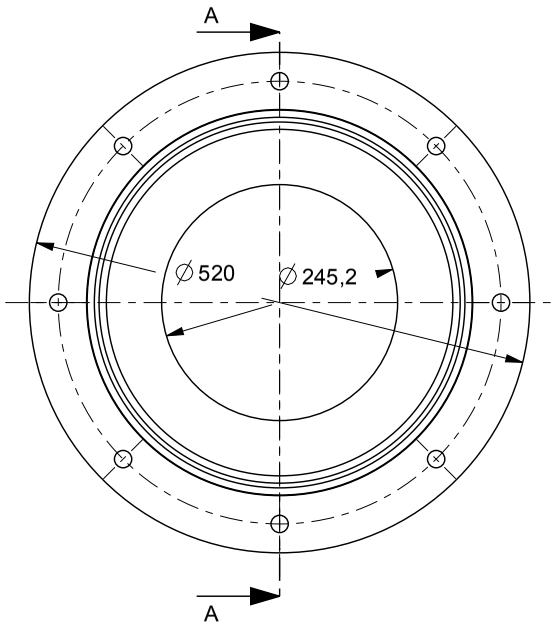

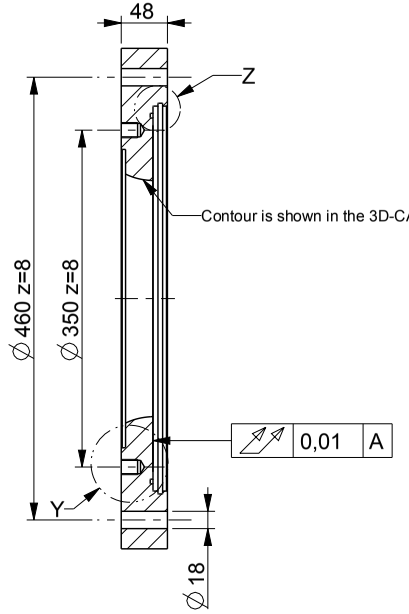

Section A-A

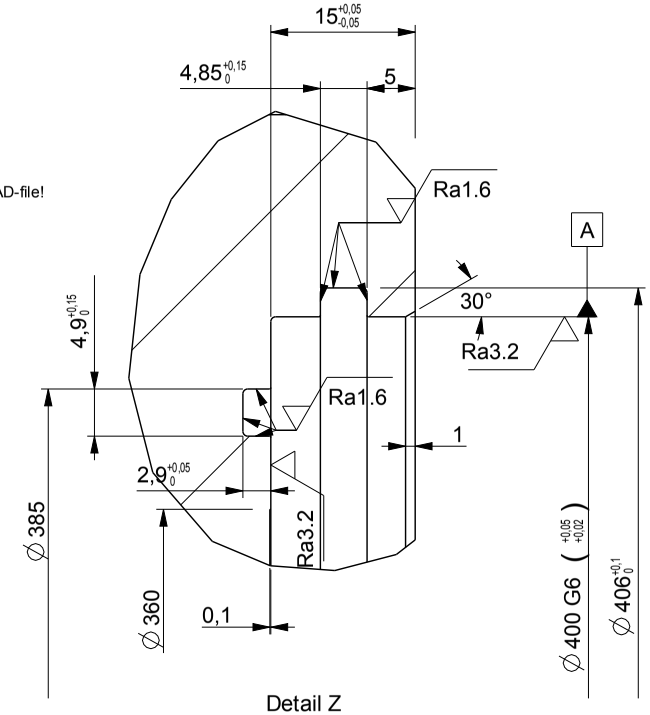

Detail Z
Scale 2.000

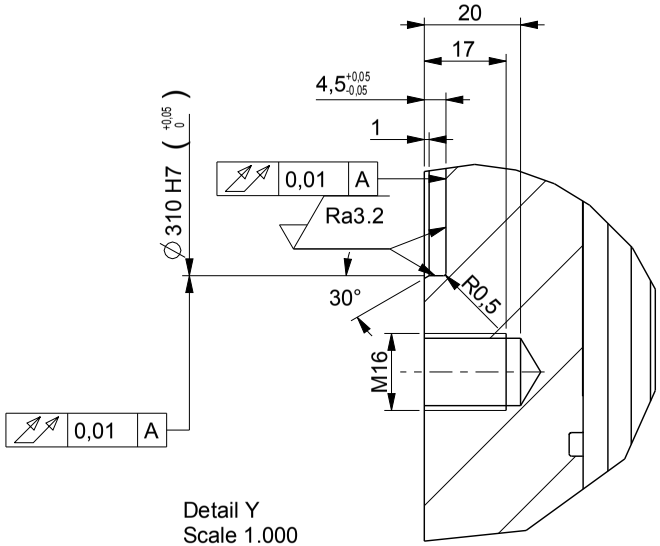

Detail Y
Scale 1.000

-0.2 +0.5

Ra25 (Ra3.2 Ra1.6)

Dateiname des Zeichnungsobjektes / Name of the drawingobject: 1040_003_FLANSCH_SS	Dateityp / File-type: PART	Dateiname der Zeichnung / Name of the drawing: 1040_003_FLANSCH	
Tolerierung/Tolerance ISO 8015; Allg. Toleranz/Gen. tolerance DIN ISO 2768 m-K	Oberflaeche / Surface quality DIN ISO 1302; Werkst.-Kanten / Part-edges DIN ISO 13715	Maßstab/Scale 0,200	Gew./Weight: 50.4 kg
		Werkstoff / Material: S355J2	
		Halbzeug / Raw material: Thermal Cut D=520; d=240; s=50	
	Datum/Date	Name	
Bearb. / Edit.	2013-04-19	Hopfgartner	
Gepr. / Cert.			
Norm / Standard			
Graz, University of Technology, Institute for Hydraulic Fluidmachinery		Benennung/Denotation: Flange Impeller casing	
		Zeichnungsnummer/Drawing number: BT 1040_003	Blatt/Page 1; 1 Bl./P.

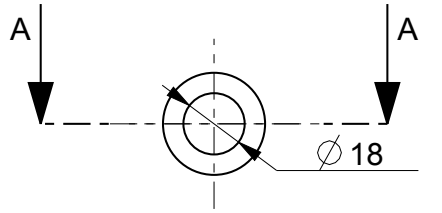

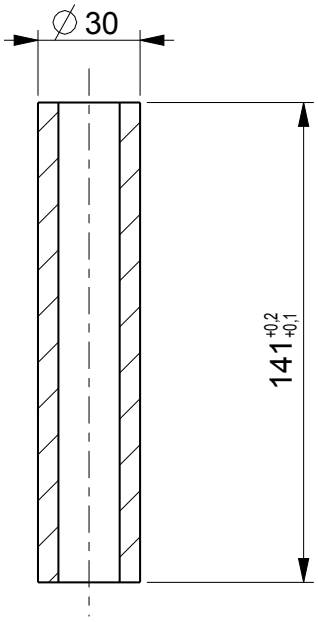

Section A-A

Dateiname des Zeichnungsobjektes / Name of the drawingobject: 1040_004_HUELSE	Dateityp File-type: PART	Dateiname der Zeichnung / Name of the drawing: 1040_004_HUELSE	
	Tolerierung ISO 8015 Allg. Toleranz DIN ISO 2768 m-K	Oberflaeche DIN ISO 1302 Werkst.-Kanten DIN ISO 13715	Maßstab/Scale 0,500 Gew./Weight: 0.5 kg Werkstoff/Material: S355J2 Halbzeug/Feedstock:
	Datum/Date	Name	Benennung/Denotation: Bushing Impeller casing
	Bear. Edit 2013-04-23	Hopfgartner	
	Gepr. Cert.		
	Norm		
	Graz University of Technology Institute for hydraulic fluidmachinery		Zeichnungsnummer / Drawing number: BT 1040_004
			Blatt/Page 1 / 1 Bl./P.

B.5 Diffuser casing

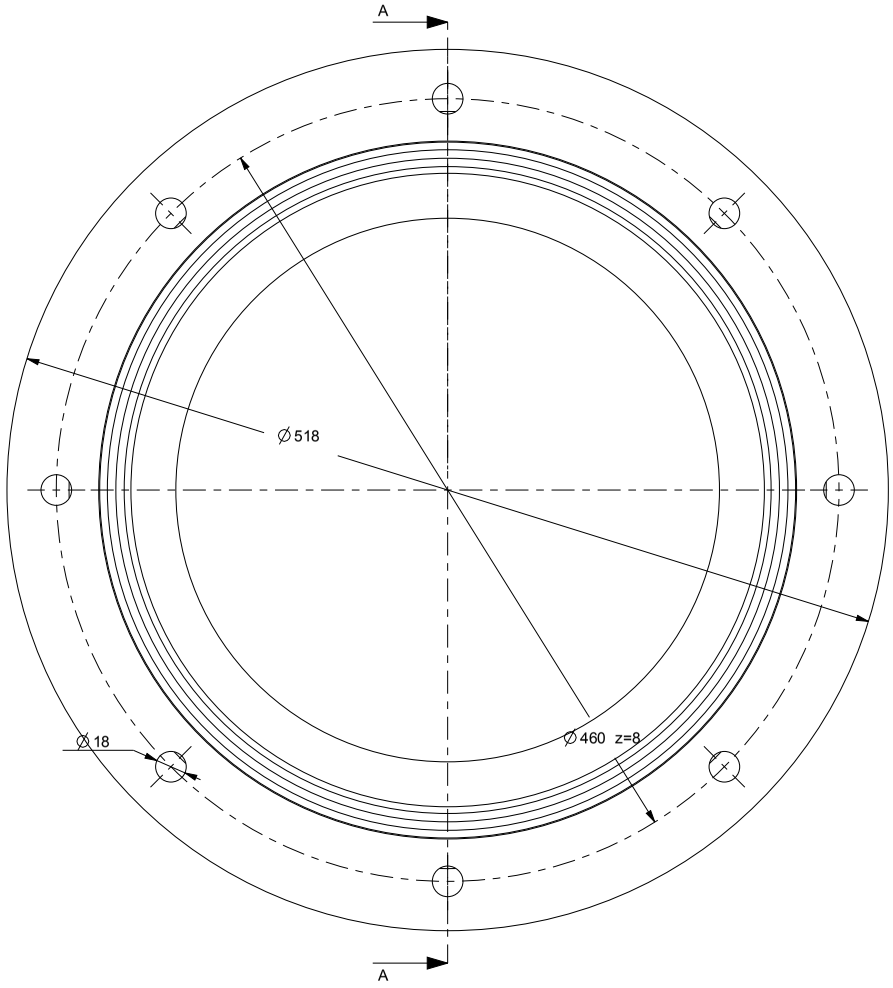

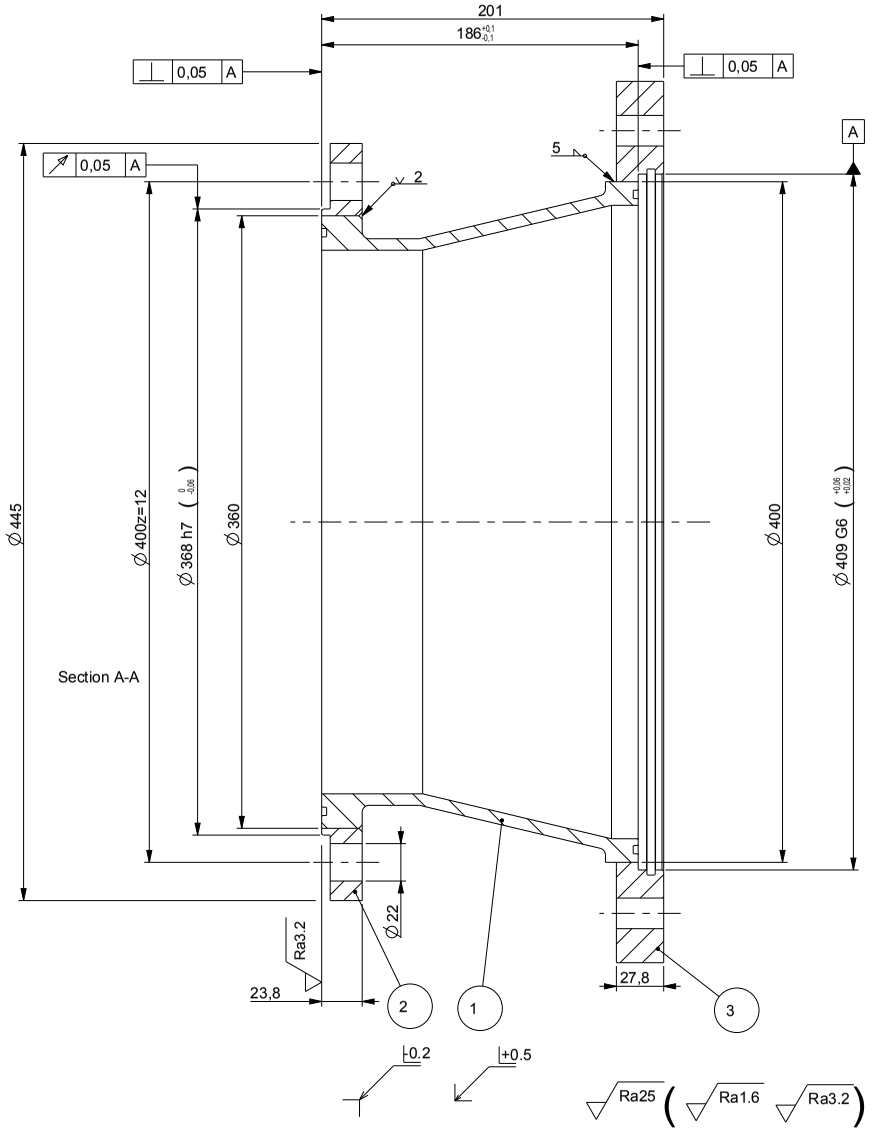

No.	Qnty	DRAWING No.	DENOTATION	STANDARD	MATERIAL	RAW MATERIAL
3	1	BT.1050_003	Flange		S355J2	
2	1	BT.1050_002	Flange		S355J2	
1	1	BT.1050_001	Casing		1.4301	

Missing dimensions are shown in the single-part drawings!

Datei name des Zeichnungsobjektes /Name of the drawing object:
1050_000_LEITRADMANTEL

Dateityp. / File type: ASSEM

Datei name der Zeichnung / Name of the drawing:
1050_000_LEITRADMANTEL

Tolerierung/Tolerance: ISO 8015
Allg. Toleranz/Gen. tolerance: DIN ISO 2768 m-K

Oberfläche / Surface quality: DIN ISO 1302
Werkst.-Kanten / Part edges: DIN ISO 13715

Maßstab/Scale 0,500

Gew./Weight 42.5 kg

Werkstoff/Material:

Halbzeug/Raw material:

	Datum/Date	Name
Bearb./Draft	21.04.18	Hofgärtner
Gepr./Check		
Norm/Standard		

Benennung/Denotation:

Diffuser casing

Graz, University of Technology
Institute for Hydraulic Fluidmachinery

Zeichnungsnummer/Drawing number:
BG 1050_000

Blatt/Page 1
1 BLP

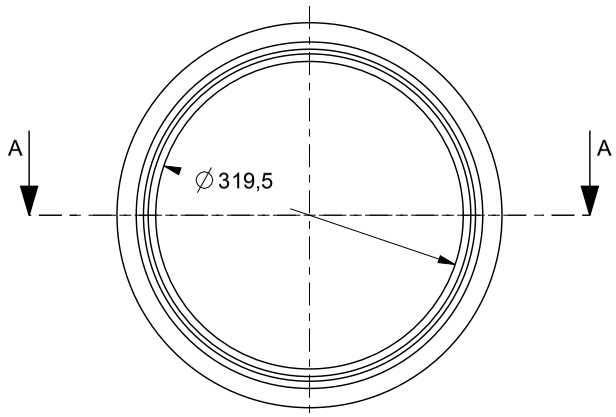

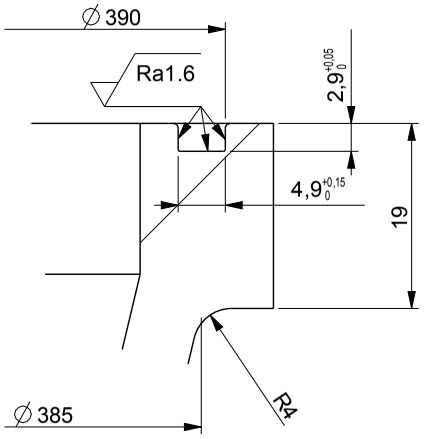

Detail Y
Scale 2.000

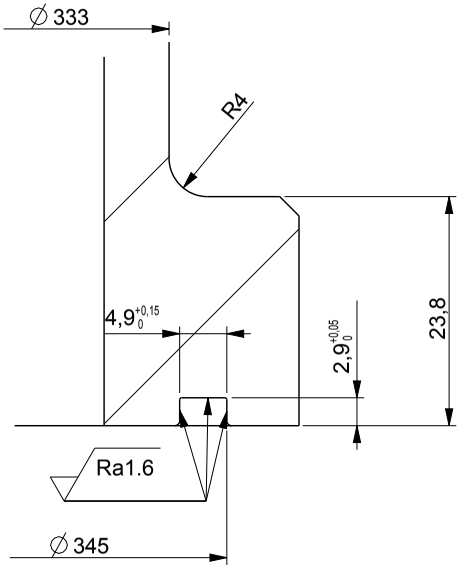

Detail Z
Scale 2.000

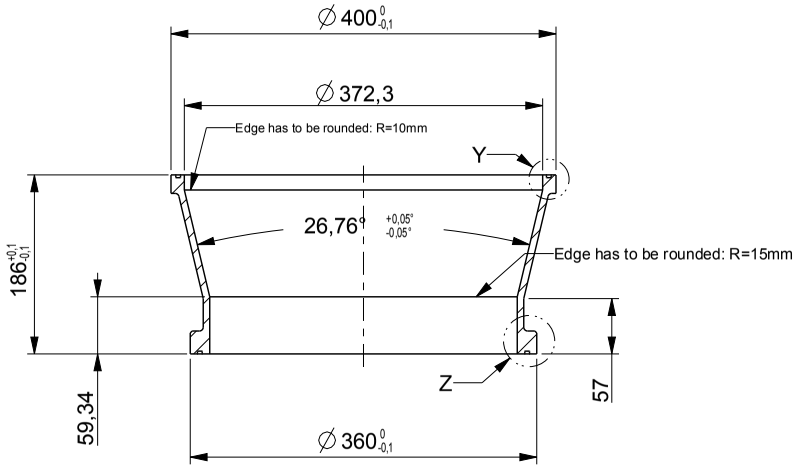

Section A-A

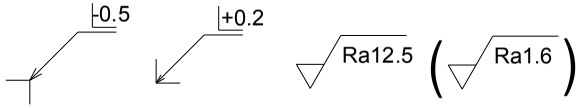

Dateiname des Zeichnungsobjektes / Name of the drawingobject: 1050_001_MANTEL		Dateityp File-type: PART	Dateiname der Zeichnung / Name of the drawing: 1050_001_MANTEL
	Tolerierung/Tolerance ISO 8015 Allg. Toleranz/Gen. tolerance DIN ISO 2768 m-K	Oberflaeche Surface quality DIN ISO 1302 Werkst.-Kanten Part-edges DIN ISO 13715	Maßstab/Scale 0,200 Gew./Weight: 16.1 kg Werkstoff / Material: 1.4301 Halbzeug/ Raw material: Pipe D=400; d=300
	Datum/Date	Name	Benennung/Denotation: Casing Diffuser casing
Bearb. Edit. 2013-04-18 Hopfgartner Gepr. Genh. Norm Standard			
	Graz, University of Technology Institute for Hydraulic Fluidmachinery		Zeichnungsnummer/Drawing number: BT 1050_001 Blatt/Page 1 / 1 Bl./P.

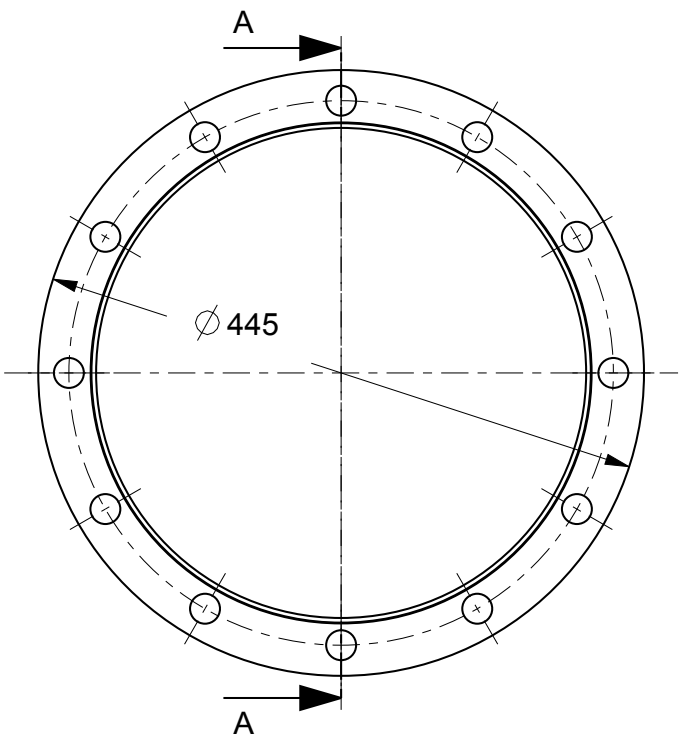

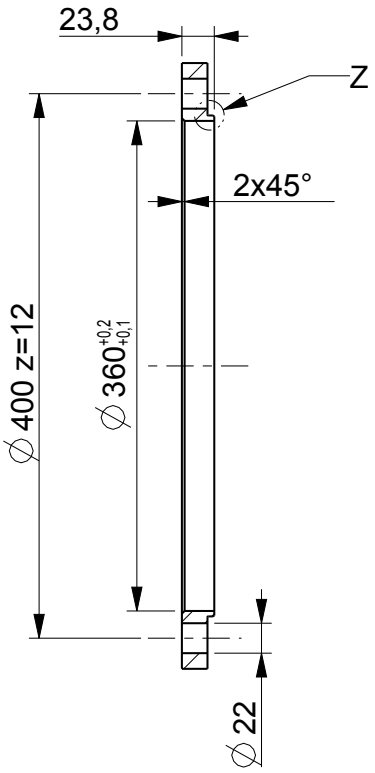

Section A-A

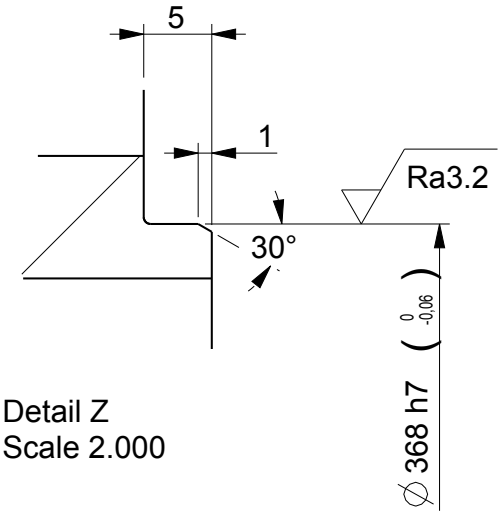

Detail Z
Scale 2.000

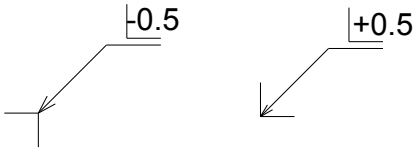

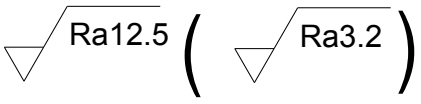

Dateiname des Zeichnungsobjektes / Name of the drawingobject: 1050_002_FLANSCH_DS		Dateityp File-type: PART	Dateiname der Zeichnung / Name of the drawing: 1050_002_FLANSCH
	Tolerierung/Tolerance ISO 8015 Allg. Toleranz/Gen. tolerance DIN ISO 2768 m-K	Oberflaeche Surface quality DIN ISO 1302 Werkst.-Kanten Part-edges DIN ISO 13715	Maßstab/Scale 0,200 Gew./Weight: 7.9 kg
			Werkstoff/Material: S355J2
			Halbzeug/Raw material: Thermal cut D=450; d=310; s=25
	Datum/Date / Name		Benennung/Denotation: Flange Diffuser casing
	Bear. / Edit. 2013-04-18 Hopfgartner		
	Gepr. / Cert.		
	Norm / Standard		
	Graz, University of Technology Institute for Hydraulic Fluidmachinery		Zeichnungsnummer / Drawing number: BT 1050_002
			Blatt/Page 1 — 1 Bl./P.

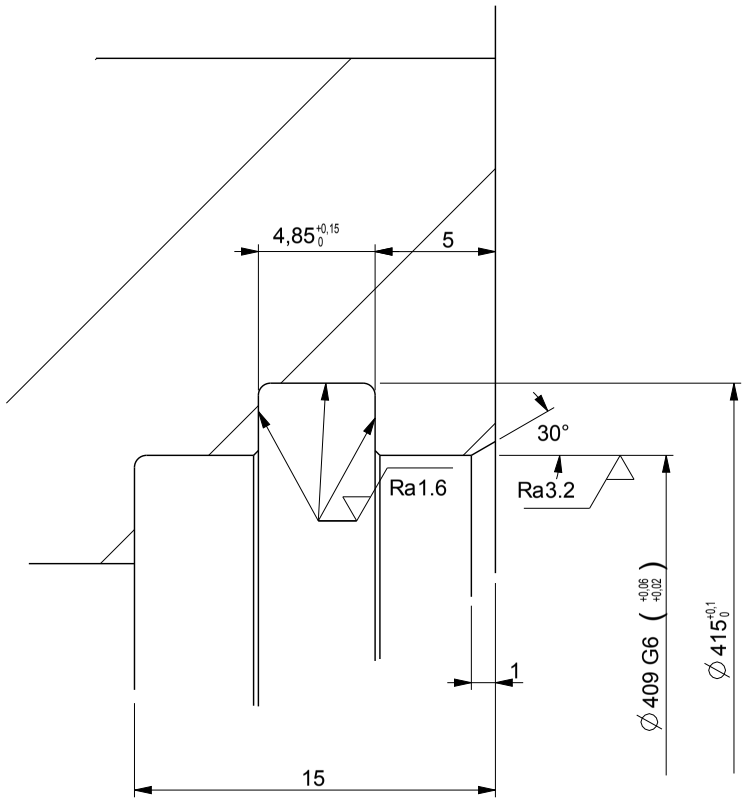

Detail Z
Scale 5.000

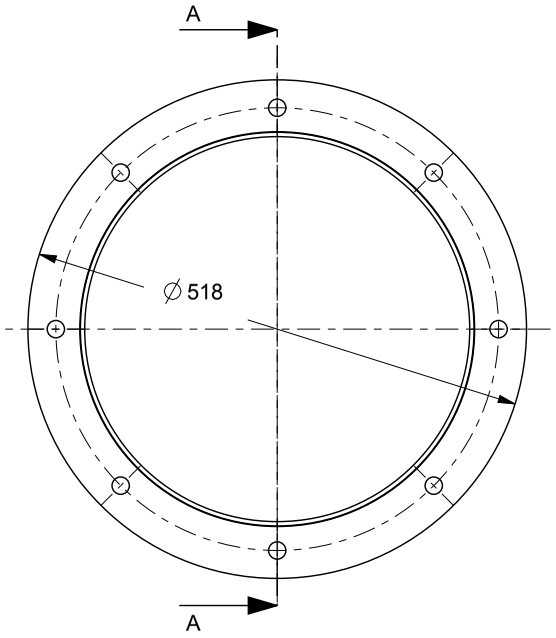

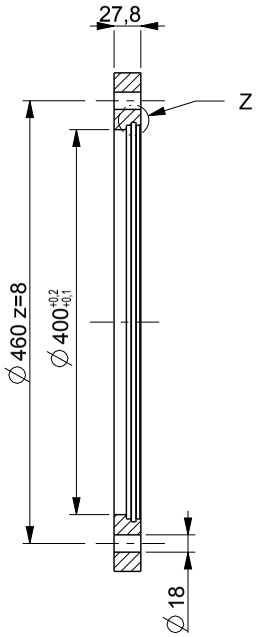

Section A-A

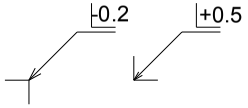

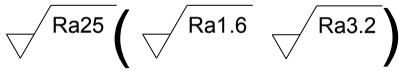

Dateiname des Zeichnungsobjektes / Name of the drawingobject: 1050_003_FLANSCH_SS		Dateityp File-type: PART	Dateiname der Zeichnung / Name of the drawing: 1050_003_FLANSCH
	Tolerierung/Tolerance ISO 8015 Allg. Toleranz/Gen. tolerance DIN ISO 2768 m-K	Oberfläche Surface quality DIN ISO 1302 Werkst.-Kanten Part-edges DIN ISO 13715	Maßstab/Scale 0,200 Gew./Weight: 18.5 kg Werkstoff / Material: S355J2 Halbzeug / Raw material: Thermal cut D=520; d=350; s=30
	Datum/Date	Name	Benennung/Denotation: Flange Diffuser casing
Bearb. Edit. 2013-04-18 Hopfgartner Gepr. Cert. Norm Standard			
	Graz, University of Technology Institute for Hydraulic Fluidmachinery		Zeichnungsnummer/Drawing number: BT 1050_003 Blatt/Page 1 / 1 Bl./P.

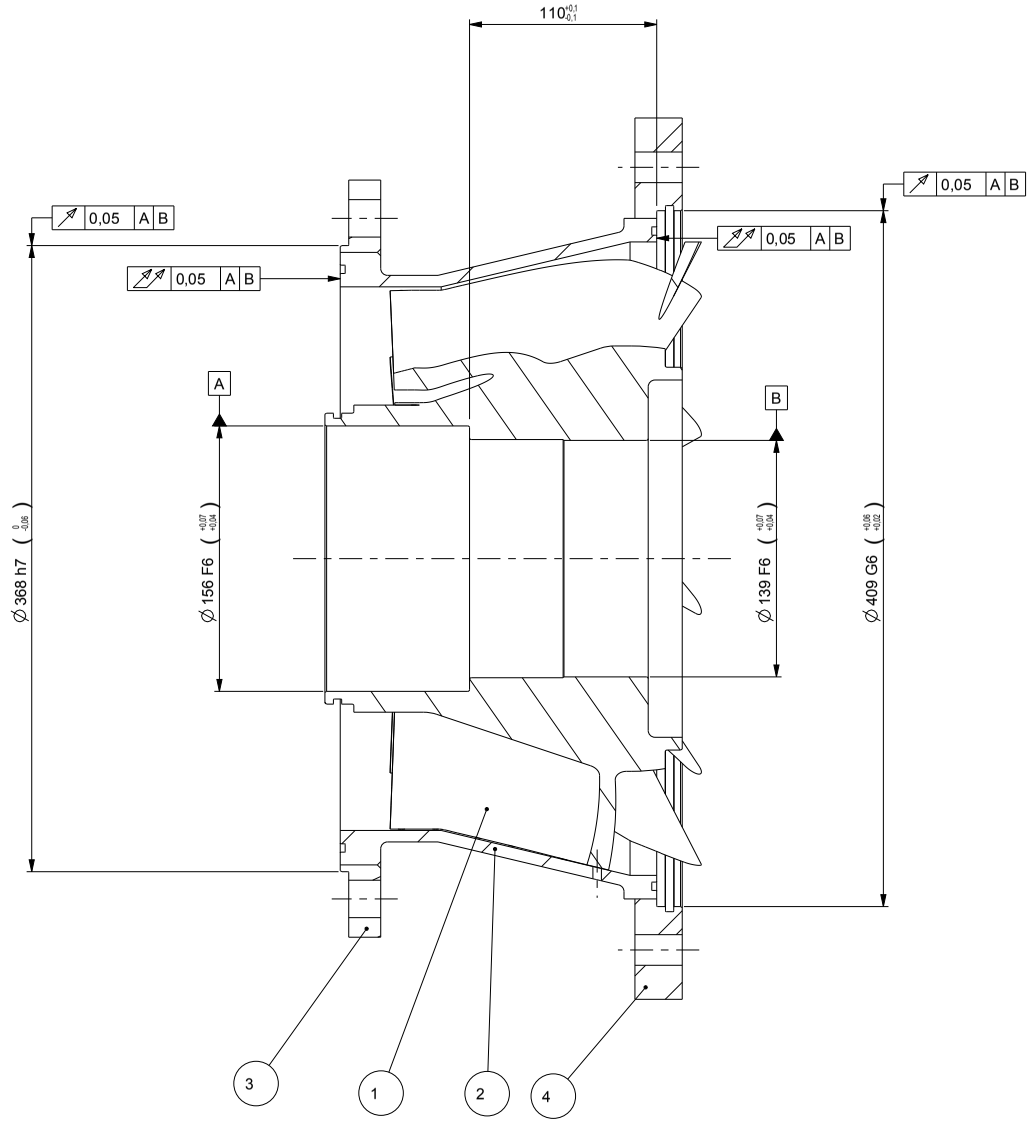

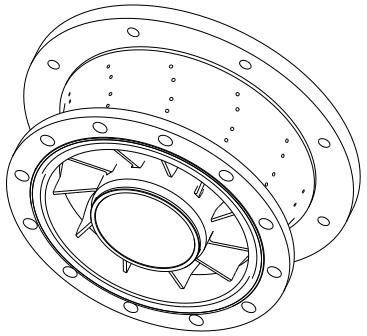

Scale 0.200

The diffuser and the casing are connected together by welding (bore holes). These bore holes are bored into the vanes of the diffuser from outside, after the two parts are assembled.

Missing dimensions and explanatary notes are shown in the single-part drawings!

No.	Qnty	DRAWING No.	DENOTATION	STANDARD	MATERIAL	RAW MATERIAL
4	1	BT.1050_003	Flange		S355J2	
3	1	BT.1050_002	Flange		S355J2	
2	1	BT.1050_001	Casing		1.4301	
1	1	BT.1010_006	Diffuser		1.4301	

Datenname des Zeichnungsobjektes /Name of the drawing object: 1050_100_LEITAPPARAT_MONT

Dateityp. /File-type: ASSEM

Datenname der Zeichnung / Name of the drawing: 1050_100_LEIT_MONT

Toleranzung/Tolerance: ISO 8015; Allg. Toleranz/Gen. tolerance: DIN ISO 2768 m-K

Oberfläche/Surface quality: DIN ISO 1302

Werkst.-Kanten/Part edges: DIN ISO 13715

Maßstab/Scale: 0,500

Gew./Weight: 78kg

Werkstoff/Material:

Halbzeug/Raw material:

	Datum/Date	Name
Bearb./Draft	21.04.14	Hofgärtner
Gepr./Check		
Norm/Standard		

Benennung/Denotation:

Diffuser with casing

Graz, University of Technology
Institute for Hydraulic Fluidmachinery

Zeichnungsnummer/Drawing number: BG 1050_100

Blatt/Page 1

1 BLP

B.6 Outer pipe

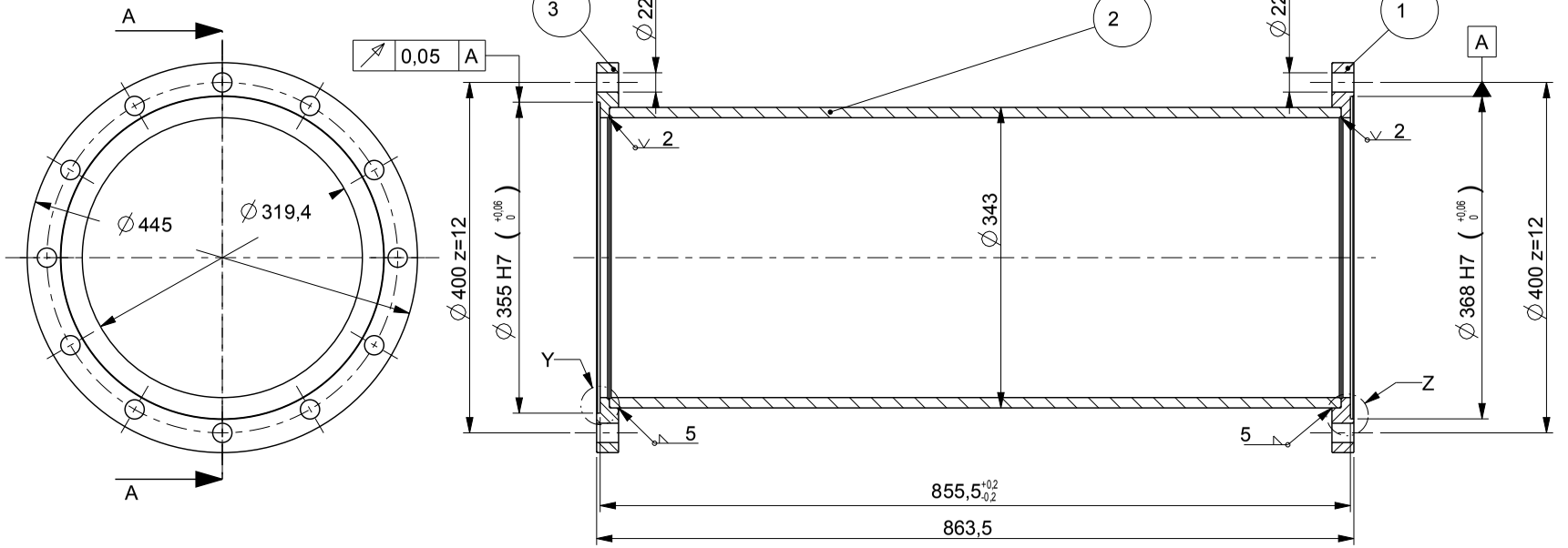

Section A-A

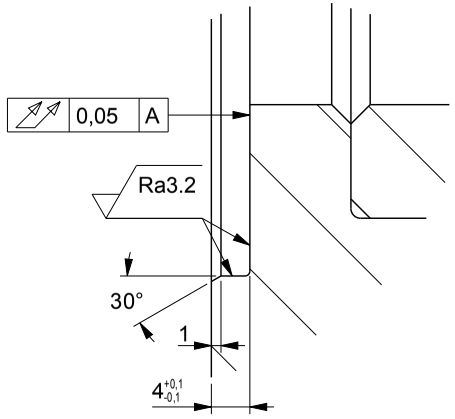

Detail Y
Scale 2.000

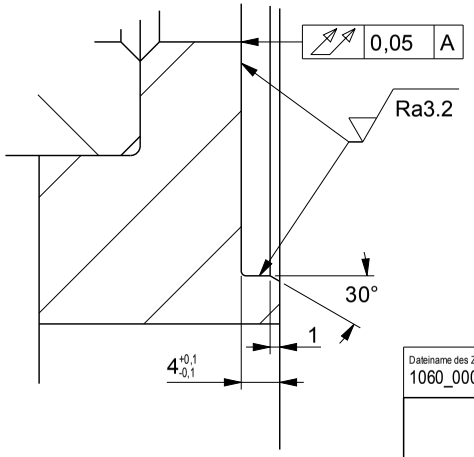

Detail Z
Scale 2.000

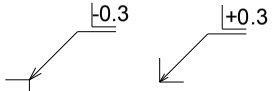

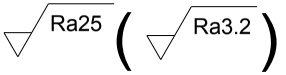

Missing dimensions are shown in the single-part drawings!

No.	Qnty	DRAWING No.	DENOTATION	STANDARD	MATERIAL	RAW MATERIAL
3	1	BT 1060_004	Flange		S355J2	
2	1	BT 1060_002	Casing		S355J2	343x17,5
1	1	BT 1060_001	Flange		S355J2	

Dateiname des Zeichnungsobjektes / Name of the drawingobject:	1060_000_AUSSENROHR
Dateityp / File-type:	ASSEM
Dateiname der Zeichnung / Name of the drawing:	1060_000_AUSSENROHR
Tolerierung/Tolerance	ISO 8015
Allg. Toleranz/Gen. tolerance	DIN ISO 2768 m-K
Oberflaeche / Surface quality	DIN ISO 1302
Werkst.-Kanten / Part-edges	DIN ISO 13715
Maßstab/Scale	0,200
Gew./Weight:	103.8 kg
Werkstoff / Material:	
Halbzeug/ Raw material:	

	Datum/Date	Name
Bearb.	2013-04-19	Hopfgartner
Edit.		
Gepr.		
Cert.		
Norm		
Standard		

Benennung/Denotation:

Outer pipe

Graz, University of Technology
Institute for Hydraulic
Fluidmachinery

Zeichnungsnummer/Drawing number:
BG 1060_000

Blatt/Page 1
1 Bl./P.

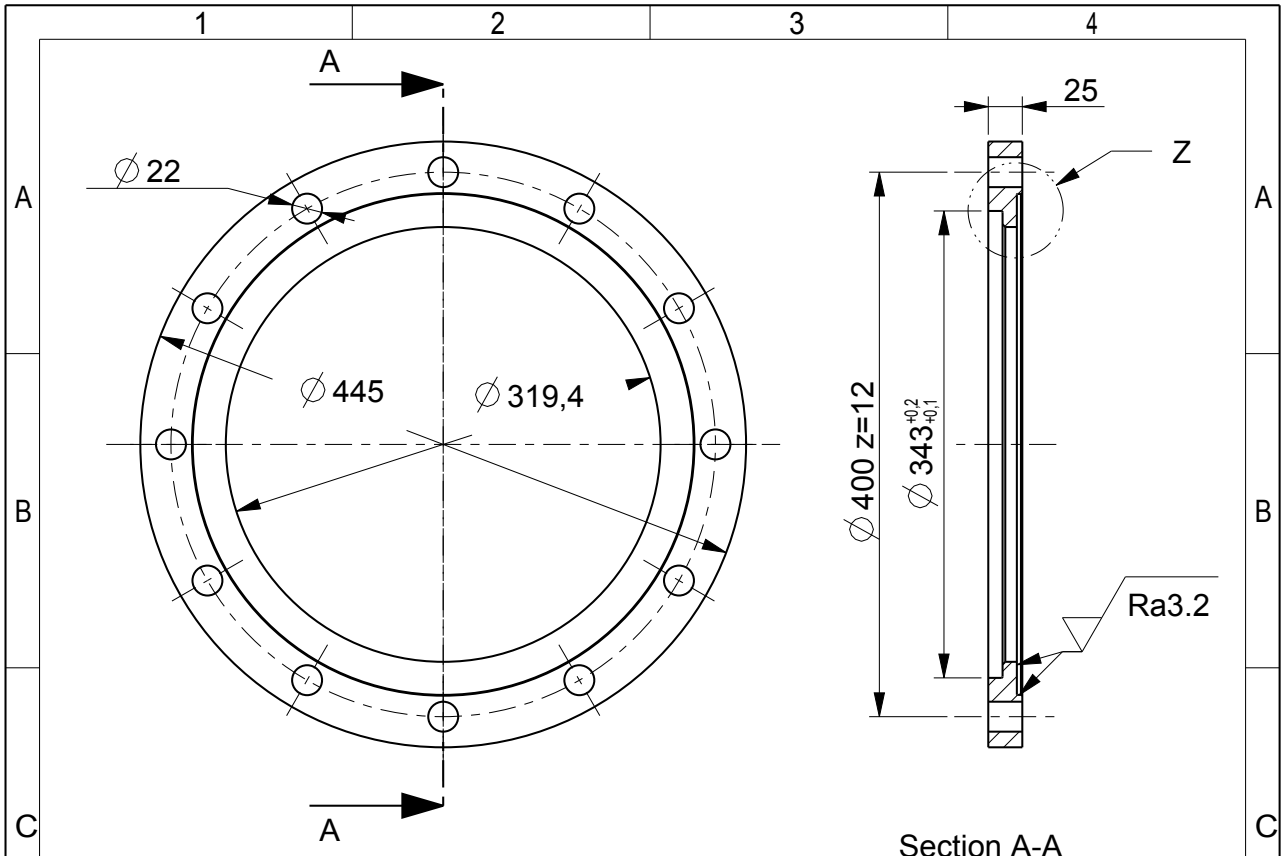

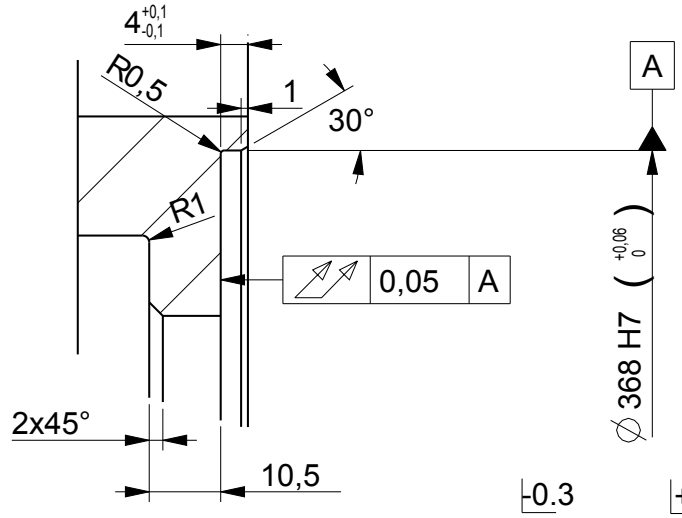

Detail Z
Scale 1.000

-0.3 +0.5

Ra25 (Ra3.2)

Dateiname des Zeichnungsobjektes / Name of the drawingobject: 1060_001_FLANSCH_SS		Dateityp File-type: PART	Dateiname der Zeichnung / Name of the drawing: 1060_001_FLANSCH
	Tolerierung/Tolerance ISO 8015 Allg. Toleranz/Gen. tolerance DIN ISO 2768 m-K	Oberflaeche Surface quality DIN ISO 1302 Werkst.-Kanten Part-edges DIN ISO 13715	Maßstab/Scale 0,200 Gew./Weight: 12.3 kg
			Werkstoff/Material: S355J2
			Halbzeug/Raw material: Breaker Plate D=450; d=310; s=25
	Datum/Date	Name	Benennung/Denotation:
	Bear. / Edit. 2013-04-19	Hopfgartner	Flange Outer pipe
	Gepr. / Cert.		
	Norm / Standard		
Graz, University of Technology Institute for Hydraulic Fluidmachinery			Zeichnungsnummer / Drawing number: BT 1060_001
			Blatt/Page 1
			1 Bl./P.

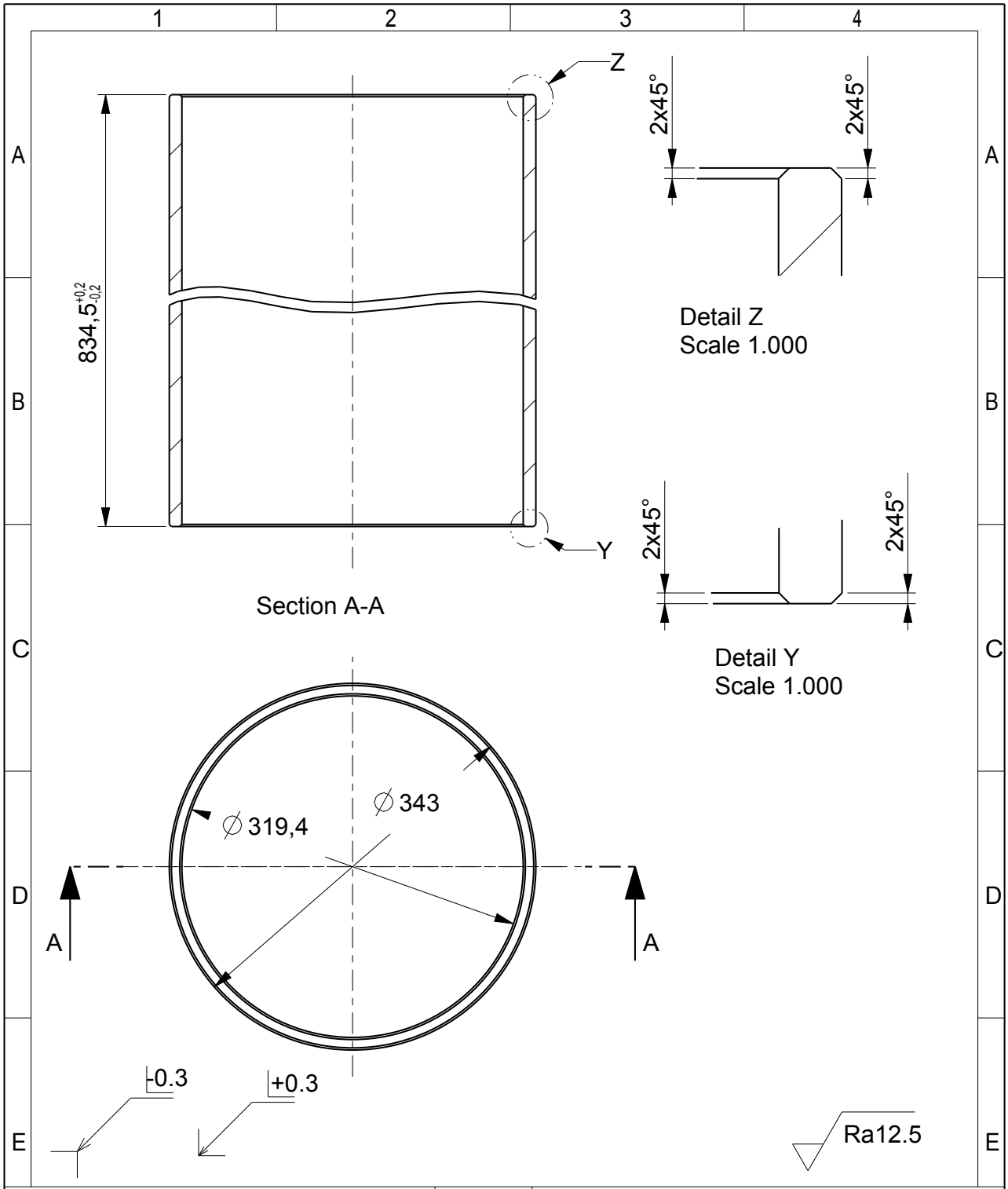

Dateiname des Zeichnungsobjektes / Name of the drawingobject: 1060_002_MANTEL		Dateityp File-type: PART	Dateiname der Zeichnung / Name of the drawing: 1060_002_MANTEL
	Tolerierung/Tolerance ISO 8015 Allg. Toleranz/Gen. tolerance DIN ISO 2768 m-K	Oberflaeche Surface quality DIN ISO 1302 Werkst.-Kanten Part-edges DIN ISO 13715	Maßstab/Scale 0,200 Gew./Weight: 39.6 kg Werkstoff/Material: S355J2 Halbzeug/Raw material: Pipe 343x17.5
	Datum/Date / Name Bear. / Edit. 2013-05-29 Hopfgartner Gepr. / Cert. Norm / Standard		Benennung/Denotation: Pipe Outer Pipe
	Graz, University of Technology Institute for Hydraulic Fluidmachinery		Zeichnungsnummer / Drawing number: BT 1060_002 Blatt/Page 1 1 Bl./P.

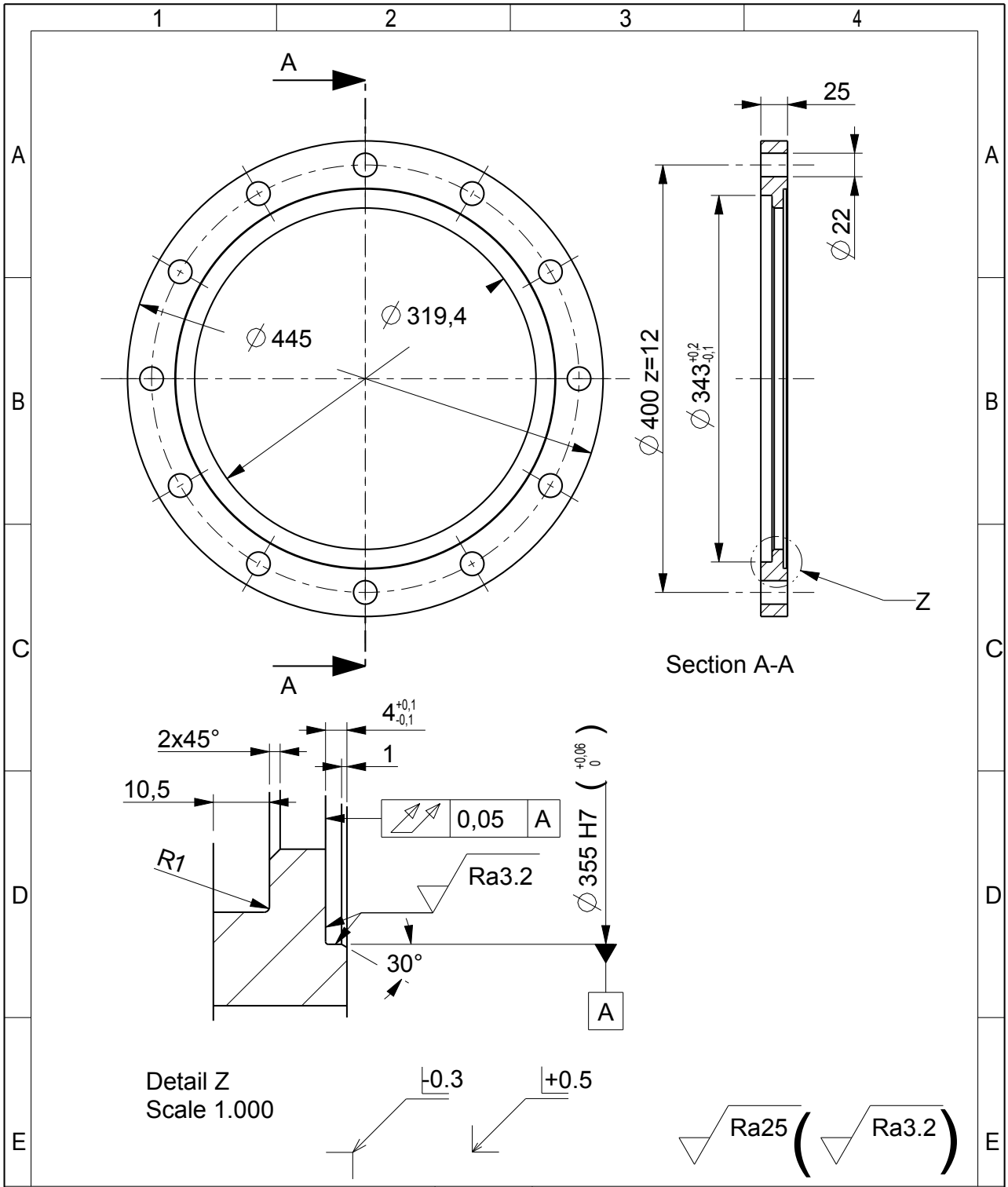

Dateiname des Zeichnungsobjektes / Name of the drawingobject: 1060_004_FLANSCH_DS		Dateityp File-type: PART	Dateiname der Zeichnung / Name of the drawing: 1060_004_FLANSCH
	Tolerierung/Tolerance ISO 8015 Allg. Toleranz/Gen. tolerance DIN ISO 2768 m-K	Oberflaeche Surface quality DIN ISO 1302 Werkst.-Kanten Part-edges DIN ISO 13715	Maßstab/Scale 0,200 Gew./Weight: 12.3 kg
			Werkstoff/Material: S355J2
			Halbzeug/Raw material: Thermal cut D=450; d=310; s=25
	Datum/Date	Name	Benennung/Denotation:
	Bear. / Edit. 2013-04-19	Hopfgartner	Flange Outer pipe
	Gepr. / Cert.		
	Norm / Standard		
Graz, University of Technology Institute for Hydraulic Fluidmachinery			Zeichnungsnummer / Drawing number: BT 1060_004
			Blatt/Page 1
			1 Bl./P.

B.7 Suction pipe

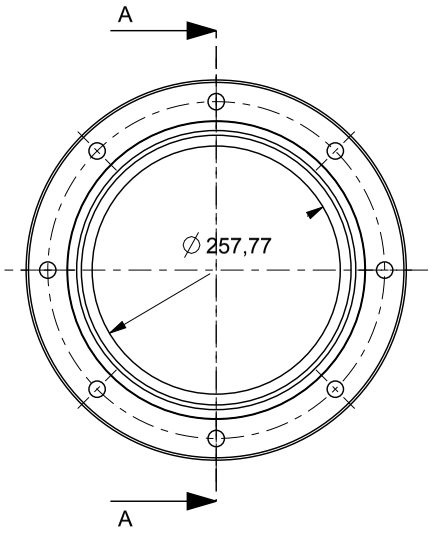

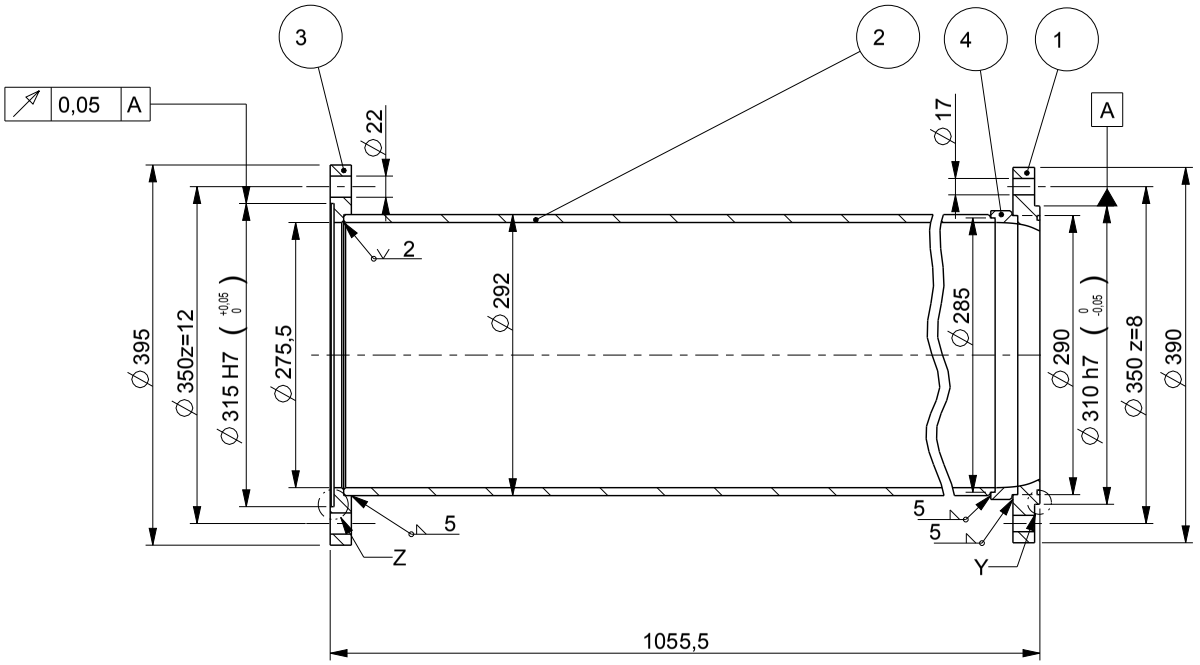

Section A-A

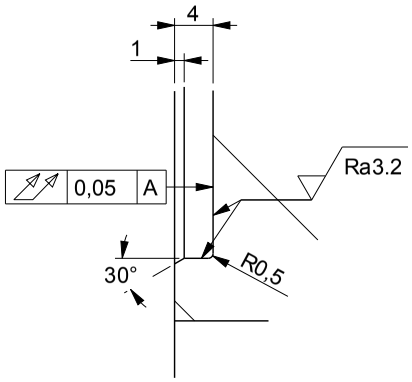

Detail Z
Scale 2.000

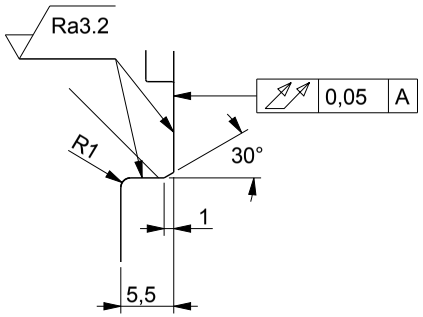

Detail Y
Scale 2.000

Missing dimensions are shown in the single-part drawings!

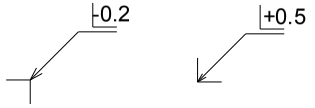

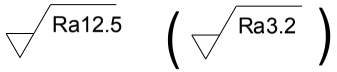

No.	Qnty	DRAWING No.	DENOTATION	STANDARD	MATERIAL	RAW MATERIAL
4	1	BT 1070_006	Adapter flange		S355J2	
3	1	BT 1070_003	Flange		S355J2	
2	1	BT 1070_002	Pipe		S355J2	292x10
1	1	BT 1070_001	Flange		S355J2	

Dateiname des Zeichnungsobjektes / Name of the drawingobject: 1070_000_SAUGROHR					Dateityp File-type: ASSEM	Dateiname der Zeichnung / Name of the drawing: 1070_000_SAUGROHR		
				Toleranz/Tolerance ISO 8015 Allg. Toleranz/Gen. tolerance DIN ISO 2768 m-K	Oberflaeche Surface quality DIN ISO 1302 Werkst.-Kanten Part-edges DIN ISO 13715	Maßstab/Scale 0,200	Gew./Weight: 82.7 kg	
						Werkstoff / Material: Halbzeug/ Raw material:		
				Datum/Date	Name	Benennung/Denotation:		
				Bearb. Edit.	2013-04-19	Hopfgartner		
				Gepr. Cert.				
				Norm Standard				
				Graz, University of Technology Institute for Hydraulic Fluidmachinery		Suction Pipe		
						Zeichnungsnummer/Drawing number: BG 1070_000	Blatt/Page 1	1 Bl./P.

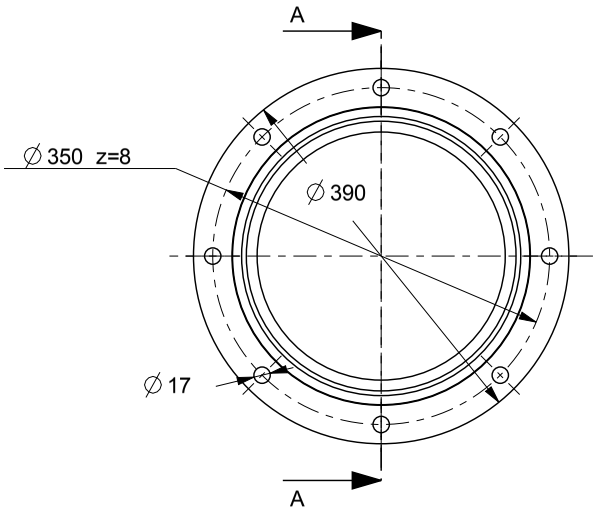

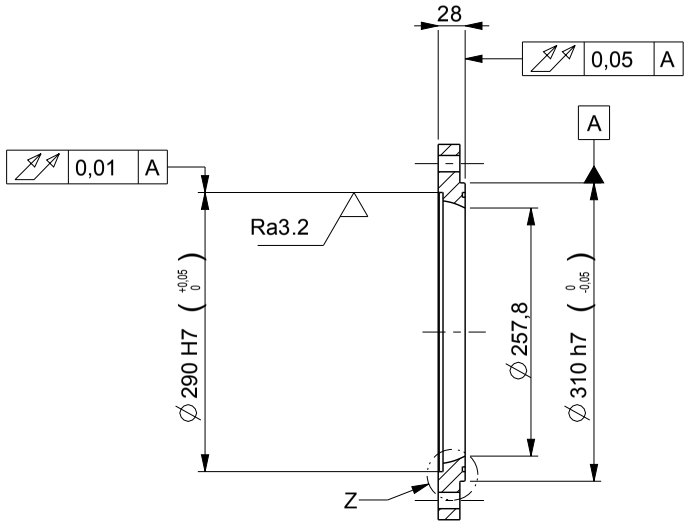

Section A-A

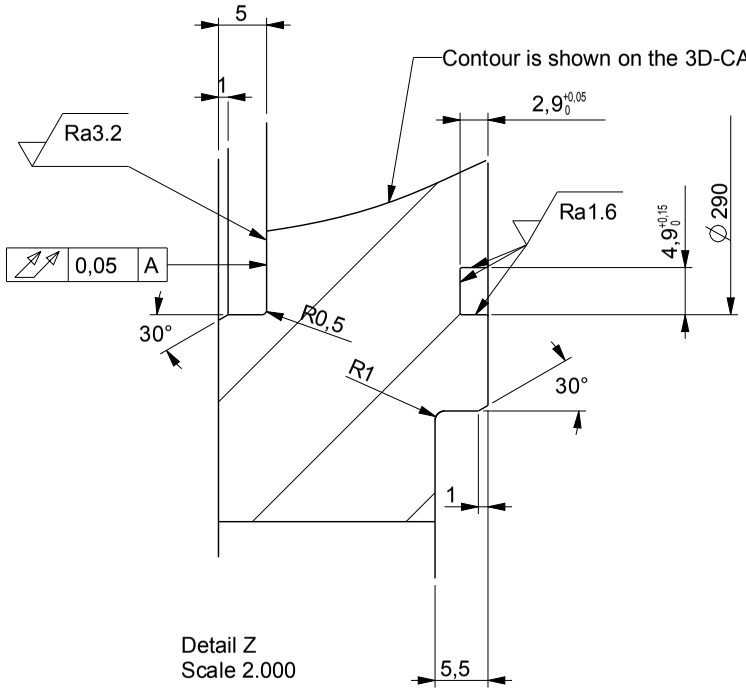

Detail Z
Scale 2.000

0.2 +0.5

Ra12.5 (Ra1.6 Ra3.2)

Dateiname des Zeichnungsobjektes / Name of the drawingobject: 1070_001_FLANSCH		Dateityp / File-type: PART	Dateiname der Zeichnung / Name of the drawing: 1070_001_FLANSCH
	Tolerierung/Tolerance ISO 8015; Allg. Toleranz/Gen. tolerance DIN ISO 2768 m-K	Oberflaeche / Surface quality DIN ISO 1302; Werkst.-Kanten / Part-edges DIN ISO 13715	Maßstab/Scale 0,200; Gew./Weight: 12.4 kg; Werkstoff / Material: S355J2; Halbzeug / Raw material: Thermal cut D=520; d=240; s=30
	Datum/Date; Name		Benennung/Denotation: Flange Suction pipe
	Bearb. / Edit. 2013-04-19 Hopfgartner; Gepr. / Cert.; Norm / Standard		
	Graz, University of Technology Institute for Hydraulic Fluidmachinery		Zeichnungsnummer/Drawing number: BT 1070_001; Blatt/Page 1; 1 Bl./P.

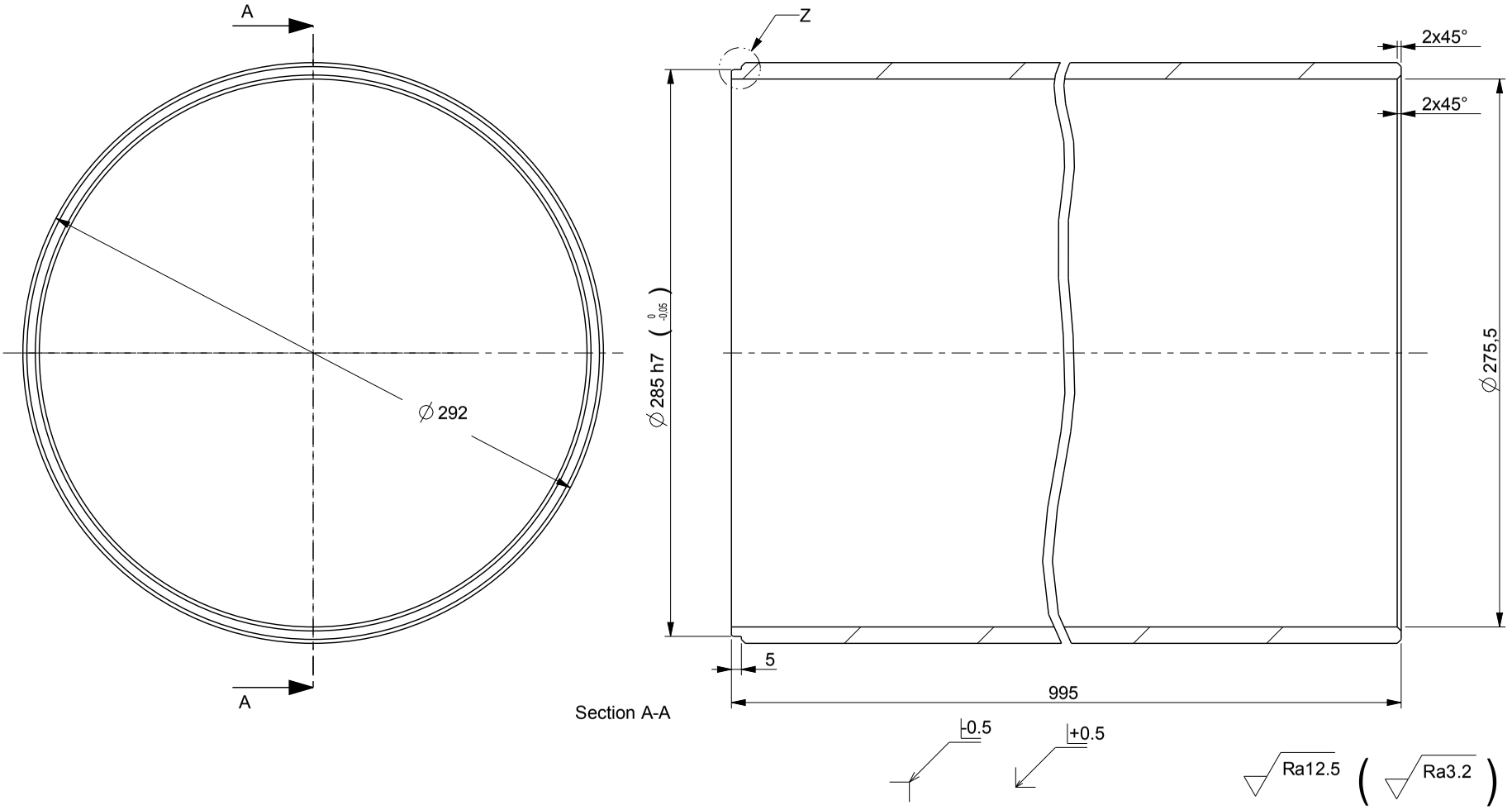

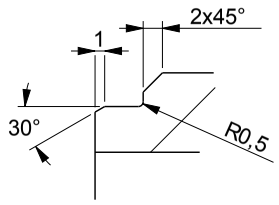

Detail Z
Scale 2.000

Dateiname des Zeichnungsobjektes / Name of the drawingobject: 1070_002_ROHR		Dateityp File-type: PART	Dateiname der Zeichnung / Name of the drawing: 1070_002_ROHR
	Tolerierung/Tolerance ISO 8015 Allg. Toleranz/Gen. tolerance DIN ISO 2768 m-K	Oberflaeche Surface quality DIN ISO 1302 Werkst.-Kanten Part-edges DIN ISO 13715	Maßstab/Scale 0,500 Gew./Weight: 29.3 kg Werkstoff / Material: S355J2 Halbzeug / Raw material: Pipe 292x10
	Datum/Date	Name	Benennung/Denotation: Pipe Suction pipe
Bearb. Edit.	2013-05-29	Hopfgartner	
Gepr. Cert.			
Norm Standard			
	Graz, University of Technology Institute for Hydraulic Fluidmachinery		Zeichnungsnummer/Drawing number: BT 1070_002
			Blatt/Page 1 1 Bl./P.

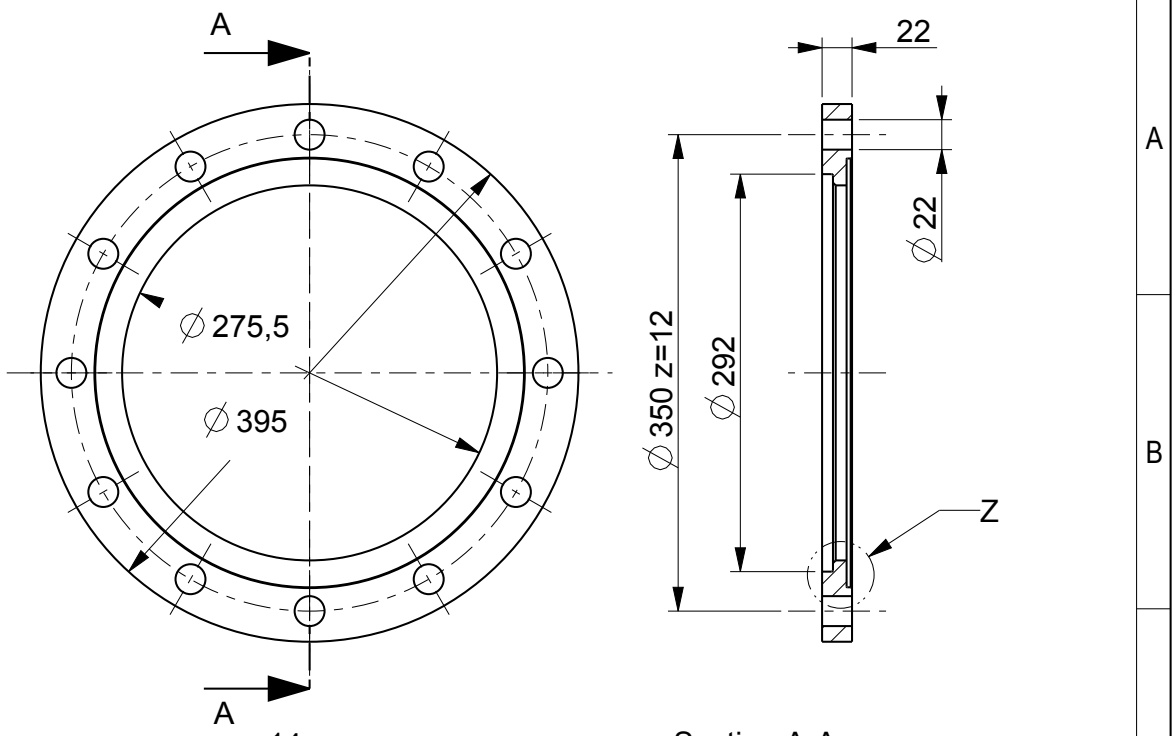

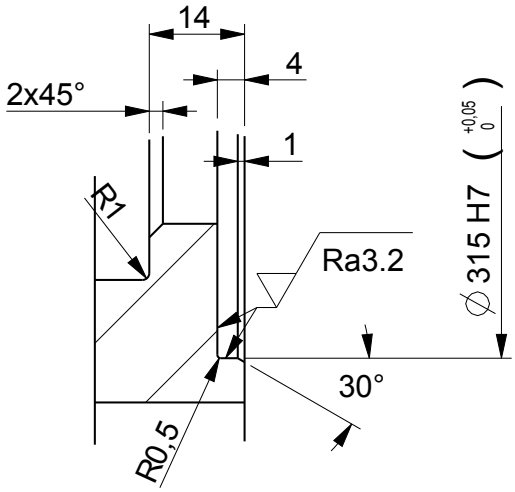

Detail Z
Scale 1.000

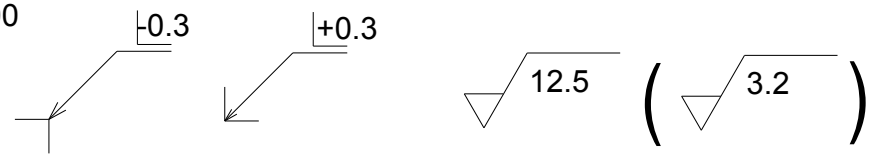

Dateiname des Zeichnungsobjektes / Name of the drawingobject: 1070_003_FLANSCH		Dateityp File-type: PART	Dateiname der Zeichnung / Name of the drawing: 1070_003_FLANSCH
	Tolerierung/Tolerance ISO 8015 Allg. Toleranz/Gen. tolerance DIN ISO 2768 m-K	Oberflaeche Surface quality DIN ISO 1302 Werkst.-Kanten Part-edges DIN ISO 13715	Maßstab/Scale 0,200 Gew./Weight: 10.0 kg Werkstoff/Material: S355J2 Halbzeug/Raw material: Plate D=400; s=25
	Datum/Date	Name	Benennung/Denotation:
	Bear. / Edit. 2013-04-19	Hopfgartner	Flange Suction pipe
	Gepr. / Cert.		
	Norm / Standard		
Graz, University of Technology Institute for Hydraulic Fluidmachinery			Zeichnungsnummer / Drawing number: BT 1070_003
			Blatt/Page 1 1 Bl./P.

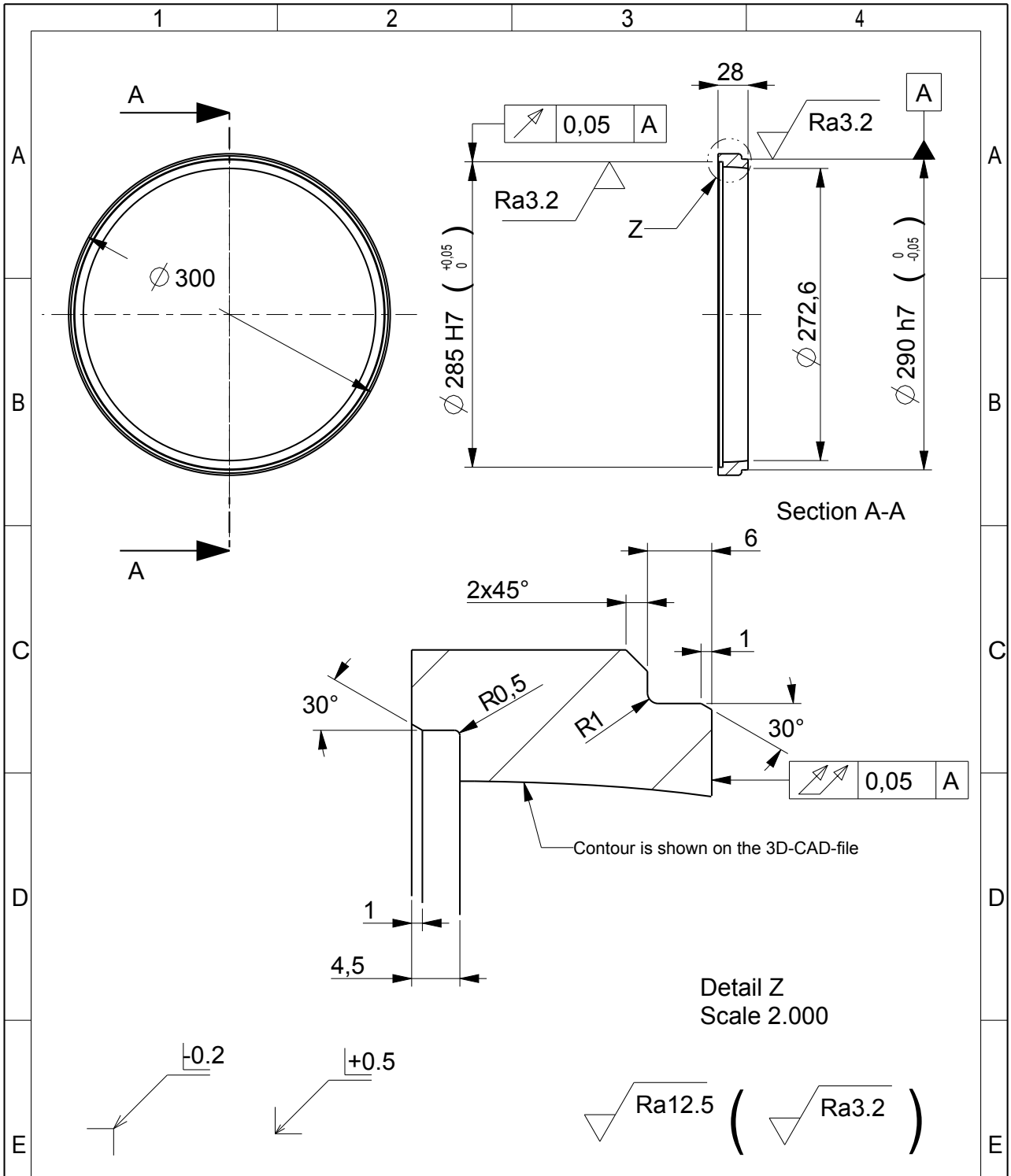

Dateiname des Zeichnungsobjektes / Name of the drawingobject: 1070_006_FLANSCH		Dateityp File-type: PART	Dateiname der Zeichnung / Name of the drawing: 1070_006_FLANSCH
	Tolerierung/Tolerance ISO 8015 Allg. Toleranz/Gen. tolerance DIN ISO 2768 m-K	Oberflaeche Surface quality DIN ISO 1302 Werkst.-Kanten Part-edges DIN ISO 13715	Maßstab/Scale 0,200 Gew./Weight: 2.7 kg Werkstoff/Material: S355J2 Halbzeug/Raw material: Thermal cut D=315; d=250; s=30
	Datum/Date / Name Bear. / Edit. 2013-04-19 Hopfgartner Gepr. / Cert. Norm / Standard		Benennung/Denotation: Adapter flange Suction pipe
	Graz, University of Technology Institute for Hydraulic Fluidmachinery		Zeichnungsnummer / Drawing number: BT 1070_006 Blatt/Page 1 1 Bl./P.

B.8 Conus

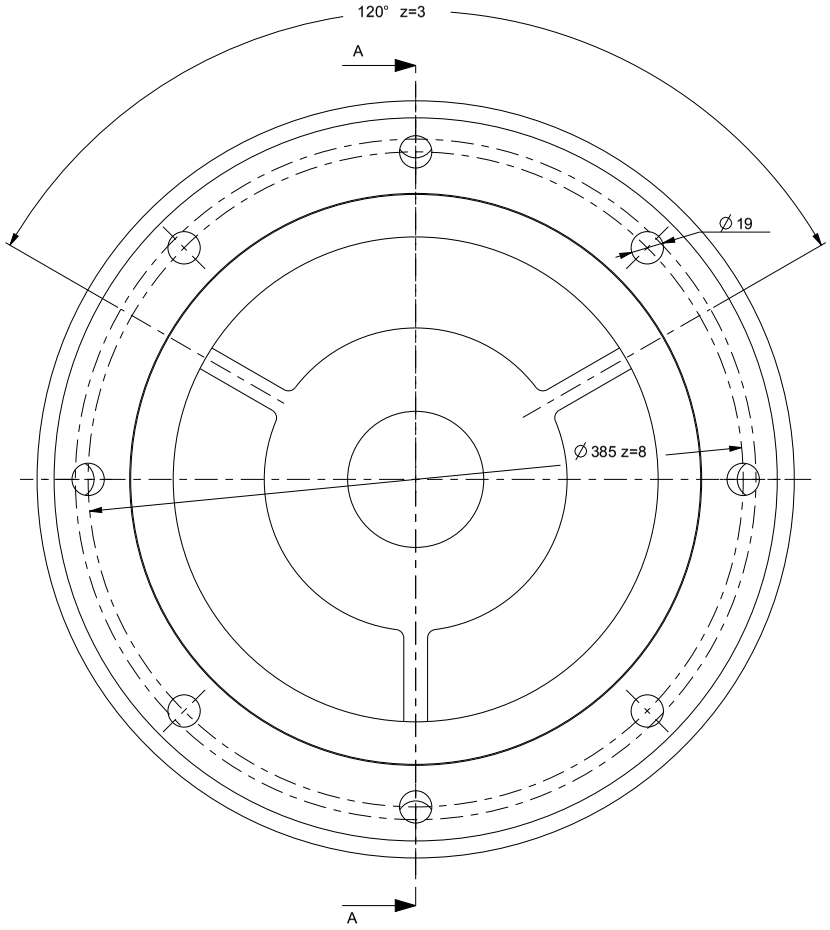

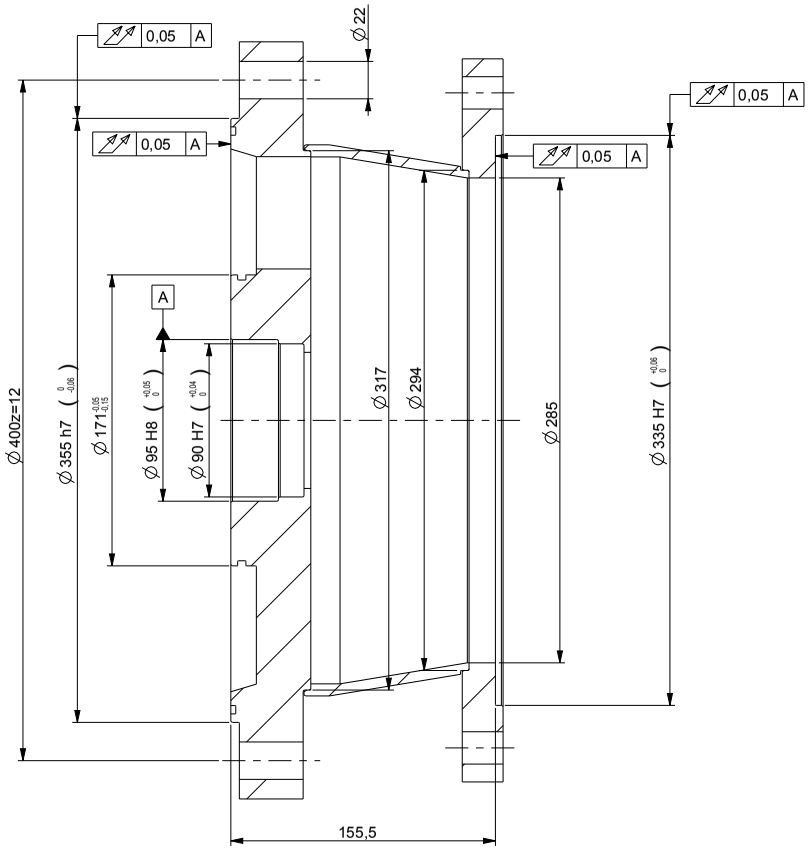

Section A-A

Missing dimensions are shown in the single-part drawings!

No.	Qnty	DRAWING No.	DENOTATION	STANDARD	MATERIAL	RAW MATERIAL
3	1	BT 1080_003	Flange		S355J2	
2	1	BT 1080_002	Casing		S355J2	
1	1	BT 1080_001	Flange		S355J2	

Datei-Name des Zeichnungsobjektes /Name of the drawing object:
1080_000_KONUS

Dateityp
File-type:
ASSEM

Datei-name der Zeichnung / Name of the drawing:
1080_000_KONUS

Toleranzen/Tolerance
ISO 8015
Allg. Toleranz/Gen. tolerance
DIN ISO 2768 m-K

Oberfläche
Surface quality
DIN ISO 1302
Werkst.-Kanten
Part edges
DIN ISO 13715

Maßstab/Scale 0,500
Gew./Weight 47.3 kg
Werkstoff/Material:
Halbzeug/Raw material:

	Datum/Date	Name
Bearb./Draft	2015-04-24	Hofgärtner
Gepr./Check		
Norm/Standard		

Benennung/Denotation:
Conus

Graz, University of Technology
Institute for Hydraulic
Fluidmachinery

Zeichnungsnummer/Drawing number:
BG 1080_000

Bl.n/Pg.n 1
1 Bl./P.

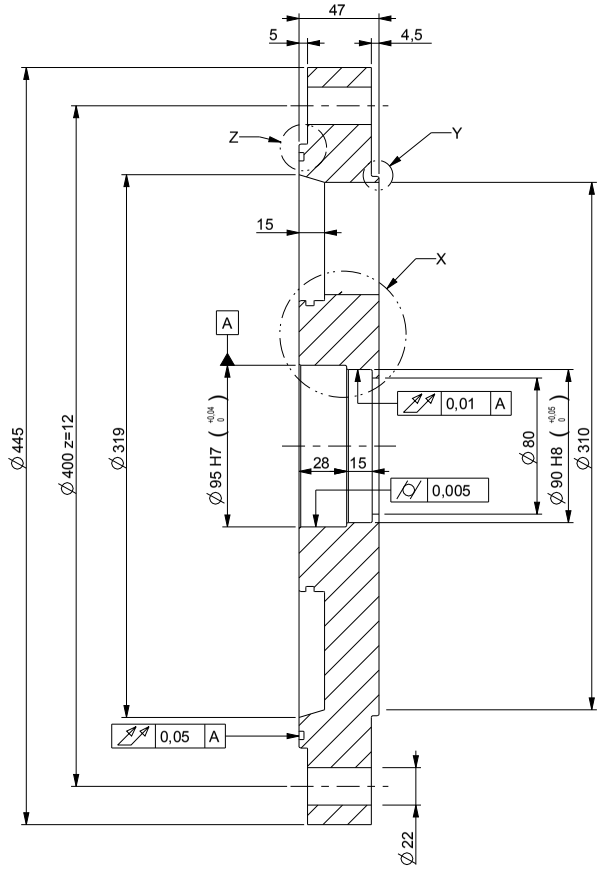

Section A-A

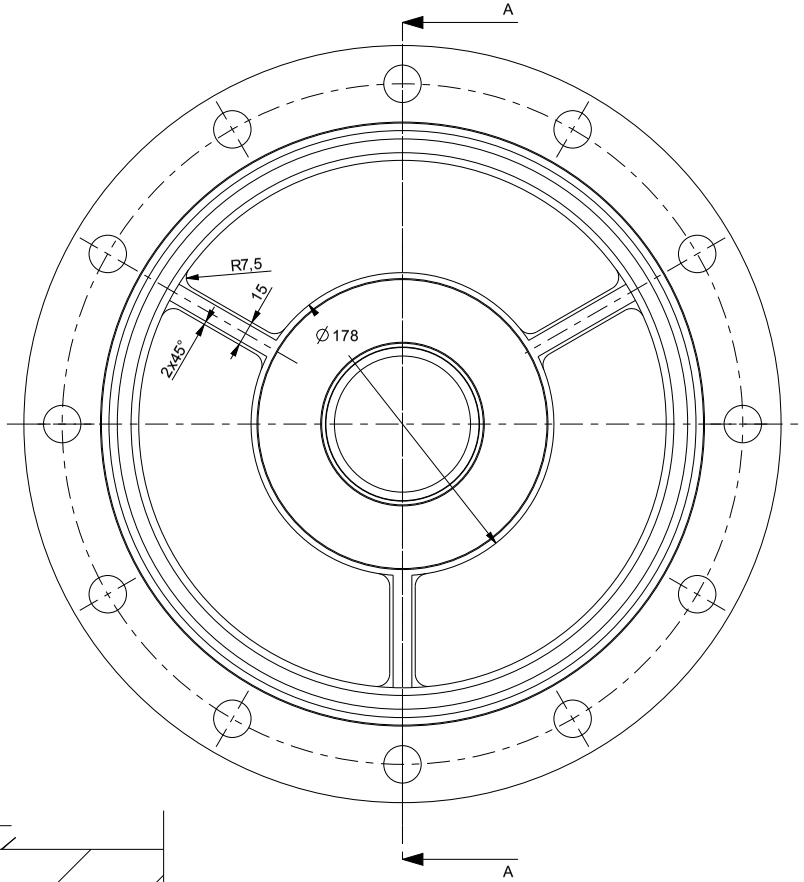

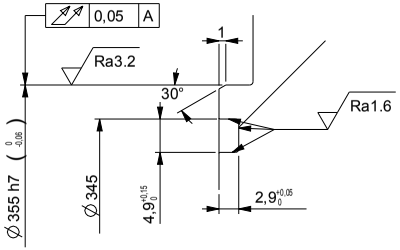

Detail Z
Scale 2.000

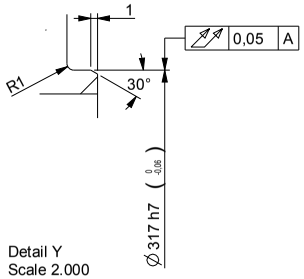

Detail Y
Scale 2.000

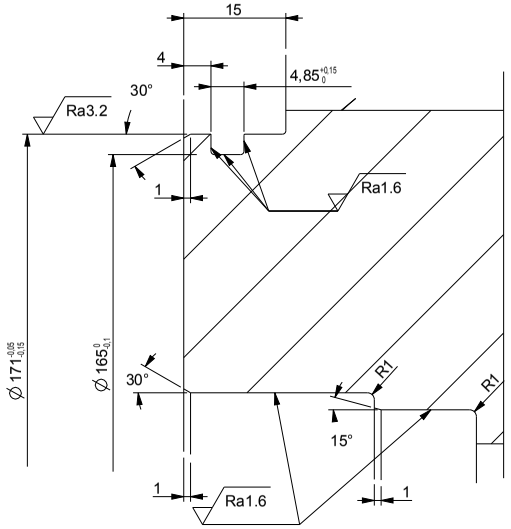

Detail X
Scale 2.000

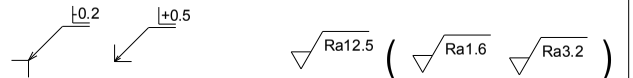

Dateiname des Zeichnungsobjektes /Name of the drawing object: 1080_001_FLANSCH		Dateityp. File-type: PART	Dateiname der Zeichnung / Name of the drawing: 1080_001_FLANSCH
	Toleranzen/Tolerance ISO 8015 Allg. Toleranz/Gen. tolerance DIN ISO 2768 m-K	Oberfläche Surface quality DIN ISO 1302 Werkst.-Kanten Part edges DIN ISO 13715	Maßstab/Scale 0,500 Gew./Weight 30.6 kg Werkstoff Material S355J2 Halbzeug Raw material Plate D=450; s=50
	Datum/Date	Name	Benennung Denomination: Flange Conus
Bearb./Draft.	31.04.19	Hofgärtner	
Gepr./Check.			
Norm Standard			
Graz, University of Technology Institute for Hydraulic Fluidmachinery			Zeichnungsnummer/Drawing number: BT 1080_001 Blatt/Page 1 / 1 BLP

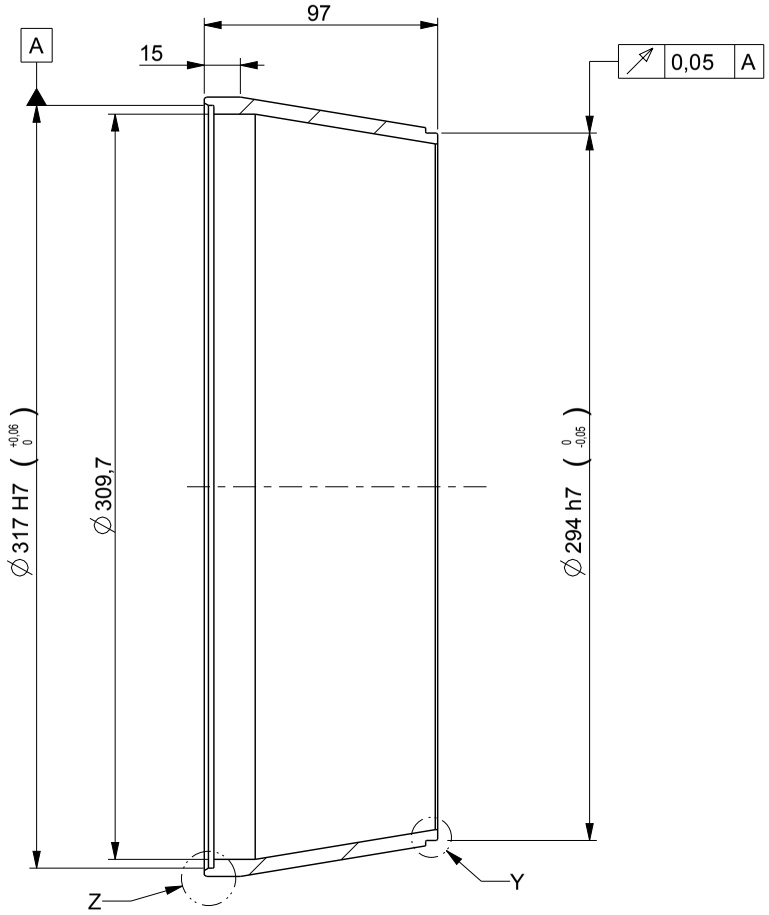

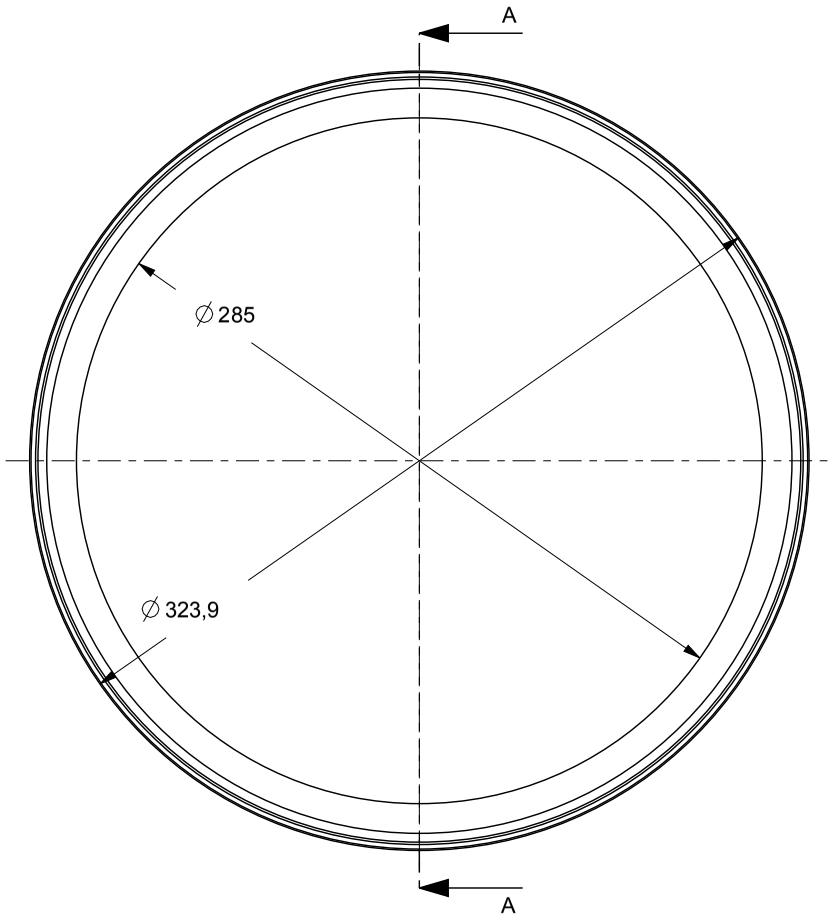

Section A-A

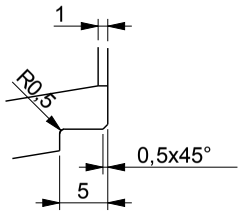

Detail Y
Scale 2.000

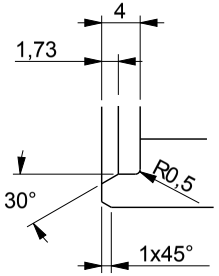

Detail Z
Scale 2.000

Dateiname des Zeichnungsobjektes / Name of the drawingobject: 1080_002_MANTEL		Dateityp File-type: PART	Dateiname der Zeichnung / Name of the drawing: 1080_002_MANTEL
	Tolerierung/Tolerance ISO 8015; Allg. Toleranz/Gen. tolerance DIN ISO 2768 m-K	Oberflaeche Surface quality DIN ISO 1302; Werkst.-Kanten Part-edges DIN ISO 13715	Maßstab/Scale 0,500; Gew./Weight: kg; Werkstoff / Material: S355J2; Halbzeug / Raw material: Reducing piece 323,9x7,1/273x6,3/203
	Datum/Date	Name	Benennung/Denotation: Reducing piece Conus
	Bearb. / Edit. 2013-04-24	Hopfgartner	
	Gepr. / Cert.		
	Norm / Standard		
Graz, University of Technology Institute for Hydraulic Fluidmachinery			Zeichnungsnummer/Drawing number: BT 1080_002; Blatt/Page 1; 1 Bl./P.

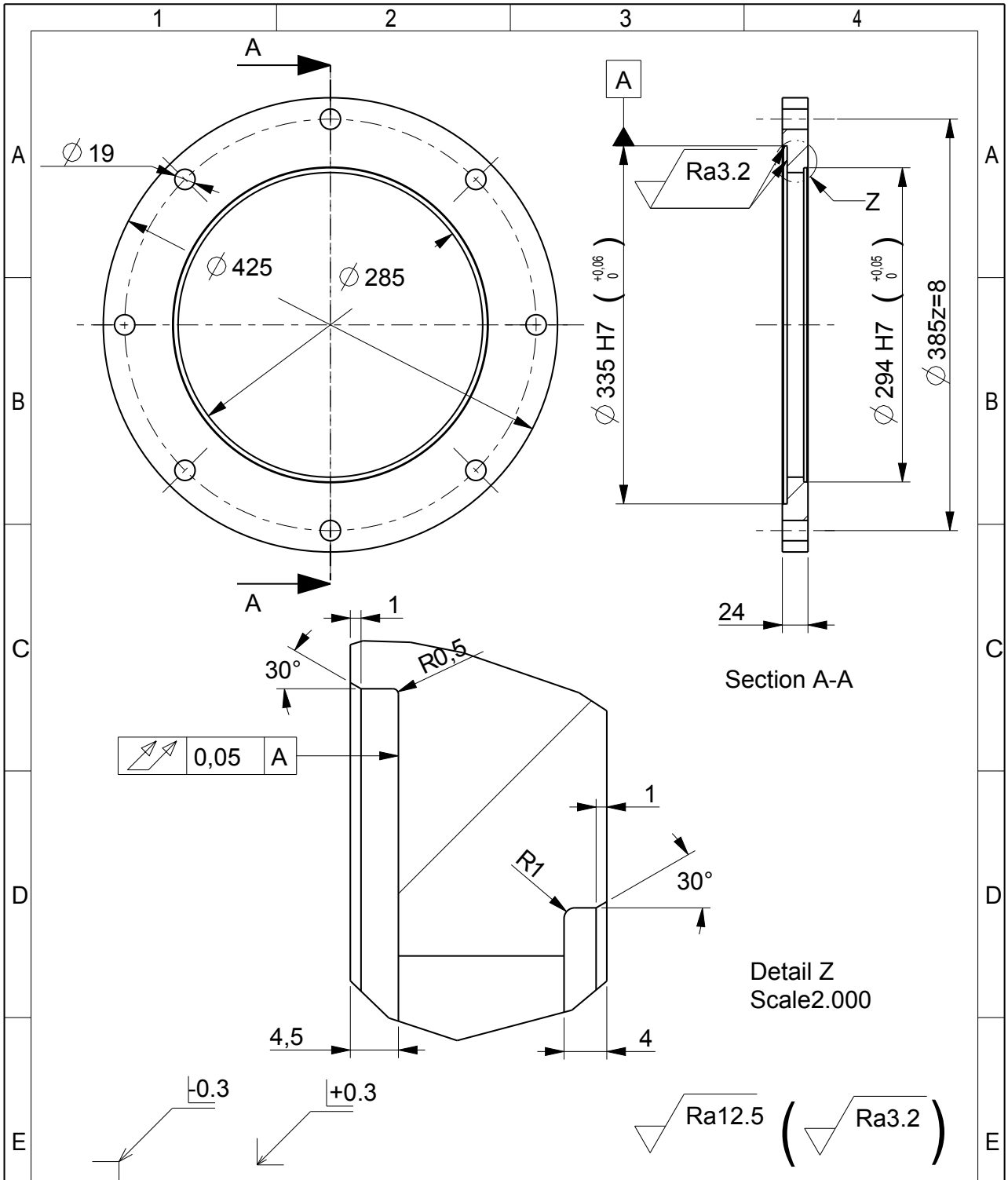

Dateiname des Zeichnungsobjektes / Name of the drawingobject: 1080_003_FLANSCH	Dateityp File-type: PART	Dateiname der Zeichnung / Name of the drawing: 1080_003_FLANSCH	
	Tolerierung/Tolerance ISO 8015 Allg. Toleranz/Gen. tolerance DIN ISO 2768 m-K	Oberflaeche Surface quality DIN ISO 1302 Werkst.-Kanten Part-edges DIN ISO 13715	Maßstab/Scale 0,200 Gew./Weight: 13.7 kg
			Werkstoff/Material: S355J2
			Halbzeug/Raw material: Breaker Plate D=450; d=270; s=25
	Datum/Date	Name	Benennung/Denotation:
	Bear. / Edit. 2013-04-24	Hopfgartner	Flange Conus
	Gepr. / Cert.		
	Norm / Standard		
Graz, University of Technology Institute for Hydraulic Fluidmachinery			Zeichnungsnummer / Drawing number: BT 1080_003
			Blatt/Page 1
			1 Bl./P.

B.9 Driving shaft

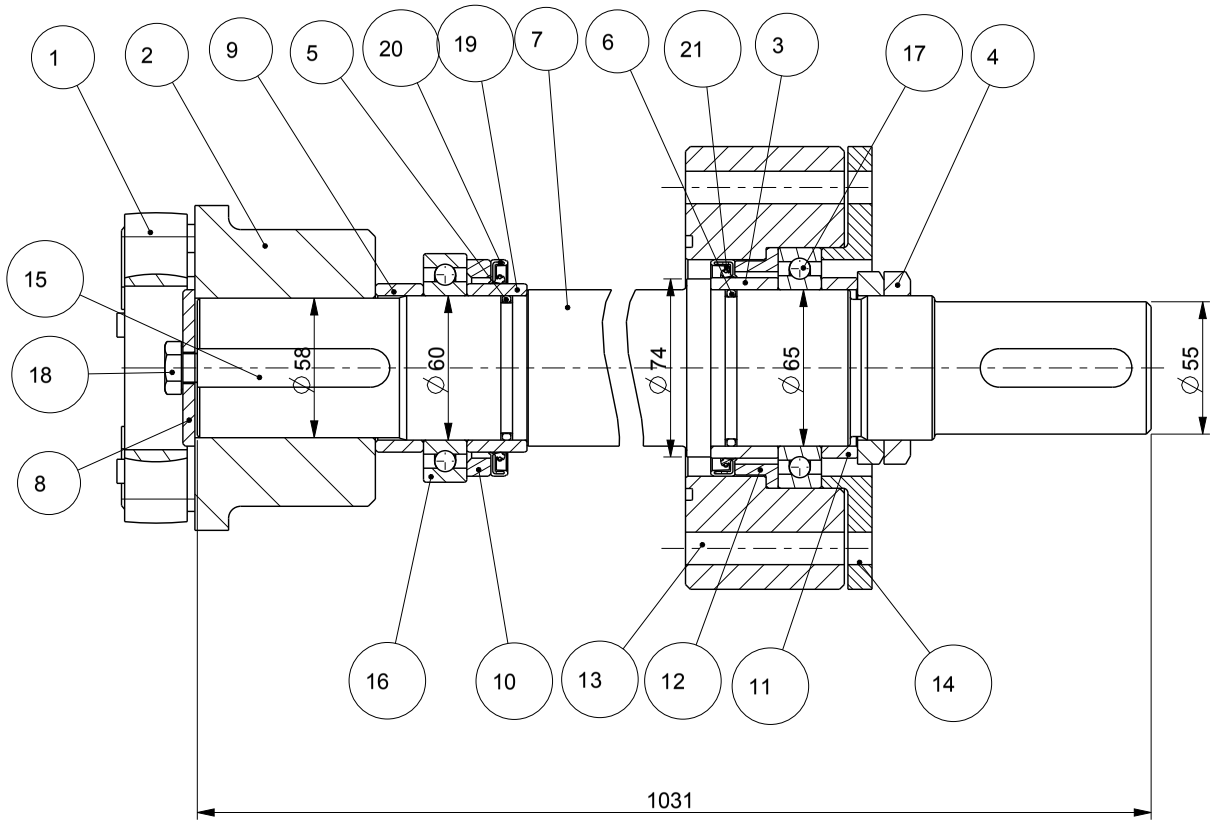

No.	Qnty	DRAWING No.	DENOTATION	STANDARD	MATERIAL	RAW MATERIAL
21	1		Radial shaft sealing	Simrit BABSL1 75x90x10	72 NBR 902	
20	1		Radial shaft sealing	Simrit BABSL1 70x90x7x0	72 NBR 902	
19	1		Inner ring	IR 60x70x25		
18	1		Hexagonal screw	DIN 933 M12x30	A2-70	
17	1		Grooved ball bearing	6013-2RS1		
16	1		Grooved ball bearing	6012-2RSR		
15	1		Fitting key	DIN 6885 A 16x10x80		
14	1	BT 1090_008	Cover plate		1.4301	
13	1	BT 1090_007	Bearing bushing		1.4301	
12	1	BT 1090_006	Space ring		1.4301	
11	1	BT 1090_005	Space ring		1.4301	
10	1	BT 1090_004	Space ring		1.4301	
9	1	BT 1090_003	Space ring		1.4301	
8	1	BT 1090_002	Disk		1.4301	
7	1	BT 1090_001	Shaft		42CrMo4	
6	1		O-ring d=59		NBR70Sh	Cord 3.6
5	1		O-ring d=54		NBR70Sh	Cord 3.6
4	2		Lock nut	KM12		
3	1		Inner ring	IR 65x75x28		
2	1		Cuppling d=58	GE-T 65		
1	1		Cuppling - toothed ring	GE-T 65 E	94 Shore	

Dateiname des Zeichnungsobjektes / Name of the drawingobject:
1090_000_ANTRIEBSWELLE

Dateityp / File-type: ASSEM

Dateiname der Zeichnung / Name of the drawing:
1090_000_ANTRIEBSWELLE_NEU

Tolerierung/Tolerance: ISO 8015
Allg. Toleranz/Gen. tolerance: DIN ISO 2768 m-K

Oberflaeche / Surface quality: DIN ISO 1302
Werkst.-Kanten / Part-edges: DIN ISO 13715

Maßstab/Scale: 0,500

Gew./Weight: 44.6 kg

Werkstoff / Material:
Halbzeug / Raw material:

	Datum/Date	Name
Bearb. / Edit.	2013-06-25	Hopfgartner
Gepr. / Cert.		
Norm / Standard		

Benennung/Denotation:

Driving shaft

Graz, University of Technology
Institute for Hydraulic Fluidmachinery

Zeichnungsnummer/Drawing number:
BG 1090_000

Blatt/Page 1
1 Bl./P.

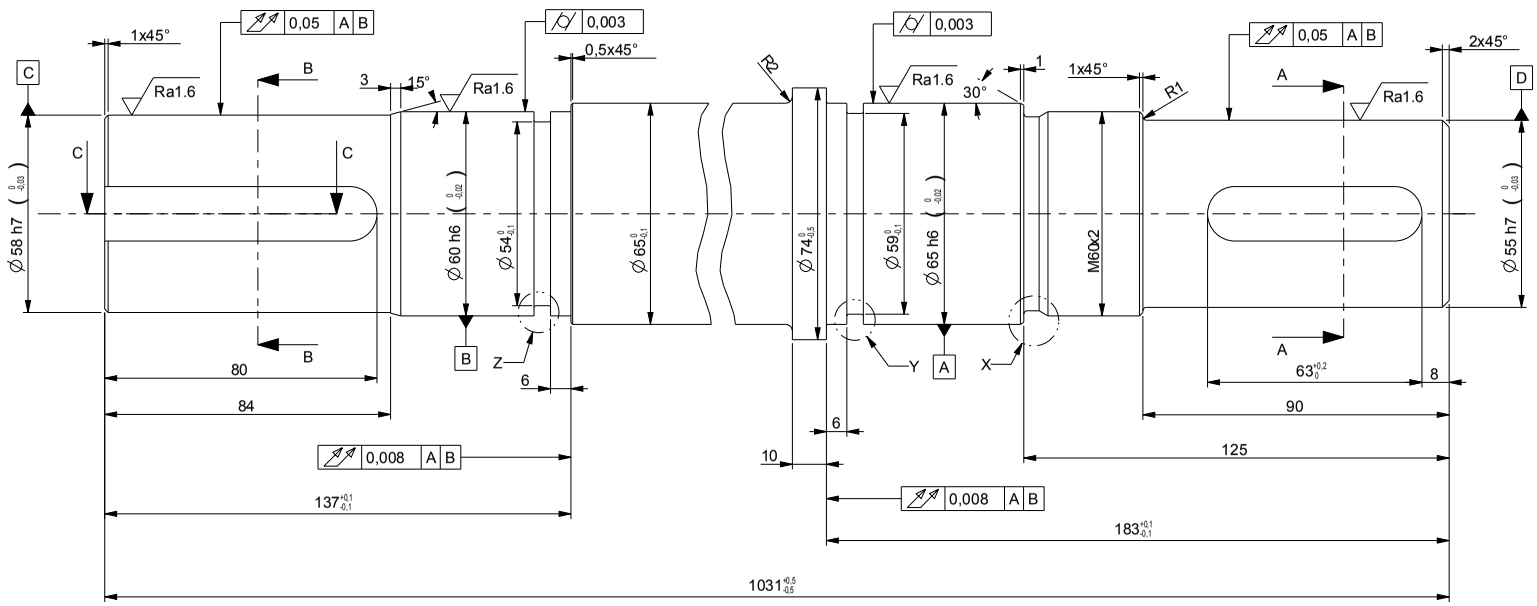

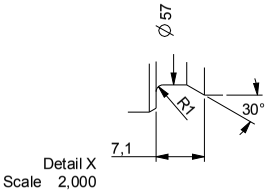

Detail X
Scale 2,000

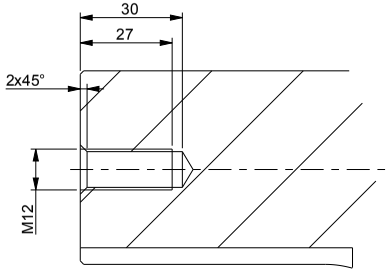

Section C-C

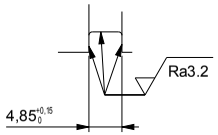

Detail Z
Scale 2,000

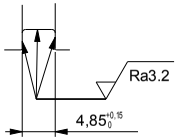

Detail Y
Scale 2,000

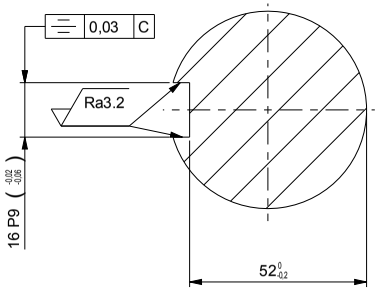

Section B-B

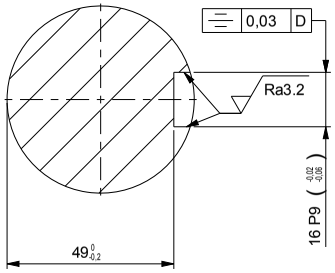

Section A-A

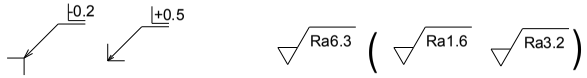

Dateiname des Zeichnungsobjektes /Name of the drawing object: 1090_001_WELLE_NEU		Dateityp File type: PART	Dateiname der Zeichnung / Name of the drawing: 1090_001_WELLE_NEU
	Tolerierung/Tolerance ISO 8015 Allg. Toleranz/Gen. tolerance DIN ISO 2768 m-K	Oberfläche Surface quality DIN ISO 1302 Werkst.-Kanten Part edges DIN ISO 13715	Maßstab/Scale 1,000 Gew./Weight 25.2 kg
			Werkstoff Material 42CrMo4 Härtung Raw material
	Datum/Date	Name	Benennung Denomination: Shaft Driving shaft
Bearb./Draft.	21-06-24	Hofgärtner	
Gepr./Cert.			
Norm Standard			
Graz, University of Technology Institute for Hydraulic Fluidmachinery			Zeichnungsnummer/Drawing number: BT 1090_001 Blatt/Page 1 / 1 BLP

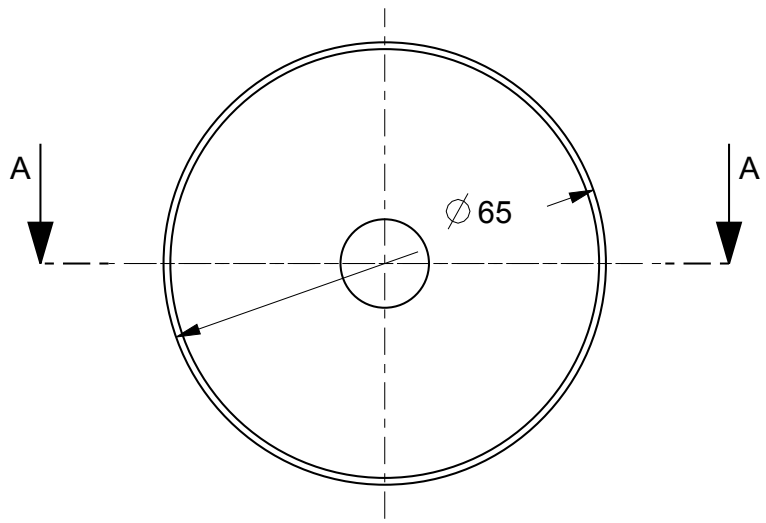

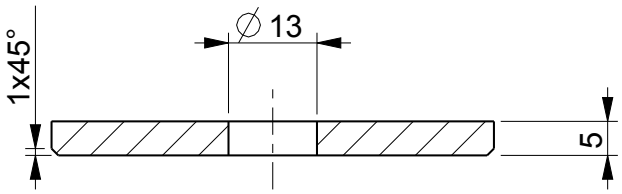

Section A-A

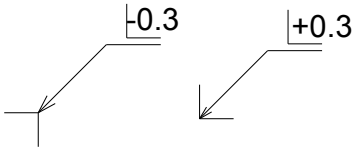

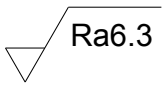

Dateiname des Zeichnungsobjektes / Name of the drawingobject: 1090_002_SCHEIBE		Dateityp File-type: PART	Dateiname der Zeichnung / Name of the drawing: 1090_002_SCHEIBE
	Tolerierung/Tolerance ISO 8015 Allg. Toleranz/Gen. tolerance DIN ISO 2768 m-K	Oberflaeche Surface quality DIN ISO 1302 Werkst.-Kanten Part-edges DIN ISO 13715	Maßstab/Scale 1,000 Gew./Weight: 0.12 kg Werkstoff/Material: 1.4301 Halbzeug/Raw material:
	Datum/Date / Name		Benennung/Denotation: Disk Driving shaft
	Bear. / Edit. 2013-04-24 Hopfgartner Gepr. / Cert. Norm / Standard		
	Graz, University of Technology Institute for Hydraulic Fluidmachinery		Zeichnungsnummer / Drawing number: BT 1090_002
			Blatt/Page 1 1 Bl./P.

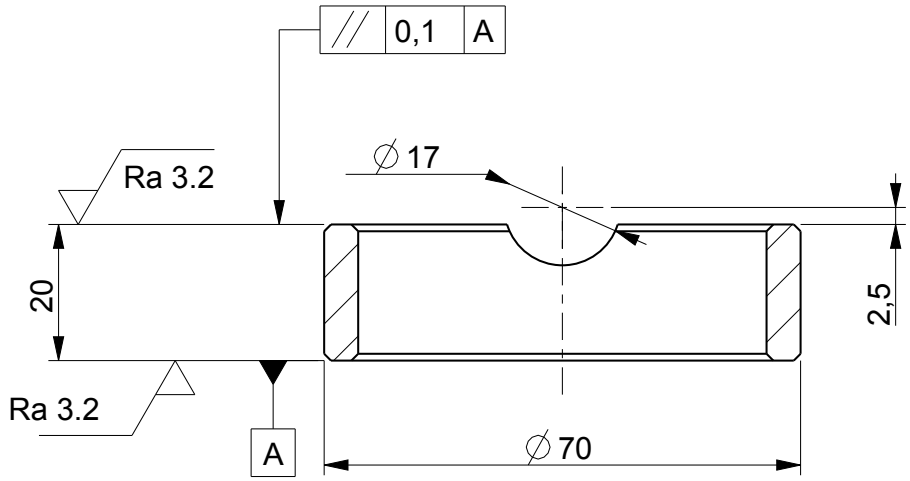

Section A-A

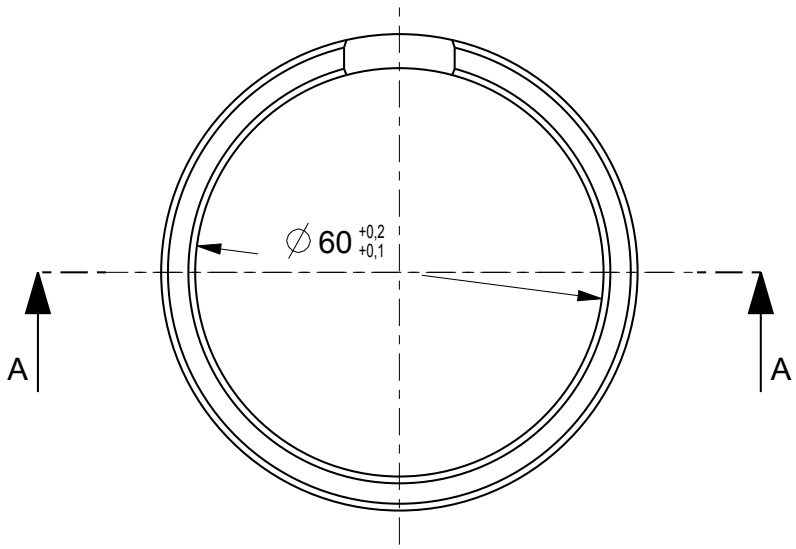

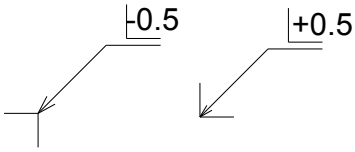

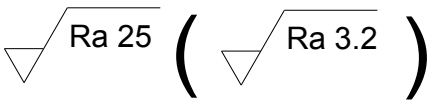

Dateiname des Zeichnungsobjektes / Name of the drawingobject: 1090_003_DISTANZRING_B	Dateityp File-type: PART	Dateiname der Zeichnung / Name of the drawing: 1090_003_DISTANZRING	
Tolerierung/Tolerance ISO 8015 Allg. Toleranz/Gen. tolerance DIN ISO 2768 m-K	Oberflaeche Surface quality DIN ISO 1302 Werkst.-Kanten Part-edges DIN ISO 13715	Maßstab/Scale 1,000	Gew./Weight: 0.15 kg
		Werkstoff/Material: 1.4301	
		Halbzeug/Raw material:	
	Datum/Date / Name	Benennung/Denotation: Space ring Driving shaft	
Bear. Edit. 2013-04-24 Hopfgartner			
Gepr. Cert.			
Norm Standard			
Graz, University of Technology Institute for Hydraulic Fluidmachinery		Zeichnungsnummer / Drawing number: BT 1090_003	Blatt/Page 1 / 1 Bl./P.

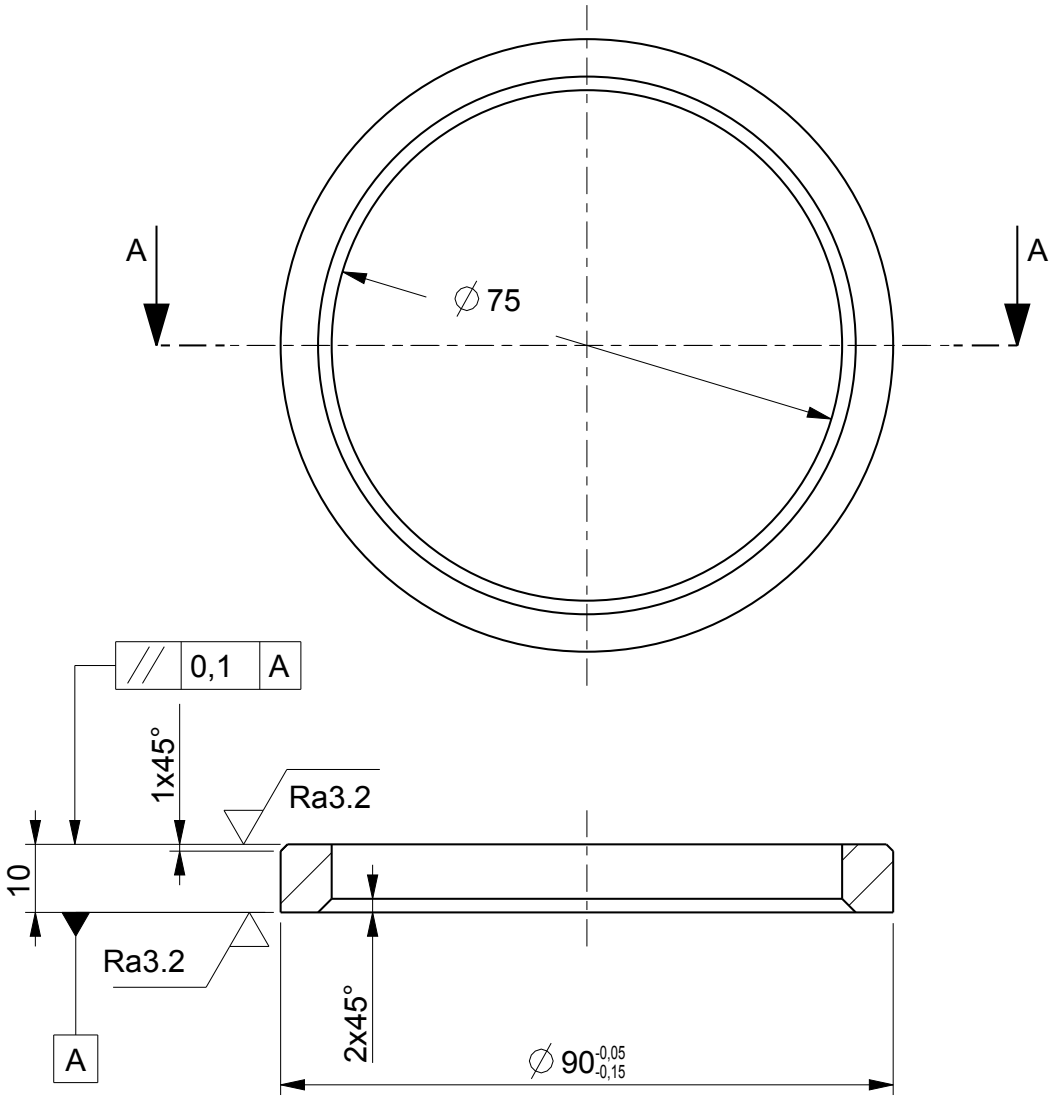

Section A-A

Ra12.5 (Ra3.2)

Dateiname des Zeichnungsobjektes / Name of the drawingobject: 1090_004_DISTANZRING_C		Dateityp File-type: PART	Dateiname der Zeichnung / Name of the drawing: 1090_004_DISTANZRING
	Tolerierung/Tolerance ISO 8015 Allg. Toleranz/Gen. tolerance DIN ISO 2768 m-K	Oberflaeche Surface quality DIN ISO 1302 Werkst.-Kanten Part-edges DIN ISO 13715	Maßstab/Scale 1,000 Gew./Weight: 0.15 kg Werkstoff/Material: 1.4301 Halbzeug/Raw material:
	Datum/Date / Name Bear. / 2013-04-24 / Hopfgartner Edit. Gepr. / Cert. Norm / Standard		Benennung/Denotation: Space ring Driving shaft
	Graz, University of Technology Institute for Hydraulic Fluidmachinery		Zeichnungsnummer / Drawing number: BT 1090_004 — Blatt/Page 1 — 1 Bl./P.

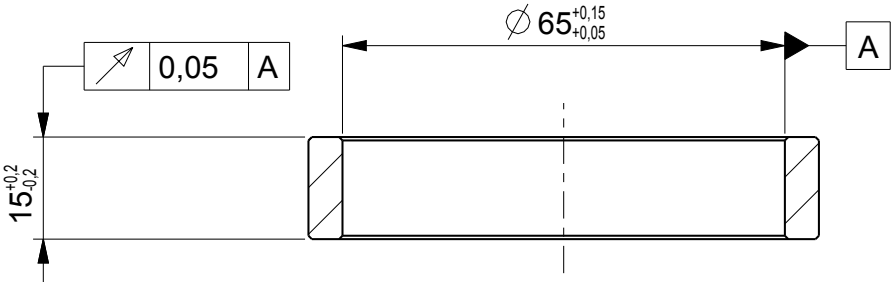

Section A-A

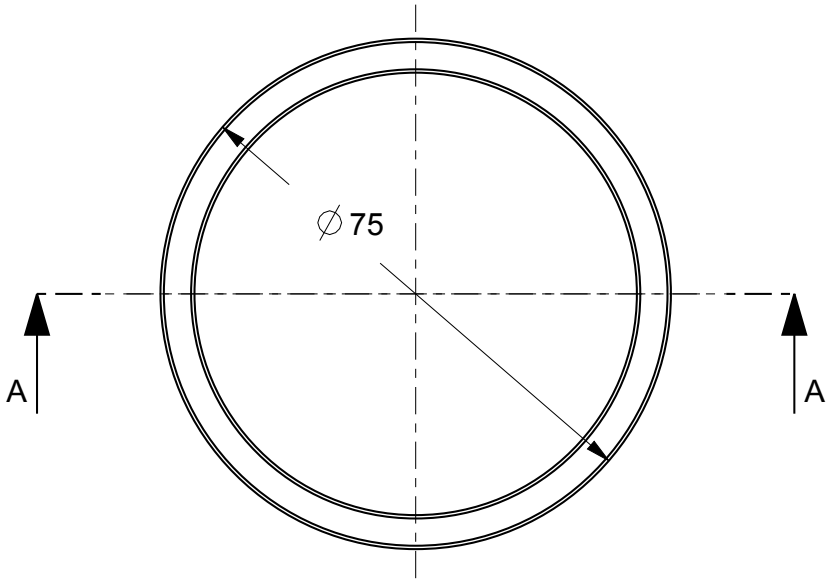

Dateiname des Zeichnungsobjektes / Name of the drawingobject: 1090_005_DISTANZRING	Dateityp File-type: PART	Dateiname der Zeichnung / Name of the drawing: 1090_005_DISTANZRING	
	Tolerierung/Tolerance ISO 8015 Allg. Toleranz/Gen. tolerance DIN ISO 2768 m-K	Oberflaeche Surface quality DIN ISO 1302 Werkst.-Kanten Part-edges DIN ISO 13715	Maßstab/Scale 1,000 Gew./Weight: 0.13 kg
			Werkstoff/Material: 1.4301
			Halbzeug/Raw material:

	Datum/Date	Name
Bear. Edit.	2013-06-24	Hopfgartner
Gepr. Cert.		
Norm Standard		

Benennung/Denotation:

Space ring
Driving shaft

Graz, University of Technology
Institute for Hydraulic
Fluidmachinery

Zeichnungsnummer / Drawing number:

BT 1090_005

Blatt/Page 1

1 Bl./P.

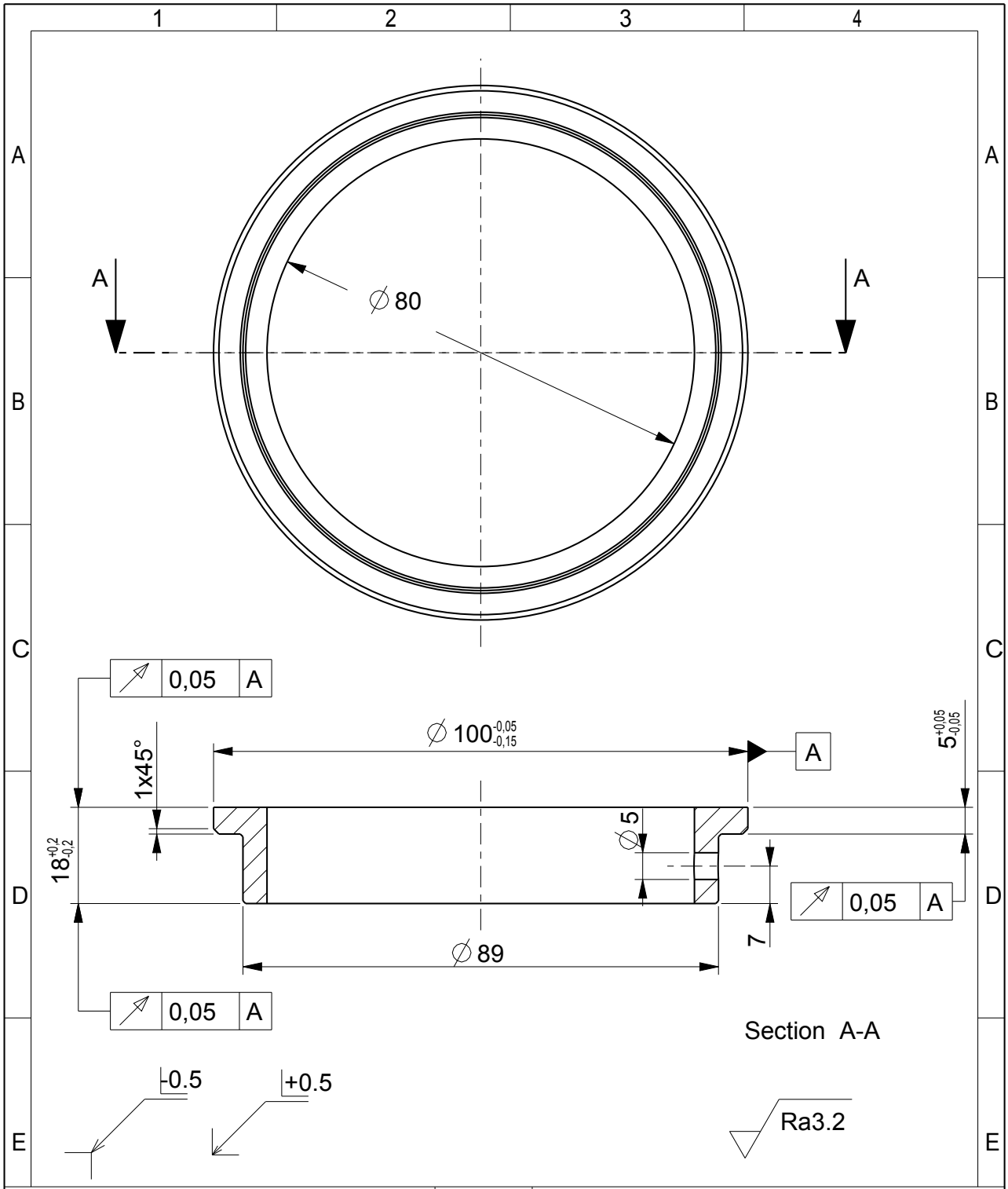

Dateiname des Zeichnungsobjektes / Name of the drawingobject: 1090_006_DISTANZRING	Dateityp File-type: PART	Dateiname der Zeichnung / Name of the drawing: 1090_006_DISTANZRING	
	Tolerierung/Tolerance ISO 8015 Allg. Toleranz/Gen. tolerance DIN ISO 2768 m-K	Oberflaeche Surface quality DIN ISO 1302 Werkst.-Kanten Part-edges DIN ISO 13715	Maßstab/Scale 1,000 Gew./Weight: 0.23 kg
			Werkstoff/Material: 1.4301
			Halbzeug/Raw material:
	Datum/Date	Name	Benennung/Denotation:
	Bear. Edit. 2013-06-24	Hopfgartner	Space ring Driving shaft
	Gepr. Cert.		
	Norm Standard		
Graz, University of Technology Institute for Hydraulic Fluidmachinery		Zeichnungsnummer / Drawing number: BT 1090_006	Blatt/Page 1 1 Bl./P.

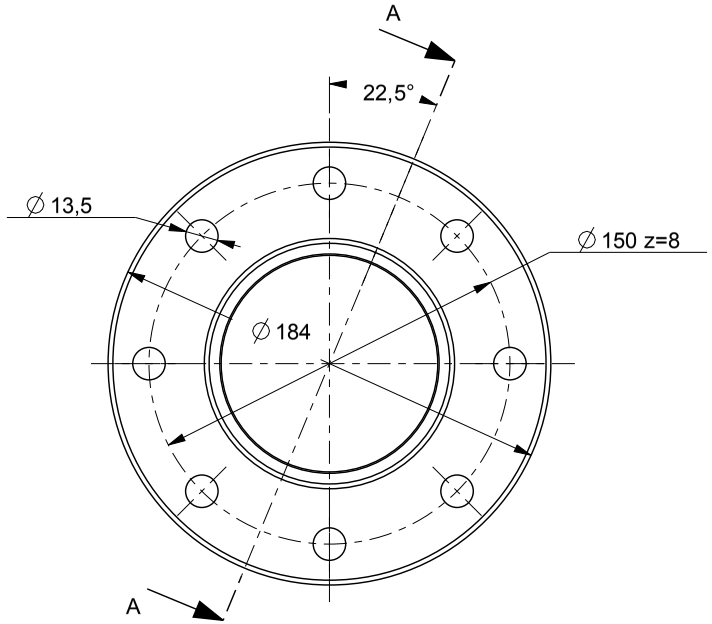

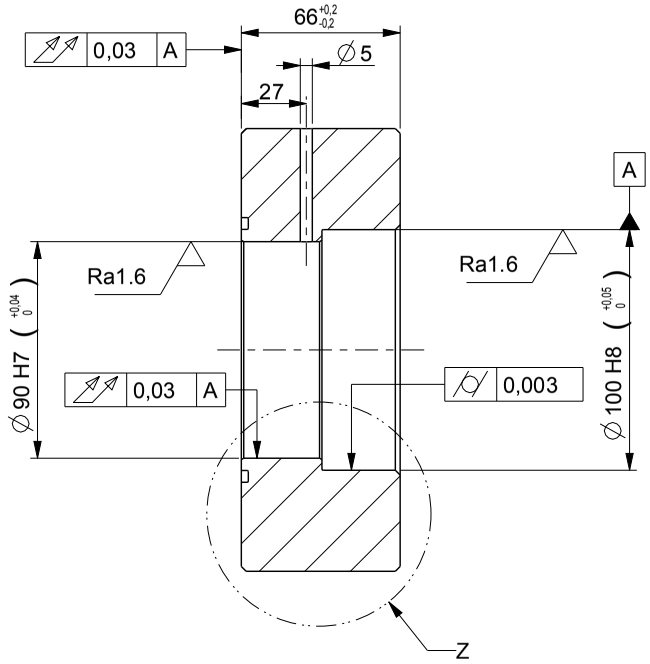

Section A-A

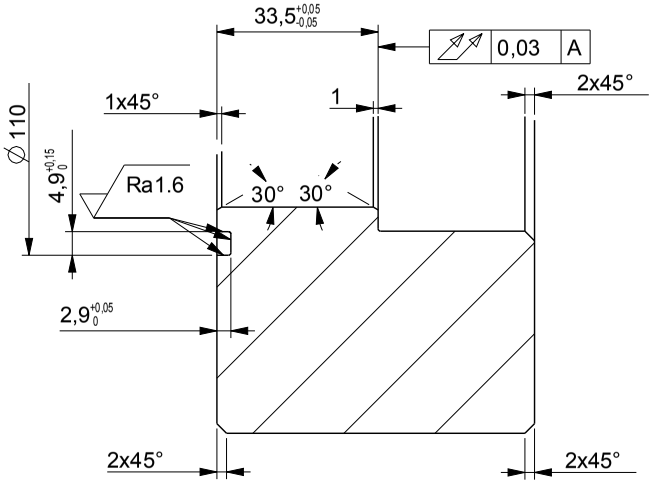

Detail Z
Scale 1,000

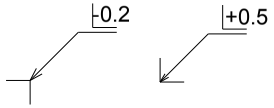

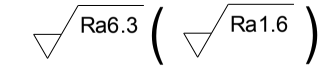

Dateiname des Zeichnungsobjektes / Name of the drawingobject: 1090_007_HUELSE		Dateityp File-type: PART	Dateiname der Zeichnung / Name of the drawing: 1090_007_HUELSE
	Tolerierung/Tolerance ISO 8015 Allg. Toleranz/Gen. tolerance DIN ISO 2768 m-K	Oberflaeche Surface quality DIN ISO 1302 Werkst.-Kanten Part-edges DIN ISO 13715	Maßstab/Scale 0,500 Gew./Weight: 8.7 kg Werkstoff / Material: S355J2 Halbzeug / Raw material:
	Datum/Date	Name	Benennung/Denotation: Bearing bushing Driving shaft
Bearb. Edit. 2013-06-24 Gepr. Cert. Norm Standard		Hopfgartner	
Graz, University of Technology Institute for Hydraulic Fluidmachinery			Zeichnungsnummer/Drawing number: BT 1090_007 Blatt/Page 1 1 Bl./P.

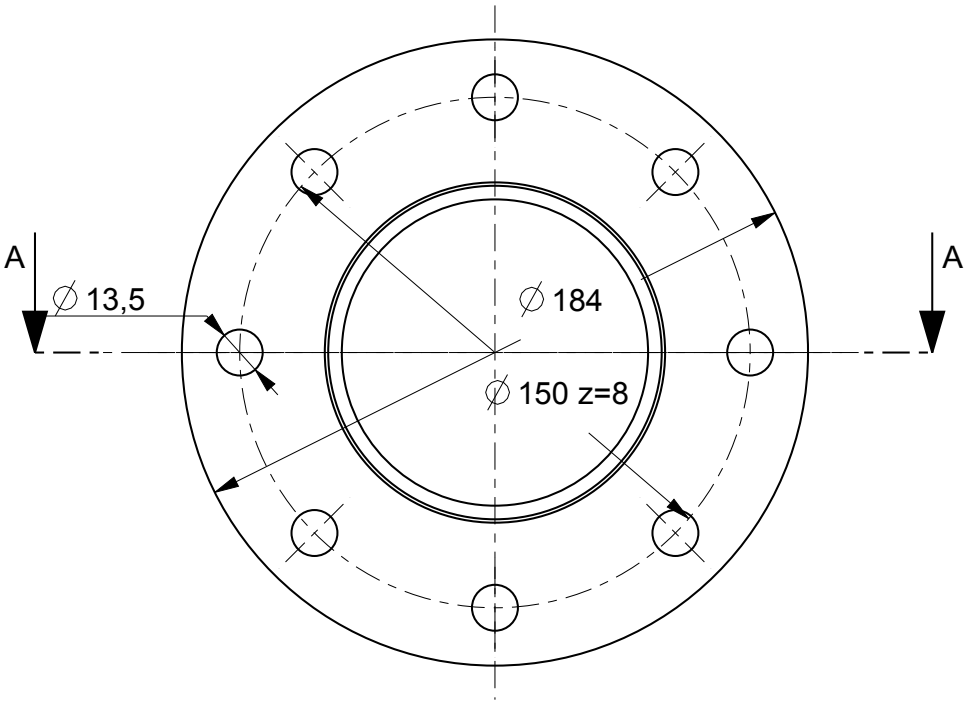

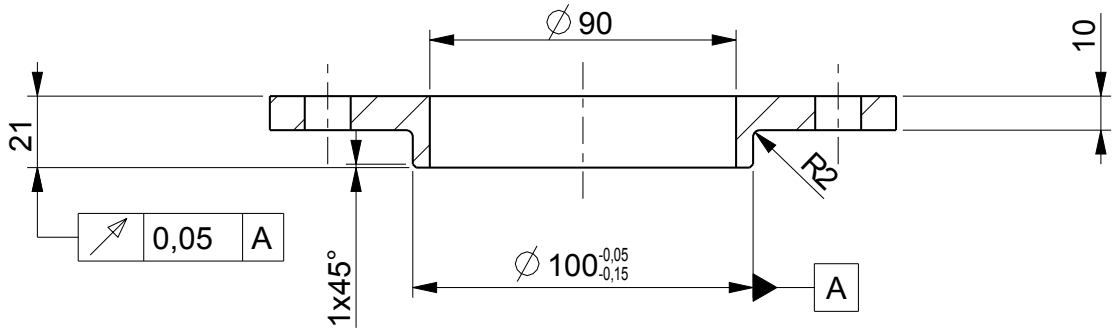

Section A-A

Dateiname des Zeichnungsobjektes / Name of the drawingobject: 1090_008_DECKEL		Dateityp File-type: PART	Dateiname der Zeichnung / Name of the drawing: 1090_008_DECKEL
	Tolerierung/Tolerance ISO 8015 Allg. Toleranz/Gen. tolerance DIN ISO 2768 m-K	Oberflaeche Surface quality DIN ISO 1302 Werkst.-Kanten Part-edges DIN ISO 13715	Maßstab/Scale 0,500 Gew./Weight: 1.2 kg
			Werkstoff/Material: S355J2
			Halbzeug/Raw material:
	Datum/Date	Name	Benennung/Denotation:
	Bear. Edit. 2013-06-24	Hopfgartner	Cover plate Driving shaft
	Gepr. Cert.		
	Norm Standard		
Graz, University of Technology Institute for Hydraulic Fluidmachinery			Zeichnungsnummer / Drawing number: BT 1090_008
			Blatt/Page 1
			1 Bl./P.